

## Durham E-Theses

---

*Studies on the ring-opening metathesis polymerization  
of functionalised bicyclic olefins using well-defined  
molybdenum initiators*

Edward L. Marshall

### How to cite:

---

Marshall, Edward L. (1992) Studies on the ring-opening metathesis polymerization of functionalised bicyclic olefins using well-defined molybdenum initiators. Doctoral thesis, Durham University.

### Use policy

---

The full-text may be used and/or reproduced, and given to third parties in any format or medium, without prior permission or charge, for personal research or study, educational, or not-for-profit purposes provided that:

- a full bibliographic reference is made to the original source
- a <https://etheses.durham.ac.uk/id/eprint/5766/> is made to the metadata record in Durham E-Theses
- the full-text is not changed in any way

The full-text must not be sold in any format or medium without the formal permission of the copyright holders.

Please consult the [full Durham E-Theses policy](#) for further details.

**Studies on the Ring-Opening Metathesis Polymerization of Functionalised  
Bicyclic Olefins using Well-Defined Molybdenum Initiators**

by

Edward L. Marshall, B.Sc. (Dunelm)

University of Durham

A thesis submitted in part fulfilment of the requirements for the degree of  
Doctor of Philosophy at the University of Durham.

December 1992

The copyright of this thesis rests with the author.  
No quotation from it should be published without  
his prior written consent and information derived  
from it should be acknowledged.



- 2 JUL 1993

## **Statement of Copyright**

The Copyright of this thesis rests with the author. No quotation from it should be published without his prior written consent and information derived from it should be acknowledged.

## **Declaration**

The work described in this thesis was carried out in the Department of Chemistry at the University of Durham between October 1989 and September 1992. All the work is my own, unless stated to the contrary, and it has not been submitted previously for a degree at this or any other university.

## **Financial Support**

The Science and Engineering Research Council is gratefully acknowledged for providing a grant for the work described herein, administered through the Interdisciplinary Research Centre in Polymer Science and Technology.

This thesis is dedicated with all my love to my mother.

## Acknowledgements

In reality, the work described in this thesis is not all my own, as it states in the declaration, but the product of many friends and colleagues. Of these my most sincere gratitude is extended towards my supervisor, Dr. Vernon C. Gibson. Appreciation is also expressed to Professor W. James Feast for innumerable helpful suggestions and to Jim's group, especially Drs. Ezat Khosravi and Brian Wilson who did much of the ground work for this thesis; Ezat also provided two of the monomers polymerized in chapter five. Professor Ken Ivin is also acknowledged for his invaluable help in assigning the N.M.R. spectra described in chapters two and three, as is Dr. Alan Kenwright. I would also like to thank Professor Richard R. Schrock from M.I.T. and several of his students, particularly John Oskam, for ideas and unselfish early communication of their own findings. Dr. Geoff Davies, Dr. Huw Hubbard, and Professor Ian Ward from the Department of Physics at Leeds University are thanked for the dielectric measurements reported herein and advice with the general aims of the study.

Vernon must also be praised for assembling such a wonderful group of students to work with. Dr. Alan Shaw, Dr. David Williams, and Dr. Jonathan Mitchell all share equal blame for me doing a Ph.D. (I've got three bullets with your names on, boys). I've shared so many laughs and so many good times with Phil Dyer and Matt Jolly that to wish them both the very best for the future doesn't seem enough. The remaining members, Tina, Martyn, Mike, Leela and Brenda have all earned a place in my heart. I could not forget all the other members of lab 101 / 19 from the past, especially Andy and Oliver as well as Eduardo, Ulrich, Jens and Kayumars who are also fondly remembered.

My housemates over the last few years also deserve a special mention, particularly Martin, Jon, Gail, and Angela. I'm sure we'll all remember the smelly-cheese fondue with both happiness and a touch of sadness for the rest of our living days. I mustn't forget the others who put up with me: Karen, Julie, Jane, Elke, Rebecca and Edward. Special thanks must go to Ian and all my friends from CG100; to Paul, Mark and Chris from CG27, Alan and Nigel from CG115, all the Tuesday afternoon footballers, and the survivors of Euan's minibus driving to Hayesdale '92!

And now, the people who really matter; thanks to all my family, especially my Mother, Debbie, Robert, my Grandfather and Grandmother, Catherine and Jeffrey, Sean, Patricia, Michael, Anne, Mike, Michaela, Bob, Bet, and all the folks from Eire, for all the support and love they've given me over the past twenty-four years. This thesis is for them.

## Abstract

### Studies into the Ring-Opening Metathesis Polymerization of Functionalised Bicyclic Olefins using Well-Defined Molybdenum Initiators

This thesis describes studies into the living ring-opening metathesis polymerization (R.O.M.P.) of several fluorinated norbornenes and norbornadienes, using a series of well-defined initiators of general formula  $\text{Mo}(\text{N}-2,6\text{-i-Pr}_2\text{-C}_6\text{H}_3)(\text{CHR})(\text{OR}')_2$ .

Chapter 1 highlights areas of R.O.M.P. and of fluoropolymers of relevance to the general themes of the thesis.

Chapter 2 describes the R.O.M.P. of 2,3-bis(trifluoromethyl)bicyclo[2.2.1]hepta-2,5-diene, using both  $\text{Mo}(\text{N}-2,6\text{-i-Pr}_2\text{-C}_6\text{H}_3)(\text{CHCMe}_2\text{Ph})(\text{OCMe}_3)_2$  and  $\text{Mo}(\text{N}-2,6\text{-i-Pr}_2\text{-C}_6\text{H}_3)(\text{CHCMe}_2\text{Ph})(\text{OCMe}(\text{CF}_3)_2)_2$ . In the former case a very high trans polymer has previously been reported; by changing the ancillary alkoxide ligands to hexafluorobutoxides the geometry of the polymer is completely reversed to very high cis. Dielectric measurements on both materials have been carried out and these have been used to determine the tacticity of the polymers in conjunction with high frequency  $^{13}\text{C}$  N.M.R. spectroscopy. This information has then been considered in terms of mechanistic implications.

Chapter 3 details how an equilibrium mixture of the two initiators used in the previous chapter can provide access to any desired cis and trans content poly[1,4-(2,3-bis(trifluoromethyl)cyclopentenylene) vinylene]. The  $^{13}\text{C}$  N.M.R. spectra of a series of such intermediate samples are assessed and the observed splitting of the methylene resonance is described. This information is combined with preliminary dielectric measurements to arrive at a full unambiguous assignment of polymer microstructure.

Chapter 4 continues the theme of controlling the stereoregular nature of poly[1,4-(2,3-bis(trifluoromethyl)cyclopentenylene) vinylene] synthesized from the four-coordinate 'Schrock' initiators. A series of experiments are described which investigate the effect of chiral components at or near the metal centre in an attempt to increase the selectivity of one face of the active site towards the approach of the monomer. Most of these are found to be ineffective in terms of changing the tacticity of the polymer produced. However, the employment of chiral bidentate alkoxides has been found to exhibit some influence which is described.

Chapter 5 reports on the synthesis of three other related fluoropolymers using similar techniques to those employed in the previous chapters.  $^{13}\text{C}$  N.M.R. spectroscopy has again been used to determine the stereoregularity of the polymers prepared. Attention is then turned to the first-ever syntheses of fluorinated block-copolymers via living R.O.M.P.. These species have been fully characterised and indeed shown to possess genuine block structures.

Chapter 6 presents experimental details for chapters 2-5.

Edward L. Marshall (December 1992)

## Abbreviations

N.M.R.	Nuclear magnetic resonance	I.R.	Infra-red
G.P.C.	Gel permeation chromatography	D.S.C.	Differential scanning calorimetry
T.S.C.	Thermally stimulated current	T.G.A.	Thermal gravimetric analysis
W.A.X.D.	Wide angle X-ray diffraction	D.M.T.A.	Dynamic mechanical tension apparatus
NAr	2,6-di-iso-propyl-arylimido (DIPP)	THF	Tetrahydrofuran
DME	Dimethoxyethane	BN(OH) <sub>2</sub>	1,1'-Bi-2-naphthol
Cp	Cyclopentadienyl ligand	Cp*	Pentamethylcyclopentadienyl
c	Cis	t	Trans
$\sigma_c$	Cis vinylene fraction	$\sigma_t$	Trans vinylene fraction
HH	Head-head	TT	Tail-tail
HT	Head-tail	TH	Tail-head
r	Racemic (syndiotactic)	m	Meso (isotactic)
$\delta$	Chemical shift	ppm	Parts per million
$\epsilon_0$	Vacuum permittivity	$\tan \delta$	Mechanical loss tangent
$\epsilon_U$	Unrelaxed dielectric constant	$\epsilon_R$	Relaxed dielectric constant
g	Kirkwood g-factor	$\mu$	Dipole moment
k	Boltzmann constant	T	Temperature (Kelvin)
$k_p$	Rate constant of propagation	$k_i$	Rate constant of initiation
[I]	Concentration of initiator	[M]	Concentration of monomer
$M_n$	Number average molecular weight	$M_w$	Weight average molecular weight
PDI	Polydispersity index	LUMO	Lowest unoccupied molecular orbital

## Contents

	Page
<b>Chapter One - An Overview of Ring-Opening Metathesis Polymerization and Fluorinated Polymers</b>	<b>1</b>
1.1 Introduction	2
1.2 Olefin Metathesis	4
1.2.1 The mechanism for olefin metathesis and ring-opening metathesis polymerization	5
1.2.2 Thermodynamic considerations	7
1.3 Metathesis initiators	9
1.3.1 Classical initiator systems	9
1.3.2 Transition metal carbene complexes	10
1.3.3 Metallacyclobutane catalysts	12
1.4 A comparison of the structure and bonding in metal alkylidenes and metal carbenes	13
1.5 Living R.O.M.P.	15
1.5.1 Living polymerizations	15
1.5.2 Well-defined initiators for the living R.O.M.P. of cycloalkenes	15
1.5.3 Titanacyclobutanes	16
1.5.4 Four coordinate imido-alkylidene complexes of tungsten and molybdenum	18
1.5.5 Aqueous living R.O.M.P.	21
1.6 The ring-opening metathesis polymerization of fluorinated cycloolefins	23
1.6.1 Classically initiated R.O.M.P.	23
1.6.2 The R.O.M.P. of fluorinated bicyclic olefins using well-defined Schrock initiators	25
1.7 Fluorinated polymers	28
1.7.1 Poly(tetrafluoroethylene)	30

1.7.2	Poly(vinylidene fluoride)	31
1.7.3	The origin of piezoelectricity in poly(vinylidene fluoride)	33
1.7.4	The applications of poly(vinylidene fluoride) arising from its piezoelectricity	33
1.8	Summary	35
1.9	References	36
 <b>Chapter Two - The Living R.O.M.P. of 2,3-Bis(trifluoromethyl) Bicyclo[2.2.1]hepta-2,5-diene</b>		 41
2.1	Introduction	42
2.1.1	Historical background	42
2.1.2	A highly stereoregular fluoropolymer synthesized via living R.O.M.P.	44
2.2	Tacticity	48
2.3	The influence of reaction conditions upon cis / trans content in poly[1,4-(2,3-bis(trifluoromethyl)cyclopentenylene) vinylene]	51
	a) Temperature	51
	b) Solvent	52
	c) Monomer concentration	55
	d) Stirring	56
2.3.1	Conclusions	56
2.4	The R.O.M.P. of 2,3-bis(trifluoromethyl)bicyclo[2.2.1]hepta-2,5-diene using Mo(N-2,6-i-Pr <sub>2</sub> -C <sub>6</sub> H <sub>3</sub> )(CHCMe <sub>2</sub> Ph)(OCMe(CF <sub>3</sub> ) <sub>2</sub> ) <sub>2</sub> as the initiator	58
2.4.1	N.M.R. spectroscopic study	58
2.4.2	Molecular weight distribution	65
2.4.3	Differential scanning calorimetry	66
2.5	A kinetic study on the metathesis polymerization of 2,3-bis(trifluoromethyl)bicyclo[2.2.1]hepta-2,5-diene	67

2.6	The R.O.M.P. of 2,3-bis(trifluoromethyl)bicyclo[2.2.1]hepta-2,5-diene using Mo(N-2,6-i-Pr <sub>2</sub> -C <sub>6</sub> H <sub>3</sub> )(CHCMe <sub>2</sub> Ph)(OCMe <sub>2</sub> CF <sub>3</sub> ) <sub>2</sub> as the initiator	71
2.7	Dielectric measurements and the microstructure of high trans poly(1,4-(2,3-bis(trifluoromethyl)cyclopentenylene) vinylene)	74
2.8	Discussion	82
2.9	Summary	96
2.10	References	97
 <b>Chapter Three - A Mixed Initiator System for the Living R.O.M.P. of 2,3-Bis(trifluoromethyl)bicyclo[2.2.1]hepta-2,5-diene</b>		<b>98</b>
3.1	Ligand exchange between transition metal centres	99
3.2	Alkoxide exchange reactions in four-coordinate molybdenum-based metathesis initiators	101
3.2.1	The reaction between Mo(NAr)(CHCMe <sub>2</sub> Ph)(OCMe <sub>3</sub> ) <sub>2</sub> and Mo(NAr)(CHCMe <sub>2</sub> Ph)(OCMe(CF <sub>3</sub> ) <sub>2</sub> ) <sub>2</sub>	101
3.2.2	The mechanism of alkoxide exchange	105
3.2.3	The reaction of Mo(NAr)(CHCMe <sub>2</sub> Ph)(OCMe <sub>3</sub> ) <sub>2</sub> with LiOCMe(CF <sub>3</sub> ) <sub>2</sub> and of Mo(NAr)(CHCMe <sub>2</sub> Ph)(OCMe(CF <sub>3</sub> ) <sub>2</sub> ) <sub>2</sub> with LiOCMe <sub>3</sub>	106
3.2.4	The reaction of Mo(NAr)(CHCMe <sub>2</sub> Ph)(OCMe <sub>3</sub> ) <sub>2</sub> with (CF <sub>3</sub> ) <sub>2</sub> MeCOH and of Mo(NAr)(CHCMe <sub>2</sub> Ph)(OCMe(CF <sub>3</sub> ) <sub>2</sub> ) <sub>2</sub> with Me <sub>3</sub> COH	107
3.3	The use of a mixed alkoxide molybdenum neophylidene complex as an initiator for the R.O.M.P. of 2,3-bis(trifluoromethyl)bicyclo[2.2.1]hepta-2,5-diene	109
3.3.1	The addition of 2,3-bis(trifluoromethyl)bicyclo[2.2.1]hepta-2,5-diene to a 1:1 mixture of <b>I<sub>A</sub></b> and <b>I<sub>B</sub></b> in benzene-D <sub>6</sub>	109
3.3.2	The large scale polymerization of 2,3-bis(trifluoromethyl)bicyclo[2.2.1]hepta-2,5-diene using the 1:1 mixture of <b>I<sub>A</sub></b> and <b>I<sub>B</sub></b>	111

3.3.3	Polymer structural control via changes in the composition of the mixed initiator equilibrium	111
3.3.4	The use of the mixed initiator system to R.O.M.P. 2,3-bis(trifluoromethyl)bicyclo[2.2.1]hepta-2,5-diene in $\alpha,\alpha,\alpha$ -trifluorotoluene	114
3.4	The microstructure of poly(1,4-(2,3-bis(trifluoromethyl)cyclopentenylene) vinylene)	117
3.4.1	Microstructural assignment via $^{13}\text{C}$ spectroscopy - the C7 methylene region	117
3.4.2	Further microstructural information from other resonances in the $^{13}\text{C}$ N.M.R. spectrum	121
3.4.3	Microstructural assignment via $^{19}\text{F}$ N.M.R. spectroscopy	126
3.5	Summary	129
3.6	References	130

**Chapter Four - Studies into Tacticity Control in the Living R.O.M.P. of 2,3-bis(trifluoromethyl)bicyclo[2.2.1]hepta-2,5-diene**

4.1	Introduction	132
4.2	Five-coordinate chiral base adducts of $\text{Mo}(\text{NAr})(\text{CHR})(\text{OR}')_2$	133
4.2.1	The reaction between $\text{Mo}(\text{NAr})(\text{CHR})(\text{OR}')_2$ and (S)-(-)- $\alpha$ -methyl benzylamine	134
4.2.2	The polymerization of 2,3-bis(trifluoromethyl)bicyclo[2.2.1]hepta-2,5-diene in the presence of (S)-(-)- $\alpha$ -methylbenzylamine	135
4.2.3	Polymerization of 2,3-bis(trifluoromethyl)bicyclo[2.2.1]hepta-2,5-diene by $\text{Mo}(\text{NAr})(\text{CHR})(\text{OR}')_2$ in the presence of (+)-camphor	137
4.2.4	The reaction between $\text{Mo}(\text{NAr})(\text{CHCMe}_2\text{Ph})(\text{OR})_2$ and (+)-camphor in benzene- $\text{d}_6$	139
4.3	Chiral ancillary ligands	144
4.3.1	The $^1\text{H}$ N.M.R. reaction of $\text{Mo}(\text{NAr})(\text{CHCMe}_2\text{Ph})(\text{OCMe}_3)_2$ with	144

	1-adamantanol, (S)-endo-borneol, and (-)-menthol in C <sub>6</sub> D <sub>6</sub>	
4.3.2	Synthesis of Mo(NAr)(CHCMe <sub>2</sub> Ph)(OR) <sub>2</sub> {ROH = adamantanol, (S)-endo-borneol, and (-)-menthol}	145
4.3.3	The polymerization of 2,3-bis(trifluoromethyl)bicyclo[2.2.1]hepta-2,5-diene initiated by Mo(NAr)(CHCMe <sub>2</sub> Ph){(S)-endo-borneoxide}	147
4.4	The synthesis of bidentate alkoxide analogues of the molybdenum R.O.M.P. initiators	152
4.4.1	Studies employing 3,5-di-tert-butyl-catechol	152
4.4.2	Studies on 1,1'-bi-2-naphthol as a chelating ligand to the Mo(NAr)(CHCMe <sub>2</sub> Ph) fragment	154
4.5	Conclusions	160
4.6	References	161
<b>Chapter Five - The Synthesis of Fluorinated Homopolymers and Block Copolymers via Living R.O.M.P.</b>		<b>163</b>
5.1	Introduction	164
5.2	The synthesis of fluorinated homopolymers via living R.O.M.P.	165
5.2.1	The living R.O.M.P. of fluorinated monomers <b>II</b> , <b>III</b> , and <b>IV</b> with Mo(NAr)(CHCMe <sub>2</sub> Ph)(OCMe <sub>3</sub> ) <sub>2</sub>	165
5.2.2	Scaled up homopolymerizations of <b>II</b> , <b>III</b> , and <b>IV</b>	170
5.2.3	<sup>13</sup> C N.M.R. spectroscopic analysis of poly <b>II</b>	170
5.2.4	<sup>13</sup> C N.M.R. spectroscopic analysis of poly <b>III</b>	184
5.2.5	<sup>1</sup> H and <sup>13</sup> C N.M.R. spectroscopic analysis of poly <b>IV</b>	190
5.2.6	Gel permeation chromatographic analysis of the fluoropolymers	195
5.3	The synthesis of fluorinated block copolymers:- a model for PVDF	199
5.3.1	<sup>1</sup> H N.M.R. study of living fluorinated block copolymers	200
5.3.2	Scaled-up syntheses of the fluorinated block copolymers	203
5.4	Structural characterisation of the fluorinated block copolymers	204
5.4.1	<sup>13</sup> C N.M.R. spectroscopic analysis of the block copolymers	204

5.4.2	$^{13}\text{C}$ N.M.R. analysis of the copolymer of <b>I</b> and <b>III</b>	204
5.4.3	$^{13}\text{C}$ and $^{19}\text{F}$ N.M.R. analysis of block copolymers <b>I - II</b> , <b>IV - I</b> and <b>IV - III</b>	208
5.4.4	Differential scanning calorimetric analysis	211
5.4.5	Dielectric measurements	214
5.4.6	Gel permeation chromatographic analysis	215
5.5	Summary	220
5.6	References	221
 <b>Chapter Six - Experimental Details</b>		 222
6.1	General	223
6.1.1	Experimental techniques	223
6.1.2	Solvents and Reagents	224
6.2	Experimental details to chapter two	226
6.2.1	Investigations into the effect of reaction conditions upon the trans content of poly[1,4-(2,3-bis(trifluoromethyl)cyclopentenylene) vinylene]	226
6.2.2	The reaction between 2,3-bis(trifluoromethyl)bicyclo[2.2.1]hepta- 2,5-diene with $\text{Mo}(\text{NAr})(\text{CHCMe}_2\text{Ph})(\text{OCMe}(\text{CF}_3)_2)_2$ in $\text{C}_6\text{D}_6$	227
6.2.3	The scaled up reaction between 2,3-bis(trifluoromethyl)bicyclo [2.2.1]hepta-2,5-diene and $\text{Mo}(\text{NAr})(\text{CHCMe}_2\text{Ph})(\text{OCMe}(\text{CF}_3)_2)_2$ in $\alpha,\alpha,\alpha$ -trifluorotoluene	228
6.2.4	Determination of $k_p / k_i$ for the R.O.M.P. of 2,3-bis(trifluoromethyl) bicyclo[2.2.1]hepta-2,5-diene initiated by $\text{Mo}(\text{NAr})(\text{CHR})(\text{OCMe}(\text{CF}_3)_2)_2$ { $\text{R} = \text{CMe}_3, \text{CMe}_2\text{Ph}$ }	229
6.2.5	Determination of $k_p$ for the R.O.M.P. of 2,3-bis(trifluoromethyl) bicyclo[2.2.1]hepta-2,5-diene initiated by $\text{Mo}(\text{NAr})(\text{CHR})(\text{OCMe}(\text{CF}_3)_2)_2$ { $\text{R} = \text{CMe}_3, \text{CMe}_2\text{Ph}$ }	230

6.2.6	The reaction between 2,3-bis(trifluoromethyl)bicyclo[2.2.1]hepta-2,5-diene and $\text{Mo}(\text{NAr})(\text{CHCMe}_3)(\text{OCMe}_2\text{CF}_3)_2$ in $\text{C}_6\text{D}_6$	230
6.2.7	The scaled-up reaction between 2,3-bis(trifluoromethyl)bicyclo[2.2.1]hepta-2,5-diene and $\text{Mo}(\text{NAr})(\text{CHCMe}_3)(\text{OCMe}_2\text{CF}_3)_2$ in $\alpha,\alpha,\alpha$ -trifluorotoluene	231
6.3	Experimental details to chapter three	233
6.3.1	Reaction of $\text{Mo}(\text{NAr})(\text{CHCMe}_2\text{Ph})(\text{OCMe}(\text{CF}_3)_2)_2$ with one equivalent of $\text{Mo}(\text{NAr})(\text{CHCMe}_2\text{Ph})(\text{OCMe}_3)_2$	233
6.3.2	Reaction of $\text{Mo}(\text{NAr})(\text{CHCMe}_2\text{Ph})(\text{OCMe}_3)_2$ with 2 equivalents of $\text{LiOCMe}(\text{CF}_3)_2$	233
6.3.3	Reaction of $\text{Mo}(\text{NAr})(\text{CHCMe}_2\text{Ph})(\text{OCMe}(\text{CF}_3)_2)_2$ with 2 equivalents of $\text{LiOCMe}_3$	233
6.3.4	Reaction of $\text{Mo}(\text{NAr})(\text{CHCMe}_2\text{Ph})(\text{OCMe}_3)_2$ with 2 equivalents of $(\text{CF}_3)_2\text{MeCOH}$	234
6.3.5	Reaction of $\text{Mo}(\text{NAr})(\text{CHCMe}_2\text{Ph})(\text{OCMe}(\text{CF}_3)_2)_2$ with 2 equivalents of $\text{Me}_3\text{COH}$	234
6.3.6	The addition of 2,3-bis(trifluoromethyl)bicyclo[2.2.1]hepta-2,5-diene to a 1:1 mixture of $\text{Mo}(\text{NAr})(\text{CHCMe}_2\text{Ph})(\text{OCMe}(\text{CF}_3)_2)_2$ and $\text{Mo}(\text{NAr})(\text{CHCMe}_2\text{Ph})(\text{OCMe}_3)_2$ in $\text{C}_6\text{D}_6$	234
6.3.7	The large scale polymerisation of 2,3-bis(trifluoromethyl)bicyclo[2.2.1]hepta-2,5-diene with a 1:1 mixture of $\text{Mo}(\text{NAr})(\text{CHCMe}_2\text{Ph})(\text{OCMe}(\text{CF}_3)_2)_2$ and $\text{Mo}(\text{NAr})(\text{CHCMe}_2\text{Ph})(\text{OCMe}_3)_2$	235
6.4	Experimental details to chapter four	
6.4.1	The reaction of $\text{Mo}(\text{NAr})(\text{CHR})(\text{OR}')_2$ with (S)-(-)- $\alpha$ -methylbenzyl amine	236
6.4.2	The R.O.M.P. of 2,3-bis(trifluoromethyl)bicyclo[2.2.1]hepta-2,5-diene by $\text{Mo}(\text{NAr})(\text{CHR})(\text{OR}')_2$ in the presence of (S)-(-)- $\alpha$ -methylbenzylamine	236
6.4.3	The R.O.M.P. of 2,3-bis(trifluoromethyl)bicyclo[2.2.1]hepta-2,5-diene by $\text{Mo}(\text{NAr})(\text{CHR})(\text{OR}')_2$ in the presence of (+)-camphor	237

6.4.4	The reaction of Mo(NAr)(CHR)(OR') <sub>2</sub> with (+)-camphor in C <sub>6</sub> D <sub>6</sub>	238
6.4.5	The reaction between Mo(NAr)(CHCMe <sub>2</sub> Ph)(OCMe <sub>3</sub> ) <sub>2</sub> and 2 equivalents of ROH in C <sub>6</sub> D <sub>6</sub>	238
6.4.6	The synthesis of Mo(NAr)(CHCMe <sub>2</sub> Ph){(S)-endo-borneoxide} <sub>2</sub>	239
6.4.7	The synthesis of Mo(NAr)(CHCMe <sub>2</sub> Ph){(-)-mentholate} <sub>2</sub>	241
6.4.8	The attempted synthesis of Mo(NAr)(CHCMe <sub>2</sub> Ph)(3,5-di-t-butyl catecholate)	243
6.4.9	The synthesis of Mo(NAr)(CHCMe <sub>2</sub> Ph)(η <sup>2</sup> -binaphtholate)	243
6.5	Experimental details to chapter five	245
6.5.1	The reaction between Mo(NAr)(CHR)(OR') <sub>2</sub> and 10 equivalents of the fluorinated monomers <b>II</b> , <b>III</b> , and <b>IV</b>	245
6.5.2	Scaled-up homopolymerizations of monomers <b>II</b> , <b>III</b> , and <b>IV</b> initiated by Mo(NAr)(CHR)(OR') <sub>2</sub>	246
6.5.3	Characterising data on the high trans ring-opened polymer of 2-trifluoromethylbicyclo[2.2.1]hepta-2,5-diene	247
6.5.4	Characterising data on the high trans ring-opened polymer of endo/exo-5-trifluoromethylbicyclo[2.2.1]hept-2-ene	247
6.5.5	Characterising data on the high trans ring-opened polymer of 5,5,6-trifluoro-6-trifluoromethylbicyclo[2.2.1]hept-2-ene	248
6.5.6	Block copolymer syntheses	249
6.5.7	Characterisation data on block copolymer <b>I - III</b>	250
6.5.8	Characterisation data on block copolymer <b>I - II</b>	251
6.5.9	Characterisation data on block copolymer <b>IV - I</b>	251
6.5.10	Characterisation data on block copolymer <b>IV - III</b>	252
6.6	References	253
<b>Appendices</b>		254
Appendix I	The relationship between dielectric constants and polymer microstructure	255
Appendix II	Kinetic derivation for the calculation of k <sub>p</sub> /k <sub>i</sub>	258

Appendix III First year Induction Courses : October 1989	261
Appendix IV Colloquia, lectures and seminars given by invited speakers	262
Appendix V Conferences attended	270
Appendix VI Publications	271

## **Chapter One**

### **A Short Overview of Ring-Opening Metathesis Polymerization and the Importance of Fluorinated Polymers**

## 1.1 Introduction

This thesis describes research aimed towards the development of piezoelectric fluoropolymers synthesised by the living ring-opening metathesis polymerization (R.O.M.P.) of appropriately substituted bicyclo[2.2.1]-hept-2-enes and -hepta-2,5-dienes.

Highly piezoelectric polymers, such as poly(vinylidene fluoride), possess correspondingly high dielectric constants, arising from substantial alignment of dipolar moments. At an early stage therefore, stereoregularity in the fluorinated ring-opened polymers to be synthesised was identified as highly desirable.

It has previously been reported that  $\text{Mo}(\text{NAr})(\text{CHCMe}_3)(\text{OCMe}_3)_2$  initiates the living R.O.M.P. of 2,3-bis(trifluoromethyl)bicyclo[2.2.1]hepta-2,5-diene to yield a 98% trans, possibly tactic polymer. Chapter two of this thesis reports attempts to increase the trans content of this polymer and the effect that such changes have upon its electrical properties. During this study the synthesis of 98% cis poly[1,4-(2,3-bis(trifluoromethyl)cyclopentenylene) vinylene] was discovered, initiated via  $\text{Mo}(\text{NAr})(\text{CHCMe}_3)(\text{OCMe}(\text{CF}_3)_2)_2$ . The conformations of both polymers have also been analysed in the light of dielectric measurements.

Structure-property correlation studies are of crucial importance to the understanding of how the physical properties of a polymer, such as piezoelectricity, can be controlled via subtle variations in its microstructural architecture. In order to undertake such a study two requirements prevail; there must exist a method for synthesising a wide range of stereoisomers of the polymer, and a full microstructure determination must be supplied for each sample prepared.

The exploitation of the living R.O.M.P. of 2,3-bis(trifluoromethyl)bicyclo[2.2.1]hepta-2,5-diene to synthesise such a range of samples using an equilibrium mixture of initiators is described in chapter three. Further, a full microstructure assignment is then made on the evidence of  $^{13}\text{C}$  N.M.R. spectroscopic data and dielectric measurements.

Among the conclusions drawn from the dielectric measurements carried out as part of the work described in chapters two and three possibly the most important is the key role that chain tacticity has in controlling physical properties. Chapter four therefore relates endeavours to alter the tacticity of poly[1,4-(2,3-bis(trifluoromethyl)cyclopentenylene) vinylene] via several methods, but especially by changing the identity of the ancillary alkoxide ligands at the metal centre of the initiator.

Chapter five recounts the synthesis of three other ring-opened fluoropolymers, and several fluorinated block copolymers, again via four-coordinate Schrock metathesis initiators. In the context of material science block copolymers offer potentially unique possibilities not attainable with other polymeric materials.

Experimental details for all the above chapters and full characterising data for all novel compounds prepared are then presented in chapter six.

The remainder of this chapter provides an overview of areas relevant to this thesis. Pertinent features of R.O.M.P. are discussed with particular emphasis upon the recent developments in well-defined initiators and living R.O.M.P.; this is followed by a brief review of the properties and commercial importance of fluoropolymers.

## 1.2 Olefin metathesis

The term 'metathesis' is widely used in chemistry to describe reactions in which two small units of a molecule are interchanged between pairs of such molecules (figure 1.1). Olefin metathesis<sup>1</sup> therefore involves the exchange of alkylidene fragments between two molecules of an olefin, as shown in figure 1.2.

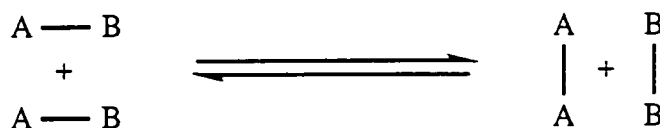


Fig 1.1: Schematic interpretation of a metathesis reaction

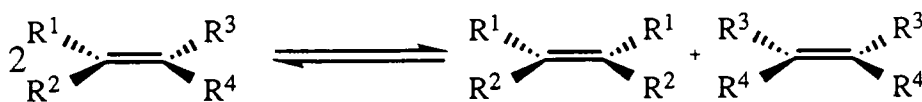
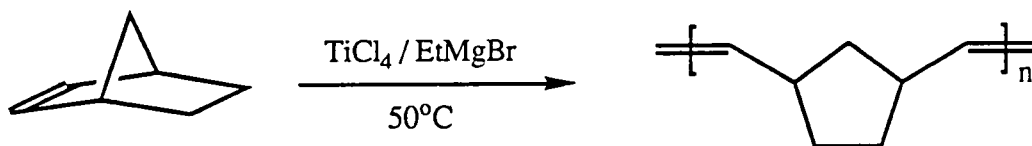


Figure 1.2: The olefin metathesis reaction

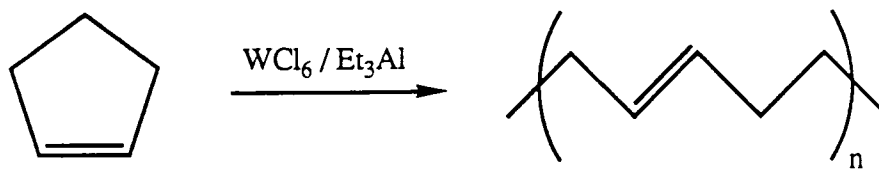
The first example of olefin metathesis (albeit only recognised as such some years later) was the ring-opening polymerization of bicyclo[2.2.1]hept-2-ene ('norbornene'), reported in a Du Pont patent in 1955<sup>2</sup>, equation 1.



Equation 1

In 1964 Natta discovered that WCl<sub>6</sub> / Et<sub>3</sub>Al initiates the ring-opening polymerization of cyclopentene to give highly trans polypentenamer (equation 2), whereas when the

initiator was a mixture of  $\text{MoCl}_5$  and  $\text{Et}_3\text{Al}$  a polymer with high cis content resulted<sup>3</sup>. Further, the cis/trans ratio in the polymer could be altered by variations in the catalyst, the cocatalyst, the stoichiometry of the catalyst : co-catalyst ratio, and the polymerization temperature.



Equation 2

Calderon is widely credited with introducing the expression 'olefin metathesis'<sup>4</sup>, as well as realising that the ring-opening metathesis polymerization (R.O.M.P.) of cycloalkenes and the disproportionation (alkylidene exchange) of acyclic olefins are examples of the same reaction type.

### 1.2.1 The mechanism for olefin metathesis and ring-opening metathesis polymerization

In 1970 Chauvin and Herisson proposed the now generally accepted mechanism behind olefin metathesis<sup>5</sup>. Featuring the reversible [2+2] cycloaddition of the olefinic carbon-carbon double bond to a metal carbene species, it proceeds via a metallacyclobutane intermediate as shown in figure 1.3. This then ring-opens to either regenerate the original reaction mixture or to lead to a new olefin (and a new metal carbene). R.O.M.P. transpires via the same metal-carbene initiated mechanism; however, since the carbon-carbon double bond is enclosed within a ring, productive metathesis results in an unsaturated polymer chain, figure 1.4.

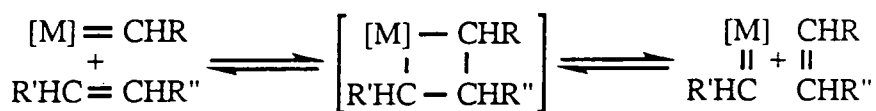


Figure 1.3: The Herisson and Chauvin olefin metathesis mechanism

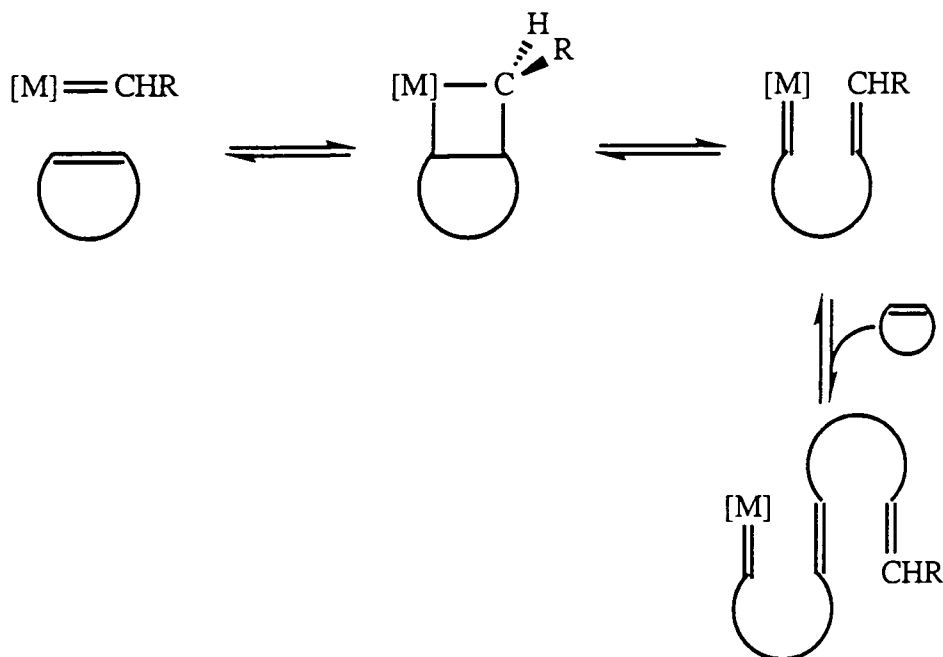


Figure 1.4: General reaction mechanism for the ring-opening metathesis of cycloolefins

A considerable amount of research has been undertaken into the metathesis polymerization of highly strained bicyclic olefin systems such as norbornene (bicyclo[2.2.1]hept-2-ene); such monomers typically undergo R.O.M.P. more favourably than their monocyclic counterparts, an observation usually explained as the thermodynamic consequence of ring-strain relief<sup>6</sup> (although this argument has been challenged<sup>7</sup>). Indeed, a form of poly(norbornene) containing approximately 90% trans double bonds is sold commercially by Chimie CdF under the tradename Norsorex.

In the past twenty years there have also been many reports on the R.O.M.P. of functionalized bicyclo[2.2.1]hept-2-enes. For example, 5-substituted norbornenes have

been R.O.M.P.ed for all the following substituents; Me<sup>8-11</sup>, i-Pr<sup>12</sup>, C<sub>n</sub>H<sub>2n+1</sub> (n = 8 - 12)<sup>13</sup>, CH<sub>2</sub>CH<sub>2</sub>CH=CH<sub>2</sub><sup>14</sup>, CH<sub>2</sub>OH<sup>15,16</sup>, COOH<sup>15,16</sup>, COCH<sub>3</sub><sup>17</sup>, CONH<sub>2</sub><sup>18,19</sup>, CN<sup>15,20</sup>, 3-C<sub>5</sub>H<sub>4</sub>N<sup>20</sup>, Cl<sup>19,21</sup>, Br<sup>19</sup>, and SiCl<sub>3</sub><sup>22</sup>. The reader is referred to reference 6 for further details of the polymers of these and other 5-substituted norbornenes, as well as 5,5- and 5,6- difunctionalized bicyclo[2.2.1]hept-2-enes.

### 1.2.2 Thermodynamic considerations

Acyclic olefin metathesis can be considered as a thermoneutral process; as a result a statistical mixture of all the olefin products is expected to eventually form<sup>1</sup>. It should therefore be possible to predict the eventual equilibrium position given the relevant thermodynamic data. However, the situation is complicated, in all but the most simple examples, by the presence of a series of competing equilibria (which can give rise to a degree of stereoselectivity in the product distribution).

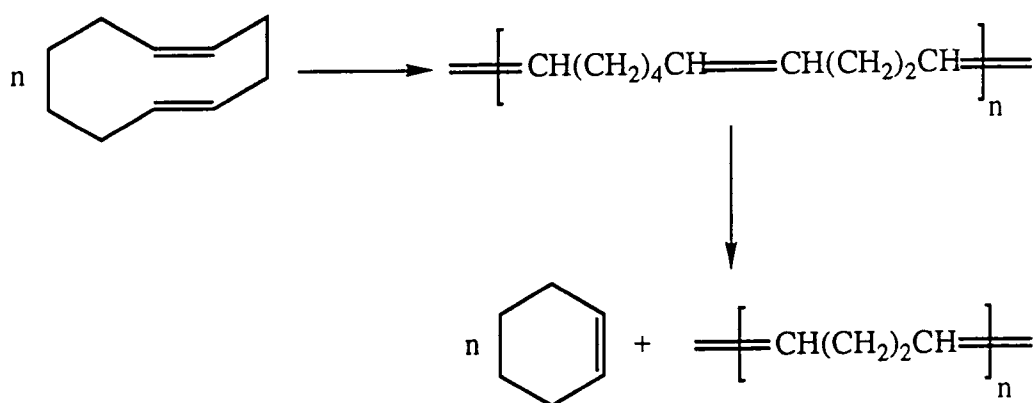
An interesting exploitation of the equilibrium situation is the removal of ethylene from the product mixture arising from the metathesis of a terminal olefin. This forces the equilibrium position over towards production of more ethylene (which is also removed) and the desired dimerised non-methylidene fragment<sup>23</sup>; e.g. the conversion of styrene (PhCH=CH<sub>2</sub>) into stilbene (PhCH=CHPh).

The thermodynamic picture for the R.O.M.P. of cyclic olefins is rather less complex<sup>6,24</sup>. It is well-documented that for 3 and 4-membered rings and for rings with 8 or more atoms, ring-opening polymerization is favoured, and will proceed if a suitable mechanism is available.

However, in the case of 5-, 6-, and 7-membered rings the thermodynamic parameters are often finely balanced<sup>25</sup>. For such examples the sign of  $\Delta G$  may depend upon both subtle variations in physical conditions (monomer concentration, temperature, pressure) and chemical factors (e.g. the position and the size of ring-substituents).

Attempts to correlate monomer structure with polymerizability have drawn two main conclusions. The first of these is that although cyclopentene and cycloheptene can be polymerized, cyclohexene is much more resistant towards R.O.M.P., as a result of its low strain energy (i.e.  $\Delta H$  is too small to offset the positive value of  $-T\Delta S$ ).

Consequences of the non-polymerizable nature of cyclohexene are often encountered in R.O.M.P.. For example, attempts to polymerize cis,trans - cyclodeca-1,5-diene using  $WCl_6 / Et_2AlCl$  only succeed in producing polybutenamer, equation 3, due to the elimination of cyclohexene from the propagating chain<sup>26</sup>.



Equation 3

Secondly, substituted rings are generally less likely to undergo ring-opening polymerization than unsubstituted cycloalkenes. For example, 1-methylcyclopentene will generally not undergo R.O.M.P.<sup>27</sup>, but 3-methylcyclopentene will<sup>28</sup>; the more bulky 3-isopropylcyclopentene will not<sup>28</sup>. In general, substituents upon the double bond to be opened hinder attack on the propagating carbene, whilst bulky substituents located elsewhere on the ring tend to give rise to unfavourable steric interactions in the open polymer chain.

### 1.3 Metathesis initiators

There are three distinct classes of transition metal initiators for olefin metathesis and ring-opening metathesis polymerization. The first and historically most important are ill-defined dual component systems, known as 'classical initiators'. These are usually transition-metal chlorides or complexes thereof, mixed with Lewis acid co-catalysts and occasionally an oxygen-containing promoter (e.g. ethanol). The initiating mixtures can be homogeneous or heterogeneous, although distinguishing between the two is not always straightforward.

The other two categories encompass well-defined species, namely transition metal carbenes (including both Fischer-type carbene complexes, and more recently Schrock alkylidenes of the early transition metals), and metallacyclobutanes, first predicted by Chauvin when he proposed his original mechanism for metathesis.

#### 1.3.1 Classical initiator systems

Until recently most R.O.M.P. initiators were based upon transition metal halides in the presence of a Lewis acid co-catalyst. These so-called 'classical initiators' are often commercially available and relatively inexpensive. The following halides and halide complexes have all been used as R.O.M.P. catalysts:  $\text{TiCl}_4$ ,  $\text{ZrCl}_4$ ,  $\text{VCl}_4$ ,  $\text{VOCl}_3$ ,  $\text{NbCl}_5$ ,  $\text{TaCl}_5$ ,  $\text{MoCl}_5$ ,  $\text{Mo}(\text{NO})_2(\text{PPh}_3)_2\text{Cl}_2$ ,  $\text{WF}_6$ ,  $\text{WCl}_6$ ,  $\text{WOCl}_4$ ,  $\text{W}(\text{OR})_2\text{Cl}_4$ ,  $\text{ReCl}_5$ ,  $\text{RuCl}_3 \cdot 3\text{H}_2\text{O}$ ,  $\text{OsCl}_3$ , and  $\text{IrCl}_3 \cdot 3\text{H}_2\text{O}$ . Not all of these require co-catalysts in order to initiate R.O.M.P. (e.g.  $\text{ReCl}_5$  will polymerize 1-methylnorbornene to give an all cis, all head-tail, syndiotactic polymer, an alternating copolymer of two enantiomers<sup>29</sup>).

However, such classical systems suffer from many disadvantages. Of primary significance, such initiating systems are ill-defined; in other words the precise nature of the active site at the metal centre is not known.

In addition, the metal carbene must first be generated before initiation and subsequent propagation can commence<sup>30-32</sup>, (the major role of the Lewis acid is to aid the formation of the active site). This process usually proceeds in very low yield and the activity of a given initiating system is dependent upon its chemical, thermal, and mechanical history, and upon the order and the rate of mixing of the catalyst, the co-catalyst, and the monomer. The reader is warned that this sometimes gives rise to an element of irreproducibility, a point worth considering when referring to the literature on such systems.

### 1.3.2 Transition metal carbene complexes

In 1964 Fischer reported the synthesis of the first heteroatom-stabilised metal carbene  $[(CO)_5W=C(OMe)Me]$ <sup>33,34</sup>. Although this complex displays a disappointingly low activity as an olefin metathesis catalyst, it does effect the R.O.M.P. of highly strained cycloalkenes, such as cyclobutene and bicyclo[2.2.1]hept-2-ene<sup>35</sup>. More importantly, its isolation heralded a new era in organotransition metal chemistry; that of metal-carbon multiple bonds<sup>36</sup>.

The chemistry of Fischer carbene complexes is influenced largely by the heteroatom substituent, particularly if the heteroatom possesses an accessible  $\pi$ -symmetry orbital<sup>37,38</sup>. This allows for the conjugation of the heteroatom lone pair with the metal-ligand  $\pi$ -orbitals, leading to a significant reduction in the metal-carbon bond-order, as shown in figure 1.5.



Figure 1.5: Canonical forms of a Fischer-carbene

Such carbene complexes display a pronounced tendency to behave as carbon electrophiles<sup>37</sup>. It is evident that such electrophilic properties are shared by other non-heteroatom stabilised carbenes such as that shown below (figure 1.6)<sup>39</sup>. Examples of such species are typically complexes of a low-valent metal centre.

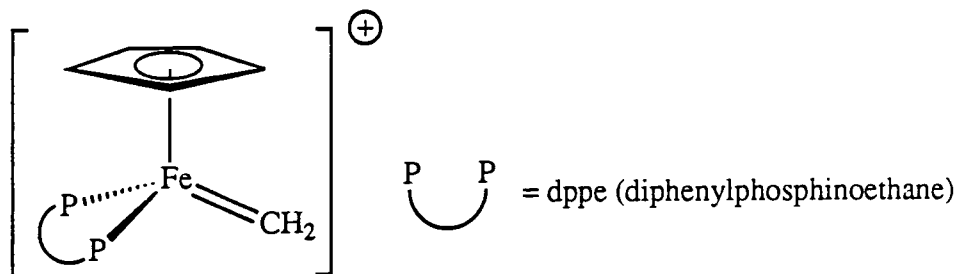


Figure 1.6: An atypical Fischer-carbene containing no heteroatom carbene substituent

In the years that followed a second class of transition metal complexes containing metal-carbon double bonds was discovered. The so-called 'Schrock' alkylidenes are high-valent nucleophilic species bearing no heteroatom substituent upon the carbene carbon atom<sup>40</sup>. The first example to be reported was  $[\text{Ta}(\text{CHCMe}_3)(\text{CH}_2\text{CMe}_3)_3]$ , which was prepared from the addition of two equivalents of neopentyl magnesium chloride to  $\text{Ta}(\text{CH}_2\text{CMe}_3)_3\text{Cl}_2$ <sup>41</sup>.

To date high-valent alkylidene complexes have also been reported for titanium<sup>42,44</sup>, zirconium<sup>43,44</sup>, niobium<sup>45</sup>, molybdenum<sup>46</sup>, tungsten<sup>47-49</sup> and rhenium<sup>50</sup>, and their syntheses have recently been the subject of an excellent review<sup>51</sup>.

Metal-alkylidene complexes have rapidly become established as the initiators of choice for R.O.M.P.. Although their synthesis generally requires competence in organometallic techniques, they are preferable over the more widely-available dual component classical systems for several reasons. Most importantly the identity of the active site on the initiator is known and can be studied during the course of initiation and propagation by several methods. Furthermore, the polymerizations are usually 'living'; i.e.

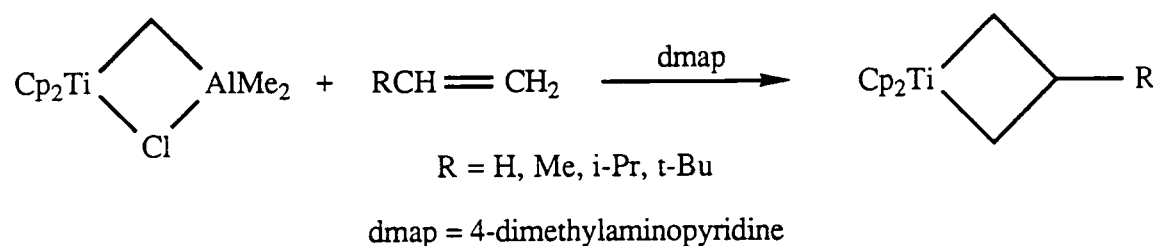
the propagating chain is continuously bonded to the metal centre, until the addition of a suitable 'capping' reagent (which cleaves the metal from the polymer chain in a controllable termination step).

### 1.3.3 Metallocyclobutane catalysts

Chauvin's [2+2] cycloaddition mechanism for olefin metathesis was proposed prior to the observation of any metallacyclobutane complexes. In fact, metallacyclobutanes were long believed to be transient non-isolable species.

However, it is now known that metallacyclobutanes and metal carbenes are energetically very similar<sup>52</sup>, and as Osborn and co-workers have shown, may occasionally be observed simultaneously during a metathesis reaction<sup>53</sup>. In some cases the metallocycle form may even be the catalyst resting state.

The first metallacycle metathesis initiators to be isolated were prepared by Grubbs from the reaction of Tebbe's titanocene methylenide reagent with various olefins in the presence of nitrogen containing bases (equation 4)<sup>54,55</sup>.



Equation 4

## 1.4 A comparison of the structure and bonding in metal alkylidenes and metal carbenes

Metal-ligand multiple bonds (most commonly encountered with oxo, imido, alkylidene, or alkylidyne ligands) consist of one  $\sigma$  bond and one or two  $\pi$  bonds<sup>36</sup>. The  $\pi$  interactions result from the overlap of metal d-orbitals with ligand p-orbitals of suitable symmetry orthogonal to the  $\sigma$  bond. However metal-alkylidenes are fundamentally different from metal-oxo, metal-imido, and metal-alkylidyne fragments, primarily because the alkylidene ligand is a single-faced  $\pi$ -donor; i.e. at most it can only form a double bond (one  $\sigma$  bond and one  $\pi$  bond).

Heteroatom-stabilised carbenes differ from metal-alkylidenes in several respects. Both Goddard<sup>52,56,57</sup> and Hall<sup>37</sup> have suggested that the  $M=CR_2$  bond can act either as a covalent bond (as in ethylene) or as a donor-acceptor bond.

The former case is described as the interaction of a triplet metal centre with a triplet carbene fragment, schematically shown in the top half of figure 1.7. This picture closely mirrors that found in the so-called 'Schrock' alkylidenes; indeed, free carbenes with only hydrogen and alkyl substituents ( $CH_2$ ,  $CHR$ , and  $CR_2$ ) have been observed to favour triplet ground states<sup>58,59</sup>.

In the case of Fischer carbenes the carbene fragment exists in a singlet state (figure 1.7). The metal-ligand bonding consists of the donation of the singlet carbene lone pair into a vacant metal d-orbital, and backbonding from a filled metal d-orbital into the vacant p-orbital. This is essentially the same as the well-known Dewar-Chat-Duncanson model for an olefin binding to a metal centre<sup>60,61</sup>, in which metal electron density is off-loaded into the olefin  $\pi^*$  LUMO. This type of donor-acceptor bonding is favoured by metal fragments with filled d-orbitals, i.e. low-valent, late transition metals. These contrast with high valent, early transition metal species which have few d electrons and hence are more suited to bond with triplet carbene fragments.

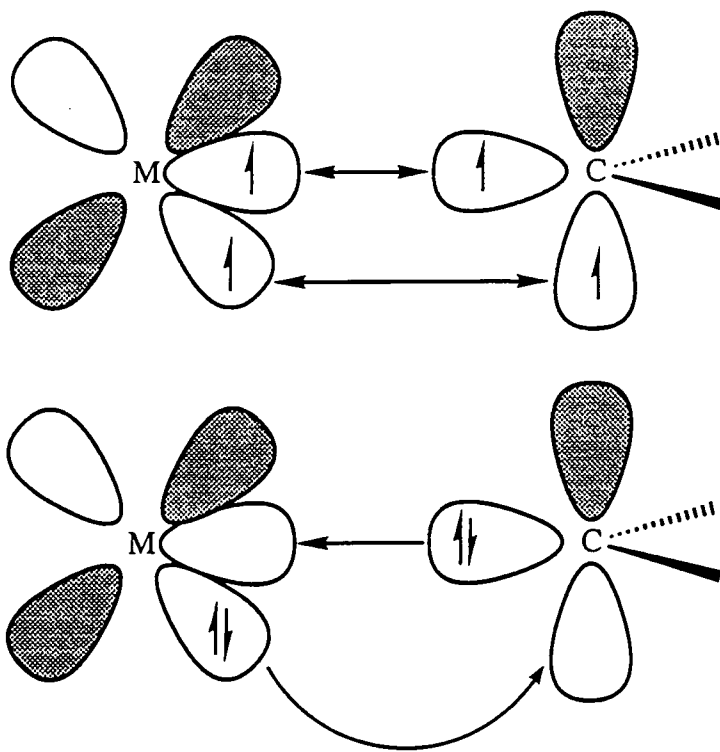


Figure 1.7: Schematic bonding picture for Schrock alkylidenes (top) and Fischer carbenes (bottom)

This simple summary can be used to explain several features of alkylidene and carbene chemistry. For example, complexes of singlet carbenes are electrophilic because they possess an empty orbital located on the carbene carbon (albeit stabilised by synergic back-bonding). On the other hand in triplet carbene complexes (i.e. Schrock alkylidenes) where there are two covalent bonds the carbon centre is nucleophilic.

## 1.5 Living R.O.M.P.

### 1.5.1 Living polymerizations

A living polymerization is a chain propagation reaction which proceeds in the absence of kinetic steps of termination or chain transfer<sup>62-64</sup>. Consequently such polymerizations provide the maximum degree of control for the synthesis of polymers with well-defined structures.

Among the features of a genuine living polymerization<sup>65</sup>, perhaps the singly most important is that the number average molecular weight,  $M_n$ , is a linear function of conversion; this implies that  $M_n$  can therefore be controlled by the stoichiometry of the reaction. Furthermore, if the rate constant of initiation,  $k_i$ , is greater than or comparable to  $k_p$ , the rate constant of propagation, then narrow molecular weight distributions are achievable (although polydispersities can approach unity even if  $k_p$  is many more times greater than  $k_i$ <sup>66</sup>). Although monodisperse polymers are often not required for applications, such materials are desirable in many areas, including adhesives, coatings, biological systems, and in Langmuir-Blodgett techniques.

A further advantage of a living polymerization is the ability to synthesize block copolymers<sup>67</sup>, simply by sequential monomer addition following the total consumption of the previous monomer fraction. Further discussion is deferred until chapter five which describes the synthesis of several fluorinated block copolymers via living R.O.M.P..

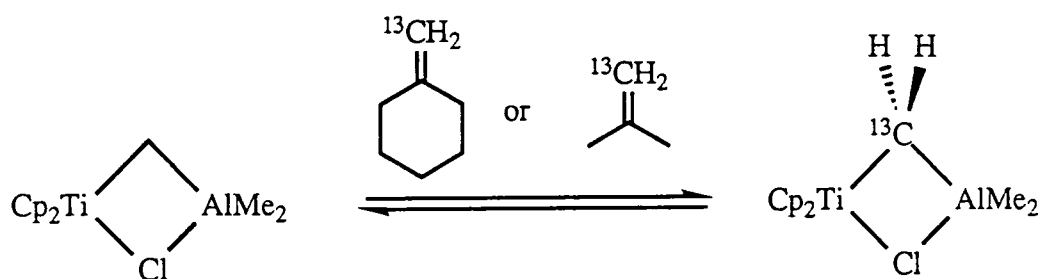
### 1.5.2 Well-defined initiators for the living R.O.M.P. of cycloalkenes

As mentioned previously, one of the major advantages of certain well-defined R.O.M.P. initiators over their classical counterparts is that they catalyse living polymerizations. The following sections discuss the reactions of two classes of such initiators, titanacyclobutanes and four-coordinate imido-alkylidene complexes of tungsten

and molybdenum. Finally a brief account is given of aqueous R.O.M.P. initiators developed by Grubbs and co-workers.

### 1.5.3 Titanacyclobutanes

The first example of a well-defined carbene complex in which olefin incorporation could be observed via N.M.R. was reported in 1979 by Tebbe et al<sup>68</sup>. By adding <sup>13</sup>C labelled 1,1-disubstituted olefins to a titanacyclobutane it is possible to observe the slow incorporation of <sup>13</sup>C atoms into the metallacyclobutane as the labelled methylenide unit exchanges into the bridging site of the complex (equation 5).



Equation 5

The first well-documented example of the living R.O.M.P. of a cycloalkene was the polymerization of norbornene with related titanacyclobutane complexes<sup>69,70</sup>. The metallacyclobutane exists in equilibrium with its ring-opened carbene form, which R.O.M.P.s the bicyclic olefin in a living manner (figure 1.8). In order to terminate the chain propagation, the metal site can be capped by adding a ketone (typically benzophenone) or an aldehyde. This class of initiator has been exploited to produce diblock and triblock copolymers of norbornene, substituted norbornenes, and dicyclopentadiene<sup>71,72</sup>. Copolymers have also been produced by grafting living ring-opened polymers onto carbonyl-containing polymers<sup>73</sup>, and by capping the living polymer with

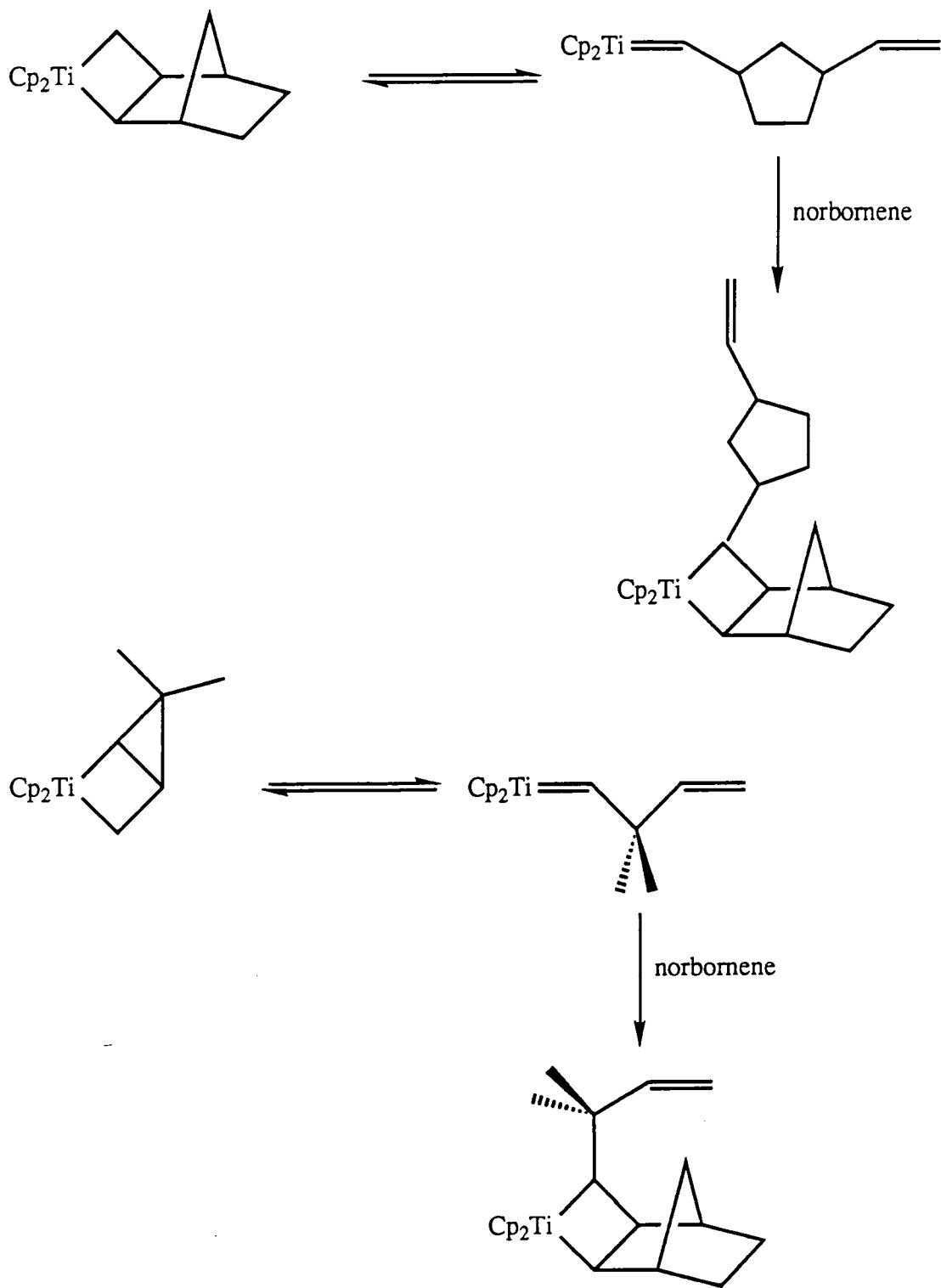


Figure 1.8: The first reported examples of the living R.O.M.P. of norbornene

terephthalaldehyde prior to an Aldol condensation polymerization of silyl vinyl ethers<sup>74,75</sup>. It is even possible to synthesize 'star' polymers by generating di- or tetrafunctional initiators<sup>76</sup>.

However, there are two drawbacks associated with this initiator system. Firstly titanacyclobutanes require temperatures of 50°C in order to ring-open. Also these titanium complexes are notoriously reactive towards functionalities due to the highly electrophilic nature of the metal centre. Therefore the range of suitable monomers is limited to relatively stable hydrocarbons.

Nevertheless, Grubbs and co-workers have produced a range of interesting polymeric structures<sup>77,78</sup> one example of which is shown below (figure 1.9).

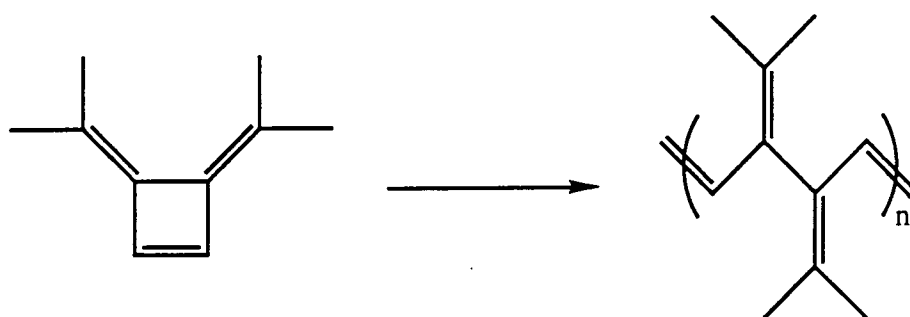


Figure 1.9: The R.O.M.P. of 3,4-di(iso-propylidene)cyclobutene using a titanacyclobutane initiator

#### 1.5.4 Four coordinate imido-alkylidene complexes of tungsten and molybdenum

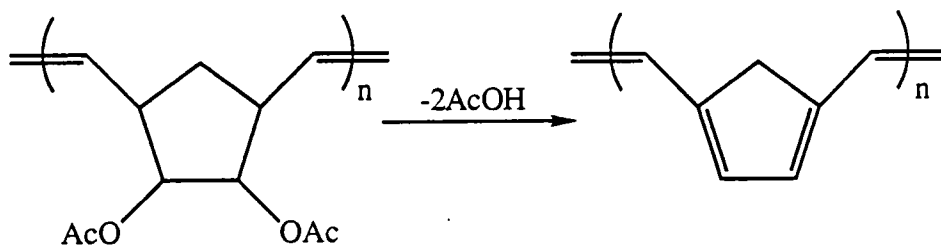
$W(NAr)(CHCMe_3)(OCMe(CF_3)_2)_2$ <sup>79,80</sup> metathesizes cis-pent-2-ene at the rate of  $10^3$  turnovers/minute in toluene at room temperature; however, under the same conditions the non-fluorinated analogue  $W(NAr)(CHCMe_3)(OCMe_3)_2$  will achieve a rate of just 2 turnovers/hour<sup>80</sup>. Since olefin metathesis can be thought of as the nucleophilic attack of the carbon-carbon double bond upon the metal centre, this marked difference in reactivity is

ascribed to the more electrophilic nature of the metal centre in the former case (due to the highly electronegative fluorinated alkoxide ligands).

Both tungsten and molybdenum complexes of the general type  $M(\text{NAr})(\text{CHR})(\text{OR}')_2$  will effect the rapid metathesis polymerization of norbornene and norbornadiene in a living manner<sup>81</sup>. The chains can be terminated with aldehydes (typically benzaldehyde or pivaldehyde) in a Wittig-type capping reaction, to yield near-monodisperse materials ( $M_n/M_w = 1.03$  for a 500-mer of poly(norbornene) initiated by  $W(\text{NAr})(\text{CHCMe}_3)(\text{OCMe}_3)_2$ )<sup>82</sup>.

The use of the tungsten initiators to R.O.M.P. functionalized norbornenes and norbornadienes is problematic for reasons that are still not clear, although it appears to be related to the enhanced electrophilicity of tungsten. Nonetheless the molybdenum-based analogues will R.O.M.P. several functionalized monomers some of which are listed in table 1.1.

One of the many reasons for investigating the R.O.M.P. of functionalized monomers is the potential for elimination of one or more relatively small molecules from the polymer to generate an unsaturated system. Just such an example is the ring-opened polymer of *exo-cis*-2,3-norbornenediacetate, which when subjected to temperatures between 250 - 300°C eliminates two equivalents of acetic acid (equation 6)<sup>83</sup>.



Equation 6

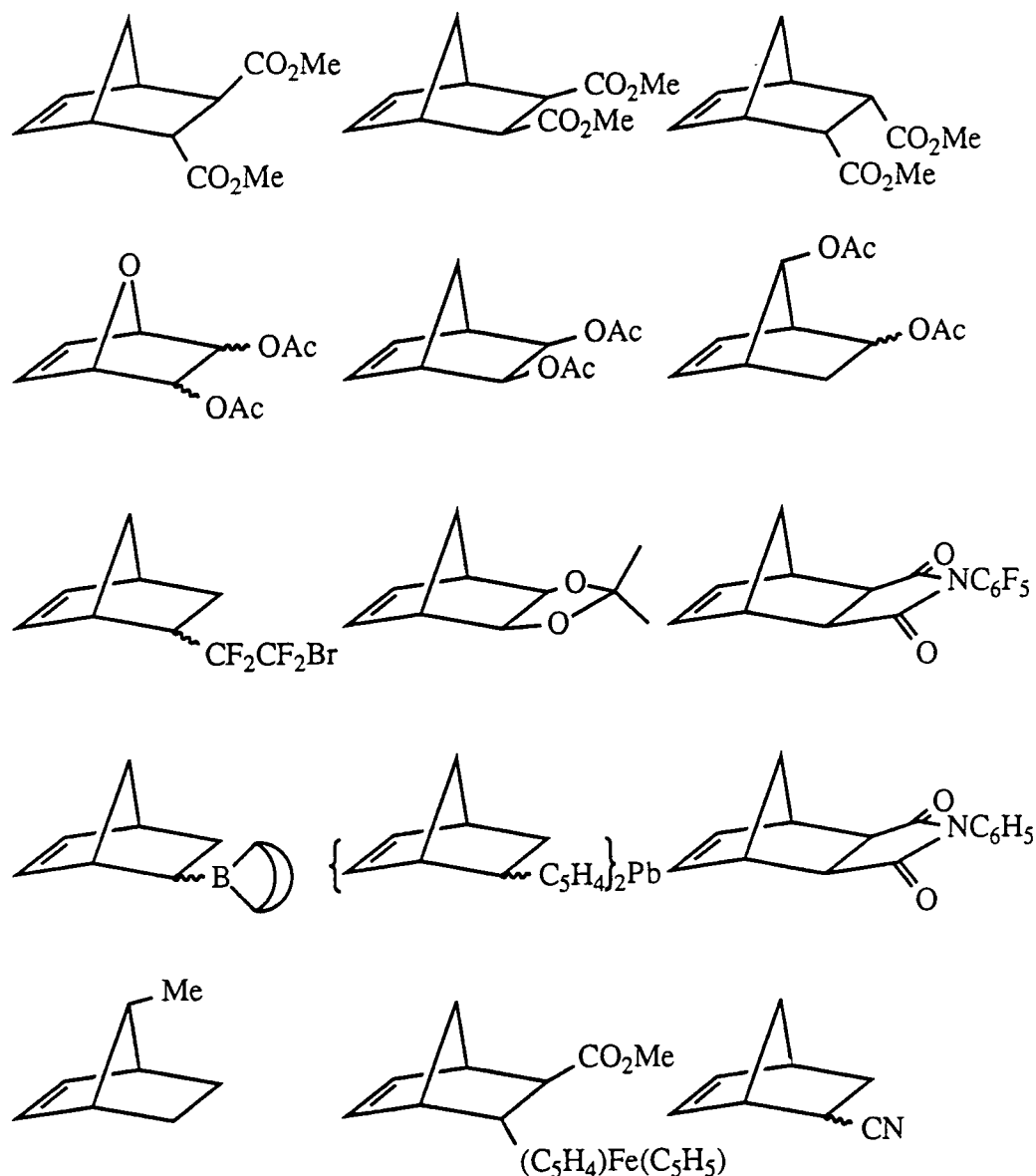
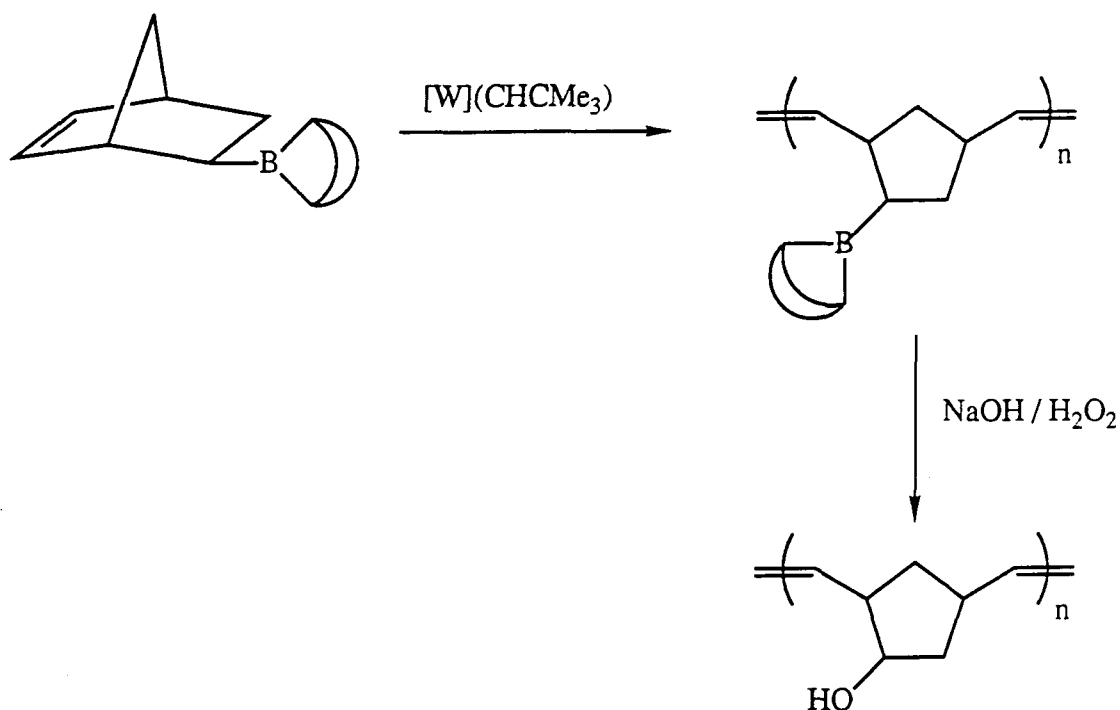


Table 1.1: Examples of functionalized norbornenes that have been polymerized using  $\text{Mo}(\text{NAr})(\text{CHR})(\text{OR}')_2$  <sup>83-86</sup>

The incorporation of functionalized groups into hydrocarbon polymers is also an important method for modifying the chemical and physical properties of the material. Recent work by Chung and co-workers has opened this field up even further; they have reported the living metathesis polymerization of norbornenyl-9-borabicyclononane<sup>85</sup>. Since organoboranes are such synthetically-versatile intermediates, a whole host of functional groups can be attached onto the hydrocarbon backbone. For example, hydroxyl groups can

be introduced under mild oxidation conditions using alkaline hydrogen peroxide (equation 7). This is particularly important since the Schrock initiators are unstable with respect to the alcohol functionality.



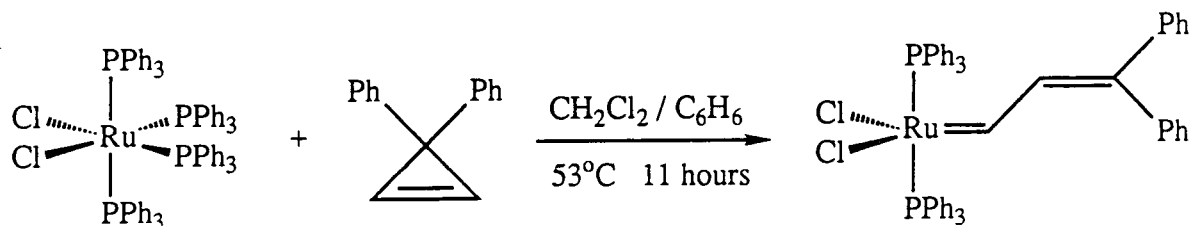
Equation 7

Other interesting reactions featuring this class of initiator include the preparation of PbS clusters embedded in a poly(norbornene) matrix<sup>86</sup>, the R.O.M.P. of cyclooctatetraene to poly(acetylene)<sup>87</sup>, and the synthesis of star-shaped polymers<sup>88</sup>.

### 1.5.5 Aqueous living R.O.M.P.

A recent discovery in the field of metathesis polymerization is Grubb's observation that  $RuCl_3 \cdot 3H_2O$  initiates the polymerization of 7-oxa-norbornenes in aqueous solution<sup>89</sup>. This implies that the system must somehow generate a water stable, late transition-metal (hence presumably low valent) carbene species.

Recently Grubb's group have reported the synthesis and isolation of a moisture-insensitive ruthenium carbene<sup>90</sup>, shown in equation 8. This complex is stable in the presence of deoxygenated water (but unfortunately is insoluble in water and alcohols), and will polymerize norbornene in deoxygenated organic solvents in a living fashion. The propagating carbene is also moisture stable, and has been observed via <sup>1</sup>H N.M.R... Although this work is still far from complete, enormous interest in an air- and water-stable, living metathesis initiator still exists.



Equation 8

## 1.6 The ring-opening metathesis polymerization of fluorinated cycloolefins

Most industrially-produced fluoropolymers are prepared by radical chain polymerization. However, in 1979 Feast and Wilson reported the first example of the ring-opening metathesis polymerization of a fluorinated cycloolefin<sup>91,92</sup>.

### 1.6.1 Classically initiated R.O.M.P.

2,3-Bis(trifluoromethyl)bicyclo[2.2.1]hepta-2,5-diene was the first fluorinated bicyclic olefin to be successfully R.O.M.P.ed using an initiating mixture of  $WCl_6$  and  $SnMe_4$  at room temperature in toluene. Further studies revealed that catalyst systems based upon molybdenum and ruthenium could also bring about the R.O.M.P. of this monomer in various yields, and that the microstructure of the polymer produced (in particular the cis and trans content) was dependent upon the initiating system<sup>93</sup>.

This is a particularly convenient monomer to study; it is simple to synthesize, and the resultant polymer has a relatively uncomplicated  $^{13}C$  N.M.R. spectrum, because only four possible assembly modes exist for the ring-opened polymer of a symmetrical 2,3-difunctionalized norbornadiene<sup>1</sup> (see chapters two and three).

In subsequent studies Feast's group polymerized a variety of other polar, fluorinated norbornenes and norbornadienes, and were able to assign polymer microstructure (using infra-red and  $^{13}C$  N.M.R. spectroscopy), and relate the structures to the initiating systems used, with the long term aim of synthesising highly stereoregular fluoropolymers<sup>94-98</sup>. Table 1.2 summarizes some of the fluorinated monomers studied.

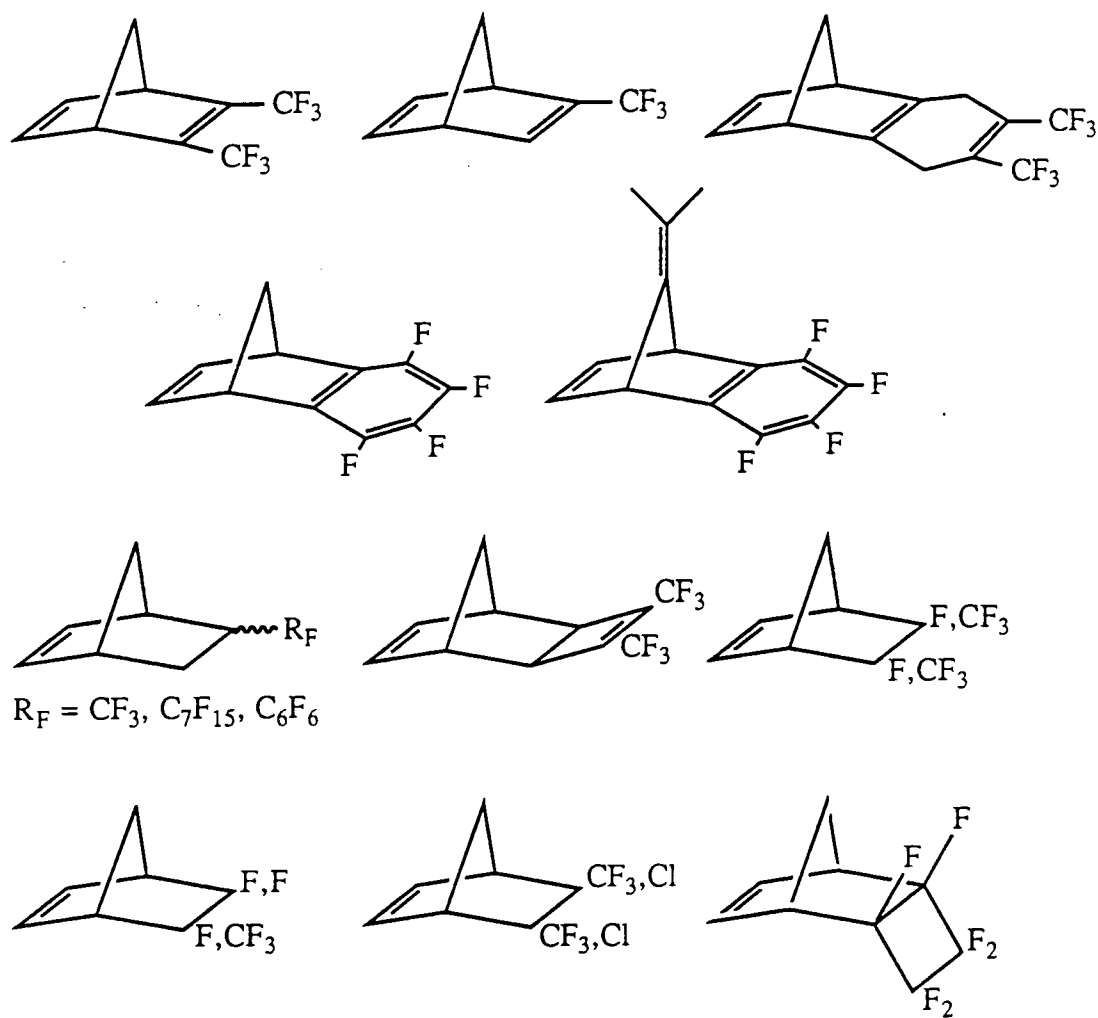
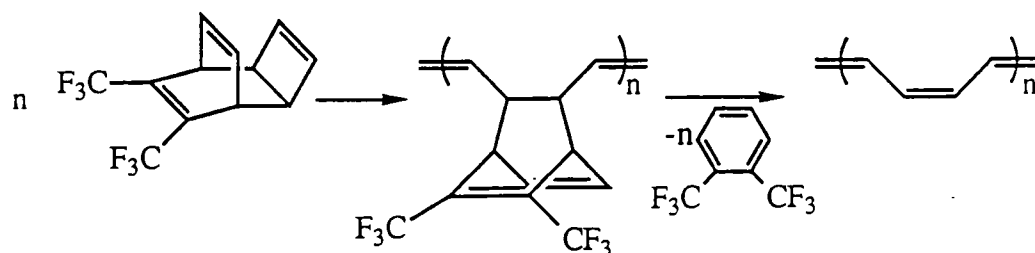


Table 1.2: A selection of fluorinated derivatives of norbornene and norbornadiene studied by Feast and co-workers<sup>99</sup>.

An important application of the R.O.M.P. of fluorinated bicyclic olefins is the synthesis of poly(acetylene) by the Durham precursor route<sup>100,101</sup>. In this process 7,8-bis(trifluoromethyl)tricyclo[4.2.2.0<sup>2,5</sup>]deca-3,7,9-triene (TCDT-F6) is polymerized to give a material from which hexafluoro-ortho-xylene can be eliminated upon heating, (equation 9). This method is particularly useful since films of poly(acetylene) can be prepared simply by casting the precursor polymer prior to the intermolecular elimination step. This is not usually possible when poly(acetylene) is synthesized by other techniques<sup>102</sup>.

This idea has since been exploited by Grubbs<sup>78</sup> (figure 1.9) and Schrock<sup>103</sup> (see section 1.6.2), also to produce poly(acetylene) using well-defined initiators.



Equation 9

### 1.6.2 The R.O.M.P. of fluorinated bicyclic olefins using well-defined Schrock initiators

Further investigation by Schrock's group on TCDT-F6 (see section 1.5.1) using  $W(NAr)(CHCMe_3)(OCMe_3)_2$ , has led to the synthesis of a homologous series of polyenes that contain up to 15 double bonds<sup>103-106</sup>. Such polyenes have also been included in polynorbornene diblock or triblock co-polymers<sup>103</sup>.

An interesting aspect of this study is the discovery that hexafluoro-ortho-xylene may be eliminated from the living polymer chain; i.e. it is possible to bring about the elimination step prior to capping at the metal centre. Schrock has also investigated the direct polymerization of acetylene, in a reaction closely related to R.O.M.P. (figure 1.10).

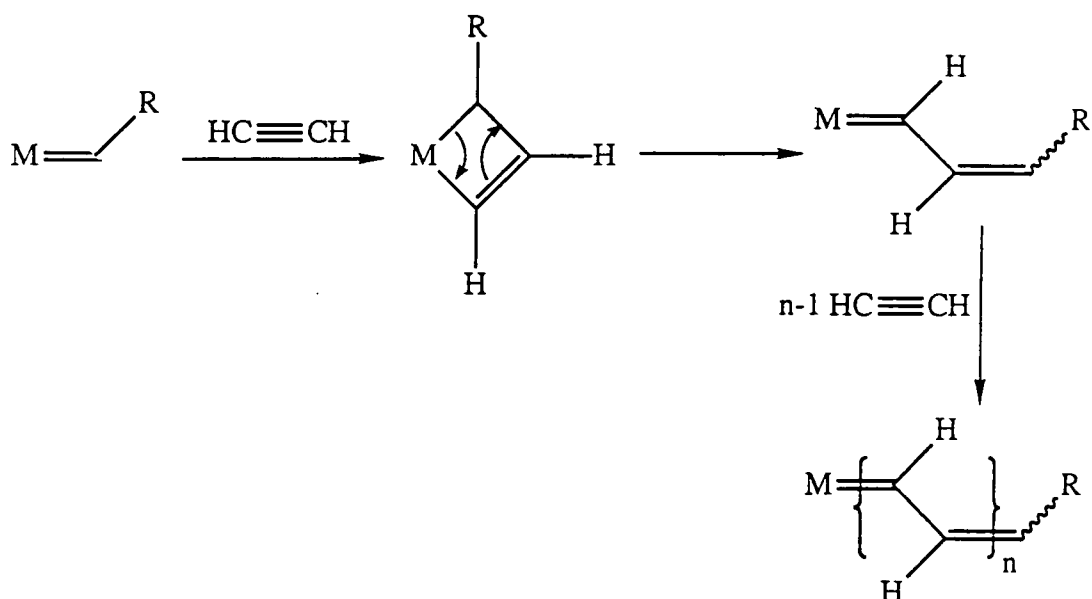


Figure 1.10: Acetylene metathesis polymerization

Indeed this work proved moderately successful; between three and thirteen equivalents of acetylene can be polymerized in a controllable manner by  $W(NAr)(CHCMe_3)(OCMe_3)_2$  in the presence of five equivalents of quinuclidene.<sup>107</sup> It is believed that the quinuclidene binds to the living polyacetylene metal site more than it does to the unreacted initiator, hence reducing the difference in  $k_p$  and  $k_i$ , allowing for a reduction in the polydispersity of the final material.

A similar technique has recently been used by Grubbs to polymerize cyclobutene with  $W(NAr)(CHCMe_3)(OCMe_3)_2$  in the presence of  $PMe_3$ . The base co-ordinates reversibly to the metal centre, and thereby partially deactivates it towards R.O.M.P., allowing the polymer produced to have a narrow molecular weight distribution<sup>108</sup>.

The R.O.M.P. of several other fluorinated cyclic olefins has also been investigated with these initiators. Most significantly, in 1989 it was reported that 2,3-bis(trifluoromethyl)bicyclo[2.2.1]hepta-2,5-diene can be polymerized using  $Mo(NAr)(CHCMe_3)(OCMe_3)_2$  to give a material which contains in excess of 98% trans vinylenes in the polymer backbone<sup>83,109</sup>. Moreover, comparison of the  $^{13}C$  N.M.R. spectrum of this

product with that of 55% trans material prepared using the classical system  $WCl_6 / SnMe_4$ , seemed to indicate that the highly trans polymer might be tactic (i.e. containing a regular arrangement of cyclopentenylene rings between the trans double bonds). Since work on this system forms the basis of chapters two and three of this thesis, further discussion will be deferred.

## 1.7 Fluorinated polymers

Dramatic changes in the physical properties and chemical reactivities of organic materials can be brought about by fluorination, as the amazingly diverse and constantly expanding commercial range of fluoro-organic products bears witness (e.g. drugs, dyes; surfactants, liquid crystals, refrigerants, anaesthetics, blood substitutes, and agrochemicals). Unsurprisingly therefore, although generally quite expensive, fluorinated polymers have a large commercial market. Some of the most common are listed in table 1.3.

The main drawback of organofluorines is their relatively high cost; therefore most applications of fluoropolymers are highly specialised<sup>110</sup>. With a handful of exceptions, summarised in figure 1.11, the industrial production of fluorinated polymers takes place on a small-tonnage scale. For comparison the corresponding figure for low density polyethylene is 5,200,000 tonnes.

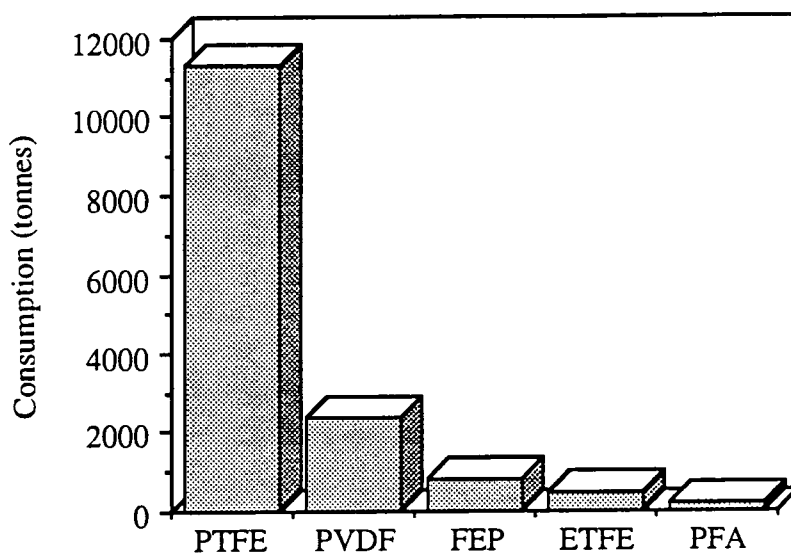
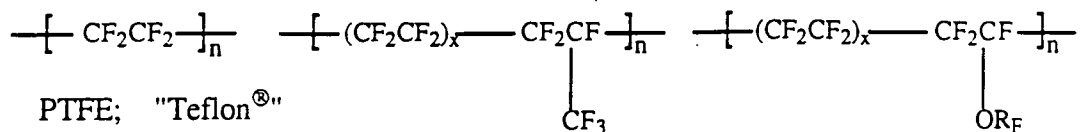


Figure 1.11: The 1989 consumption of various fluorinated plastics in Western Europe:

PTFE = poly(tetrafluoroethylene), PVDF = poly(vinylidene fluoride), FEP = tetrafluoroethylene /

hexafluoropropylene copolymer, ETFE = ethylene / tetrafluoroethylene copolymer,

PFA = tetrafluoroethylene / perfluoroalkylvinylether copolymer<sup>111</sup>.



PTFE; "Teflon<sup>®</sup>"

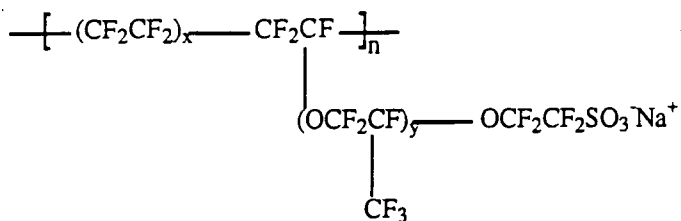
FEP

$\text{R}_F = n\text{-C}_3\text{F}_7$

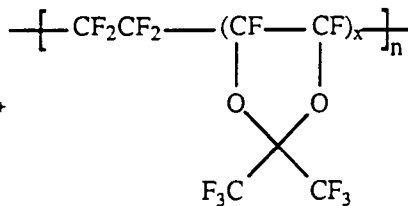
"PFA"

$\text{R}_F = \text{CF}_3$

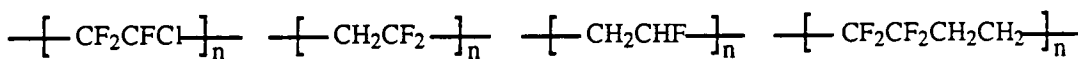
"Kalrez<sup>®</sup>"



"Nafion<sup>®</sup>"



"Teflon<sup>®</sup> AF"

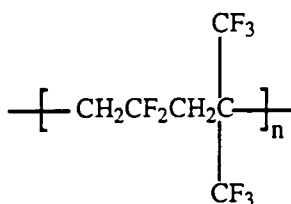


PCTFE

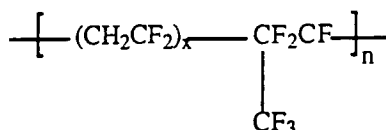
PVDF

PVF

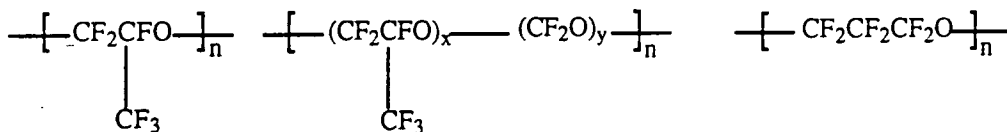
ETFE



"CM-X"



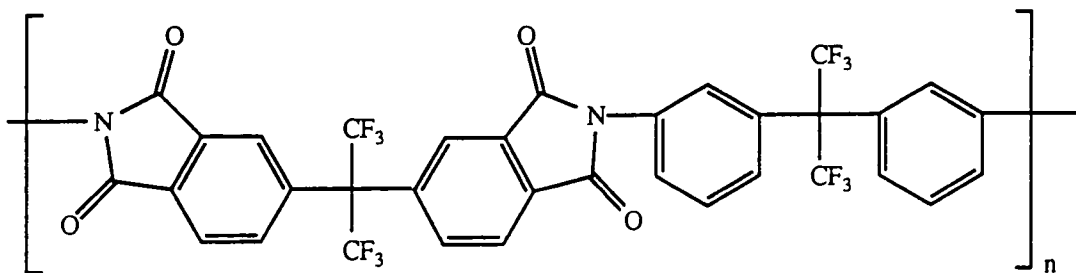
"Viton<sup>®</sup> A"



"Galden<sup>®</sup>"; "Krytox<sup>®</sup>"

"Fomblin<sup>®</sup> Y"

"Demnum<sup>®</sup>"



A<sub>6</sub>-F Polyimide

### 1.7.1 Poly(tetrafluoroethylene)

The history of fluorinated polymers dates back to 1938, when Plunkett at Du Pont serendipitously discovered poly(tetrafluoroethylene), PTFE. This polymer was found to be highly stable (both thermally and chemically-resistant), and soon found use in gaskets, valve packings, and electrical insulation in chemical plant handling of uranium hexafluoride. Fifty years later, PTFE finds widespread use, encountered in numerous everyday applications, from non-stick coatings to surgical implants and fire protection devices.

The extraordinary resistance of fluoroorganics to violently reactive chemicals (including concentrated acids and alkalis, and harsh oxidising and reducing reagents) is well-documented; this inertness is also encountered in many fluorinated polymers. For example, PTFE is attacked chemically by only a handful of compounds (e.g. molten alkali metals, elemental fluorine and other vigorous fluorinating agents e.g.  $\text{ClF}_3$  at elevated temperatures). It is non-flammable (it has a measured oxygen index of 95%<sup>112</sup>, compared with carbon, 65%, uPVC, 45%, and poly(propylene) 17%), shows excellent stability towards ultra-violet radiation, and is soluble only in high-boiling point perfluorocarbons (e.g. in perfluorokerosene at 350°C<sup>113</sup>).

The reason behind this stability is the shielding of the carbon backbone by an almost impenetrable sheath of fluorine atoms, coupled with the great strength of C-F bonds and their lack of polarisability.

The same argument also explains why partially-fluorinated polymers are less resistant to chemical attack than their perfluorocarbon analogues; commercially, this results in a balancing act between fluorine content and hence cost, with desired chemical stability and physical properties.

### 1.7.2 Poly(vinylidene fluoride)

Owing to the strength of the C-F bond dipole, partially-fluorinated polymers can display significantly polar characteristics. Indeed, poly(vinylidene fluoride),  $-(\text{CH}_2\text{CF}_2)_n$  has become the archetypal piezoelectric polymeric material, a property derived from the presence of a high degree of alignment of its C-F dipoles. A piezoelectric material is one which when subjected to a straining force responds in such a way as to generate an electrical current (the related concept of pyroelectricity arises from the application of heat).

The contrasting piezoelectric character of the isomeric polymers poly(vinylidene fluoride), PVDF, and poly(ethylene-co-tetrafluoroethylene), ETFE, provides a good example of the key role polar C-F bonds can play. Poling PVDF results in significant alignment of its C-F dipoles, and the resultant material displays outstanding piezoelectric properties; ETFE, however, cannot adopt a polar configuration, and hence has negligible piezoelectric character (figure 1.12).

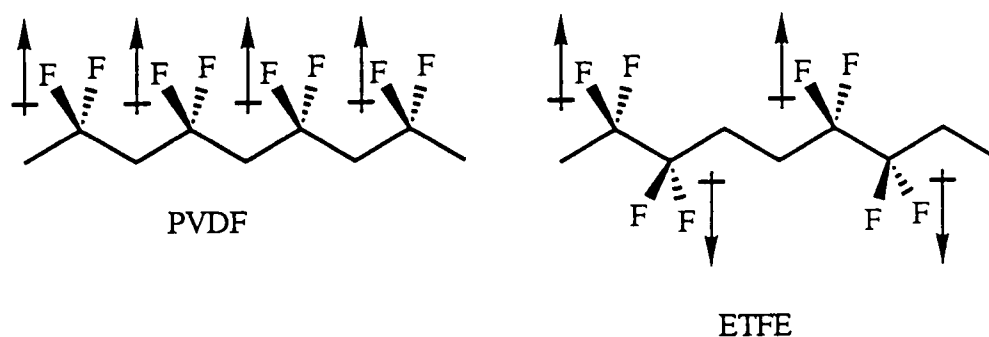


Figure 1.12: The alignment of dipoles in poly(vinylidene fluoride) compared to that in the copolymer of ethylene and tetrafluoroethylene.

The strong piezoelectric effect in poly(vinylidene fluoride) was first detected in 1969 by Kawai<sup>14</sup>. As figure 1.13 demonstrates, PVDF exhibits considerably stronger piezoelectric activity than other polymers. This behaviour is due in part to its high dielectric constant.

The discovery of the piezoelectric effect in PVDF, and later of its pyroelectric properties led to extensive research in the mid- to late- 1970's, and much of this work has since been reviewed<sup>115</sup>.

PVDF is commercially available as a semi-crystalline polymer, with typical molecular weights of  $10^6$  (corresponding to approximately 2000 repeat units). It is predominantly head-tail, although some head-head (i.e. a  $CF_2$  group adjacent to another  $CF_2$ ) and tail-tail ( $CH_2$  followed by  $CH_2$ ) defects do occur. The crystalline regions are embedded in an amorphous phase which has a glass-transition temperature of about  $-40^\circ C$  when measured at low frequencies.

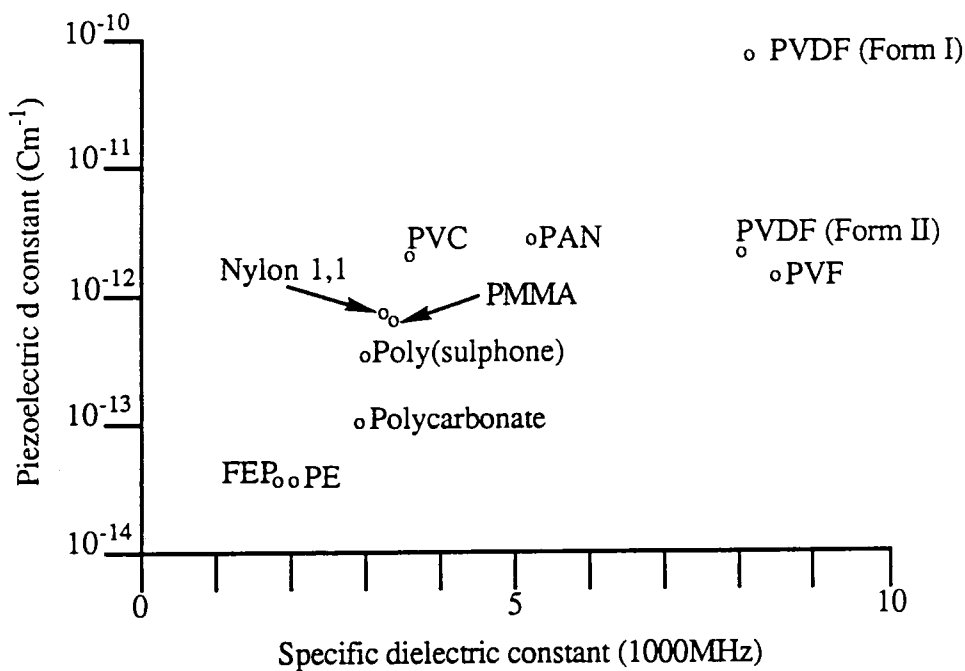


Figure 1.13: The general trend of increasing piezoelectricity with increasing dielectric constant<sup>115</sup>

{PAN = Poly(acetonitrile), PE = poly(ethylene), PMMA = Poly(methylmethacrylate), PVC = Poly(vinylchloride), PVF = Poly(vinylfluoride), PVDF Form I and II are two of the four crystalline conformations of poly(vinylidene fluoride)}

### 1.7.3 The origin of piezoelectricity in poly(vinylidene fluoride)

Models on the piezoelectric effect in PVDF are based on the assumption that the material consists of crystalline and amorphous phases differing in dielectric and elastic properties<sup>116-118</sup>. Piezoelectricity can therefore arise in many ways:

(a) the dielectric constant of the crystalline and amorphous regions have different strain dependence. Hence, in the presence of a polarisation, this yields a piezoelectric effect, known as the 'electrostrictive contribution'.

(b) The elastic constants of the crystalline and amorphous parts are different. Again, in a polarised sample, this yields a strain dependence and thus contributes to the piezoelectric effects observed (dimensional contribution).

(c) The crystalline parts have an intrinsic piezoelectricity due to the strain dependence of their polarisation (crystal contribution).

Despite much work in this area many details concerning the origin of piezoelectricity in PVDF are still to be worked out. In particular, the effect of neutralizing counter charges<sup>118</sup> and the contribution of those parts of the amorphous phase neighbouring the crystals<sup>119</sup>, are not well understood.

### 1.7.4 The applications of poly(vinylidene fluoride) arising from its piezoelectricity

There are basically three main areas in which PVDF is used in order to exploit its piezoelectric character. PVDF transducers for audio-frequency applications are found in microphones, headphones, loudspeakers (tweeters), and in medical sensors. Secondly, PVDF is used in ultrasonics and underwater transducers; for example, in Rayleigh- and Lamb- wave detectors. Finally PVDF has found many uses as an electromechanical transducer, for example in computer keyboards, telephone dials, optical fibre switches, variable-focus mirrors, impact detectors, and coin sensors. The reader is directed to

reference 115 and the references contained therein for a full and detailed account of this subject.

PVDF is also used to a lesser extent because of its pyroelectric and optical properties. For example, it has been used widely in infra-red detectors, photocopiers, and Vidicons (for night-light surveillance).

## 1.8 Summary

The resurgence of interest in olefin metathesis over the past few years has stemmed from the advances in well-defined initiator synthesis made by several organometallic groups around the world, but particularly those led by Osborn<sup>53,120</sup>, Grubbs<sup>90,120,121</sup>, and Schrock<sup>51,82,83,122</sup>. The range of ring-opened polymers being produced is constantly increasing and future commercial production is a strong possibility.

As polymer architecture control becomes increasingly available with living systems, the ability to produce functionalized polymers of predetermined microstructure has become a real possibility. The work on which the following chapters are based describes attempts to apply this idea to fluorinated bicyclic olefins using well-defined Schrock molybdenum initiators, and to explore property-structure correlations via dielectric, pyro- and piezoelectric measurements.

## 1.9 References

1. K.J. Ivin 'Olefin Metathesis', Academic Press, London (1983)
2. A.W. Anderson, N.G. Merckling U.S. Patent 2721 189; Chem. Abstr. **50** 3008 (1955)
3. G. Natta, G. Dall'Asta, G. Mazzanti Angew. Chem. Int. Ed. Engl. **3** 723 (1964)
4. Chem. Eng. News, **45** 51 (1967)
5. J.L. Herisson, Y. Chauvin Makromol. Chem. **141** 161 (1970)
6. K.J. Ivin, T. Saegusa 'Ring-opening Polymerization', Elsevier Applied Science, London (1984)
7. P.A. Patton, T.J. McCarthy Macromolecules **20** 778 (1987)
8. K.J. Ivin, D.T. Lavery, J.J. Rooney, P. Watt Rec. Trav. Chim. Pays Bas **96** M54 (1977)
9. K.J. Ivin, L.M. Lam, J.J. Rooney Makromol. Chem. **182** 1847 (1981)
10. K.J. Ivin, G. Lapienis, J.J. Rooney J. Chem. Soc., Chem. Commun. 1068 (1979)
11. K.J. Ivin, G. Lapienis, J.J. Rooney Polymer **21** 436 (1980)
12. G.I. Devine, H.T. Ho, K.J. Ivin, M.A. Mohamed, J.J. Rooney J. Chem. Soc., Chem. Commun. 1229 (1982)
13. L.P. Tenney, P.C. Lane Chem. Abstr. **90** 187884 (1979)
14. L.P. Tenney Chem. Abstr. **90** 169556 (1979)
15. H.G.G. Dekking J. Polym. Sci. **55** 525 (1961)
16. F.W. Michelotti, J.H. Carter Polym. Prepr. Am. Chem. Soc. **6** 224 (1965)
17. R.E. Rinehart Chem. Abstr. **68** 87750 (1968)
18. R.E. Rinehart, H.P. Smith J. Polym. Sci., Polym. Lett. **B3** 1049 (1965)
19. K. Komatsu, S. Matsumoto, S. Aotani Chem. Abstr. **86** 56201 (1977)
20. M. Kobayashi, T. Kamijima., S. Kobayshi Chem. Abstr. **88** 38328 (1978)
21. P. Hepworth Chem. Abstr. **78** 98287 (1973)

22. M. Zimmermann, G. Pampus, D. Maertens *Chem. Abstr.* **85** 95539 (1976)
23. P. Chevalier, D. Sinou, G. Descotes *Bull. Soc. Chim. France* 2254 (1975)
24. K.J. Ivin in 'Reactivity, Mechanism and Structure in Polymer Chemistry' (Eds A.D. Jenkins and A. Ledwith), Wiley, London (1974), Chapter 16.
25. V.M. Cherednichenko *Polymer Sci. USSR* **A20** 1225
26. L. Hocks, D. Berck, A.J. Hubert, P. Teyssie *J. Polym. Sci., Polym. Lett.* **13** 391
27. S.J. Lee, J. McGinnis, T.J. Katz *J. Am. Chem. Soc.* **98** 7818
28. P. Gunther, F. Haas, G. Marwede, K. Nutzelt, W. Oberkirch, G. Pampus, N. Schon, J. Witte *Angew. Makromol. Chem.* **14** 87
29. J.G. Hamilton, K.J. Ivin, J.J. Rooney, L.C. Waring *J. Chem. Soc., Chem. Commun.* 159 (1983)
30. R.H. Grubbs, C.R. Hoppin *J. Chem. Soc., Chem. Commun.* 634 (1977)
31. M.F. Farona, R.L. Tucker *J. Mol. Catal.* **8** 85 (1980)
32. R.H. Grubbs, S. Swemick *J. Mol. Catal.* **8** 25 (1980)
33. E.O. Fischer, A. Maasbol *Angew. Chem. Int. Ed. Engl.* **3** 580 (1964)
34. E.O. Fischer *Adv. Organomet. Chem.* **14** 1 (1976)
35. T.J. Katz, N. Acton *Tetrahedron Lett.* 4251 (1976)
36. See for example, W.A. Nugent, J. M. Mayer 'Metal-Ligand Multiple Bonds', Wiley, New York (1988)
37. T.E. Taylor, M.B. Hall *J. Am. Chem. Soc.* **106** 1576 (1984)
38. D. Seyferth (editor) 'Transition Metal Carbene Complexes', Verlag Chemie, Weinheim (1983)
39. M. Brookhart, J.R. Tucker, T.C. Flood, J. Jensen *J. Am. Chem. Soc.* **102** 1203 (1980)
40. R.R. Schrock *J. Organomet. Chem.* **300** 249 (1986)
41. R.R. Schrock *J. Am. Chem. Soc.* **96** 6796 (1974)
42. L.R. Gilliom, R.H. Grubbs *Organometallics* **5** 721 (1986)

43. F.W. Hartner, J. Schwartz, S.M. Clift *J. Am. Chem. Soc.* **105** 640 (1983);  
S.M. Clift, J. Schwartz *J. Am. Chem. Soc.* **106** 8300 (1984)
44. P. Binger, P.P. Muller, R. Benn, R. Mynott *Angew. Chem.* **101** 647 (1989)
45. R.R. Schrock, J.D. Fellmann *J. Am. Chem. Soc.* **100** 3359 (1978)
46. J.S. Murdzek, R.R. Schrock *Organometallics* **6** 1373 (1987)
47. J. Kress, M. Wesolek, J.A. Osborn *J. Chem. Soc., Chem. Commun.* 514 (1982)
48. A. Agüero, J. Kress, J.A. Osborn *J. Chem. Soc., Chem. Commun.* 793 (1985)
49. J. Kress, A. Agüero, J.A. Osborn *J. Mol. Catal.* **36** 1 (1986)
50. D.S. Edwards, L.V. Biondi, J.W. Ziller, M.R. Churchill, R.R. Schrock  
*Organometallics* **2** 1505 (1983)
51. J. Feldman, R.R. Schrock *Progr. Inorg. Chem.* **39** 1 (1991)
52. A.K. Rappe, W.A. Goddard III *J. Am. Chem. Soc.* **104** 448 (1982)
53. J. Kress, J.A. Osborn, R.M.E. Greene, K.J. Ivin, J.J. Rooney *J. Am. Chem. Soc.*  
**109** 899 (1987)
54. T.R. Howard, J.B. Lee, R.H. Grubbs *J. Am. Chem. Soc.* **102** 6876 (1980)
55. D.A. Straus, R.H. Grubbs *J. Mol. Catal.* **28** 9 (1985)
56. E.A. Carter, W.A. Goddard III *J. Am. Chem. Soc.* **108** 2180 (1986)
57. E.A. Carter, W.A. Goddard III *J. Am. Chem. Soc.* **108** 4746 (1986)
58. A.S. Nazran, D. Griller *J. Chem. Soc., Chem. Commun.* 850 (1983) and references  
therein
59. C. Wentrup 'Reactive Molecules: The Neutral Reactive Intermediates in Organic  
Chemistry', Wiley, New York (1984) Chapter 4
60. J.P. Collman, L.S. Hege, J.R. Norton, R.G. Finke 'Principles and Applications  
of Organometallic Chemistry', University Science Press, Mill Valley, California  
(1987)
61. D.M.P. Mingos 'Bonding of Unsaturated Organic Molecules to Transition Metals',  
in 'Comprehensive Organometallic Chemistry' (Eds G. Wilkinson, F.G.A. Stone,

E.W. Abel), Pergamon, New York (1982) Volume 3 pp1-88

62. G. Odian 'Principles of Polymerization', Wiley, New York (1981)
63. A.H.E. Muller in 'Comprehensive Polymer Science', Pergamon, New York (1989)  
Volume 3 Chapter 26
64. M. Szwarc in 'Advances in Polymer Science', Springer-Verlag, Berlin (1983)  
Volume 49
65. R.P. Quirk, B. Lee *Polymer* **27** 359 (1992)
66. L. Gold *J. Chem. Phys.* **28** 91 (1958)
67. A. Noshay, J.E. McGrath 'Block Copolymers', Academic, New York (1977)
68. F.N. Tebbe, G.W. Parshall, D.W. Ovenall *J. Am. Chem. Soc.* **101** 5074 (1979)
69. L.R. Gilliom, R.H. Grubbs *J. Am. Chem. Soc.* **108** 733 (1986)
70. R.H. Grubbs, W. Tumas *Science* **243** 907 (1989)
71. L.F. Cannizzo, R.H. Grubbs *Macromolecules* **21** 1961 (1988)
72. L.F. Cannizzo, R.H. Grubbs *Macromolecules* **20** 1488 (1987)
73. W. Risse, R.H. Grubbs *Macromolecules* **22** 4462 (1989)
74. W. Risse, R.H. Grubbs *Makromol. Chem., Rapid Commun.* **10** 73 (1989)
75. W. Risse, R.H. Grubbs *Macromolecules* **22** 1558 (1989)
76. W. Risse, D.R. Wheeler, L.F. Cannizzo, R.H. Grubbs *Macromolecules* **22** 3205  
(1989)
77. T.M. Swager, R.H. Grubbs *J. Am. Chem. Soc.* **109** 894 (1987)
78. F.L. Klavetter, R.H. Grubbs *Synthetic Metals* **26** 311 (1988)
79. C.J. Schaverien, R.R. Schrock, J.C. Dewan *J. Am. Chem. Soc.* **108** 2771 (1986)
80. R.R. Schrock, R.T. DePue, J. Feldman, C.J. Schaverien, J.C. Dewan, A.H. Liu  
*J. Am. Chem. Soc.* **110** 1423 (1988)
81. R.R. Schrock, J. Feldman, R.H. Grubbs, L. Cannizzo *Macromolecules* **20** 1169  
(1987)
82. R.R. Schrock *Acc. Chem. Res.* **23** 158 (1990)

83. G.C. Bazan, E. Khosravi, R.R. Schrock, W.J. Feast, V.C. Gibson, M. O'Regan, J. Thomas *J. Am. Chem. Soc.* **112** 8378 (1990); G.C. Bazan, R.R. Schrock, H.-N. Cho, V.C. Gibson *Macromolecules* **24** 4495 (1991)
84. W.J. Feast, V.C. Gibson, K.J. Ivin, A. Kenwright, E. Khosravi, E.L. Marshall, J.P. Mitchell *Makromol. Chem* **193** 2103 (1992)
85. V. Sankaran, C.C. Cummins, R.R. Schrock, R.E. Cohen, R.J. Silbey *J. Am. Chem. Soc.* **112** 6858 (1990)
86. T.C. Chung, S. Ramakrishnan, M.W. Kim *Macromolecules* **24** 2675 (1991)
87. F.L. Klavetter, R. H. Grubbs *J. Am. Chem. Soc.* **110** 7807 (1988)
88. G.C. Bazan, R.R. Schrock *Macromolecules* **24** 817 (1991)
89. B.M. Novak, R.H. Grubbs *J. Am. Chem. Soc.* **110** 7542
90. S.T. Nguyen, L.K. Johnson, R.H. Grubbs *J. Am. Chem. Soc.* **114** 3974 (1992)
91. W.J. Feast, B. Wilson *Polymer* **20** 1183 (1979)
92. W.J. Feast, B. Wilson *J. Mol. Cat.* **8** 277 (1980)
93. Ab. Alimuniar, P.M. Blackmore, J.H. Edwards, W.J. Feast, B. Wilson *Polymer* **27** 1281 (1986)
94. W.J. Feast, L.A.H. Shahada *Polymer* **27** 1289 (1986)
95. P.M. Blackmore, W.J. Feast *Polymer* **27** 1296 (1986)
96. P.M. Blackmore, W.J. Feast *J. Mol. Cat.* **36** 145 (1986)
97. P.M. Blackmore, W.J. Feast, P. C. Taylor *Brit. Pol. J.* **19** 205 (1987)
98. P.M. Blackmore, W.J. Feast *J. Fluorine Chem.* **35** 235 (1987)
99. See also N. Seehof, W. Risse *Makromol. Chem., Rapid Commun.* **12** 107 (1991)
100. J.H. Edwards, W.J. Feast *Polymer* **21** 595 (1980)
101. J.H. Edwards, W.J. Feast, D.C. Bott *Polymer* **25** 395 (1984)
102. G. Natta, G. Mazzanti, P. Corradini *Atti. Acad. Nazl. Lincei, Rend. Classe Sci. Fis. Mat. Nat.* (8) **25** 3 (1958)
103. L.Y. Park, R.R. Schrock, S.G. Stieglitz, W.E. Crowe *Macromolecules* **24** 3489 (1991)

104. K. Knoll, S.A. Krouse, R.R. Schrock *J. Am. Chem. Soc.* **110** 4424 (1988)
105. S.A. Krouse, R.R. Schrock *Macromolecules* **21** 1885 (1988)
106. K. Knoll, R.R. Schrock *J. Am. Chem. Soc.* **111** 7989 (1989)
107. R. Schlund, R.R. Schrock, W.E. Crowe *J. Am. Chem. Soc.* **111** 8004 (1989)
108. Z. Wu, D.R. Wheeler, R.H. Grubbs *J. Am. Chem. Soc.* **114** 146 (1992)
109. G.C. Bazan, R.R. Schrock, E. Khosravi, W.J. Feast, V.C. Gibson *Polym. Commun.* **30** 258 (1989)
110. R.E. Banks, J.C. Tatlow *J. Fluorine Chem.* **68** 71 (1986)
111. B.G. Willoughby *Fluoropolymers Conference 1992, Manchester UK.*
112. R.R. Hindersinn *Chemtech* **20** 672 (1990)
113. P. Smith, K.H. Gardner *Macromolecules* **18** 1222 (1985)
114. H. Kawai *Jpn. J. Appl. Phys* **8** 975 (1969)
115. G.M. Sessler *J. Acoust. Soc. Am* **70** 1596 (1981)
116. R. Hayakawa, Y. Wada *Rep. Progr. Polym. Phys. Jpn.* **19** 321 (1976)
117. Y. Wada, R. Hayakawa *Ferroelectrics* **32** 115 (1981)
118. M.G. Broadhurst, G.T. Davis, J.E. McKinney, R.E. Collins *J. Appl. Phys.* **49** 4992 (1978)
119. G.R. Davies in 'Physics of Dielectric Solids' Conference Series Number 58 (The Institute of Physics, Bristol) (1980) pp 50-63
120. R.M.E. Greene, K.J. Ivin, J. Kress, J.A. Osborn, J.J. Rooney *Brit. Polym. J.* **21** 237 (1989) and references therein
121. R.H. Grubbs 'Alkene and Alkyne Metathesis', in 'Comprehensive Organometallic Chemistry' (Eds G. Wilkinson, F.G.A. Stone, E.W. Abel), Pergamon, New York (1982) Chapter 54
122. W.J. Feast, V.C. Gibson 'Olefin Metathesis' in 'The Chemistry of the Metal Carbon Bond', Volume 5, Wiley, New York (1989)

## **Chapter Two**

### **The Living Ring-Opening Metathesis Polymerization of 2,3-Bis(trifluoromethyl)bicyclo[2.2.1]hepta-2,5-diene**

## 2.1 Introduction

This chapter describes studies carried out into the living ring-opening metathesis polymerization of 2,3-bis(trifluoromethyl)bicyclo[2.2.1]hepta-2,5-diene, using well-defined, molybdenum-based, Schrock initiators. Initially an investigation into the production of a highly stereoregular, trans fluoropolymer, using  $\text{Mo}(\text{NAr})(\text{CHR})(\text{OCMe}_3)_2$  ( $\text{R} = \text{CMe}_3, \text{CMe}_2\text{Ph}$ ) is described, with the objective of improving upon the previously reported trans content of 98% in order to determine what effect this would have upon dielectric properties.

The synthesis of a very high cis analogue is then detailed {accessed via the hexafluorobutoxide initiator,  $\text{Mo}(\text{NAr})(\text{CHCMe}_2\text{Ph})(\text{OCMe}(\text{CF}_3)_2)_2$ }. This novel polymer has been fully characterised and preliminary dielectric measurements on both the high trans and high cis polymers are reported. The question of why replacement of butoxide ancillary ligands on the metal centre with the more electron-withdrawing fluorinated analogues should lead to a total reversal in cis and trans content is also addressed.

### 2.1.1 Historical background

The metathesis polymerization of 2,3-bis(trifluoromethyl)bicyclo[2.2.1]hepta-2,5-diene has been reported with a range of classical initiators<sup>1</sup>. A summary of some of this work is presented in table 2.1, which highlights the partial degree of control over  $\sigma_c$ , the fraction of cis vinylene bonds, offered by the employment of different initiators.

The table also serves to emphasize the absence of observed melting points. As will be explained later in this chapter, such distinct transitions are characteristic of crystalline polymers. There is therefore no evidence that any of the classically-initiated samples of poly(1,4-(2,3-bis(trifluoromethyl)cyclopentenylene) vinylene) possess a high enough degree of stereoregularity to induce the formation of crystalline domains.

Initiator system	$\sigma_c$	T <sub>g</sub> / °C	T <sub>m</sub> / °C
WCl <sub>6</sub> / SnMe <sub>4</sub>	0.46	125	-
RuCl <sub>3</sub> / SnMe <sub>4</sub>	0.30	117	-
MoCl <sub>5</sub> / SnMe <sub>4</sub>	0.13	104	-

Table 2.1: Selected physical properties of poly[1,4-(2,3 - bis(trifluoromethyl)cyclopentenylene) vinylene] prepared from a range of classical initiators (T<sub>g</sub> = glass transition temperature, and T<sub>m</sub> = melting endotherm).

### 2.1.2 A highly stereoregular fluoropolymer synthesized via living R.O.M.P.

In 1989 it was reported that 2,3-bis(trifluoromethyl)bicyclo[2.2.1]hepta-2,5-diene could be polymerized by Mo(CHCMe<sub>3</sub>)(NAr)(OCMe<sub>3</sub>)<sub>2</sub> in a well-behaved, living manner to yield the near-monodisperse fluoropolymer<sup>2,3</sup>, depicted in scheme 2.1.

<sup>13</sup>C N.M.R. spectroscopic analysis provides striking evidence that the polymer possesses a high degree of stereoregularity, containing in excess of 98% trans double bonds in the polymer backbone. Moreover, comparison of the <sup>13</sup>C N.M.R. data with that obtained on the analogous WCl<sub>6</sub> / SnMe<sub>4</sub> initiated fluoropolymer suggested that the new material was possibly tactic.



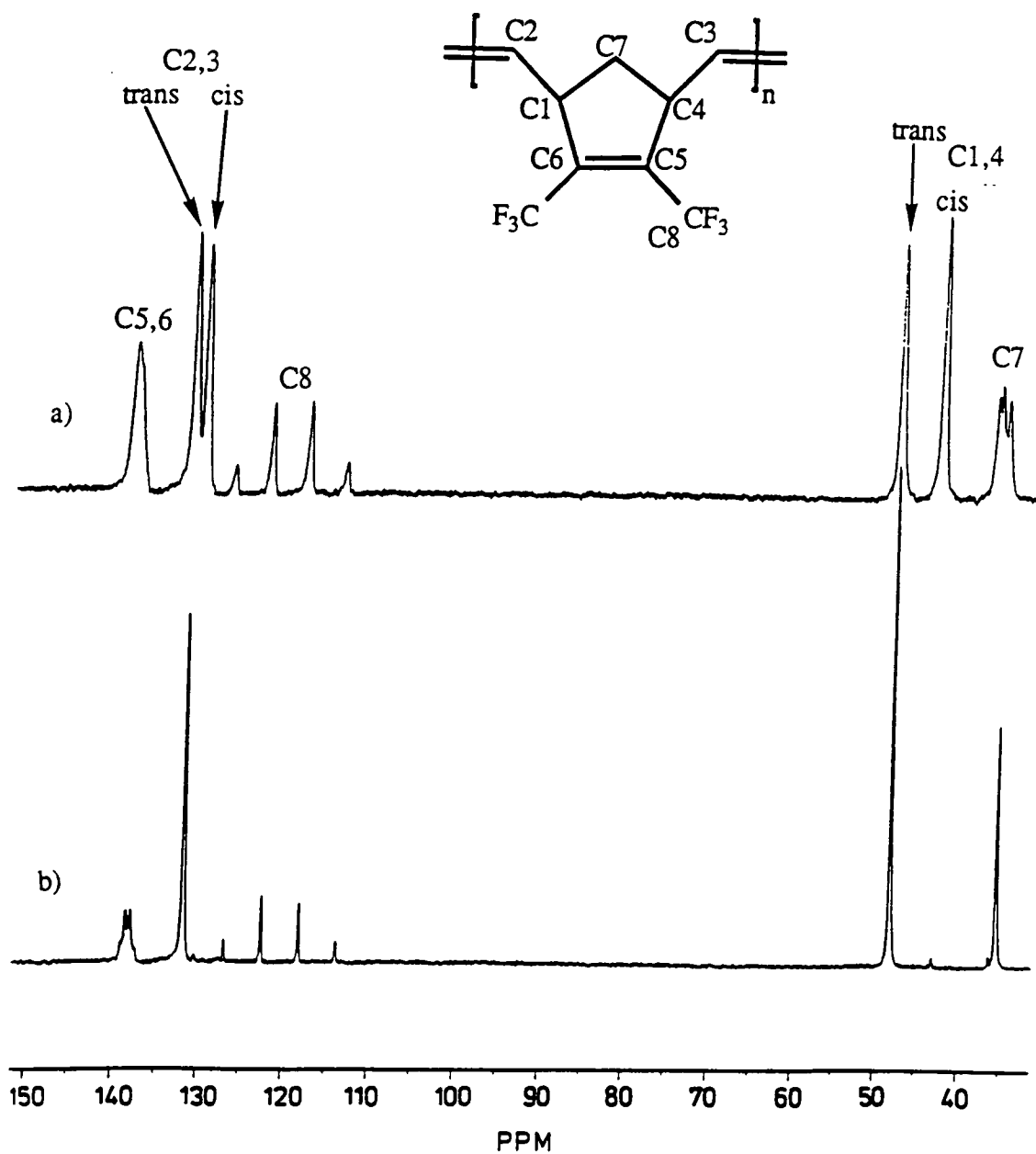


Figure 2.1 The  $^{13}\text{C}$  N.M.R. spectra (acetone- $d_6$ ) of poly[1,4-(2,3-bis(trifluoromethyl)cyclopentenylene) vinylene] initiated by

a)  $\text{WCl}_6 / \text{SnMe}_4$

b)  $\text{Mo}(\text{CHCMe}_3)(\text{NAr})(\text{OCMe}_3)_2$

As can be seen from the figure, the resonances of the 98% trans polymer are noticeably less broad than their counterparts in the sample produced using the classical initiator. Of particular interest is the single C7 methylene resonance, compared with the partially resolved multiplet in the top trace. This multiplet had previously been assigned to different ring dyad environments; the appearance of one signal would, therefore, imply the presence of just one dyad structure, and consequently a tactic polymer.

Further evidence of a high degree of tacticity was supplied by differential scanning calorimetry, revealing a well-defined melting endotherm at 190-200°C. As explained below, crystallinity is often encountered in highly stereoregular polymers. However, this is the first time that crystallinity had been observed in a fluoropolymer produced via R.O.M.P..

## 2.2 Tacticity

The regularity of successive chiral centres along a polymer chain determines the overall tacticity of that polymer. For example, poly(propylene) can adopt two regular stereochemistries, namely isotactic and syndiotactic, both of which are shown in figure 2.2, alongside the third possibility, an atactic structure.

The isotactic example has centres of the same configuration (i.e. all R or all S). However, if the centres alternate R, S, R, S, R etc, then the polymer is said to be syndiotactic. An atactic structure possesses a non-uniform sequence of chiral centres.

In order to refer to different environments in an isotactic polymer the term 'dyad' is introduced. If two successive centres have the same chiral configuration, then the two adjacent repeat units containing these atoms form a meso (m) dyad. Conversely, a racemic (r) dyad contains two atoms of opposite chirality. An isotactic polymer therefore contains all m dyads, whilst a syndiotactic polymer is composed of all r dyads<sup>4</sup>.

The stereoregularity of a polymer influences its physical properties via its ability to crystallize. In general, atactic polymers are non-crystalline, amorphous materials with little physical strength. The corresponding iso- and syndiotactic polymers are often highly crystalline, and therefore display a high physical strength and increased solvent and chemical resistance. For example, the classically-initiated samples of poly[1,4-(2,3-bis(trifluoromethyl)cyclopentenylene) vinylene] reported in table 2.1 are all atactic and hence show no observable melting points.

In a commercial sense, atactic poly(propylene) is essentially worthless, whereas isotactic poly(propylene) is a high melting, crystalline polymer which finds use as both a plastic and a fibre. It displays excellent chemical resistance, high electrical and stress-crack resistance, and with a density of  $0.9\text{gcm}^{-3}$  has a very high strength-to-weight ratio. Syndiotactic poly(propylene), like its isotactic analogue, is highly crystalline, but has a lower melting temperature and is appreciably more soluble in hydrocarbon solvents and di(ethyl) ether.

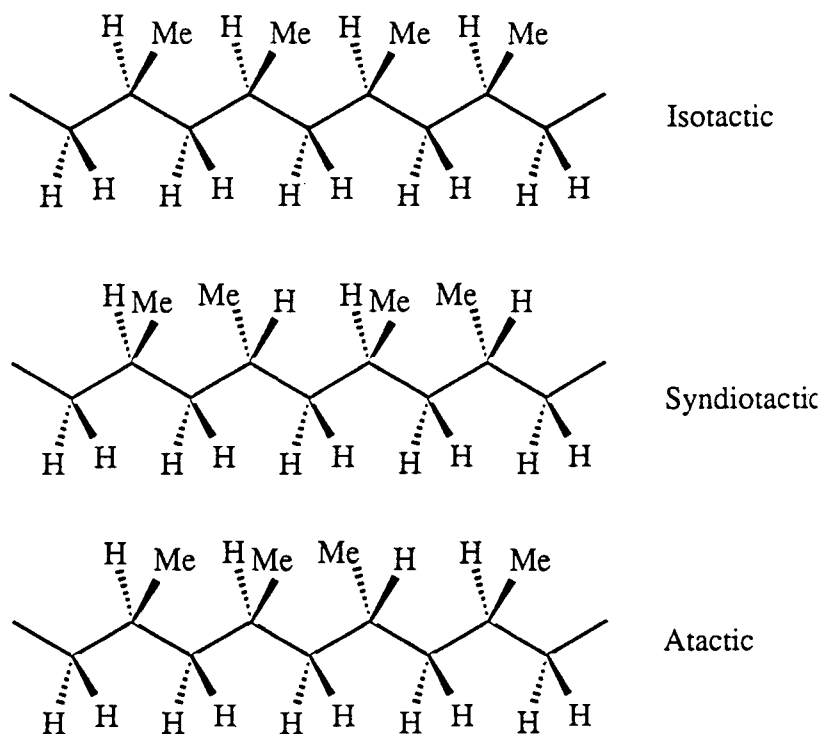


Figure 2.2 The possible stereochemical arrangements of poly(propylene)

Nuclear Magnetic Resonance has become established as the most powerful spectroscopic tool for the assignment of polymer microstructure, especially  $^{13}\text{C}$  N.M.R. which can reveal considerable detail about the distribution of dyads within a polymer chain. The increasing availability of high frequency equipment has led to the determination of triad, tetrad, and even pentad (adjacent repeat units containing 3, 4, and 5 chiral centres respectively) distributions in numerous polymers<sup>5</sup>.

The ring-opened polymers of symmetrically-substituted 2,3-difunctionalised norbornadienes are particularly well-suited to microstructure studies; the lack of head / tail regiochemistries mean that only four possible regular stereochemical structures are possible. Upon ring-opening the polymer can form a double bond with either cis or trans geometry, and can adopt either a syndiotactic or an isotactic configuration.

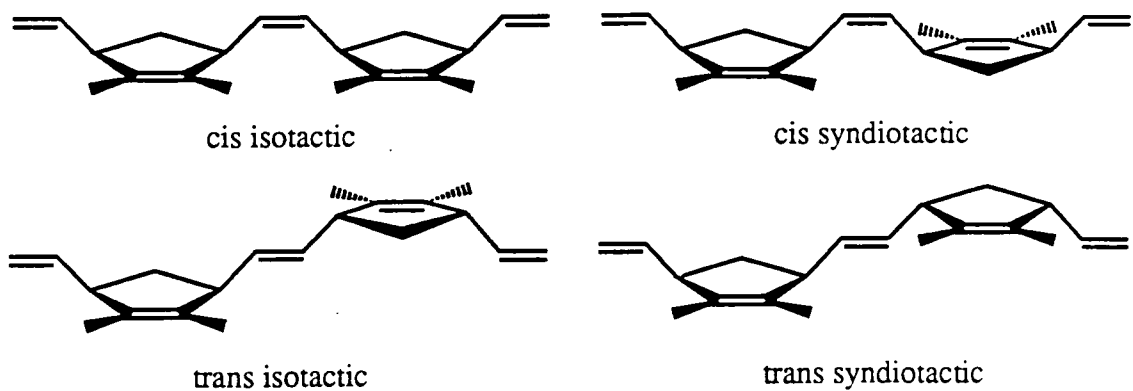


Figure 2.3 The four possible regular assembly modes for a poly(1,4-cyclopentenylene vinylene)

In poly(cyclopentenylene vinylene)s the five-membered rings are best considered as pairs of chiral centres. If they proceed (R,S), (R,S), (R,S), or (S,R), (S,R), (S,R) (i.e. every ring dyad is meso) along the backbone then the polymer is isotactic. If, however, the dyads are all racemic, {i.e. they alternate (R,S), (S,R), (R,S)} the polymer is described as syndiotactic<sup>6</sup>.

### 2.3 The influence of reaction conditions upon cis / trans content in poly[1,4-(2,3-bis(trifluoromethyl)cyclopentenylene) vinylene]

For this study variations in temperature, concentration, solvent, and even stirring rate were investigated for their effect on trans vinylene content. Although it may never be possible to conclusively stipulate precise requirements that lead to the generation of 100% trans polymer, a series of general criteria are presented which help approach that goal.

The trans contents of the polymers synthesized in this study were measured using quantitative  $^{13}\text{C}$  N.M.R. A relaxation delay of at least five times the value of  $T_1$ , the spin-lattice relaxation constant, was employed, (in this case a period of 20 seconds was found to be sufficient). In order to avoid any nuclear Overhauser contributions to the signals the proton decoupler was gated on during the acquisition, but gated off during the relaxation period.

Trans and cis fractions were then found by integrating both the vinylic and olefinic regions (C1 and C4, and C2 and C3 in figure 2.1), and an average calculated.

#### a) Temperature:

Polymerizations of 2,3-bis(trifluoromethyl)bicyclo[2.2.1]hepta-2,5-diene were carried out at 5°C, 15°C, 25°C, and 50°C in solutions of 80% toluene: 20% tetrahydrofuran (THF) using  $\text{Mo}(\text{NAr})(\text{CHCMe}_2\text{Ph})(\text{OCMe}_3)_2$ .

It was envisaged that at low temperature (and hence at a lower rate of polymerization) the proportion of trans double bonds in the polymer would increase.

As shown in table 2.2, high temperature polymerizations do lead to a significant increase in  $\sigma_c$ . However, there appears to be little gain from polymerizing below room temperature. This is especially so given the decreased rate of propagation at low temperature (and hence reduced reaction yields).

Temperature of polymerization °C	Trans content %
5	98.3
10	99.2
25	98.5
50	93.9

Table 2.2 The trans content in samples of poly[1,4-(2,3-bis(trifluoromethyl)cyclopentylene) vinylene] initiated by  $\text{Mo}(\text{NAr})(\text{CHCMe}_2\text{Ph})(\text{OCMe}_3)_2$  at different temperatures.

b) Solvent:

Previous polymerizations of this system had been conducted in a medium of approximately 80% toluene: 20% THF. The latter component helps solubilize the developing polymer chain in order to keep the polymerization homogeneous.

However, THF may play a more crucial role due to its ability to co-ordinate to electron-deficient metal centres. Although no such adduct formation is observable via  $^1\text{H}$  N.M.R. when 1 equivalent of THF is added to  $\text{Mo}(\text{NAr})(\text{CHCMe}_2\text{Ph})(\text{OCMe}_3)_2$  in benzene- $d_6$ , syn and anti rotamers of  $\text{Mo}(\text{NAr})(\text{CHCMe}_2\text{Ph})(\text{OCMe}(\text{CF}_3)_2)_2(\text{THF})$  can be detected in the analogous experiment with the fluorinated initiator. These isomers are believed to have the same geometry as the analogous trimethylphosphine adducts (figure 2.4).

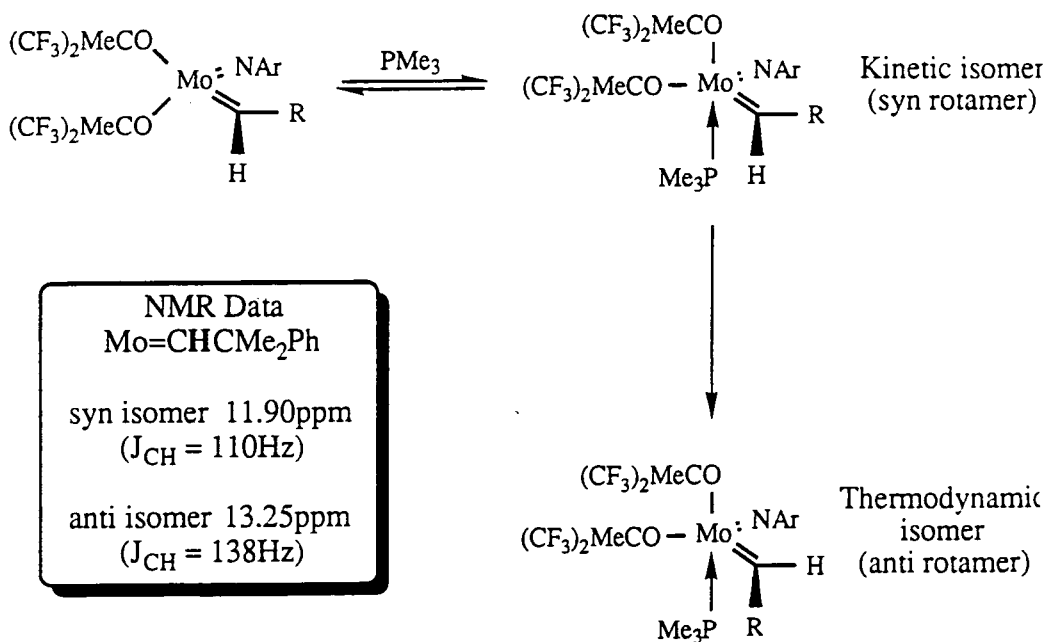


Figure 2.4 Formation of syn and anti isomers of the five-coordinate PMe<sub>3</sub> base adducts of Mo(NAr)(CHCMe<sub>2</sub>Ph)(OCMe(CF<sub>3</sub>)<sub>2</sub>)<sub>2</sub><sup>7</sup>.

The role of co-ordinating solvents in these living R.O.M.P. systems is not completely understood. However, it is known that the formation of base adducts reduces the reactivity of the catalyst (e.g. acetylene can be polymerized in a well-behaved, living fashion by tetra-coordinate neopentylidene complexes of tungsten only in the presence of a strong base such as quinuclidene<sup>8</sup>). It might therefore be expected that at higher concentrations of THF a more controlled polymerization would occur (due to a decreased reaction rate), hence leading to an increase in trans stereoregularity.

In order to study the influence of THF concentration upon polymer structure a series of polymerizations were conducted in different solvent mixtures of toluene and THF.

In neat toluene the polymerization is heterogeneous, the reaction solution turning cloudy soon after monomer addition, eventually resulting in most of the polymer falling out of the solution as a sticky solid which halts the magnetic stirring of the solution. Suspicions of a lower trans content for the resultant isolated homopolymer as a

consequence of decreased control of the reaction are confirmed by  $^{13}\text{C}$  N.M.R. Nonetheless, the recovered polymer is still very highly trans (>96%), which suggests that the mechanism which generates trans vinylene bonds operates with or without the presence of a coordinating solvent. However, higher cis contents have been observed with increasing amounts of monomer under the same conditions.

As the percentage of THF present increases the solutions become less and less cloudy, and at levels above 25% THF the solutions remain clear (obviously at higher concentrations of monomer this will not necessarily be the case). However, at increasing levels of THF content the yields of homopolymer become progressively lower. This is presumably due to the co-ordination of THF to the initiator as described above. Grubbs<sup>9</sup> has recently shown that the reversible binding of  $\text{PMe}_3$  to the corresponding tungsten-based system slows the R.O.M.P. of cyclobutene down to such an extent that polydispersities approach unity since monomer insertion into the propagating chain can only occur in the base-free species.

The trans content of the polymers is summarised in table 2.3. Most significantly, and slightly surprisingly, the decreasing rate associated with increasing THF content has little effect upon the trans content.

Attempts were also made to carry out polymerizations in different solvents, namely ethylene glycol dimethyl ether (dimethoxyethane; DME), methylene chloride, and  $\alpha,\alpha,\alpha$ -trifluorotoluene<sup>10</sup>, (all three of these have been found to be good solvents for poly[1,4-(2,3-bis(trifluoromethyl) cyclopentylene)vinylene]). The polymerization in DME proceeds in a well-behaved manner, with a yield in excess of 90%, under the standard conditions employed throughout the rest of this study. Spectroscopic analysis confirms a very high trans content between 98.5% and 99.0%.

Presumably base adduct formation is not as strong as in neat THF due to the increased size of the solvent molecule. Further the DME fragment can not chelate since a six-coordinate geometry is not accessible, and instead must act as a weak ether ligand.

Percentage of THF by weight	Trans content %	Percentage yield
0	96.4	74.9
10	99.0	81.3
25	98.0	64.7
50	97.7	57.3

Table 2.3 The trans vinylene contents and percentage yields for a series of samples of poly[1,4-(2,3-bis(trifluoromethyl)cyclopentylene)vinylene], prepared in different solvents

Methylene chloride and  $\alpha,\alpha,\alpha$ -trifluorotoluene also give high yields and high trans contents (>98%). Both of these solvents are unlikely to form adducts with the initiator, and in terms of rate are therefore preferable to mixtures of toluene and THF.

Interestingly the polymer recovered from the  $\alpha,\alpha,\alpha$ -trifluorotoluene mediated reaction has the highest trans content yet recorded (>99.6%). Further reactions in  $\alpha,\alpha,\alpha$ -trifluorotoluene confirm that the very high trans content is reproducible (typically polymers are synthesised with  $\sigma_c$  values no greater than 0.01%).

c) Monomer concentration:

0.010g of initiator was used to polymerize 1.00g of the monomer in different quantities of solvent (an 85%:15% mixture of toluene:THF). No major effect upon the stereoregular nature of the polymer was observed. As expected, polymerizations carried out at high concentrations generally gave higher yields than those in more dilute conditions.

A polymerization was also carried out in neat monomer. It was expected that due to the low solubility of the polymer in the fluorinated monomer, the living chain would rapidly fall out of solution. However, this proved not to be the case. Immediately upon addition of the monomer to the solid initiator a deep red colour forms (indicative of the first insertion molybdacyclobutane). After 15 minutes the solution is still red and just

beginning to show an increased viscosity. However, within 90 minutes the reaction mixture is completely solid. Capping with benzaldehyde, followed by isolation of the polymer confirms the high yield of the process (95%), and  $^{13}\text{C}$  N.M.R. spectroscopy reveals a remarkably high trans content of 97.5%.

#### d) Stirring:

Two identical experiments were set up in two  $20\text{cm}^3$  sample vials, each containing 0.010g of  $\text{Mo}(\text{NAr})(\text{CHCMe}_2\text{Ph})(\text{OCMe}_3)_2$  dissolved in  $3\text{cm}^3$  solvent (85% toluene: 15% THF), the only difference being the presence of a 4mm magnetic stirrer flea in one. To both solutions 1.00g 2,3-bis(trifluoromethyl)bicyclo[2.2.1]hepta-2,5-diene in a further  $3\text{cm}^3$  solvent was then added, and the polymerizations allowed to stand overnight, one being stirred, the other not.

It was thought that the lack of stirring would lead to a lower trans content due to the random generation of hot spots in the mixture giving rise to cis vinylene formation in the propagating chain. However, analysis of both polymers showed no apparent decrease in the trans content of the polymer synthesized without stirring (99.0% for the stirred polymer, 98.8% for the non-stirred sample).

Further evidence of the controlled nature of this polymerization is supplied from gel permeation chromatography. The polydispersity ( $M_w/M_n$ ) of the sample prepared without stirring has been measured at just 1.06 (compared to 1.04 for the product of the stirred reaction)

### 2.3.1 Conclusions

As mentioned previously, a method for the reproducible synthesis of 100% trans polymer was not the expected outcome of this study. However, it does appear that the trans content can be increased from 98% by combining the following suggestions.

The solvent of choice would appear to be  $\alpha,\alpha,\alpha$ -trifluorotoluene (although both DME and  $\text{CH}_2\text{Cl}_2$  are also excellent). 5  $\text{cm}^3$  of this allow for 1g of 2,3-bis(trifluoromethyl)bicyclo[2.2.]hepta-2,5-diene to be R.O.M.P.ed by 0.010g of initiator in high yield. Decreasing the reaction temperature has a slight effect upon the trans content, but the decrease in propagation rate arising needs to be borne in mind.

The final observation concerned with the stirring rate verifies just how robust this reaction is to variations in conditions; even very dramatic deviations (e.g. the addition of neat monomer) lead to only slight modifications in the stereoregular nature of the polymer.

## 2.4 The R.O.M.P. of 2,3-bis(trifluoromethyl)bicyclo[2.2.1]hepta-2,5-diene using $\text{Mo}(\text{NAr})(\text{CHCMe}_2\text{Ph})(\text{OCMe}(\text{CF}_3)_2)_2$ as the initiator

As mentioned in section 1.5.4 replacing butoxide ligands upon the metal centre with hexafluorobutoxides results in a more electrophilic alkylidene. Therefore  $\text{Mo}(\text{NAr})(\text{CHCMe}_2\text{Ph})(\text{OCMe}(\text{CF}_3)_2)_2$  is expected to be more reactive towards olefins than  $\text{Mo}(\text{NAr})(\text{CHCMe}_2\text{Ph})(\text{OCMe}_3)_2$ .

In terms of the R.O.M.P. of 2,3-bis(trifluoromethyl)bicyclo[2.2.1]hepta-2,5-diene, it was predicted that the increased reactivity of  $\text{Mo}(\text{NAr})(\text{CHCMe}_2\text{Ph})(\text{OCMe}(\text{CF}_3)_2)_2$  would manifest itself as a decrease in stereochemical selectivity; i.e. a reduction in trans content from 98%.

### 2.4.1 N.M.R. spectroscopic study

Ten equivalents of the fluorinated monomer were added to  $\text{Mo}(\text{NAr})(\text{CHCMe}_2\text{Ph})(\text{OCMe}(\text{CF}_3)_2)_2$  in 700  $\mu\text{l}$  benzene- $\text{d}_6$  and analysed by  $^1\text{H}$  N.M.R.. As expected the alkylidene signal of the initiator was absent, having been replaced by an unresolved multiplet from 12.30 to 12.51 (figure 2.5 insert).

Resolution of these signals is poor due to the low solubility of this polymer in benzene. In THF- $\text{d}_8$  two clearer multiplets are observed, but a detailed assignment has not yet proved possible (shown in figure 2.6).

Comparison of the  $\text{C}_6\text{D}_6$  spectrum with that obtained under similar conditions employing  $\text{Mo}(\text{NAr})(\text{CHCMe}_2\text{Ph})(\text{OCMe}_3)_2$  reveals substantial differences, particularly in the chemical shifts of the broadened polymer resonances.

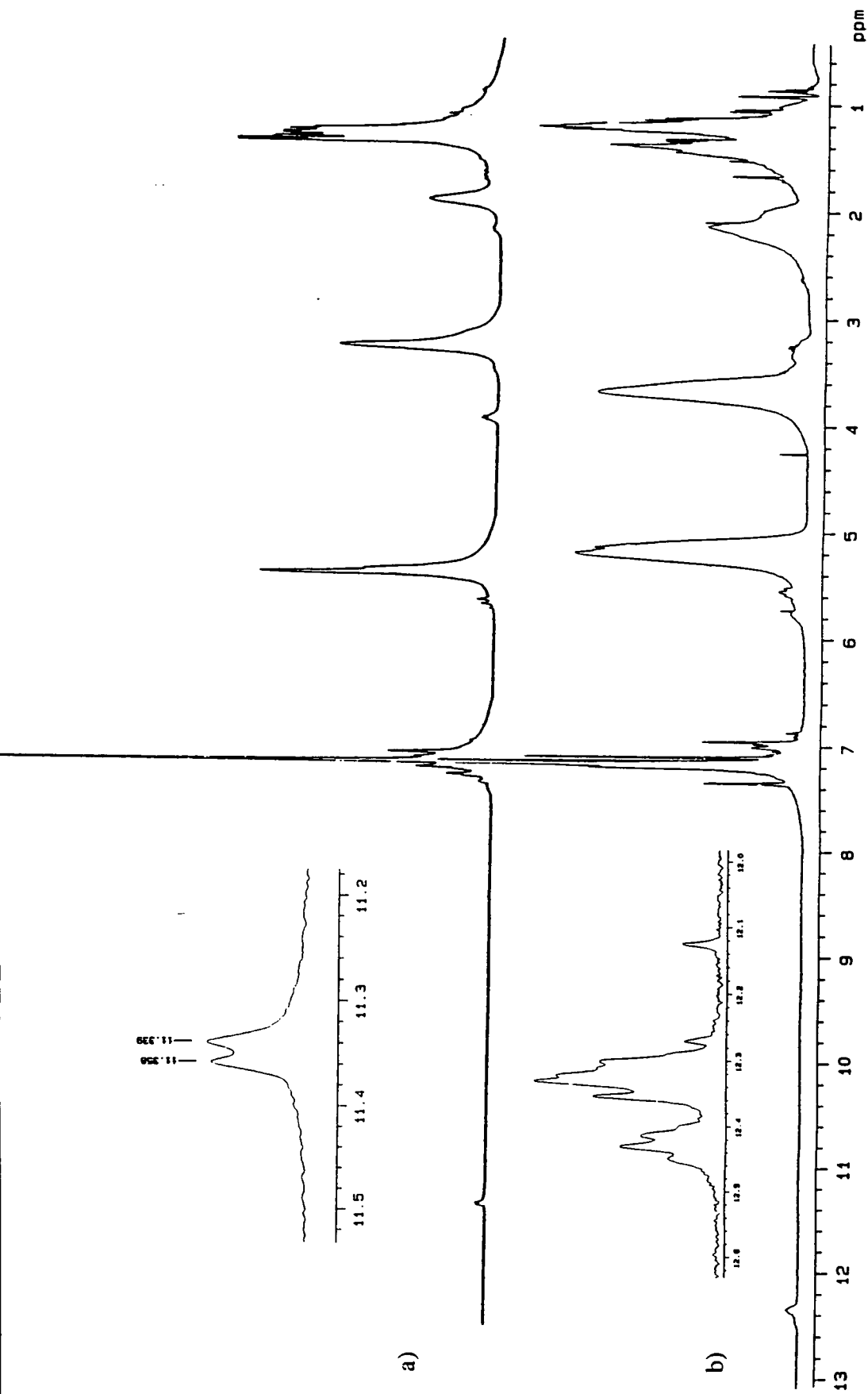


Figure 2.5 The <sup>1</sup>H N.M.R. spectra (C<sub>6</sub>D<sub>6</sub>) of living poly[1,4-(2,3-bis(trifluoromethyl)cyclopentenylene) vinylene] initiated by  
 a) Mo(NAr)(CHCMe<sub>2</sub>Ph)(OCMe<sub>3</sub>)<sub>2</sub> b) Mo(NAr)(CHCMe<sub>2</sub>Ph)(OCMe(CF<sub>3</sub>)<sub>2</sub>)<sub>2</sub>

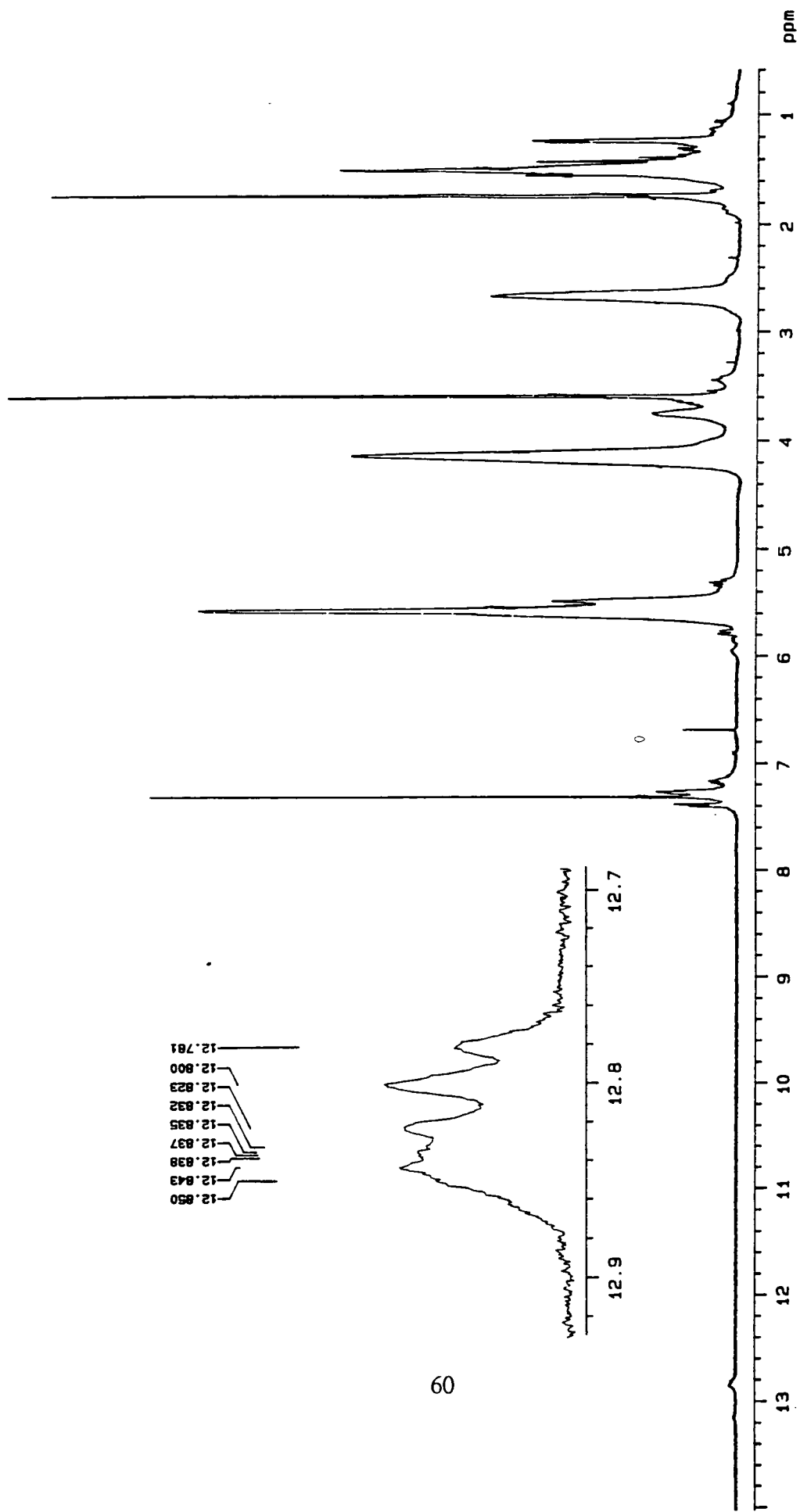


Figure 2.6  $^1\text{H}$  N.M.R. spectrum (THF- $D_8$ ) of living poly[1,4-(2,3-bis(trifluoromethyl)cyclopentenylene) vinylene] initiated by  $\text{Mo}(\text{NAr})(\text{CHCMe}_2\text{Ph})(\text{OCMe}(\text{CF}_3)_2)_2$

In order to investigate the reaction further, a small scale polymerization (1g monomer : 0.0010g Mo(NAr)(CHCMe<sub>2</sub>Ph)(OCMe(CF<sub>3</sub>)<sub>2</sub>)<sub>2</sub>) was performed in THF. After 24 hours the reaction was terminated by the addition of a large excess of benzaldehyde (50μl). Precipitation from hexane<sup>11</sup> yielded a pale yellow powder which was isolated and analysed by <sup>13</sup>C N.M.R. (figure 2.7).

Comparison of the <sup>13</sup>C spectrum with that of the high trans analogue shows that the switch from butoxide to hexafluorobutoxide ligands in the initiator results in a remarkable reversal in the cis content of the polymer produced. The fluorinated polymer now contains in excess of 98% *cis* unsaturated bonds!

Although cases of major variations in polymer structure with subtle changes in metal environment or reaction conditions are widely documented for classical transition metal / Lewis acid cocatalyst systems, to the author's knowledge only one other, (far less dramatic), case of this phenomenon has been observed with well-defined initiators<sup>12</sup>.

Note the multiplicity of the C7 methylene region in the high cis sample; the explanation for this, and its full implications, will be discussed in chapter three.

The acetone-d<sub>6</sub> <sup>1</sup>H N.M.R. spectra for both trans and cis poly[1,4-(2,3-bis(trifluoromethyl)cyclopentenylene) vinylene] are also shown (figure 2.8). Note the clear difference between the cis and trans allylic protons (4.2 and 3.8ppm respectively). Integration of these gives good agreement with the values for  $\sigma_c$  determined by integration of the <sup>13</sup>C N.M.R. signals.

The <sup>19</sup>F N.M.R. spectrum of 98% trans poly[1,4-(2,3-bis(trifluoromethyl)cyclopentenylene)vinylene] consists of a simple single resonance (although at high frequency further signals are discernible). However, the corresponding spectrum for the high cis polymer is much more complex (figure 2.9). This spectrum is discussed fully in section 3.4.3; as will be shown, it is no coincidence that the polymeric stereoisomer with the more complex <sup>19</sup>F spectrum also gives rise to the more complicated methylene (C7) region in its <sup>13</sup>C trace.

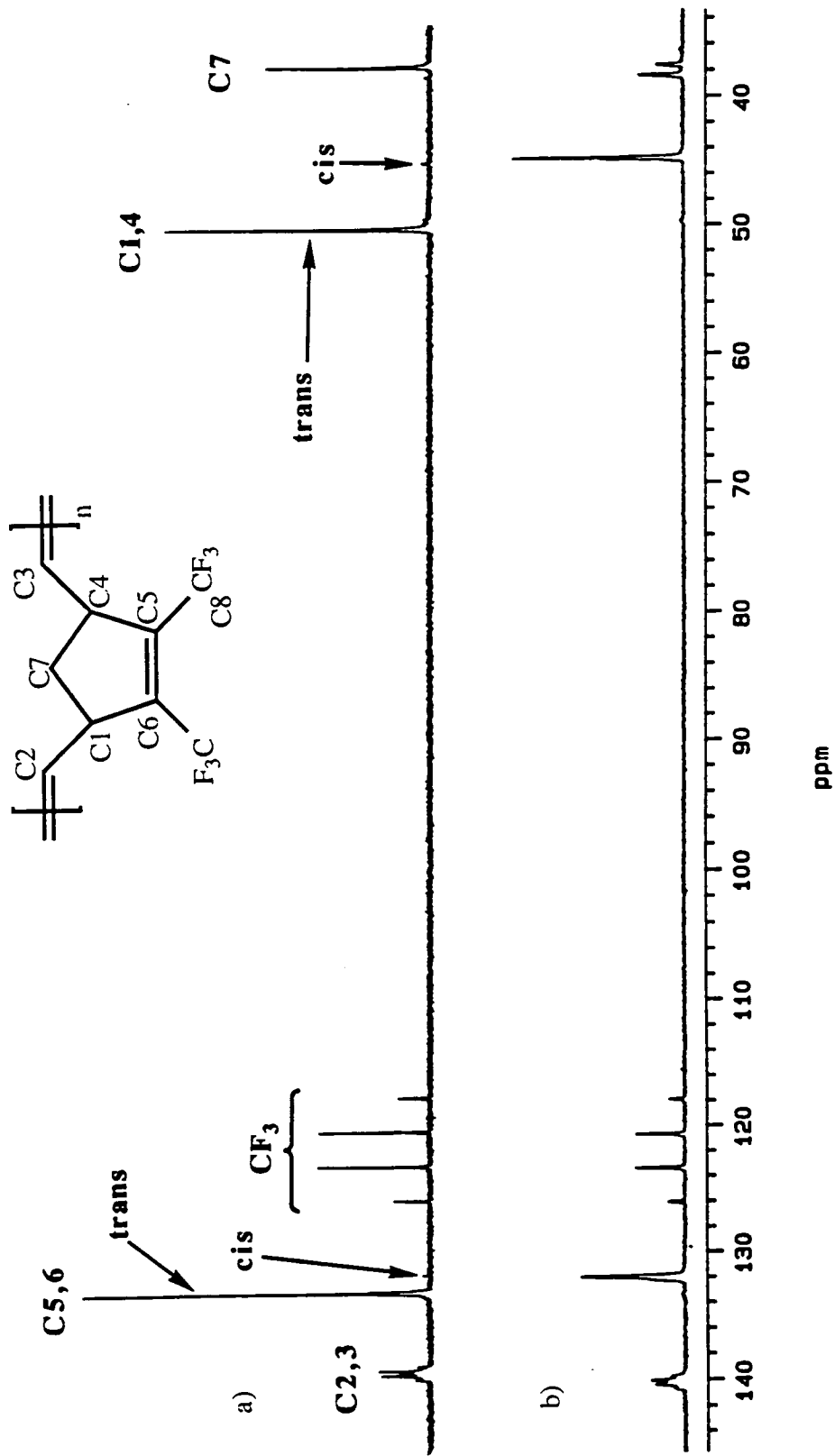


Figure 2.7 The  $^{13}\text{C}$  N.M.R. spectra (( $\text{CD}_3$ ) $_2\text{CO}$ ) of poly[1,4-(2,3-bis(trifluoromethyl)cyclopentylene)vinylene] initiated by  
 a)  $\text{Mo}(\text{NAr})(\text{CHCMe}_2\text{Ph})(\text{OCMe}_3)_2$  b)  $\text{Mo}(\text{NAr})(\text{CHCMe}_2\text{Ph})(\text{OCMe}_3)_2$

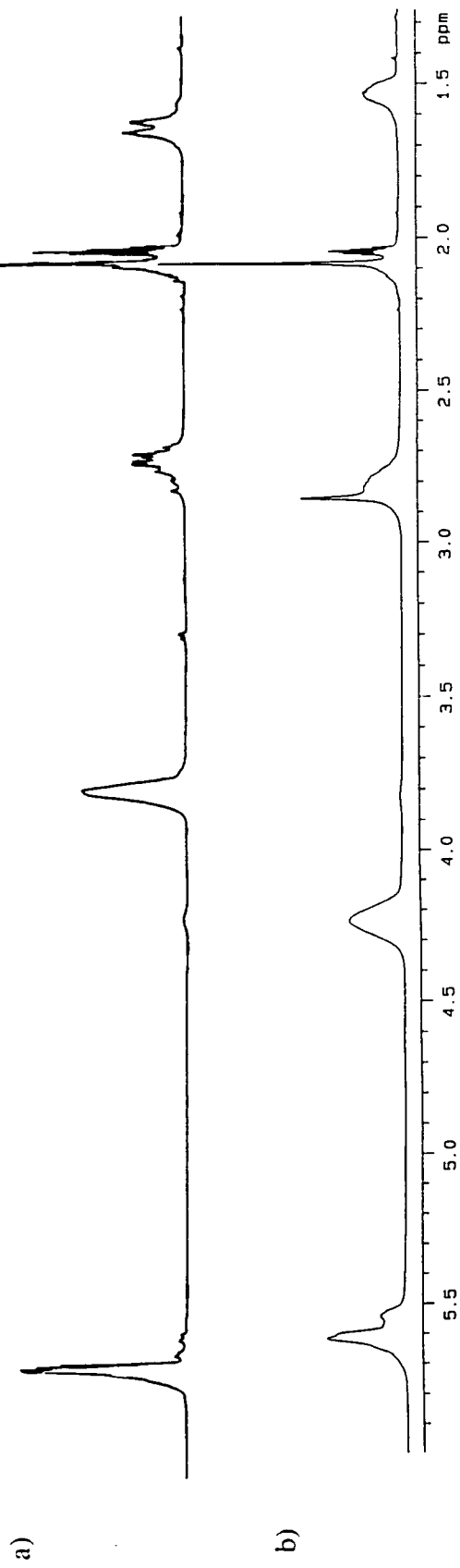


Figure 2.8 <sup>1</sup>H N.M.R. spectra ((CD<sub>3</sub>)<sub>2</sub>CO) of poly[1,4-(2,3-bis(trifluoromethyl)cyclopentenylene) vinylene] initiated by  
 a) Mo(NAr)(CHCMe<sub>2</sub>Ph)(OCMe<sub>3</sub>)<sub>2</sub> b) Mo(NAr)(CHCMe<sub>2</sub>Ph)(OCMe(CF<sub>3</sub>)<sub>2</sub>)<sub>2</sub>

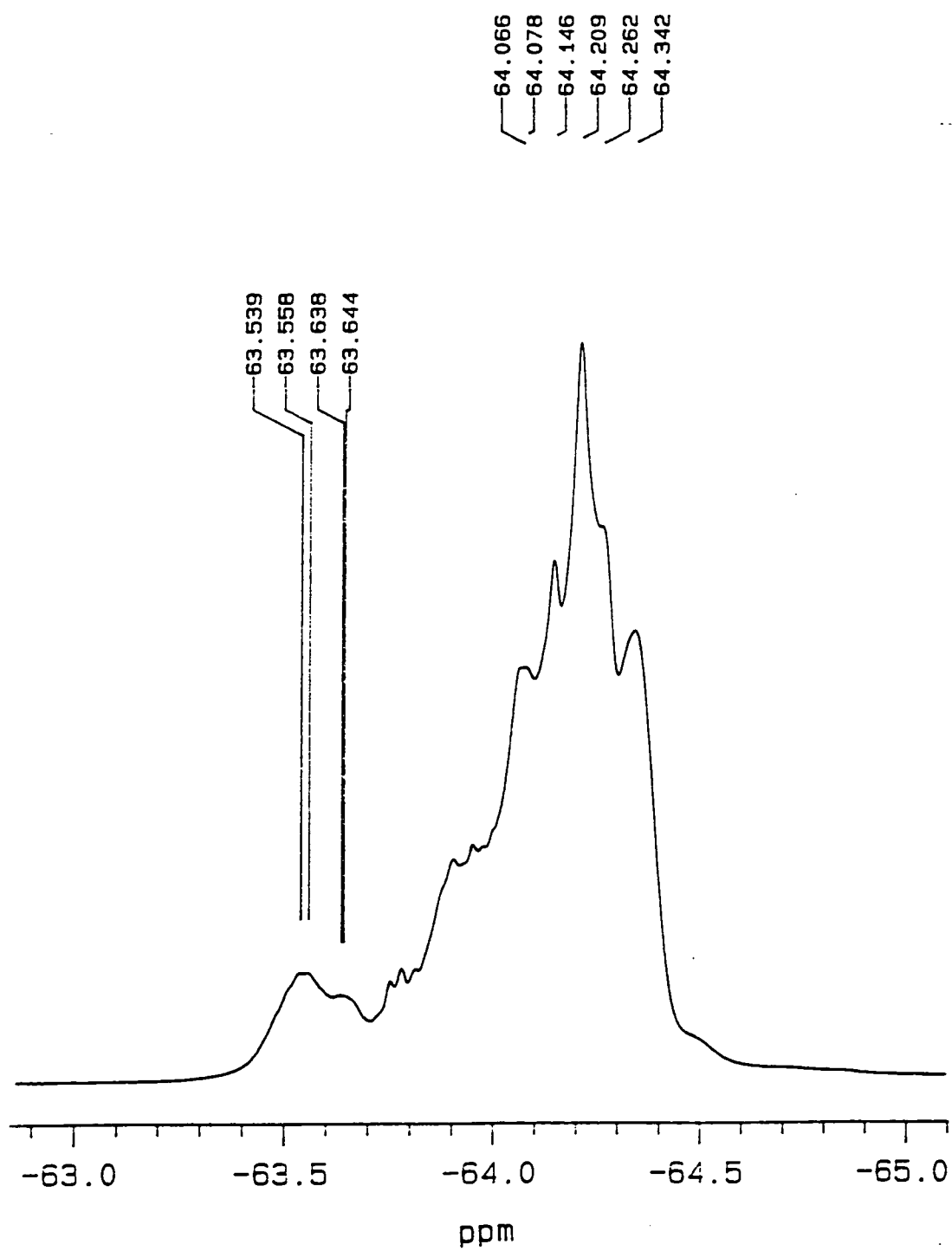


Figure 2.9 The 370MHz  $^{19}\text{F}$  N.M.R. spectrum  $\{(\text{CD}_3)_2\text{CO}\}$  of 98% cis poly[1,4-(2,3-bis(trifluoromethyl)cyclopentenylene) vinylene]

### 2.4.3 Molecular weight distribution

Gel Permeation Chromatographic studies on the R.O.M.P. of 2,3-bis(trifluoromethyl)bicyclo[2.2.1]hepta-2,5-diene using  $\text{Mo}(\text{NAr})(\text{CHCMe}_2\text{Ph})(\text{OCMe}(\text{CF}_3)_2)_2$  testify to the living nature of the polymerization, with essentially monodisperse molecular weight distributions observed (typically values in the range 1.04-1.10). Addition of 51.1 equivalents of the monomer to a rapidly stirring solution of initiator in THF (initiator concentration =  $8.26 \times 10^{-3} \text{ mol dm}^{-3}$ ) shows that after 4 hours most of the monomer is consumed, table 2.4.

Time (hours)	$M_n$ observed	Polydispersity ( $M_n/M_w$ )
2	5,500	1.04
4	9,770	1.03
8	10,230	1.05
24	11,220	1.06

Table 2.4 Gel permeation chromatographic study of the polymerization of 51.1 equivalents of 2,3-bis(trifluoromethyl)bicyclo[2.2.1]hepta-2,5-diene with  $0.0214 \text{ g Mo}(\text{NAr})(\text{CHCMe}_2\text{Ph})(\text{OCMe}(\text{CF}_3)_2)_2$  in  $3.000 \text{ g THF}$ .  $M_n$  calculated = 11,650

If the ring-opening polymerization is allowed to stir for 24 hours before addition of a capping agent (typically benzaldehyde) a small tail-off towards high molecular weight is observable on the GPC trace. This is accompanied by a slight increase in the polydispersity ( $M_n/M_w = 1.10$ ). If the reaction is stirred for 48 hours, the trace becomes obviously bimodal, with approximately 5-10% high molecular weight impurity occurring at twice the molecular weight for the major polymeric component; an example of just such a trace is shown in figure 2.10. This is in accordance with an oxygen-mediated bimolecular termination step, and will be discussed further in chapter five<sup>13</sup>.

#### 2.4.4 Differential Scanning Calorimetry analysis:

D.S.C. studies reveal a well-defined glass transition at 141.7°C for the high cis polymer. This figure has been confirmed by Dr. H. Hubbard who has determined a T<sub>g</sub> value of 144°C via thermally stimulated current (T.S.C.) measurements.

However, no detection of a melting endotherm below 250°C has been made, despite overnight annealing at 150°C.

## 2.5 A kinetic study on the metathesis polymerization of 2,3-bis(trifluoromethyl)bicyclo[2.2.1]hepta-2,5-diene

It has previously been shown that for an initial monomer concentration  $[M]_0$  and an initial initiator concentration  $[I]_0$ ...

$$\frac{[M]_0}{[I]_0} + \frac{k_p}{k_i} \ln \left\{ \frac{[I]}{[I]_0} \right\} + \left\{ 1 - \frac{k_p}{k_i} \right\} \left\{ \frac{[I]}{[I]_0} - 1 \right\} = 0$$

...where  $k_p$  and  $k_i$  are the rates of propagation and initiation respectively<sup>14,15</sup>.

When the initiator employed is  $\text{Mo}(\text{NAr})(\text{CHCMe}_2\text{Ph})(\text{OCMe}(\text{CF}_3)_2)_2$  the ratio  $[M]_0 / [I]_0$ , (the number of equivalents of monomer) can be determined by  $^{19}\text{F}$  N.M.R. spectroscopy, whilst the value of  $[I] / [I]_0$ , (i.e. the ratio of unreacted initiator to the total living species) can be found from the alkylidene region in the  $^1\text{H}$  N.M.R. spectrum. As a consequence  $k_p / k_i$  can be determined, and hence the measurement of  $k_p$  by usual kinetic techniques allows for the value of  $k_i$  to be found. Table 2.5 summarises the values of  $k_p / k_i$  for three initiators with this monomer in benzene- $d_6$ .

The rate of propagation of 2,3-bis(trifluoromethyl)bicyclo[2.2.1]hepta-2,5-diene was also measured using  $^{19}\text{F}$  N.M.R. A typical polymerization was performed in a dry-box, and at set intervals a small aliquot was withdrawn, capped and analysed for the proportion of remaining monomer to polymer. Non-deuterated benzene was employed as the solvent, along with a small amount of  $\alpha,\alpha,\alpha$ -trifluorotoluene (to act as an internal reference for the  $^{19}\text{F}$  N.M.R. spectra and to help keep the polymerization homogenous).

Initiator	$k_p / k_i$
$\text{Mo}(\text{NAr})(\text{CHCMe}_2\text{Ph})(\text{OCMe}(\text{CF}_3)_2)_2$	0.91
$\text{Mo}(\text{NAr})(\text{CHCMe}_3)(\text{OCMe}(\text{CF}_3)_2)_2$	2.63
$\text{Mo}(\text{NAr})(\text{CHCMe}_3)(\text{OCMe}_3)_2$	0.72

Table 2.5 The ratio of rate constant of propagation to rate constant of initiation for a series of well-defined molybdenum initiators with 2,3-bis(trifluoromethyl)bicyclo[2.2.1]hepta-2,5-diene in benzene- $d_6$ .

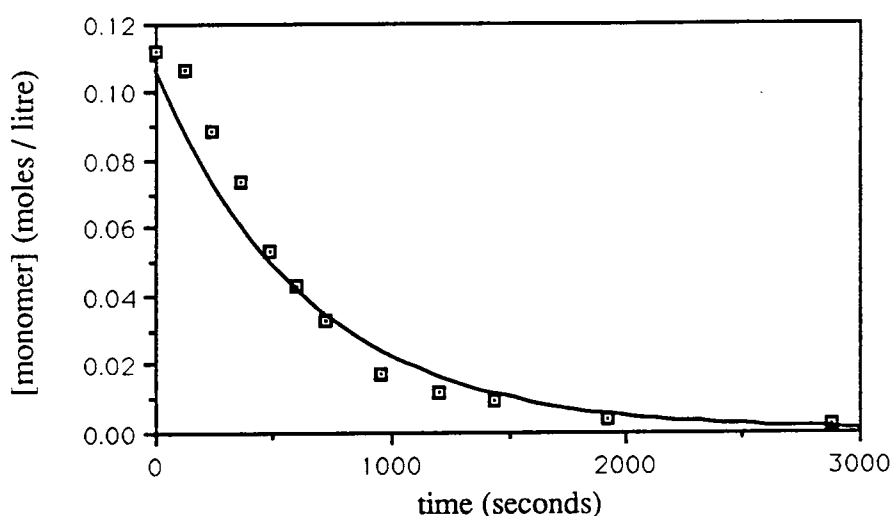


Figure 2.11: A plot of monomer concentration with time (concentration in  $\text{mol dm}^{-3}$ ) for the R.O.M.P. of 2,3-bis(trifluoromethyl)bicyclo[2.2.1]hepta-2,5-diene with  $\text{Mo}(\text{NAr})(\text{CHCMe}_2\text{Ph})(\text{OCMe}(\text{CF}_3)_2)_2$ .

For the analysis of this data first-order kinetics were assumed (this seems reasonable given the near-linear nature of figure 2.12, derived from the plot in figure 2.11).

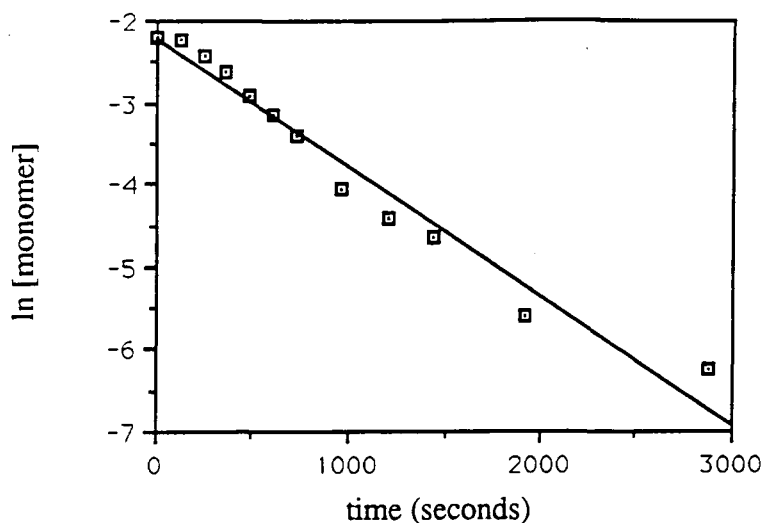


Figure 2.12 A plot of ln (monomer concentration) against time.

The data presented above leads to a  $k_p$  value of  $0.62\text{M}^{-1}\text{s}^{-1}$  for  $\text{Mo}(\text{NAr})(\text{CHCMe}_2\text{Ph})(\text{OCMe}(\text{CF}_3)_2)_2$ , and hence  $k_i = 0.68\text{M}^{-1}\text{s}^{-1}$ . For the corresponding neopentylidene initiator  $k_i = 0.24\text{M}^{-1}\text{s}^{-1}$ . The difference in these two initiation parameters reflects the subtle steric effects that are at work in this system. In the neophylidene case the planar phenyl ring can orientate itself in such a way so as to present less of an obstacle to the incoming monomer molecule than the  $\beta$ -methyl groups can in the neopentylidene group.

Initiator	$k_p / k_i$	$k_p / \text{M}^{-1}\text{s}^{-1}$	$k_i / \text{M}^{-1}\text{s}^{-1}$
$\text{Mo}(\text{NAr})(\text{CHCMe}_3)(\text{OCMe}_3)_2$	0.72	0.057	0.079
$\text{Mo}(\text{NAr})(\text{CHCMe}_3)(\text{OCMe}(\text{CF}_3)_2)_2$	2.63	0.62	0.24
$\text{Mo}(\text{NAr})(\text{CHCMe}_2\text{Ph})(\text{OCMe}_3)_2^{16}$	-	0.057	-
$\text{Mo}(\text{NAr})(\text{CHCMe}_2\text{Ph})(\text{OCMe}(\text{CF}_3)_2)_2$	0.91	0.62	0.68

Table 2.6: Summary of kinetic parameters for bis(butoxide) and bis(hexafluorobutoxide) molybdenum initiators with 2,3-bis(trifluoromethyl)bicyclo[2.2.1]hepta-2,5-diene {solvent = benzene (with a quantity of  $\alpha,\alpha,\alpha$ -trifluorotoluene for  $k_p$  determinations)}

More noticeable is the dramatic variation in  $k_p$  between the hexafluorobutoxide initiators and the non-fluorinated tert-butoxide analogues.  $\text{Mo}(\text{NAr})(\text{CHCMe}_2\text{Ph})(\text{OCMe}_3)_2$  has been reported to have a propagation rate constant of  $5.7 \times 10^{-2} \text{M}^{-1} \text{s}^{-1}$ , i.e. over an order of magnitude slower than  $\text{Mo}(\text{NAr})(\text{CHCMe}_2\text{Ph})(\text{OCMe}(\text{CF}_3)_2)_2$ . Similarly the rate of initiation of the neopentylidene bis(butoxide) initiator with 2,3-bis(trifluoromethyl)bicyclo[2.2.1]hepta-2,5-diene ( $k_i = 7.9 \times 10^{-2} \text{M}^{-1} \text{s}^{-1}$ ) is much slower than for the analogous fluorinated complex.

## 2.6 The R.O.M.P. of 2,3-bis(trifluoromethyl)bicyclo[2.2.1]hepta-2,5-diene using $\text{Mo}(\text{NAr})(\text{CHCMe}_3)(\text{OCMe}_2\text{CF}_3)_2$ as the initiator.

Having established that the bis(butoxide) initiator leads to very high trans poly[1,4-(2,3-bis(trifluoromethyl)cyclopentenylene) vinylene], whereas very high cis material is accessible from the hexafluorobutoxide parallel, attention shifted to the bis((trifluoromethyl)butoxide) complex. The following section briefly summarises the polymerization of the fluorinated monomer using  $\text{Mo}(\text{NAr})(\text{CHCMe}_3)(\text{OCMe}_2\text{CF}_3)_2$ . However, since the polymer isolated from this reaction is of rather less interest than the trans and cis examples, the account that follows is considerably less detailed than previous sections.

Figure 2.13 shows the  $^1\text{H}$  N.M.R. spectrum obtained upon the addition of ten equivalents of the monomer to  $\text{Mo}(\text{NAr})(\text{CHCMe}_3)(\text{OCMe}_2\text{CF}_3)_2$  in benzene- $d_6$ . Contrasting this with figure 2.5 suggests that the trans content (resonance at 5.40ppm) is approximately 60-70%; a figure of 65% is confirmed using quantitative  $^{13}\text{C}$  N.M.R. on the recovered polymer (figure 2.14). As in the very high cis polymer, the methylene region is no longer just one signal.

The system displays all of the characteristics associated with a living polymerization. In general the molecular weight distributions are unimodal and narrow (representative molecular weight distributions of 1.05 - 1.10). However, as with the other fluorinated initiator the presence of a small amount of dimerized polymer can be detected in samples prepared with prolonged stirring.

The polymer derived from this partially-fluorinated initiator has a glass transition temperature of  $112.3^\circ\text{C}$ , as measured by differential scanning calorimetry, but possesses no observed melting endotherms.

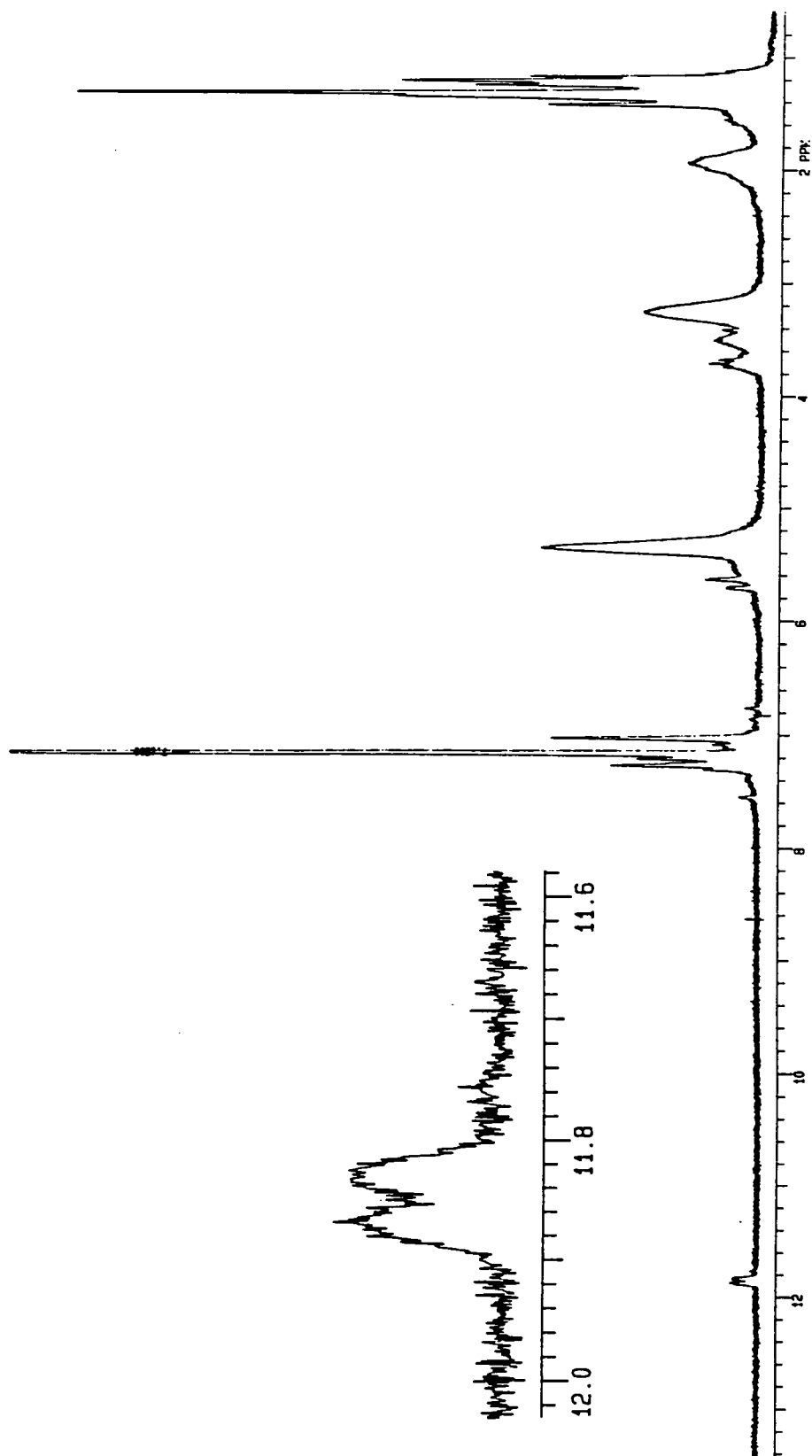


Figure 2.13 The  $^1\text{H}$  N.M.R. spectrum of  $\text{Mo}(\text{NAr})(\text{CHCMe}_3)(\text{OCMe}_2\text{CF}_3)_2$   
+ 10 equivalents 2,3-bis(trifluoromethyl)bicyclo[2.2.1]hepta-2,5-diene

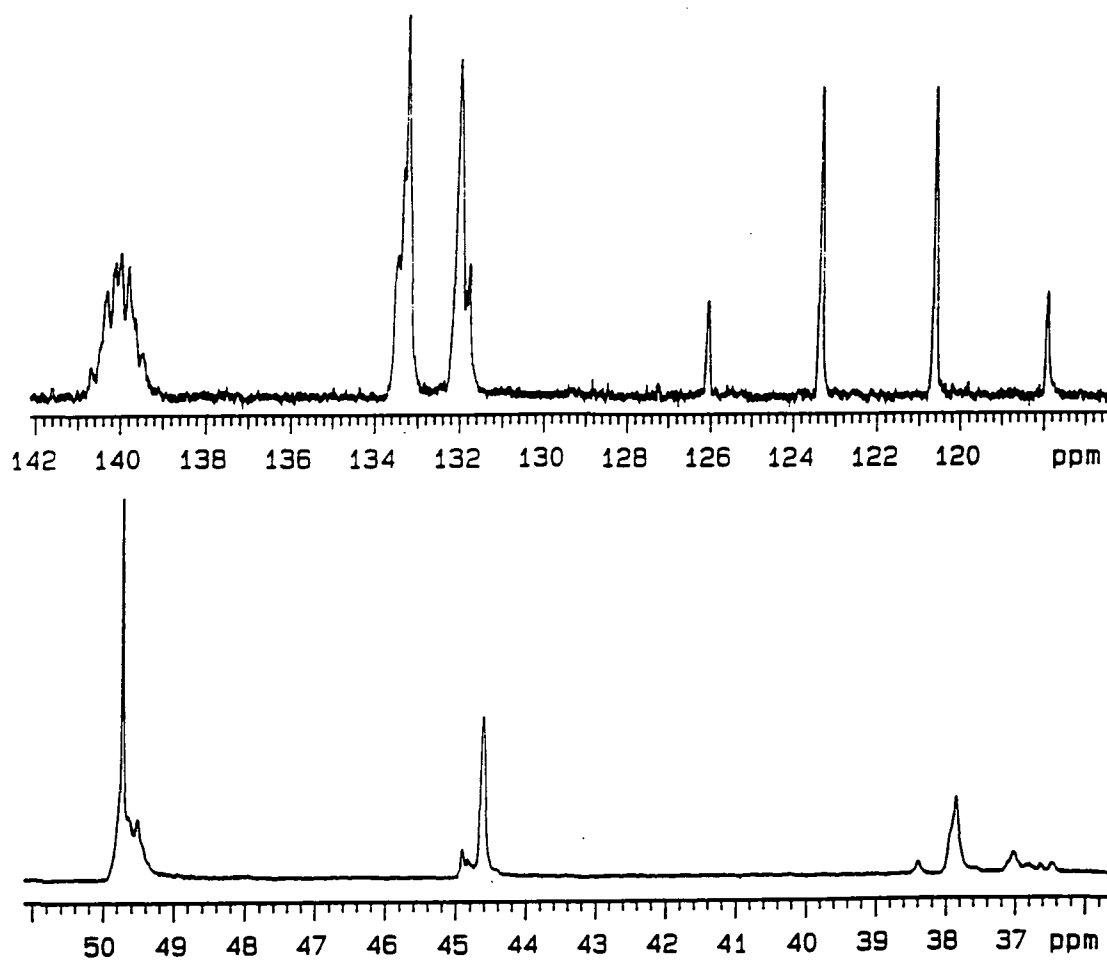


Figure 2.14 The 100MHz  $^{13}\text{C}$  N.M.R. spectrum  $\{(\text{CD}_3)_2\text{CO}\}$  of poly[1,4-(2,3-bis (trifluoromethyl)cyclopentenylene) vinylene] initiated by  $\text{Mo}(\text{NAr})(\text{CHR})(\text{OCMe}_2\text{CF}_3)_2$

## 2.7. Dielectric measurements and the microstructure of high trans poly[1,4-(2,3-bis(trifluoromethyl)cyclopentenylene) vinylene]

In the original communication on the metathesis polymerization of 2,3-bis(trifluoromethyl) bicyclo[2.2.1]hepta-2,5-diene with  $\text{Mo}(\text{CHCMe}_3)(\text{NAr})(\text{OCMe}_3)_2$ , no evidence was presented for the predominance of either trans syndio- or trans iso-tactic structure. As can be seen from figure 2.15 the two possibilities should display contrasting electrical properties (rather like poly(vinylidene fluoride) and poly(ethylene-co-tetrafluoroethylene), as discussed in section 1.7.2). In the isotactic case, the polar  $\text{CF}_3$  groups alternate from one side of the backbone to the other, whilst substantial alignment of the dipoles would be expected in the trans syndiotactic structure.

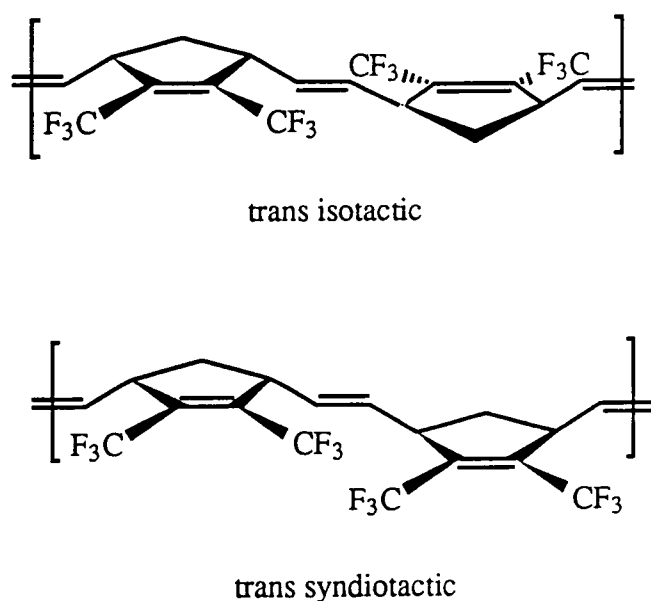


Figure 2.15: The two possible trans tactic structures of poly[1,4-(2,3-bis(trifluoromethyl)cyclopentenylene)vinylene]

Similarly, if either of the two cis tactic forms dominates then large differences would be expected in their electrical properties. In the cis-syndiotactic structure, the

fluorinated substituents would be expected to cancel out each other's dipolar effects, whilst a cis-isotactic conformation would align dipoles rather like in the trans syndiotactic form described above.

Dielectric measurements have been carried out upon a series of samples of poly[1,4-(2,3-bis(trifluoromethyl)cyclopentenylene) vinylene] by Dr. G.R. Davies and Dr. H. Hubbard at the University of Leeds. The limiting value of the relaxed,  $\epsilon_R$ , and the unrelaxed,  $\epsilon_U$ , dielectric constants (measured above and below  $T_g$  respectively) are shown in table 2.7, alongside the  $\epsilon_R$  values obtained via thermally stimulated current (T.S.C) measurements. No significant difference was observed for  $\epsilon_U$  across all the materials (values range from 2.45 - 2.75, and all the figures in the table are adjusted to an  $\epsilon_U$  value of 2.60). The sample produced from the bis(butoxide) initiator with a trans content of just 86% was produced accidentally during a large scale synthesis (8g) in toluene.

$\sigma_t$	Initiator	$\epsilon_U$	$\epsilon_R$	$\epsilon_R$ (T.S.C.)	$\frac{\epsilon_R}{\epsilon_U}$	max tan $\delta$
0.02	[Mo](OCMe(CF <sub>3</sub> ) <sub>2</sub> )	2.6	-	7.0	2.69	-
0.54	WCl <sub>6</sub> / Me <sub>4</sub> Sn	2.6	13.8	15.8	6.08	0.45
0.86	[Mo](OCMe <sub>3</sub> ) <sub>2</sub>	2.6	30.4	33.4	12.85	0.76
0.98	[Mo](OCMe <sub>3</sub> ) <sub>2</sub>	2.6	45.8	49.9	19.19	0.95

Table 2.7 Preliminary dielectric measurements upon  
poly[1,4-(2,3-bis(trifluoromethyl)cyclopentenylene) vinylene]

The maximum values of tan  $\delta$ , the mechanical loss tangent (the ratio of the loss modulus to the shear modulus) are included in the table. This parameter increases with trans content and is typically high, and confirms the  $\epsilon_R$  value obtained for the 98% trans material; single frequency Debye theory<sup>17</sup> states that tan  $\delta$  is directly proportional

to  $\left\{ (\epsilon_R - \epsilon_U) / 2 \sqrt{\epsilon_R \epsilon_U} \right\}$ . Figure 2.16 shows a typical plot of dielectric constant as a function of temperature and frequency for the highly trans polymer.

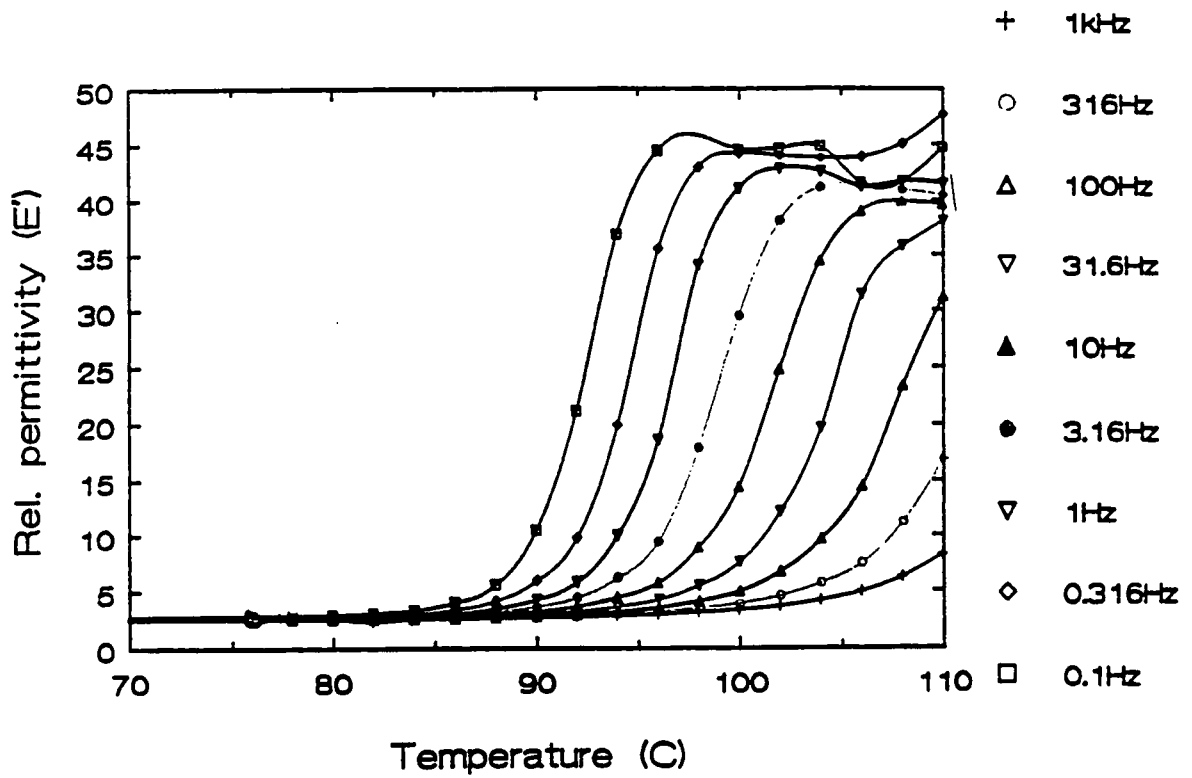


Figure 2.16

These samples have also been poled and their polarizations determined via T.S.C. recordings. In each case a sharp single peak is observable corresponding to the glass transition temperature, which is also seen in D.M.T.A. experiments. The tensile stress of the 98% trans material drops by three orders of magnitude on heating through its  $T_g$  temperature, which implies the presence of a low degree of crystallinity.

Integrating the T.S.C. with time gives the total charge released ( $\Delta Q$ ) and thence the polarization, the charge per unit area ( $\Delta P = \Delta Q / A$ ). The figures obtained from T.S.C. depoles are shown as a function of the poling field in figure 2.17. The curved appearance of the plots toward higher field is indicative of the onset of saturation of the polarization.

In order to understand the origin of the high dielectric constant of the 98% trans polymer computer modelling of the structure was carried out using several software packages. The Biosym modelling program has been used to explore adjacent ring conformations. By progressively advancing the structures about the allylic-vinyl carbon bond by a few degrees and then mapping out the energy contours obtained four minima have been identified, separated by approximately  $180^\circ$ .

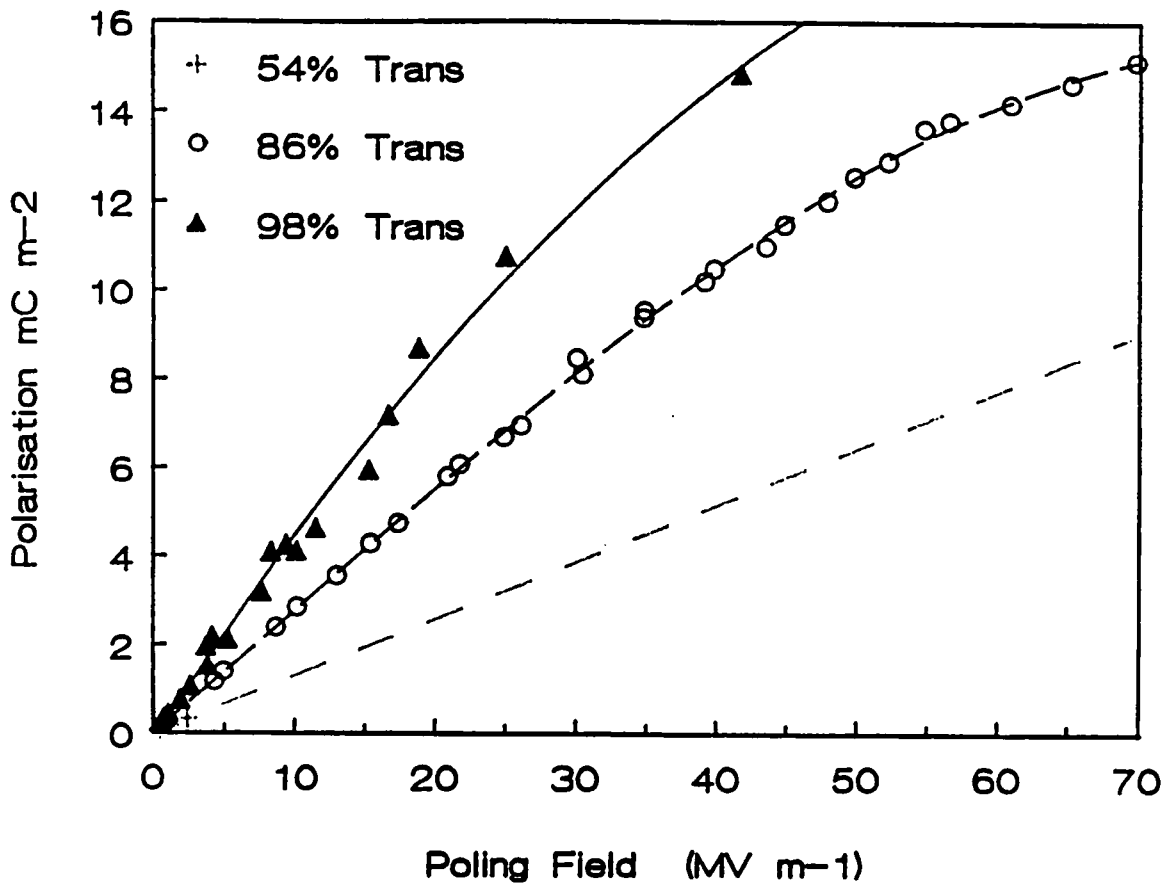


Figure 2.17

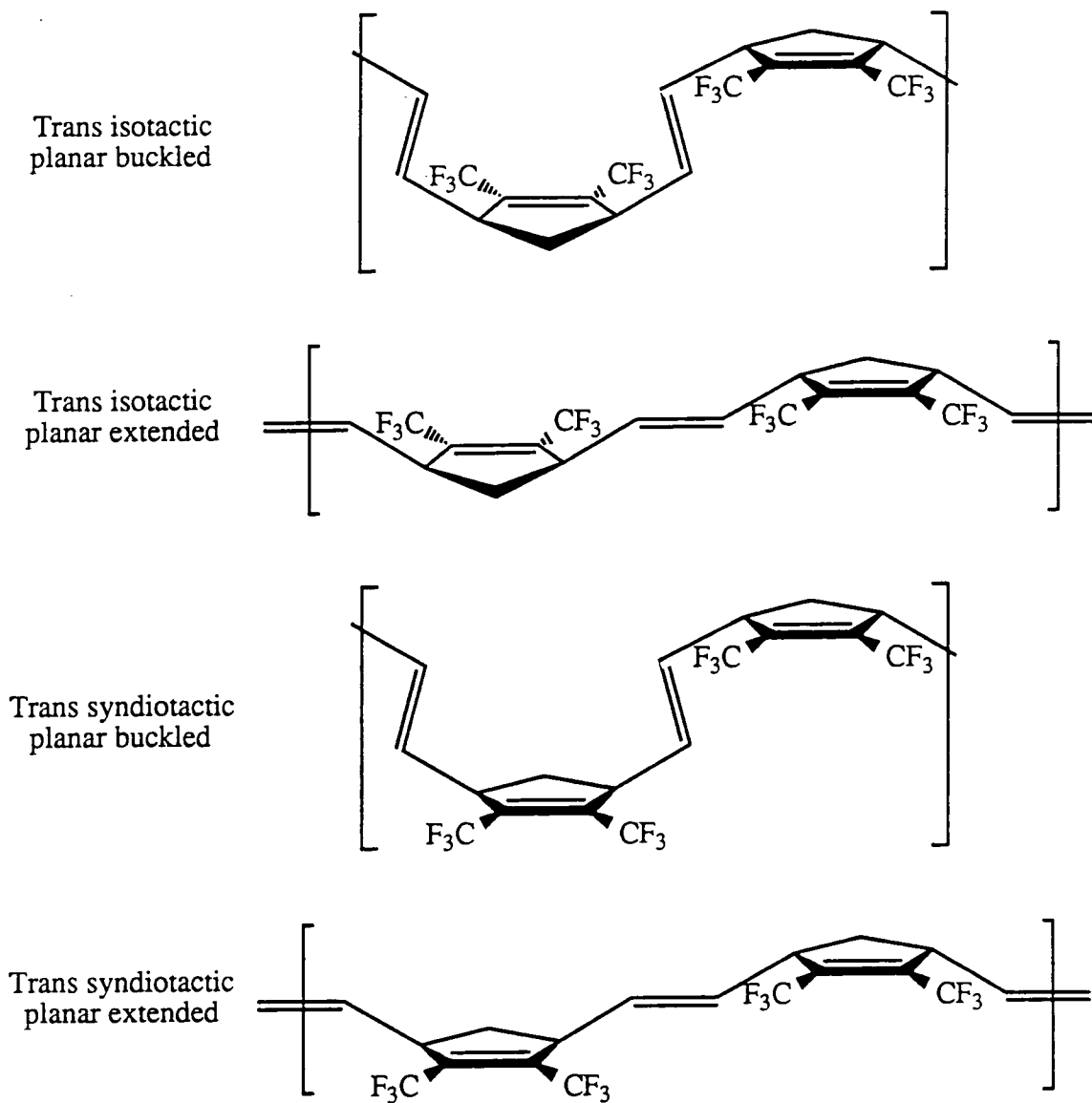


Figure 2.18 The four trans geometry energy minimizing conformations

For either trans iso- or trans syndio-tactic the four architectures available are a planar-extended, a planar-buckled, and two helical conformations. The latter two do not pack well and are immediately discarded since they would give much lower densities than are observed.

In order to determine experimentally the dipole moment of the polymer, and hence conclude which of the four conformations is adopted, it is necessary to introduce the Fröhlich form<sup>18</sup> of the Onsager equation which states:

$$\frac{(\epsilon_R - \epsilon_U)(2\epsilon_R + \epsilon_U)}{\epsilon_R(\epsilon_U + 2)^2} = \frac{n g \mu^2}{9\epsilon_0 k T} \quad (\text{Equation 2.1})$$

where  $\mu$  is the permanent dipole moment of the molecule in a vacuum,  $n$  is the number of dipoles per unit volume, and  $g$  is the Kirkwood 'g-factor', which is a correlation term used to take account of local order. If each dipole acts independently of its neighbours, then  $g$  equals unity<sup>17</sup>.

The  $g$ -factor can be found by calculating  $\mu$  for  $g = 1$  in equation 2.1. Assuming that the 54% trans material is effectively atactic (i.e. the dipoles are uncorrelated) implies that the  $g$ -factor values for all the other polymer stereoisomers should give the same value for  $\mu$  as that determined for the 54% trans sample. This dipole has been found to be 3.84D, and the resultant  $g$ -factors are tabulated below (table 2.8).

$\sigma_t$	$\epsilon_U$	$\epsilon_R$	$\mu$ (D) ( $g = 1$ )	$g$ ( $\mu = 3.84\text{D}$ )
0.02	2.6	7.0	2.39	0.39
0.54	2.6	15.8	3.84	1.00
0.86	2.6	33.4	5.61	2.13
0.98	2.6	49.9	6.84	3.17

Table 2.8 Kirkwood  $g$ -factor values determined for  
poly[1,4-(2,3-bis(trifluoromethyl)cyclopentenylene) vinylene]

The large  $g$ -factor found for the 98% trans polymer indicates that there is strong local correlation between adjacent dipoles involving 2 to 4 nearest neighbours). Such a situation could only arise from either a trans syndiotactic planar-extended or planar-buckled, or from either of the trans isotactic helical structures conformations.

Wide-angle X-ray diffraction (WAXD) measurements upon drawn fibres of the high trans polymer reveal a  $d(002)$  spacing of  $6.5\text{\AA}$ <sup>19</sup>. The repeat unit of two monomer

units is therefore  $13\text{\AA}$ , which from the modelling analysis could only be achieved in the planar-extended trans syndiotactic conformation (the Biosym package predicts a value of  $12.2\text{\AA}$ ).

As will be shown in chapter three, the 98% polymer is 92% tactic (a figure determined via  $^{13}\text{C}$  N.M.R. spectroscopy). Dielectric measurements have also been carried out upon the 99.6% trans polymer synthesised from the bis(butoxide) initiator in  $\alpha,\alpha,\alpha$ -trifluorotoluene. Since the value of the dipole moment is controlled by the average length of unbroken sequences of aligned adjacent dipoles, increasing the trans content from 98% (1 cis double bond to every 50 trans) to 99.6% (1 cis junction for every 250 trans) might be expected to have a dramatic effect upon the electrical properties.

However, this is not observed. Indeed, no significant difference was observed in any of the dielectric, T.S.C. or pyroelectric measurements carried out. The conclusion drawn is that the level of tacticity is the controlling factor in determining the values of the dipole moment and the Kirkwood  $g$ -factor. If the stereoregularity and the trans content could be refined toward 100%, then  $\epsilon_R$ ,  $\mu$ , and  $g$  could increase considerably<sup>20</sup>.

The high dielectric constant observed for the 98% trans sample of poly[1,4-(2,3-bis(trifluoromethyl)cyclopentenylene) vinylene] is easily explained in terms of the trans syndiotactic structure postulated on the evidence presented here. Appendix II of this thesis shows the mathematical relationship between  $\epsilon_R$  and the alignment of dipoles within a material.

The cis polymer afforded from the bis(hexafluorobutoxide) initiator possesses a much smaller dielectric constant (less than half that of the 54% atactic material). This would therefore seem to imply that the dipoles are not aligned, thus favouring a cis syndiotactic structure, in which the polar substituents alternate from one side of the olefinic backbone to the other. However, to date no modelling has been carried out on this system, and so it is not yet possible to completely rule out a cis isotactic helical conformation.

## 2.8 Discussion

One of the intriguing questions arising from the studies presented in this chapter is why  $\text{Mo}(\text{NAr})(\text{CHCMe}_2\text{Ph})(\text{OCMe}(\text{CF}_3)_2)_2$  should produce a very high cis poly[1,4-(2,3-bis(trifluoromethyl)cyclopentenylene) vinylene], while the bis(tert-butoxide) initiator,  $\text{Mo}(\text{NAr})(\text{CHCMe}_2\text{Ph})(\text{OCMe}_3)_2$ , affords a high trans form.

Although several possible explanations have been entertained, a detailed proton N.M.R. study by Mr. J. Oskam and Professor R.R. Schrock suggests that the whole question of stereoregularity may depend upon syn / anti rotamer interconversion rates<sup>21</sup>.

At room temperature the  $^1\text{H}$  N.M.R. spectrum of either of the two initiators shows only one alkylidene resonance, assigned to the syn alkylidene isomer, (figure 2.19).

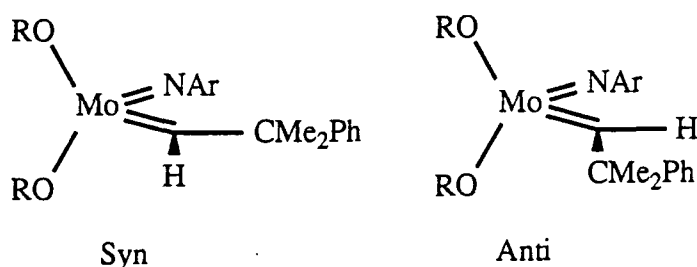


Figure 2.19 The syn and anti alkylidene rotamers of  $\text{Mo}(\text{NAr})(\text{CHCMe}_2\text{Ph})(\text{OR})_2$   
{R = CMe<sub>3</sub>, CMe<sub>2</sub>CF<sub>3</sub>, CMe(CF<sub>3</sub>)<sub>2</sub>, C(CF<sub>3</sub>)<sub>2</sub>CF<sub>2</sub>CF<sub>2</sub>CF<sub>3</sub>}

Low temperature photolysis of the bis(hexafluorobutoxide) initiator yields approximately 35% of the anti rotamer which can be observed via  $^1\text{H}$  N.M.R. spectroscopy downfield of the syn alkylidene by approximately 1ppm. By studying the relaxation of this mixture as it approaches 100% syn, the rate of rotamer conversion has been determined for a range of fluorinated initiators. The data for this study suggest that syn / anti rotamer conversion is fastest for  $\text{Mo}(\text{NAr})(\text{CHCMe}_2\text{Ph})(\text{OCMe}_3)_2$  (about five orders of magnitude greater than for its hexafluoro(butoxide) counterpart).

A related investigation has established that the anti alkylidene rotamer is much more reactive than its syn partner. Furthermore, the anti form reacts with 2,3-bis(trifluoromethyl)bicyclo[2.2.1]hepta-2,5-diene to give the syn insertion product which always contains a trans C=C double bond in the polymer.

In other words,  $\text{Mo}(\text{NAr})(\text{CHCMe}_2\text{Ph})(\text{OCMe}_3)_2$  polymerizes this monomer almost exclusively through the anti isomer, even though this form is present in immeasurably-minute amounts at room temperature. Indeed, even at  $0^\circ\text{C}$ , the anti alkylidene has only been observed via  $^1\text{H}$  N.M.R. spectroscopy after 12,000 transients at 500MHz.

Since the rate of syn / anti rotamer interconversion is much slower for the initiators bearing electron-withdrawing ancillary ligands,  $\text{Mo}(\text{NAr})(\text{CHCMe}_2\text{Ph})(\text{OCMe}(\text{CF}_3)_2)_2$  cannot significantly populate the anti rotamer state on the time scale of the polymerization at room temperature. Hence, it metathesizes 2,3-bis(trifluoromethyl)bicyclo[2.2.1]hepta-2,5-diene via the syn alkylidene to give a high cis polymer (this latter proposal simply follows on from the first study; at the time of writing it still remains to be proven experimentally). This proposition is summarised in the figure below (2.20).

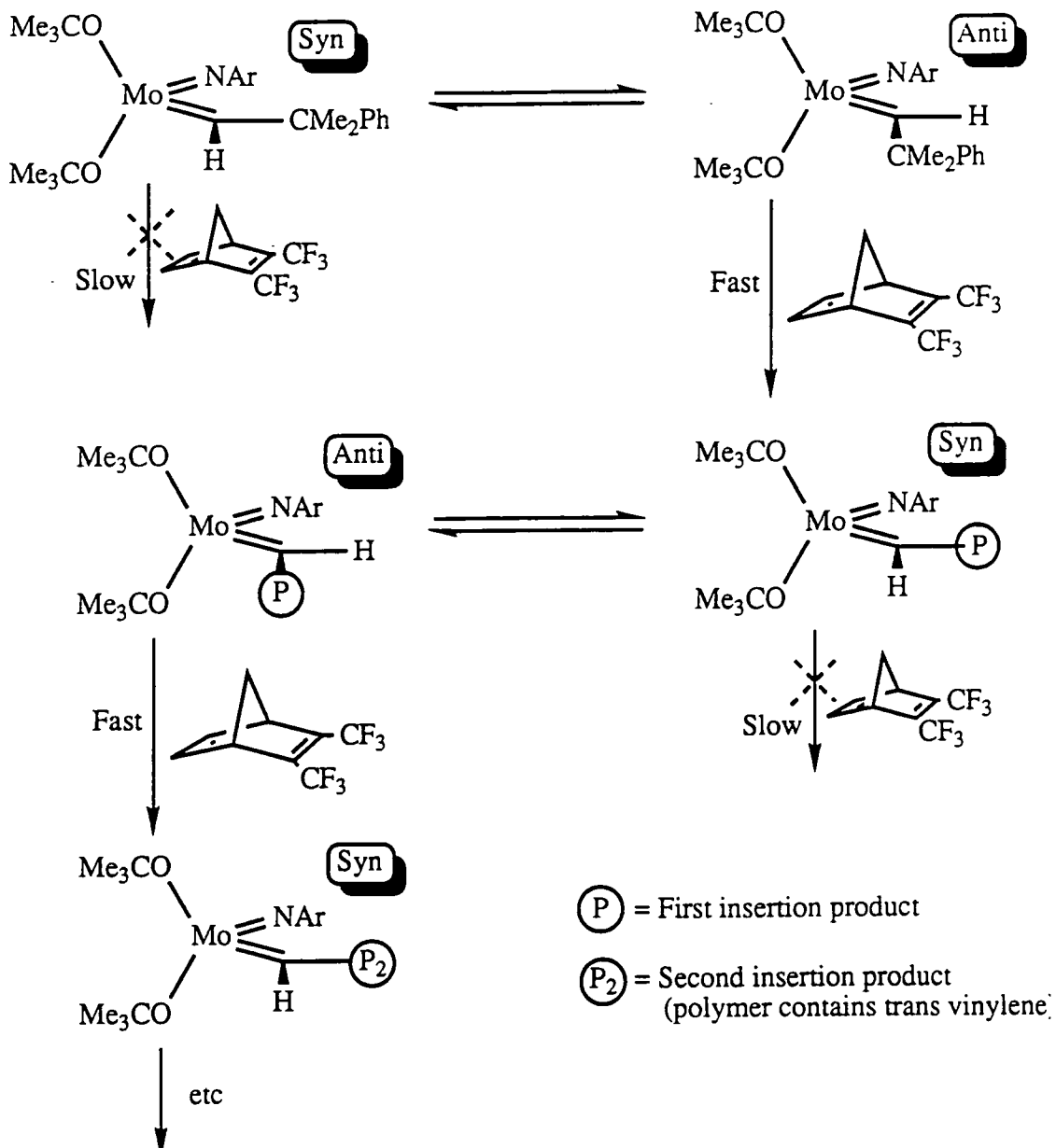


Figure 2.20 The relatively fast rate of interconversion between syn and anti rotamers for  $\text{Mo}(\text{NAr})(\text{CHCMe}_2\text{Ph})(\text{OCMe}_3)_2$  allows the more highly reactive anti alkylidene to govern the stereoregularity of the living polymer.

## 2.7.2 The origin of tacticity in well-defined living R.O.M.P. systems

As stated in chapter one, the main worker in the field of ring-opened polymer microstructure and its assignment has been Professor K.J. Ivin. One of the most creative studies in metathesis was his introduction of the idea of a 'steric fit' as a source of tacticity in such systems. A brief summary of this theory is presented here, although the reader is referred to Ivin's own publications for a more complete picture<sup>6,22,23</sup>.

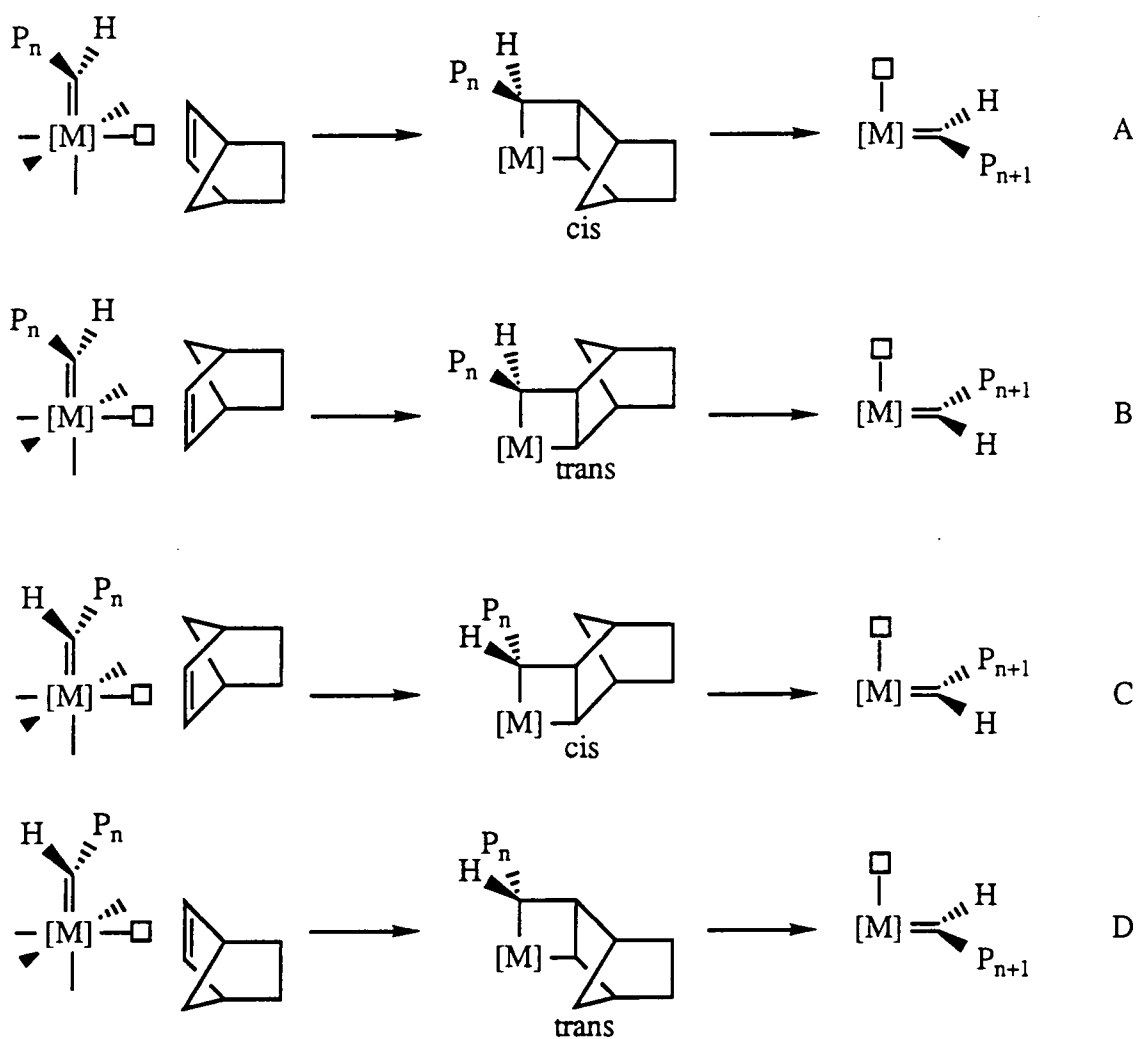


Figure 2.21 Ivin's interpretation of the origin of tacticity in R.O.M.P.<sup>6</sup>

The simplest explanation for tactic ring-opened polymers assumes that the propagating centre possesses both a left- and a right- handed form (shown in figure 2.21 as possessing an octahedral geometry). The formation of tactic polymers must involve propagation through chiral metallocarbenes, with alternating enantiomeric form associated with the formation of a cis double bond, whilst the same enantiomeric form is encountered repeatedly during the formation of trans double bonds.

Four modes of attack are shown in figure 2.21. It should now be obvious that an all cis polymer can only be formed from the alternation of propagating steps A and C. Furthermore, polymers formed from such a mechanism will also be completely syndiotactic.

Experimental evidence for such a theory cites  $\text{ReCl}_5$  initiated polymerizations which often give rise to all cis-syndiotactic poly[cyclopentylene vinylene]s (e.g. (+)-5,5-dimethylbicyclo[2.2.1]hept-2-ene<sup>24,25</sup>).

However, propagation solely through either pathway B or D will lead to the generation of a trans isotactic material. This has been found to be the case for the metathesis polymerization of ( $\pm$ )-5,5-dimethylbicyclo[2.2.1]hept-2-ene when initiated by (mesitylene) $\text{W}(\text{CO})_3$  / *exo*-2,3-epoxybicyclo[2.2.1]heptane /  $\text{EtAlCl}_2$  in chlorobenzene at 20°C<sup>23</sup>.

However, any deviation away from -ACACAC-, -BBB-, or -DDD- will lead to a drop in the level of stereoregularity in the polymer produced. Therefore in order for a polymer to be completely tactic the restrictions upon the mode of attack are enormous. The reason why several systems are known which give rise to tactic polymers is due to steric fit. Ivin proposed that the methylene unit (C7) in the monomer governed the approach pathway in order to minimize steric congestion around itself during metallocycle formation. For the trans isotactic polymers the C7 atom of the norbornene points towards the side of the vacant co-ordination site bearing the propagating chain. Conversely the monomer points towards the  $\alpha$ -proton of the carbene during formation of a cis syndiotactic polymer.

Ivin's reasoning may also be applied to well-defined alkylidene complexes; the left- and right- handed forms of the active site are envisaged as the syn and anti alkylidene rotamers. Stereoregularity is then governed by the approach of the monomer to the alkylidene rotamer. The orientation of the monomer is determined by the steric fit of the C7 methylene unit with respect to the ligands around the active site.

Schrock's study of rotamer interconversion draws three main conclusions. Firstly, polymerization of 2,3-bis(trifluoromethyl)bicyclo[2.2.1]hepta-2,5-diene via an anti alkylidene always gives a syn rotamer containing a trans double bond, whilst syn propagates to syn and results in a cis vinylene. The second point of note is that the more electrophilic metal centres (such as in the bis(hexafluorobutoxide) example) have much slower syn / anti interconversion rates than that found in the bis(butoxide) complex. Finally, anti alkylidenes are much more reactive than their syn isomers.

Figure 2.22 shows the postulated approach of the olefinic bond to the molybdenum-carbon double bond, based upon minimization of steric hindrance at the monomer C7 methylene fragment. The exceptionally bulky tertiary-butoxides disfavour attack on the OCO face of the initiator, and hence the monomer is envisaged to approach perpendicular to the NCO face. This results in a five-coordinate geometry rather like that seen in the base-adduct systems discussed before. The monomer olefinic bond acts as a  $\sigma$ -donor and the NCO face forms the equatorial plane of a trigonal bipyramid.

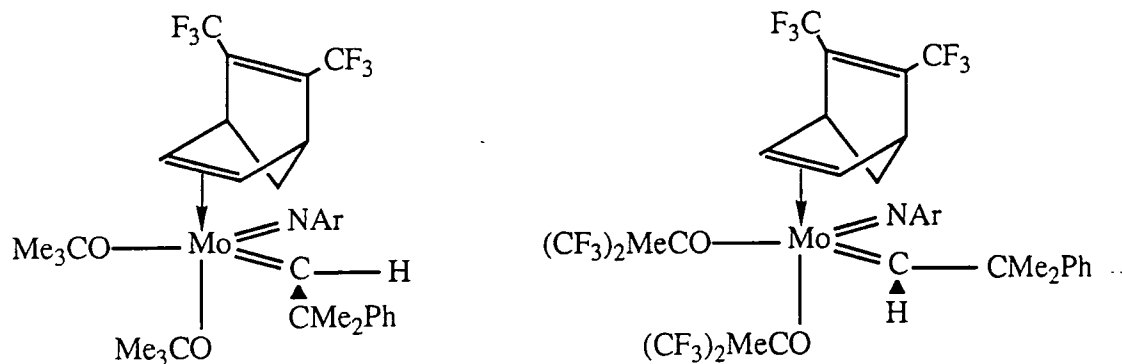


Figure 2.22 The approach pathways of the fluorinated monomer to both the bis(tert-butoxide) and the bis(hexafluorobutoxide) initiators (drawn as the anti and syn rotamer respectively)

In order to accommodate Ivin's 'steric fit' argument into this picture it is necessary to consider the effect of the two possible orientations of the monomer upon the C7 unit. Again, the inescapable bulkiness of the alkoxide ligands are believed to force the C7 methylene towards the 2,6-di(isopropyl)arylimido ligand (which is much more flexible than a tertiary-butoxide unit and can orientate itself in order to accommodate the monomer).

However, the monomer can also attack the NCO face from the opposite direction (i.e. rather than from above the plane as shown in figure 2.22, it can approach from below). As a result there are four possible regular modes of attack upon the active site that the monomer can adopt. It may attack either the syn or the anti alkylidene, and may attack either the same face, or alternating faces. It is no coincidence that there are also four possible assembly modes for a symmetrically substituted 2,3-disubstituted poly[cyclopentylene vinylene].

If Schrock's observations concerning syn and anti rotamers and Ivin's concept of steric fit are assumed then it is possible to show that all four of the regular polymer architectures are accessible, as shown in the following figures.

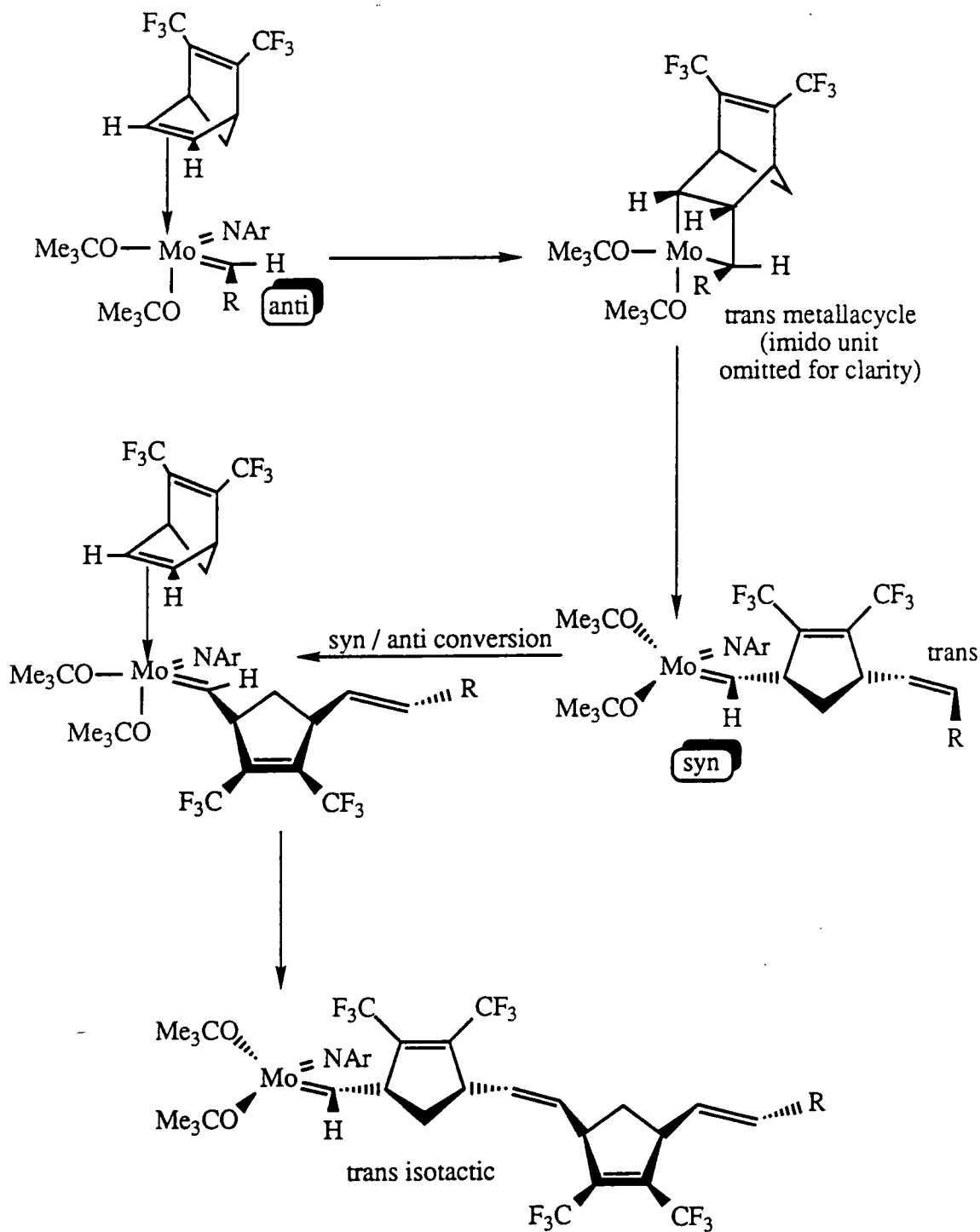


Figure 2.23 Trans isotactic polymer via attack from the same face upon the anti rotamer of  $\text{Mo}(\text{NAr})(\text{CHR})(\text{OCMe}_3)_2$

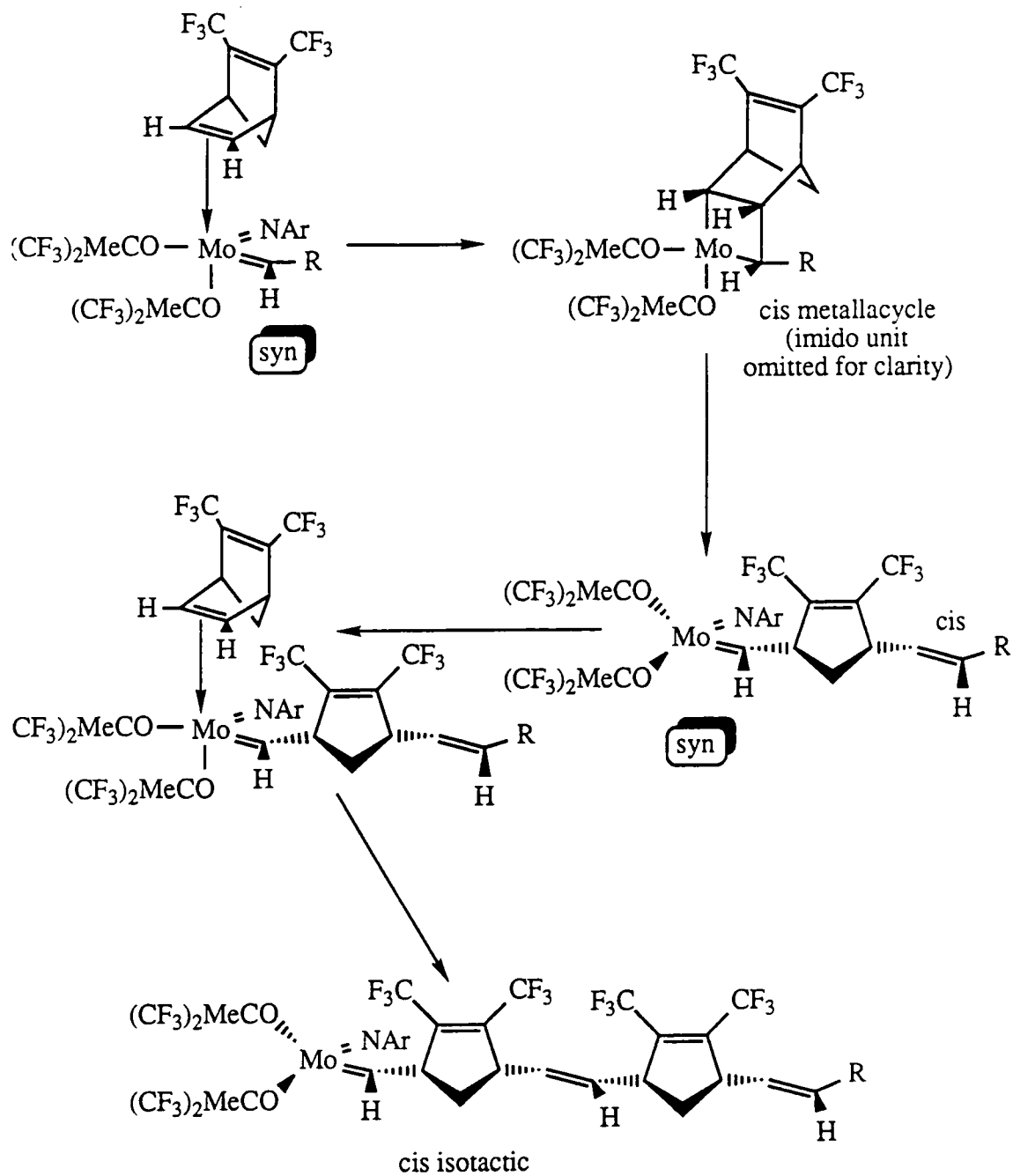


Figure 2.24 Cis isotactic polymer via attack on the same face upon the syn rotamer of  $Mo(NAr)(CHR)(OCMe(CF_3)_2)_2$

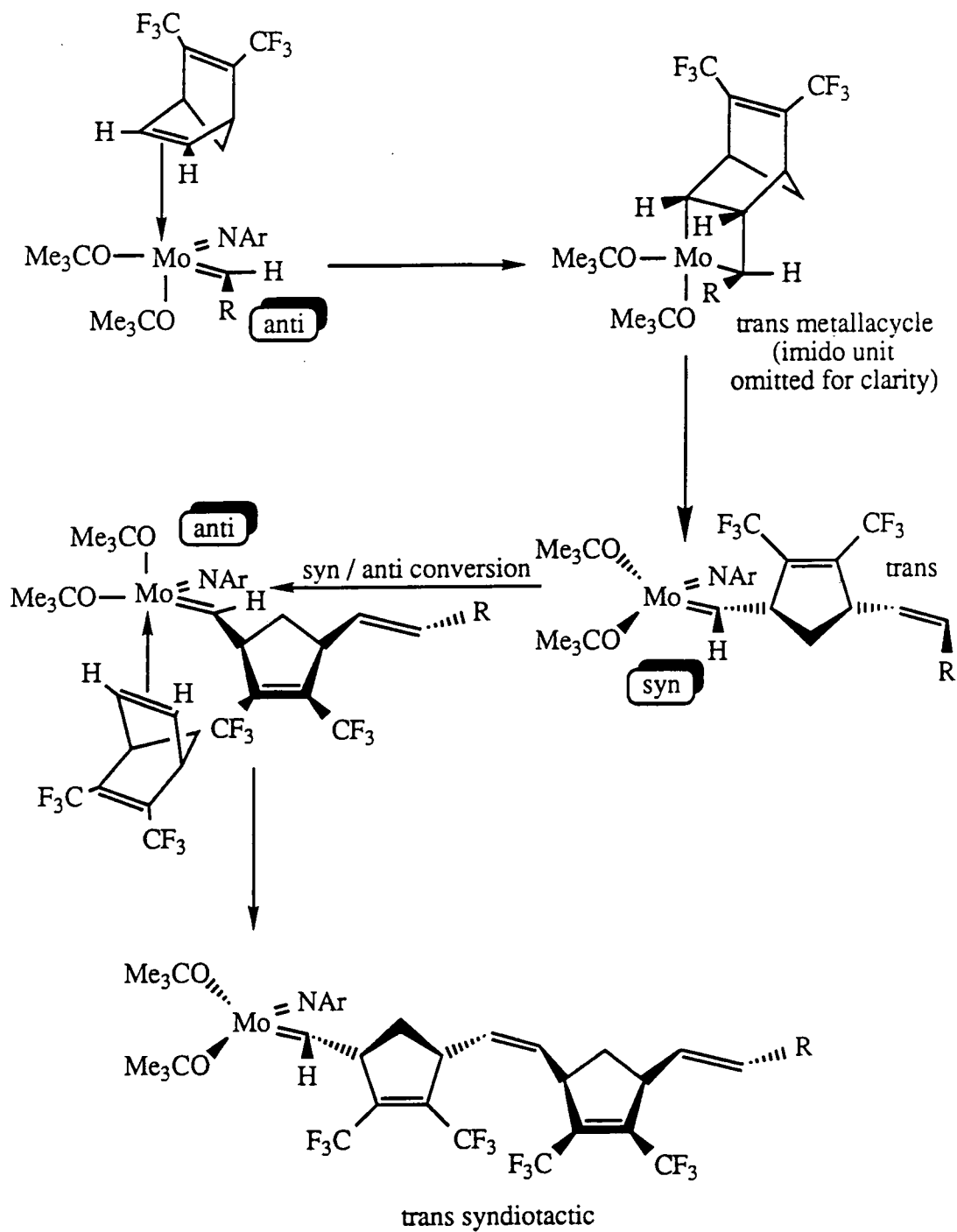


Figure 2.25 Trans syndiotactic polymer via alternating opposing approach pathways upon the anti rotamer of  $\text{Mo}(\text{NAr})(\text{CHR})(\text{OCMe}_3)_2$

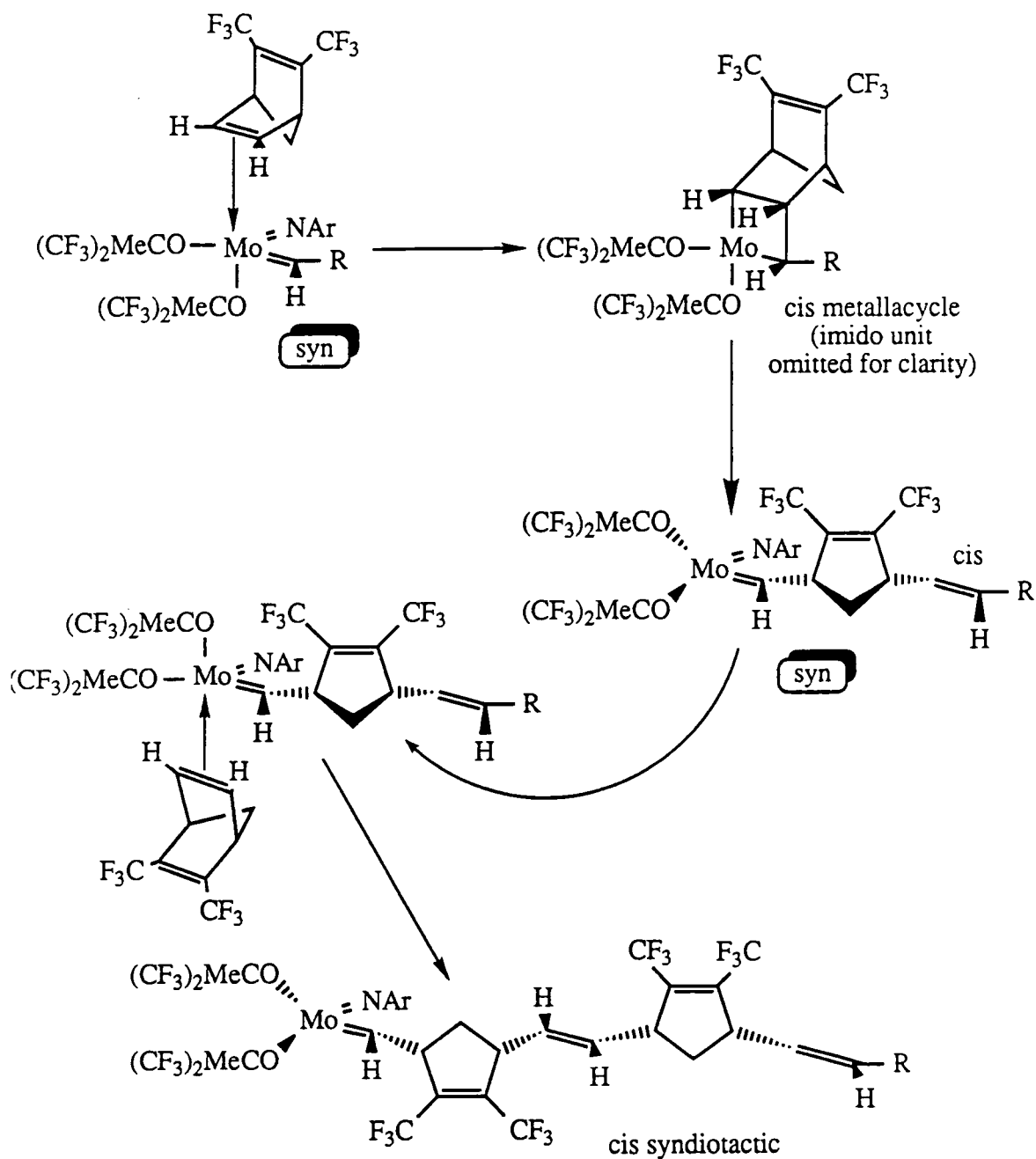


Figure 2.26 *Cis* syndiotactic polymer via alternating opposing approach pathways upon the *syn* rotamer of  $Mo(NAr)(CHR)(OCMe(CF_3)_2)_2$

From the dielectric measurements reported earlier, it appears that both the high trans and high cis polymers are predominantly syndiotactic. Having identified a likely mechanism for the formation of syndiotactic poly[1,4-(2,3-bis(trifluoromethyl) cyclopentenylene) vinylene], the question arises of why that assembly mode forms in preference to an isotactic (or an atactic) structure.

Formation of a cis isotactic polymer (whether via attack from above or from beneath the syn alkylidene) is almost certainly disfavoured because of the close proximity of the CF<sub>3</sub> substituents upon the monomer and upon the last insertion unit of the propagating chain (figure 2.27). Such a intermediate would result in intolerable fluorine-fluorine repulsions<sup>26</sup>.

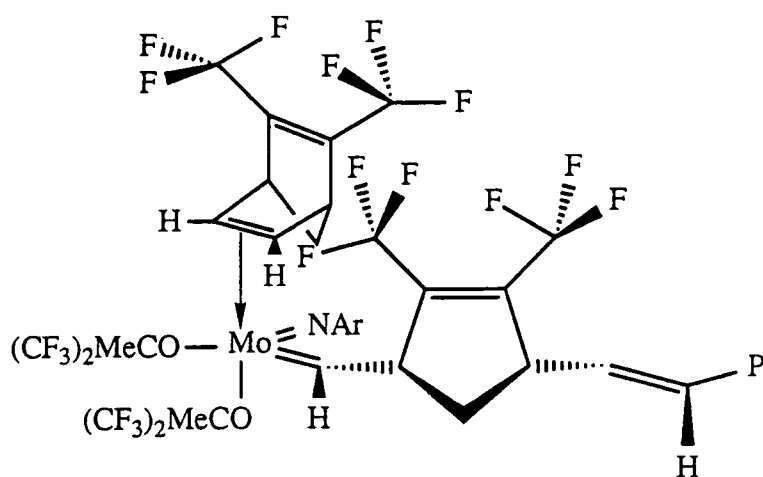


Figure 2.27 Fluorine-fluorine interactions predicted during cis isotactic polymer formation

However, the analogous intermediate in the syndiotactic mechanism places the polar fluorine-containing groups on opposite faces of the equatorial plane of the trigonal bipyramidal complex (figure 2.28). Hence F-F interactions would be minimized (further, the scope for favourable H-F interactions is also increased).

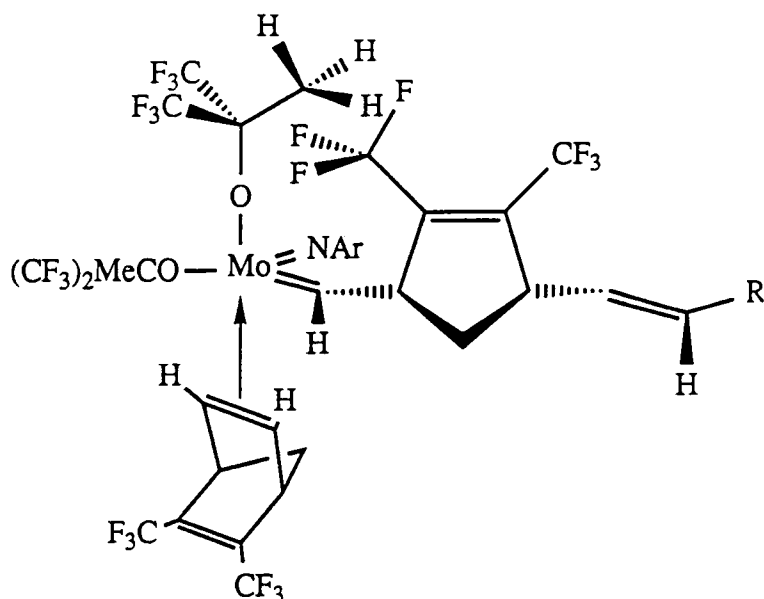


Figure 2.28 Attractive interactions during cis syndiotactic polymer formation

Although steric arguments provide an excellent rationale for cis-syndiotactic polymer formation, a similar explanation for the predominance of syndiotacticity for the trans polymer is less convincing. As figure 2.29 shows, there appears to be no overriding steric reason why the monomer should approach the N-Mo-C face from one direction rather than the other. Yet the trans polymer is known to be very much more highly tactic than the 98% cis stereoisomer.

This observation is particularly interesting; for many years proposed mechanisms to account for the formation of highly tactic polymers synthesised via R.O.M.P. have been based upon steric considerations at the metal centre. In the situation discussed above, however, this would not appear to be the case; if anything the steric influence of the last inserted (ring-opened) monomer repeat unit is more important. In other words, it would appear that the propagating mechanism is chain-end controlled (rather than metal-centre controlled).

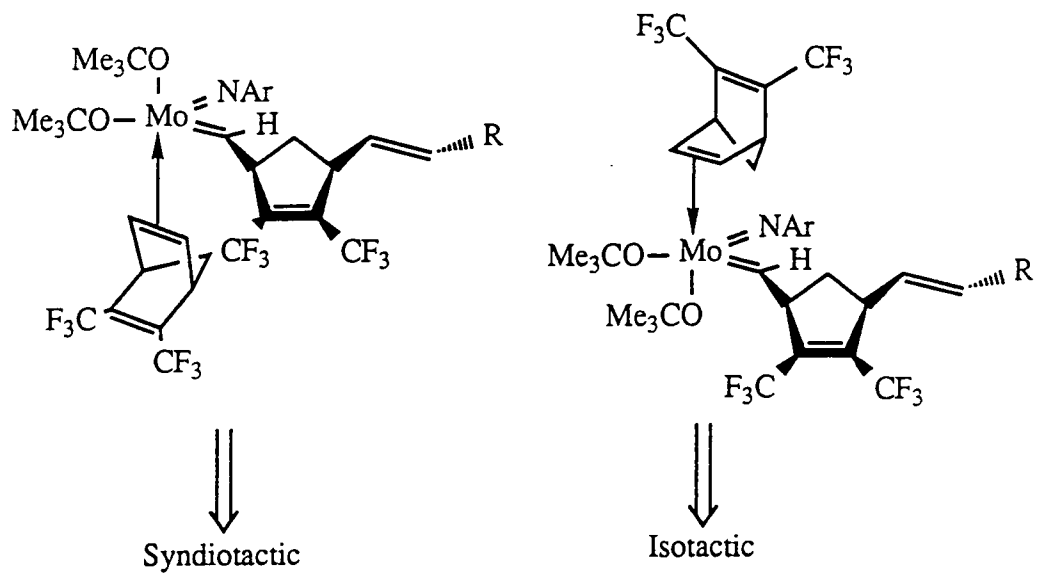


Figure 2.29 Steric considerations in the formation of the trans polymer

## 2.9 Summary

This chapter has shown that the stereoregular nature of ring-opened polymers synthesised from well-defined initiators of the general formula  $\text{Mo}(\text{NAr})(\text{CHR})(\text{OR}')_2$  is a sensitive function of the alkoxide ancillary ligands. This is particularly emphasized in the case of 2,3-bis(trifluoromethyl)bicyclo[2.2.1]hepta-2,5-diene, where the olefinic bond is deactivated and hence discrimination between polymer structures is amplified.

Furthermore, it is now believed that the mechanisms which give rise to both the cis and trans syndiotactic polymers are influenced greatly by syn / anti rotamer interconversion, the steric fit of the norbornene C7 methylene unit as it approaches the active site, and fluorine-fluorine repulsive interactions (and possibly hydrogen-fluorine attractive interactions) which lead to an alternating monomer approach pathway.

However, this area is one of much ongoing activity. Indeed recent observations by Professor R.R.Schrock suggest that a greater understanding of the mechanism for tactic polymer formation will shortly be available. In Durham attention is now being directed towards a X-ray crystallographic structure determination on both the high trans and high cis polymers, again in collaboration with the team of physicists at the University of Leeds.

## 2.10 References

1. W.J. Feast, B. Wilson *J.Mol.Cat.* **8** 277 (1980)
2. G.C. Bazan, R.R. Schrock, E. Khosravi, W.J. Feast, V.C. Gibson *Polym.Commun.* **30** 258 (1989)
3. G.C. Bazan, E. Khosravi, R.R. Schrock, W.J. Feast, V.C. Gibson, M. O'Regan, J. Thomas *J.Am.Chem.Soc.* **112** 8378 (1990)
4. H. Staudinger, A.A. Ashdown, M. Brunner, H.A. Bruson, S. Wehrli *Helv.Chim.Acta* **12** 934 (1929)
5. 'High Resolution N.M.R. Spectroscopy of Synthetic Polymers in Bulk', Ed. E.A. Komorski, VCH Publishers (1986)
6. K.J. Ivin 'Olefin Metathesis', Academic Press, London (1983)
7. G.C. Bazan, Ph.D Thesis, M.I.T. (1991)
8. R. Schlund, R.R. Schrock, W.E. Crowe *J. Am. Chem. Soc.* **111** 8004 (1989)
9. Z. Wu, D.R. Wheeler, R.H. Grubbs *J.Am.Chem.Soc* **114** 146 (1992)
10. N. Seehof, W. Risse *Makromol.Chem., Rapid Commun.* **12** 107 (1991)
11. In contrast, the polymer produced from  $\text{Mo}(\text{NAr})(\text{CHR})(\text{OCMe}_3)_2$  is recovered from methanol.
12. T. C. Chung, S. Ramakrishan, M.W. Kim *Macromolecules* **24** 2675 (1991)
13. W.J. Feast, V.C. Gibson, E. Khosravi, E.L. Marshall, J.P. Mitchell *Polymer* **30** 872 (1992)
14. L.J. Gold *J.Chem.Phys.* **28** 91 (1958)
15. The derivation of this equation is reproduced in the appendices of this thesis
16. The data for  $\text{Mo}(\text{NAr})(\text{CHCMe}_2\text{Ph})(\text{OCMe}_3)_2$  is incomplete because of the close chemical shifts of the unconsumed neophylidene  $\alpha$ -H and the propagating alkylidenes.
17. P. Debye 'Polar Molecules', Chemical Catalog Co (1929), reprinted by Dover Publications

18. H. Fröhlich 'Theory of Dielectrics', Oxford University Press (1947)
19. WAXD measurements were carried out by Dr. E.L.V. Lewis at the Department of Physics, Leeds University
20. I.M. Ward, G.R. Davies, H.V.St.A. Hubbard *Private Communication*
21. J.H. Oskam, R.R. Schrock *J.Am.Chem.Soc* **114** 7588 (1992)
22. K.J. Ivin, G. Lapienis, J.J. Rooney *J.Chem.Soc.,Chem.Comm* 1068 (1979)
23. G.I. Devine, H.T.Ho, K.J. Ivin, M.A. Mohamed, J.J. Rooney *J.Chem.Soc., Chem.Commun.* 1229 (1982)
24. H.T. Ho, K.J. Ivin, J.J. Rooney *J.,Mol.Catal.* **15** 245 (1982)
25. H.T. Ho, K.J. Ivin, J.J. Rooney *Makromol.Chem.* **183** 1629 (1982)
26. R.E. Banks 'Fluorocarbons and their Derivatives', Oldbourne Press, London (1964)

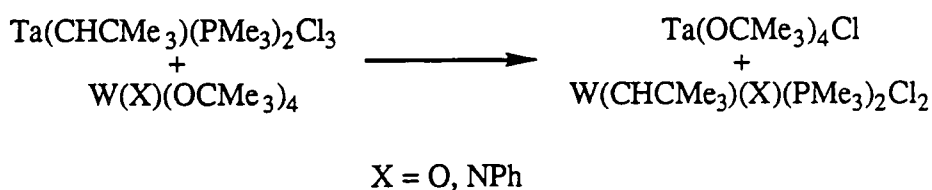
## **Chapter Three**

**A Mixed Initiator System for the Living R.O.M.P.  
of 2,3-Bis(trifluoromethyl)bicyclo[2.2.1]hepta-2,5-diene**

### 3.1 Ligand exchange between transition metal centres

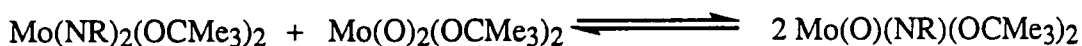
Ligand exchange is one of the most commonly encountered processes in transition metal chemistry. However, most examples of the scrambling of ligands between two transition metal compounds have been briefly reported as either unwanted side-reactions or as decomposition pathways. Relatively little use of such reactions has been made for the synthesis of novel organometallic complexes.

The classic exception is Schrock's transferral of the alkylidene unit from a tantalum neopentylidene complex to two tungsten compounds<sup>1</sup> (equation 3.1).

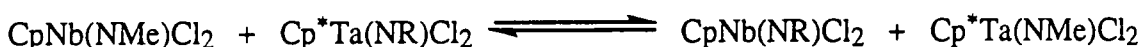


Equation 3.1

Heteroatom exchange has also recently been studied in four-coordinate molybdenum compounds, and in half-sandwich imido complexes of niobium and tantalum by Dr. V.C. Gibson and co-workers in Durham. Two such examples are listed below<sup>2,3</sup>.



Equation 3.2 {R = CMe<sub>3</sub>, 2,6-DIPP}



Equation 3.3 {R = 2,6-DIPP}

There are far more literature reports of one-electron anionic ligand exchange. The metathesis of alkoxide (and aryloxy) ligands is well-documented and has been exploited in the synthesis of many other metal-alkoxide species; for example, Wigley and co-workers have recently reported two mono(phenoxide) arene complexes of tantalum prepared via the interchange of phenoxide groups<sup>4</sup> according to equation 3.4.



Equation 3.4 { R = Me, Ph = 2,6-i-Pr<sub>2</sub>-C<sub>6</sub>H<sub>3</sub>; R = Et, Ph = 2,6-Me<sub>2</sub>-C<sub>6</sub>H<sub>3</sub> }

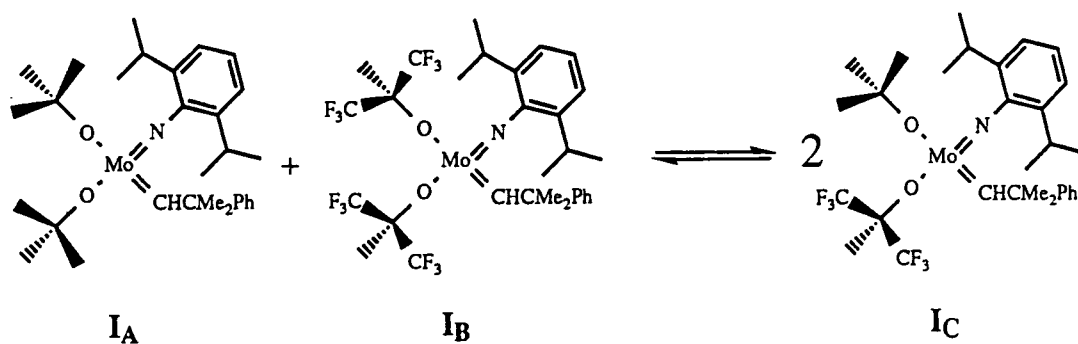
It is believed that this and similar redistribution reactions proceed via binuclear intermediates featuring bridging phenoxide (or alkoxide) groups<sup>5</sup>.

### 3.2 Alkoxide exchange reactions in 4-co-ordinate molybdenum-based metathesis initiators

Anionic ligand metathesis offers an opportunity to introduce new ancillary alkoxides through which the activity and selectivity of the initiator may be influenced. Of particular interest is the possibility for introducing chirality, either at the metal centre (i.e. the synthesis of  $\text{Mo}(\text{NAr})(\text{CHCMe}_2\text{Ph})(\text{OR})(\text{OR}')$ ) or through the introduction of chiral ligands  $\{\text{Mo}(\text{NAr})(\text{CHCMe}_2\text{Ph})(\text{OR}^*)_2\}$ . The presence of chirality at the metal centre might allow for an increased face selectivity of the monomer approach, thus increasing levels of tacticity.

#### 3.2.1 The reaction between $\text{Mo}(\text{NAr})(\text{CHCMe}_2\text{Ph})(\text{OCMe}_3)_2$ and $\text{Mo}(\text{NAr})(\text{CHCMe}_2\text{Ph})(\text{OCMe}(\text{CF}_3)_2)_2$

When one equivalent of  $\text{Mo}(\text{NAr})(\text{CHCMe}_2\text{Ph})(\text{OCMe}_3)_2$  (**I<sub>A</sub>**), is added to  $\text{Mo}(\text{NAr})(\text{CHCMe}_2\text{Ph})(\text{OCMe}(\text{CF}_3)_2)_2$  (**I<sub>B</sub>**), in benzene- $d_6$  the proton N.M.R. reveals the presence of three alkylidene signals in the ratio 7.7% : 7.7% : 84.6% as shown in figure 3.1. The two minor resonances at 11.32 and 12.12ppm correspond in chemical shift values to the two starting neophylidenes; the major signal (11.72ppm) is assigned to the neophylidene  $\text{H}_\alpha$  of the mixed alkoxide species  $\text{Mo}(\text{NAr})(\text{CHCMe}_2\text{Ph})(\text{OCMe}_3)(\text{OCMe}(\text{CF}_3)_2)$ , **I<sub>C</sub>**. This equilibrium mixture is shown in equation 3.5.



Equation 3.5

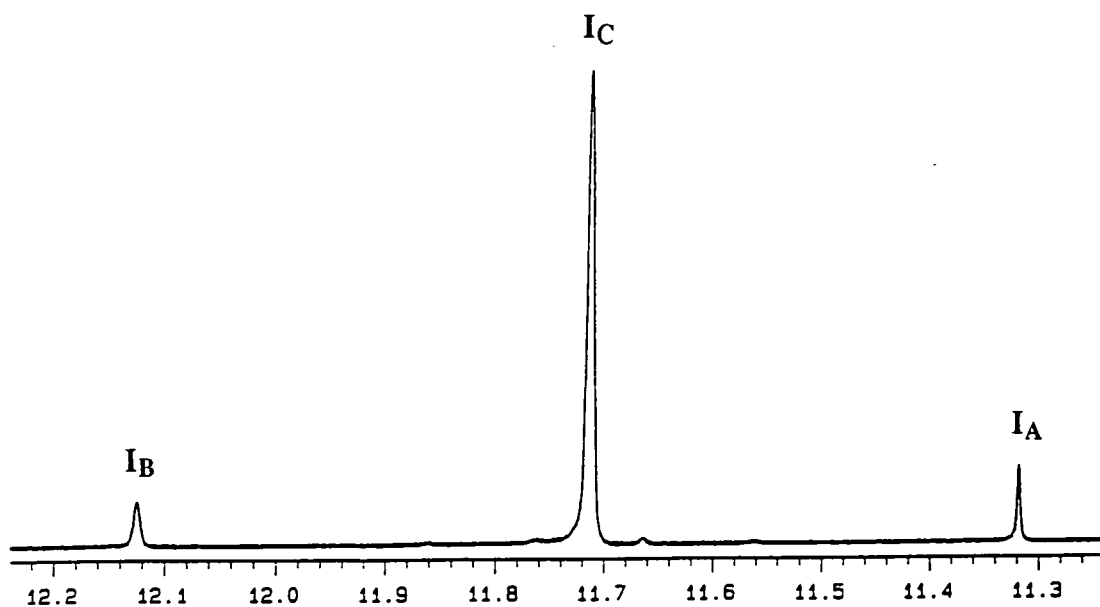


Figure 3.1 The 400MHz <sup>1</sup>H N.M.R. (C<sub>6</sub>D<sub>6</sub>) alkydene region of the equilibrium mixture resulting from the stoichiometric mixture of **I<sub>A</sub>** and **I<sub>B</sub>**

Investigation of the remainder of the <sup>1</sup>H spectrum (figure 3.2) provides further evidence that three distinct species are present. The resonances of all three imido- neophylidene complexes are resolved (with the exception of the overlapping aryl proton signals), and these are summarised in table 3.1.

As might be anticipated on simple electronegativity arguments, the chemical shifts of the intermediate species are comparable to those of Mo(NAr)(CHCMe<sub>2</sub>Ph)(OCMe<sub>2</sub>CF<sub>3</sub>)<sub>2</sub>, (**I<sub>D</sub>**). For example, consider the alkydene H<sub>α</sub> signals; **I<sub>B</sub>** is 0.84ppm upfield of **I<sub>A</sub>** because the electron density in the metal-carbon double bond is reduced due to the fluorine substituents on the ancillary ligands (less electron density results in a lower shielding of the alkydene proton). Both **I<sub>C</sub>** and **I<sub>D</sub>**, however, possesses very close alkydene chemical shifts, and both carry a total of six electron-withdrawing fluorine atoms on their alkoxide ligands.

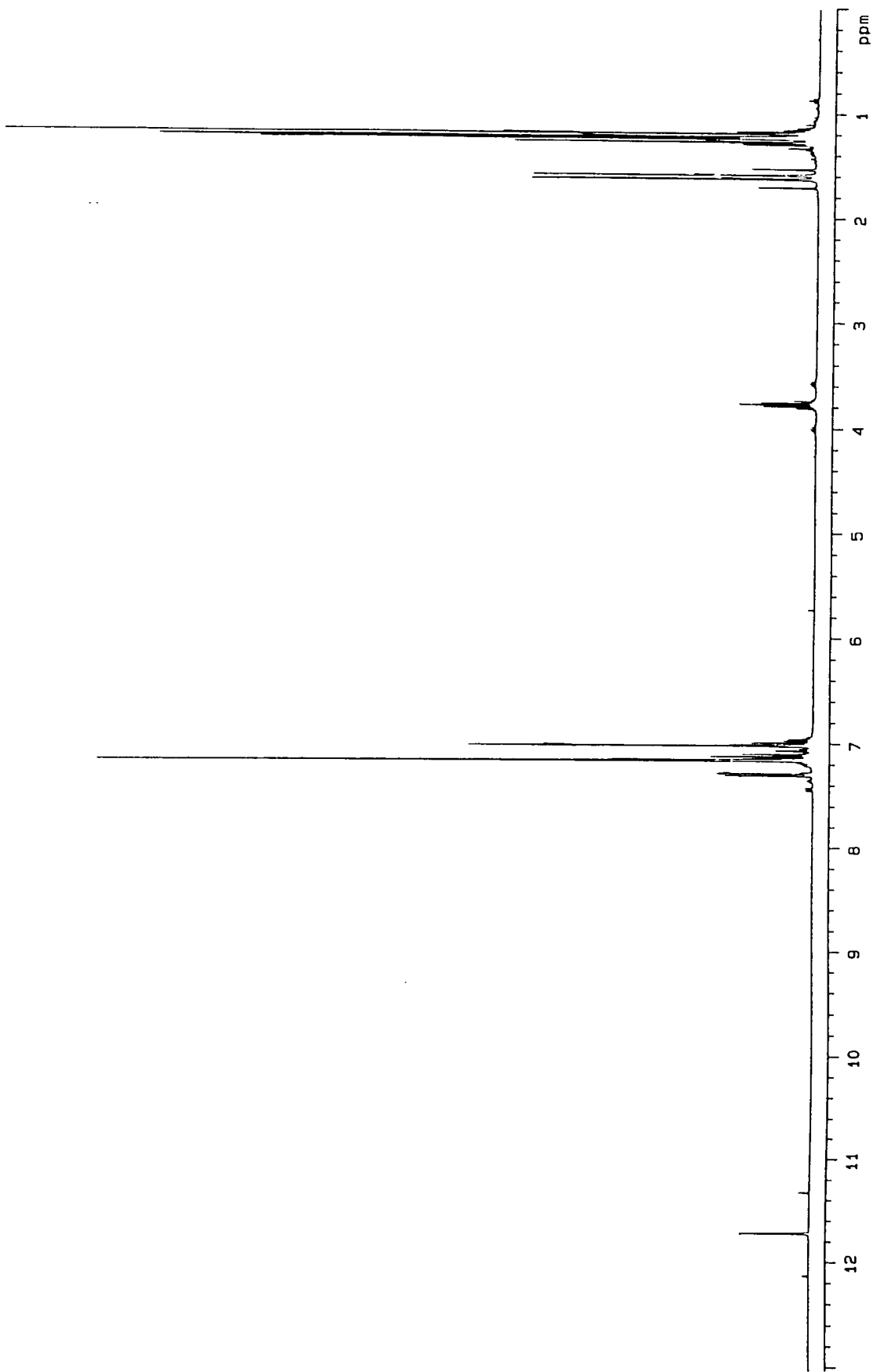


Figure 3.2 The 400MHz <sup>1</sup>H N.M.R. spectrum ( $C_6D_6$ ) of  $I_A : I_B$

Proton	I <sub>A</sub>	I <sub>B</sub>	I <sub>C</sub>	I <sub>D</sub>
[Mo]CHCMe <sub>2</sub> Ph	11.31 (s)	12.15 (s)	11.72 (s)	11.68 (s)
N-C <sub>6</sub> H <sub>3</sub> (CHMe <sub>2</sub> ) <sub>2</sub>	4.00 (sept)	3.57 (sept)	3.77 (sept)	3.75 (sept)
N-C <sub>6</sub> H <sub>3</sub> (CHMe <sub>2</sub> ) <sub>2</sub>	1.27 (d)	1.18 (d)	1.22 (d)	1.22 (d)
OCMe <sub>3</sub>	1.26 (s)	-	1.19 (s)	-
OCMe(CF <sub>3</sub> ) <sub>2</sub>	-	1.16 (s)	1.18 (s)	-
[Mo]CHCMe <sub>2</sub> Ph	1.70 (s)	1.53 (s)	1.62 (s) 1.58 (s)	1.59(s)
OCMe <sub>2</sub> CF <sub>3</sub>	-	-	-	1.17 (s)

Table 3.1 The <sup>1</sup>H N.M.R. chemical shifts for a series of molybdenum neophylidene complexes in benzene-d<sub>6</sub>

Confirmation that the mixed alkoxide is indeed the major component of the equilibrium (equation 3.5) has been achieved by selective crystallisation from n-pentane at -78°C affording I<sub>C</sub> in moderately high yield (60%). The solid state can be analysed by mass spectrometry which reveals a molecular ion mass of 659, indicative of I<sub>C</sub> (no signal at either 551 (I<sub>A</sub>) or 767 (I<sub>B</sub>) was reported)}. Satisfactory elemental analyses were also obtained.

The extremely rapid rate of alkoxide exchange in this system has been demonstrated previously by Dr. J. Mitchell in an experiment where 0.020g of the mixed alkoxide prepared as above was loaded into a 5mm N.M.R. tube fitted with a vacuum-line adaptor. Toluene-d<sub>8</sub> was then added via vacuum distillation at -196°C and the sample was sealed but kept frozen. The solution was thawed in the N.M.R. probe at -80°C and an immediate acquisition of the proton spectrum showed that the equilibrium position reported in figure 3.1 had already been established.

### 3.2.2 The mechanism of alkoxide exchange

Before considering the mechanism behind alkoxide exchange it is first necessary to briefly review the bonding modes of these ligands. As mentioned above, alkoxides are formally one-electron, anionic ligands. However, in certain cases the M-O-C angle can approach linearity as the result of sp hybridisation at the oxygen atom; the two lone pairs upon the heteroatom then become available for forming  $\pi$ -bonds with vacant metal d-orbitals. The two extreme canonical forms for such bonding modes are described below (figure 3.3).



Figure 3.3 The limiting canonical forms of metal-alkoxide bonding

A dominant feature of alkoxide ligand chemistry is their ability to bridge two metal centres via lone-pair donation (i.e. in an LX ligand type bonding mode). In the four-coordinate molybdenum (and tungsten) initiators developed by Schrock and co-workers, tert-butoxide ancillary ligands are bulky enough to prevent both dimerisation (and alkylidene coupling). However, the bis(methoxide), bis(ethoxide), and bis(n-propoxide) analogues all decompose in a matter of minutes at room temperature<sup>6,7</sup> (the smaller the alkoxide, the less stable is the complex).

As suggested earlier, the intermediate for the anionic ligand exchange almost certainly features bridging alkoxide intermediates; as a result donation of the alkoxide lone pair onto the metal centre of a second molecule gives rise to a dimer with the same geometry encountered in five-coordinate base adducts of the initiator (figure 3.4).

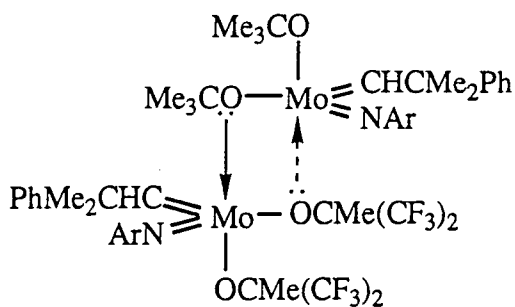


Figure 3.4 The postulated intermediate encountered during alkoxide exchange

### 3.2.3 The reaction of $\text{Mo}(\text{NAr})(\text{CHCMe}_2\text{Ph})(\text{OCMe}_3)_2$ with $\text{LiOCMe}(\text{CF}_3)_2$ and $\text{Mo}(\text{NAr})(\text{CHCMe}_2\text{Ph})(\text{OCMe}(\text{CF}_3)_2)_2$ with $\text{LiOCMe}_3$

The mixed tert-butoxide / hexafluorobutoxide complex can also be generated by the exchange of either of the homodialkoxide complexes with the complementary lithium salt,  $\text{LiOR}$  ( $\text{R} = \text{CMe}_3, \text{CMe}(\text{CF}_3)_2$ ).

Addition of two equivalents of lithium butoxide to  $\text{Mo}(\text{NAr})(\text{CHCMe}_2\text{Ph})(\text{OCMe}(\text{CF}_3)_2)_2$  gives rise to a mixture of the mixed alkoxide system and the bis(butoxide) complex in the ratio 45% : 55% (as determined by  $^1\text{H}$  N.M.R. spectroscopy). No  $\text{I}_\text{B}$  remains.

A resonance at 1.12ppm confirms that  $\text{LiOCMe}(\text{CF}_3)_2$  is a by-product of this reaction (the amount of superfluous  $\text{LiOCMe}_3$  is not discernible; its predicted chemical shift (1.27 ppm) is coincident with both the butoxide protons and one half of the aryl-imido iso-propyl methyl doublet of  $\text{Mo}(\text{NAr})(\text{CHCMe}_2\text{Ph})(\text{OCMe}_3)_2$ ). This reaction is summarised in equation 3.6.



Equation 3.6

Similarly, the reaction of  $\text{Mo}(\text{NAr})(\text{CHCMe}_2\text{Ph})(\text{OCMe}_3)_2$  with two equivalents of lithium hexafluorobutoxide in deuterated benzene leads to the formation of both the

mixed alkoxide and the bis(hexafluorobutoxide) arylimido-neophylidene species as shown in figure 3.5.

An important potential application of this reaction may be the conversion of the commercially-available  $\text{Mo}(\text{NAr})(\text{CHCMe}_2\text{Ph})(\text{OCMe}_3)_2$  into  $\mathbf{I_B}$  by trapping out the latter from the equilibrium as a five-coordinate base adduct species. In order to test this theory 5 equivalents of trimethylphosphine were introduced into a 5mm tube containing a mixture of  $\mathbf{I_A}$  and 2 equivalents  $\text{LiOCMe}(\text{CF}_3)_2$ . After standing at room temperature for five minutes  $^1\text{H}$  N.M.R. spectroscopy revealed the presence of just one alkylidene at 13.16ppm, believed to arise from the kinetic isomer (i.e. the syn rotamer) of  $\text{Mo}(\text{NAr})(\text{CHCMe}_2\text{Ph})(\text{OCMe}(\text{CF}_3)_2)_2(\text{PMe}_3)$ . However, the remainder of this spectrum displays several unassigned resonances, and to date no attempt has been made to scale up the conversion of  $\mathbf{I_A}$  into  $\mathbf{I_B}$ .

### **3.2.5 The reaction of $\text{Mo}(\text{NAr})(\text{CHCMe}_2\text{Ph})(\text{OCMe}_3)_2$ with $(\text{CF}_3)_2\text{MeCOH}$ and of $\text{Mo}(\text{NAr})(\text{CHCMe}_2\text{Ph})(\text{OCMe}(\text{CF}_3)_2)_2$ with $\text{Me}_3\text{COH}$**

Proton N.M.R. of these reactions in benzene- $\text{D}_6$  reveals that both establish the same equilibrium mixture of all three possible molybdenum complexes. The alkylidene regions of both are shown in figure 3.6 for comparison (both spectra were acquired with a recovery delay of three seconds between pulses in order to allow for full relaxation).

Further upfield the resonances of the expected complementary alcohols are observed (the chemical shifts of both  $(\text{CF}_3)_2\text{MeCOH}$  and  $\text{Me}_3\text{COH}$  methyl groups occur at 1.06ppm; the hydroxyl protons are dependent upon the reaction conditions but are usually found at 2.24 and 3.60ppm respectively) as well as all the signals expected for a mixture of the three molybdenum complexes.

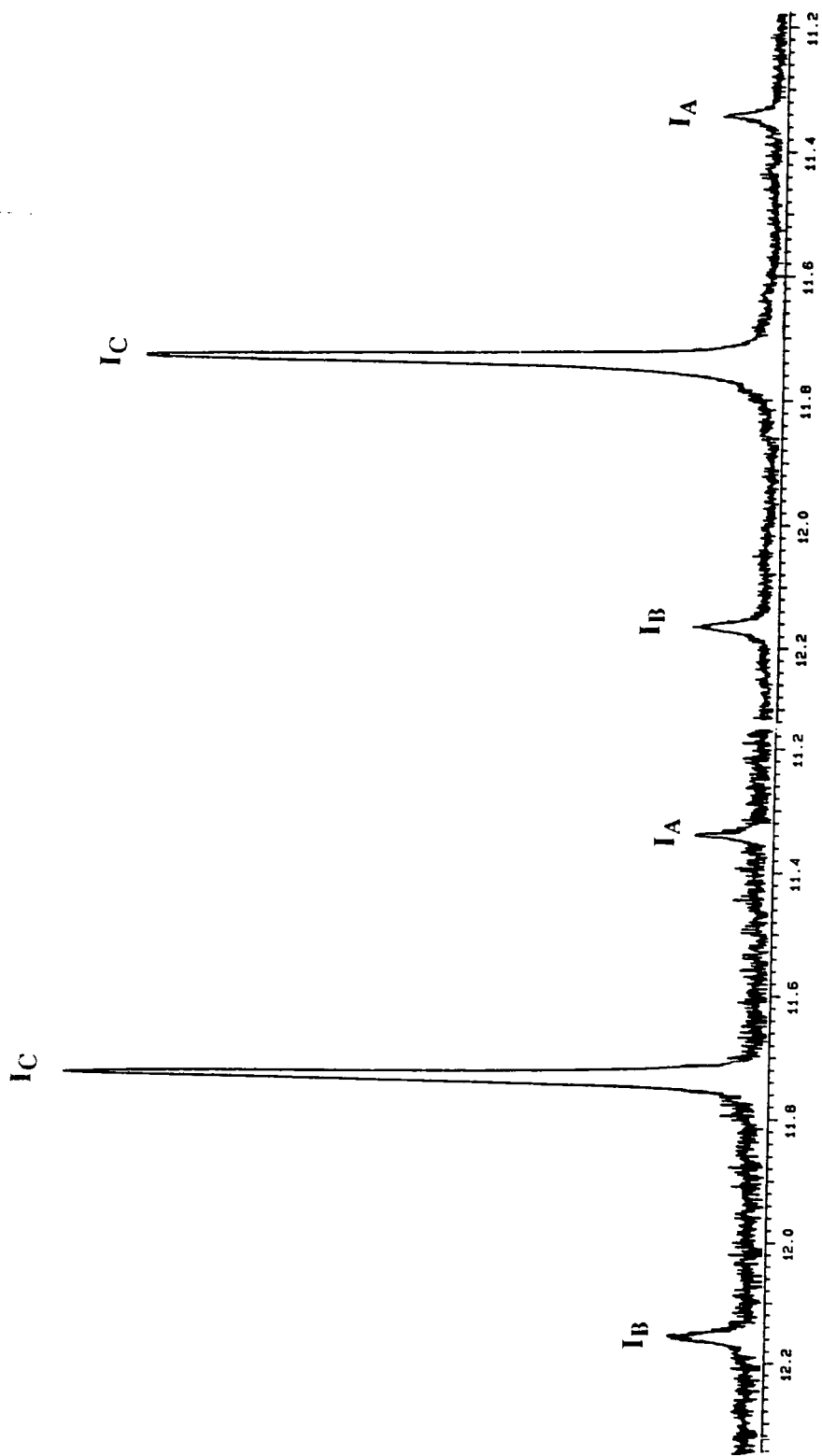


Figure 3.6 The alkydene regions of the 400MHz  $^1\text{H}$  N.M.R. spectra ( $\text{C}_6\text{D}_6$ ) of a) **I<sub>A</sub>** + 2 ( $\text{CF}_3$ )<sub>2</sub>MeCOH b) **I<sub>B</sub>** + 2 Me<sub>3</sub>COH

### 3.3 The use of the mixed alkoxide molybdenum neophylidene complex as an initiator for the R.O.M.P. of 2,3-bis(trifluoromethyl)bicyclo[2.2.1]hepta-2,5-diene.

Since both  $I_A$  and  $I_B$  are efficient initiators for R.O.M.P., it seemed likely that the mixed alkoxide analogue should also polymerize cyclic olefins. Although rapid exchange of the alkoxide ligands precludes an investigation of  $I_C$  as an initiator on its own, an opportunity presented itself to investigate for the first time a rapidly equilibrating initiator system consisting of well-defined species.

#### 3.3.1. The addition of 2,3-bis(trifluoromethyl)bicyclo[2.2.1]hepta-2,5-diene to a 1:1 mixture of $I_A$ and $I_B$ in benzene- $D_6$

If the 1:1 mixture of both homo-bis(alkoxide) complexes shown in figure 3.7 is mixed with twenty equivalents of 2,3-bis(trifluoromethyl)bicyclo[2.2.1]hepta-2,5-diene, the downfield  $^1H$  N.M.R. region of the resultant solution contains three distinct multiplets (figure 3.8). These are assigned as due to the propagating alkylidenes of  $I_A$ ,  $I_B$ , and  $I_C$ . As before the dominating resonance belongs to the mixed alkoxide with the relative ratios of all three multiplets being 6.7% ( $I_B$ ) : 86.1% ( $I_C$ ) : 7.2% ( $I_A$ ).

The propagating alkylidene for the mixed species appears to be two doublets, and this is explained as due to the orientation of the hexafluorobutoxide ligand with respect to the  $CF_3$  substituents on the inserted monomer unit. As can be seen from figure 3.9 the molybdenum centre of this species is chiral; hence the two doublets are believed to arise from the enantiomeric forms of the propagating mixed alkoxide species.

As a consequence of the different electronic nature of the ancillary alkoxides, all three initiators display different rates of initiation and propagation. Furthermore, each will give rise to different polymer chain structures. However, the extremely facile exchange of the ancillary alkoxide ligands implies that, even during the close approach of the monomer to the active site, the ligand environment around that metal centre is constantly changing. There must be some critical point during the insertion step that controls the

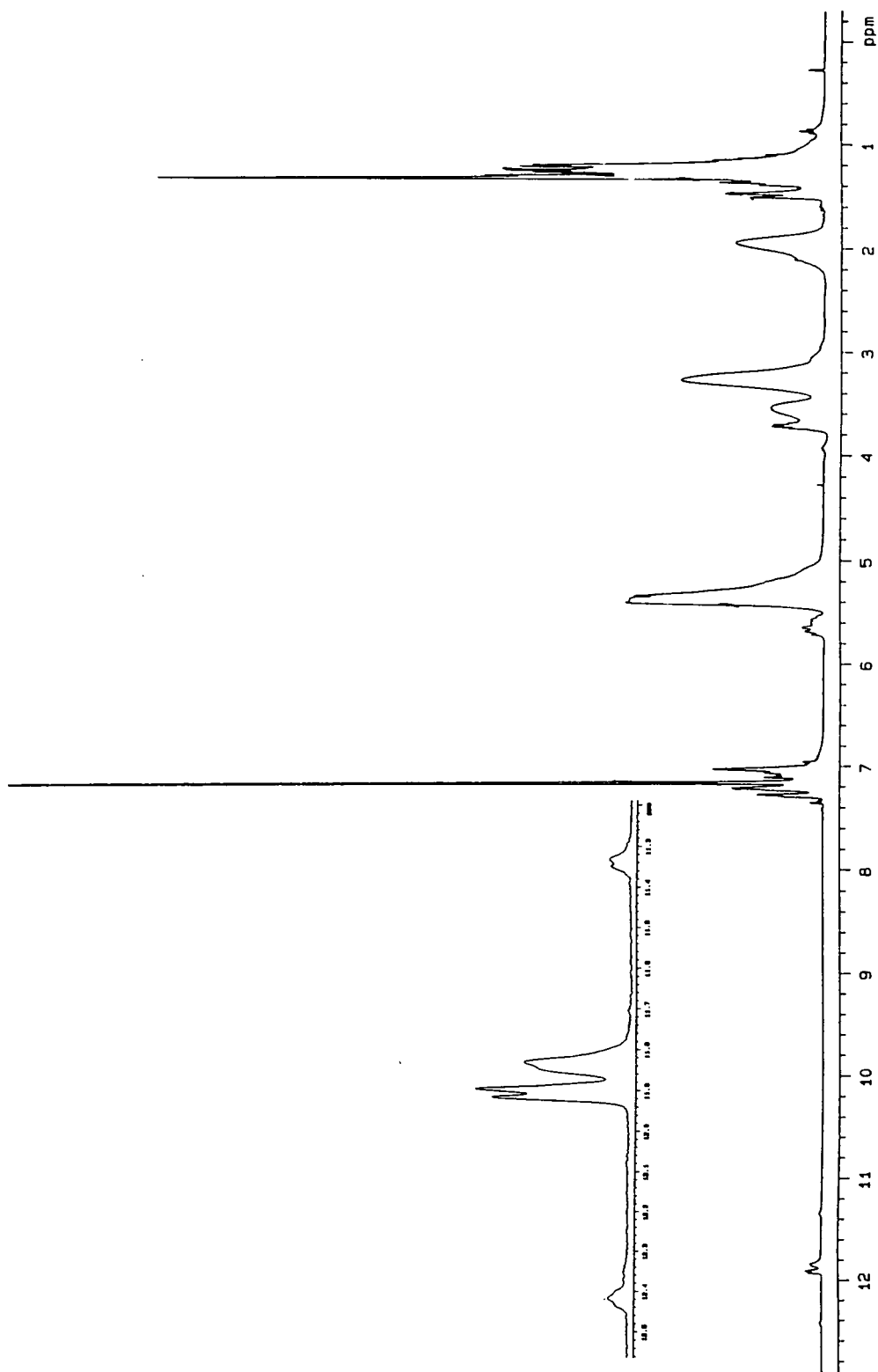


Figure 3.8 The 400MHz <sup>1</sup>H N.M.R. spectrum (C<sub>6</sub>D<sub>6</sub>) of living poly[1,4-(2,3-bis(trifluoromethyl)cyclopentylene) vinylene] initiated by a 1:1 mixture of **I<sub>A</sub>** and **I<sub>B</sub>**

nature of the polymer microstructure; it is the ancillary ligands present at that moment that will determine the outcome.

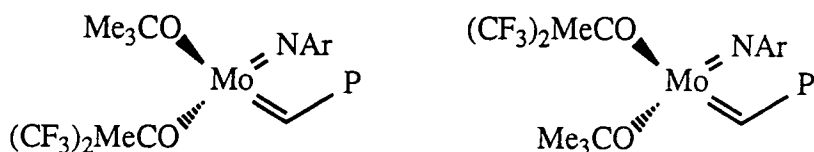


Figure 3.9 The two enantiomeric propagating forms of



{P = living poly[1,4-(2,3-bis(trifluoromethyl)cyclopentenylene)vinylene]}

### 3.3.2 The large scale polymerization of 2,3-bis(trifluoromethyl)bicyclo[2.2.1]hepta-2,5-diene using the 1:1 mixture of $I_A$ and $I_B$

The ring-opening polymerization of 2,3-bis(trifluoromethyl)bicyclo[2.2.1]hepta-2,5-diene using the equilibrium mixture discussed above has been scaled up in THF. The acetone- $d_6$   $^{13}\text{C}$  N.M.R. spectrum of the fluoropolymer produced is shown in figure 3.10 and should be compared to both high trans and high cis polymer traces (figure 2.7). The most notable feature is the intermediate cis and trans vinylene content (both  $^1\text{H}$  and quantitative  $^{13}\text{C}$  N.M.R. suggest a trans content of 64.6%), indicating a trans bias for the mixed alkoxide initiator  $I_C$ .

### 3.3.3 Control over cis / trans vinylene content using the mixed initiator equilibrium

The mixed alkoxide initiator exists in equilibrium with both the bis(tert-butoxide) and the bis(hexafluorobutoxide) complexes. Hence, increasing the proportion of one of the two starting materials (i.e. a ratio other than 1:1) results in a different equilibrium position. Figure 3.11 shows the proton N.M.R. alkylidene region obtained when two equivalents of  $\text{Mo(NAr)(CHCMe}_2\text{Ph)(OCMe}_3\text{)}_2$  are added to just one equivalent of the

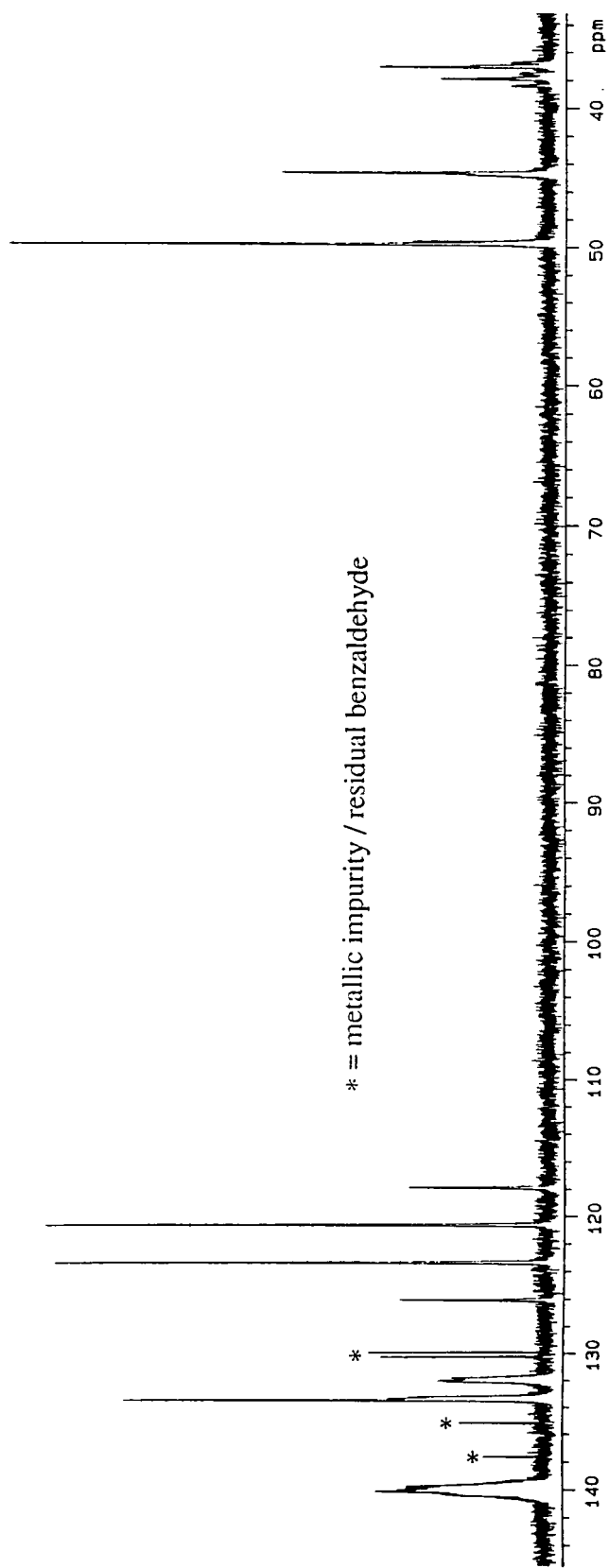


Figure 3.10 The 100MHz  $^{13}\text{C}$  N.M.R. spectrum of poly[1,4-(2,3-bis(trifluoromethyl)cyclopentenylene) vinylene] initiated by a 1:1 mixture of  $\text{I}_A$  and  $\text{I}_B$

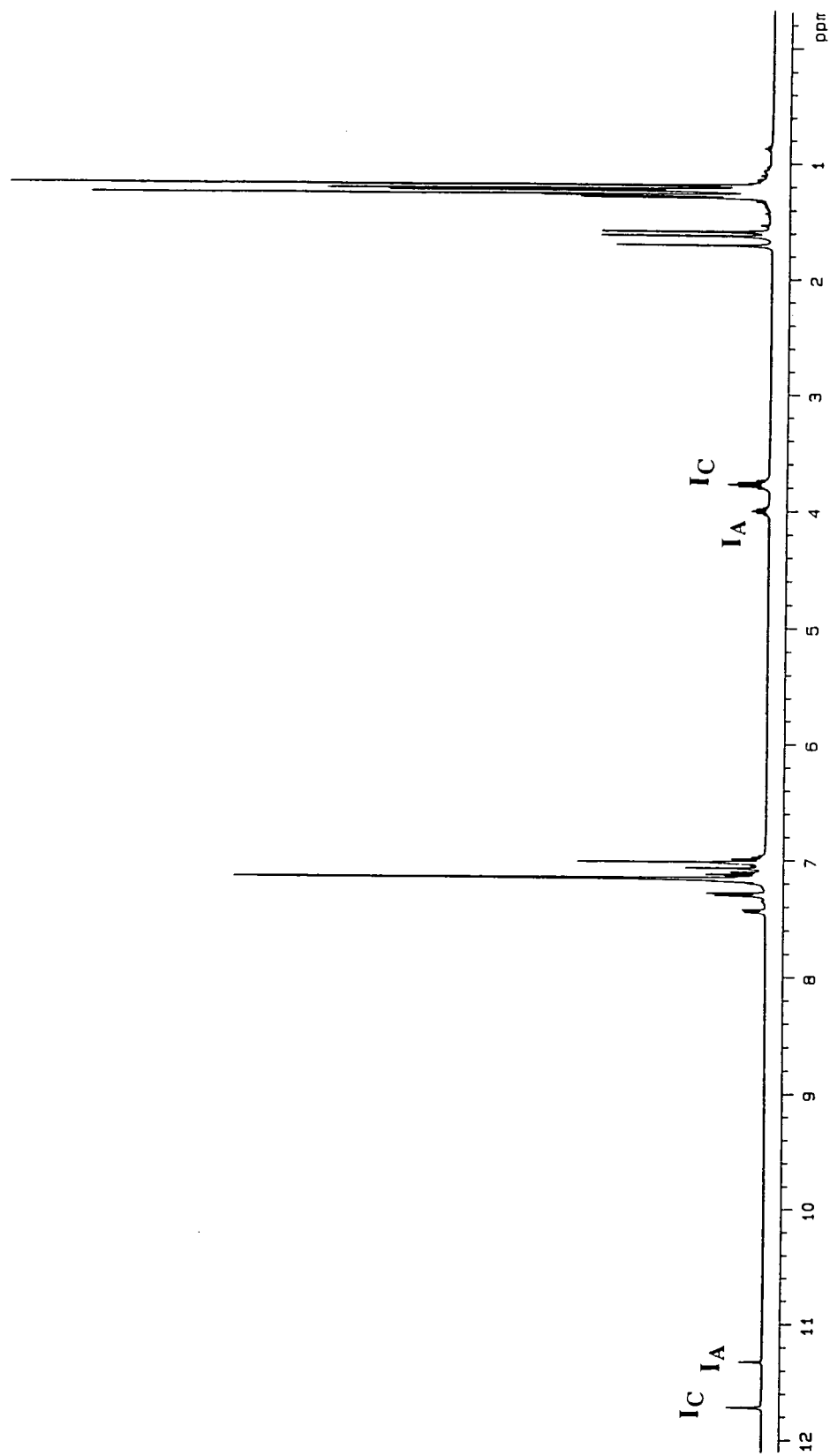


Figure 3.11 The 400MHz  $^1\text{H}$  N.M.R. spectrum ( $\text{C}_6\text{D}_6$ ) of a 2:1 mixture of **IA** : **IB**

hexafluorobutoxide analogue. Note the complete absence of any of the fluorinated starting material.

When the equilibrium is weighted over towards the bis(butoxide) initiator (as above), a sample of poly[1,4-(2,3-bis(trifluoromethyl)cyclopentenylene) vinylene] synthesized from it contains a smaller proportion of cis vinylene double bonds than in the 1:1 mixture of the bis(alkoxide) initiators. Indeed this can be exploited further; a polymer of any desired cis and trans value (between the two high extremes) can be prepared from this tri-component system, simply by altering the proportion of **I<sub>A</sub>** to **I<sub>B</sub>**. The graph in figure 3.12 displays the cis / trans vinylene content obtained as a function of the composition of the initiator mixture.

### **3.3.4 The use of the mixed initiator system to R.O.M.P. 2,3-bis(trifluoromethyl) bicyclo[2.2.1]hepta-2,5-diene in $\alpha,\alpha,\alpha$ -trifluorotoluene**

The mixed initiator system has also been used to polymerize the fluorinated norbornadiene monomer in  $\alpha,\alpha,\alpha$ -trifluorotoluene, as opposed to THF. A complete range of cis and trans contents of poly[1,4-(2,3-bis(trifluoromethyl)cyclopentenylene) vinylene] is again accessible, but there is a noticeable deviation from the results obtained in THF, as shown in table 3.2.

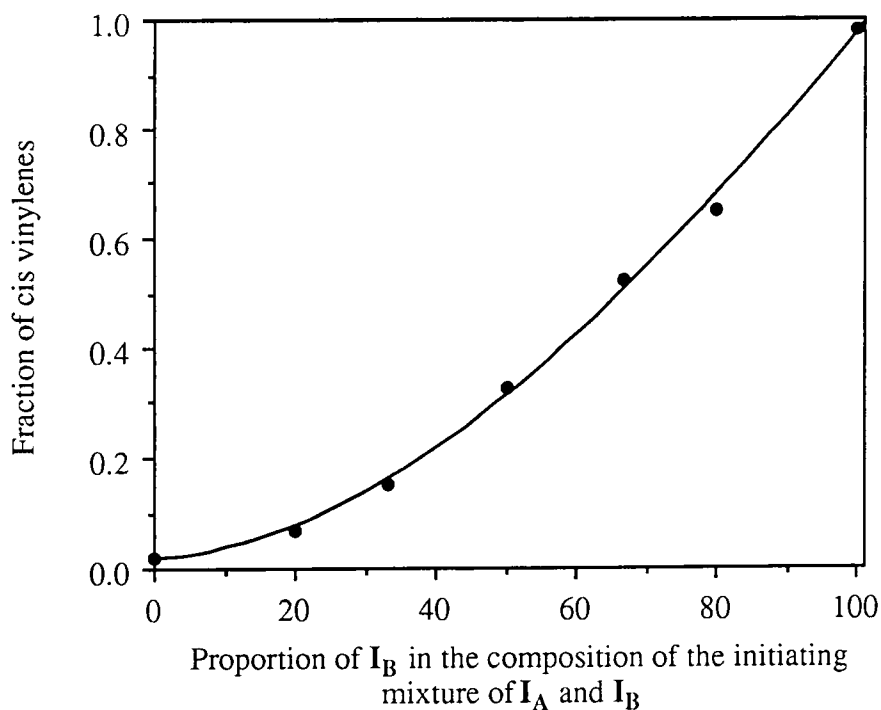


Figure 3.12  $\sigma_c$  of poly[1,4-(2,3-bis(trifluoromethyl)cyclopentenylene vinylene)] as a function of the initiating mixture in THF

Ratio of $I_A$ to $I_B$	$\sigma_t$ observed from THF polymerization	$\sigma_t$ observed from $\alpha,\alpha,\alpha$ -trifluorotoluene polymerization
1:4	0.325	0.107
1:2	0.475	0.205
1:1	0.646	0.514
2:1	0.850	0.795
4:1	0.930	0.893

Table 3.2  $\sigma_t$  of poly[1,4-(2,3-bis(trifluoromethyl)cyclopentenylene) vinylene] for samples synthesized via the mixed initiator equilibrium in  
i) THF and ii)  $\alpha,\alpha,\alpha$ -trifluorotoluene.

In  $\alpha,\alpha,\alpha$ -trifluorotoluene the polymers produced have cis contents appreciably higher than those synthesized under identical conditions in THF. This is due to the ability of the latter solvent to bind to the more electrophilic metal centres in the initiating mixture, and hence reduce their activity. In  $\alpha,\alpha,\alpha$ -trifluorotoluene no such co-ordination is expected and therefore the bis(hexafluorobutoxide) initiator plays a larger role in the propagation mechanism.

The polymers produced are found to approach monodisperse molecular weight distributions. However,  $M_n / M_w$  values are typically 1.10 - 1.20, slightly higher than those seen for the single initiator systems. Once again, small quantities of high molecular weight material with a molecular weight of approximately twice that of the major component are occasionally observed.

### 3.4 The microstructure of poly[1,4-(2,3-bis(trifluoromethyl)cyclopentenylene) vinylene]

The availability of a wide range of samples of poly[1,4-(2,3-bis(trifluoromethyl)cyclopentenylene) vinylene] differing in their cis / trans vinylene content offers an ideal opportunity for detailed physical studies. Establishing the tacticity of these polymers is also of primary importance for full structure-property correlations. The following section outlines the microstructural information relating to tacticity obtained from N.M.R. spectroscopy.

#### 3.4.1 Microstructure assignment via $^{13}\text{C}$ spectroscopy - the C7 methylene region

Sensitivity to r and m environments is often not observed in the  $^{13}\text{C}$  N.M.R. spectra of poly(cyclopentenylenes). Consequently, much of the previous work in this area has concentrated on the ring-opened polymers of optically-resolved 5-substituted norbornenes, such as 5,5-dimethylbicyclo[2.2.1]hept-2-ene<sup>8,9</sup>; in such systems the m/r effect is transformed into head/tail effects which are more readily detected by  $^{13}\text{C}$  N.M.R. spectroscopy as summarised in the figure below.

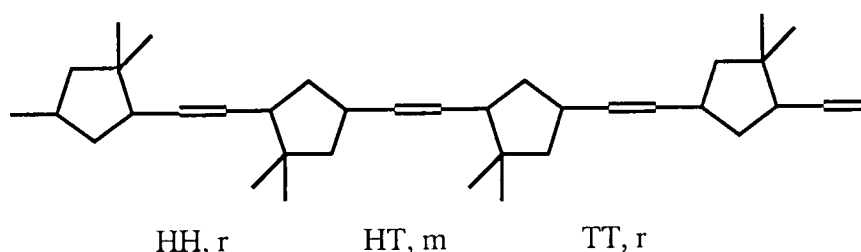


Figure 3.13 The translation of m and r dyads into head-tail effects in the ring-opened polymer of enantiomeric 5,5,-dimethylbicyclo[2.2.1]hept-2-ene (each double bond has a cis geometry)

However, optical resolution of such monomers is a laborious and low-yielding process. Quantitative measurements of tacticity are easier if the polymer gives a  $^{13}\text{C}$

N.M.R. spectrum with resonances directly sensitive to m/r dyads. Ivin et al have previously found that just such a system is the ring-opened polymer of anti-7-methylbicyclo[2.2.1]hept-2-ene<sup>10</sup>, and have determined the ring dyad tacticity with respect to cis and trans junctions for several of its polymers (formed from different classical initiating systems), and the overall tacticity from <sup>13</sup>C N.M.R. spectra of the corresponding hydrogenated macromolecules.

Fortunately, in the case of the ring-opened polymers of 2,3-bis(trifluoromethyl)bicyclo[2.2.1]hepta-2,5-diene substantial fine structure, indicative of r/m splitting and cis/trans isomerism, is revealed in the methylene C7 region. Moreover, since samples covering a large range of cis and trans contents are now available, the assignment of microstructure becomes possible.

The <sup>13</sup>C N.M.R. methylene region of poly[1,4-(2,3-bis(trifluoromethyl)cyclopentenylene) vinylene] ( $\sigma_c=0.98$ ) is shown in figure 3.14 (spectrum a). The two resonances (38.33 and 37.54ppm) are both believed to be cc, i.e. arising from methylene units between two adjacent cis vinylenes (the reader is referred to a full explanation of this terminology in Ivin's book). This assignment is based solely on the unlikelihood of observing ct or tt resonances at such a low value of  $\sigma_t$ .

The splitting of the cc resonance must be due to tacticity. The low dielectric constant for the high cis polymer would appear to rule out a predominantly isotactic structure (in which substantial alignment of polar CF<sub>3</sub> groups is expected). Therefore r dyads are believed to prevail; hence the peak of greater intensity at 38.33ppm is assigned as 'cc rr' (i.e. a methylene carbon adjacent to two cis vinylene bonds and between two syndiotactic dyads), whilst the signal at 37.54ppm is due to rm (and mr) triads.

If r and m dyads are distributed binomially along the polymer backbone, then quantitative <sup>13</sup>C N.M.R. spectroscopy suggests that  $\sigma_r=0.75$ . Given this figure, a third line (cc mm) is predicted to be present, representing 6% of the overall cc resonance; rr accounts for 56%, and rm ( $\equiv$ mr) 38% of the signal. Such a low intensity for this minor environment makes it difficult to place exactly, but the cc mm resonance is tentatively assigned to the small (but reproducible) signal at 36.40ppm.

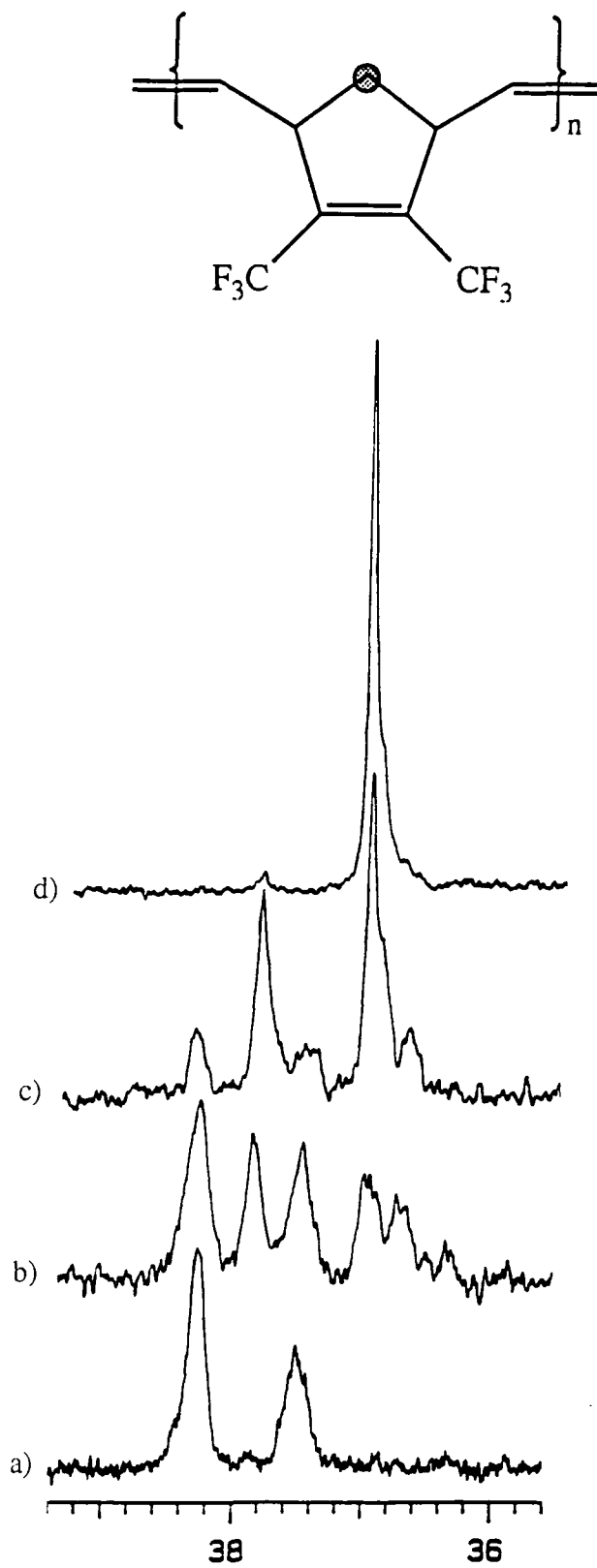


Figure 3.14 The variation in the C7 methylene region with increasing trans content (100MHz; {CD<sub>3</sub>}<sub>2</sub>CO) a)  $\sigma_c = 0.98$ , b)  $\sigma_c = 0.68$ , c)  $\sigma_c = 0.35$ , d)  $\sigma_c = 0.02$

At the other extreme, the methylene C7 region of poly[1,4-(2,3-bis(trifluoromethyl)cyclopentenylene) vinylene] ( $\sigma_c=0.004$ ), figure 3.14(d), shows one major resonance at 37.02ppm, which is obviously tt. The presence of a shoulder to high field of this signal is important; by increasing the spectrometer frequency to 125MHz resolution is enhanced considerably (the outcome is displayed in figure 3.15). Clearly the shoulder is now resolved and as in the cc resonances above, such splitting is attributed to m/r effects.

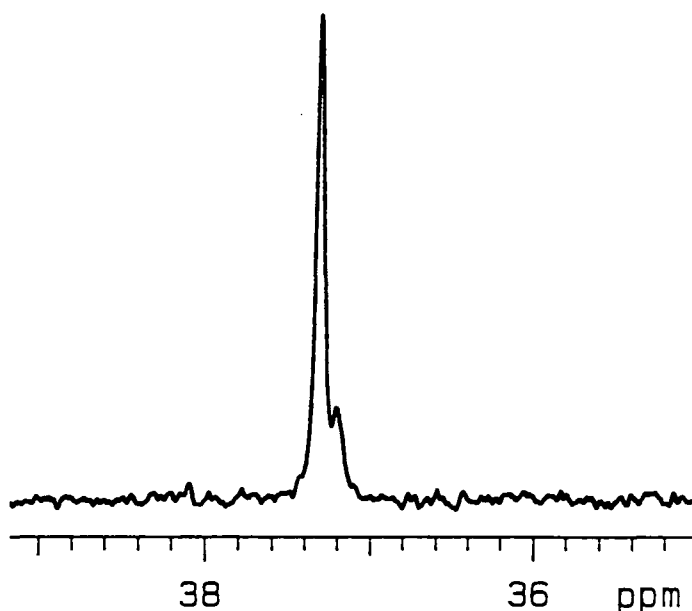


Figure 3.15 The 125MHz  $^{13}\text{C}$  N.M.R. (acetone- $\text{d}_6$ ) of the methylene carbon resonance in a sample of poly[1,4-(2,3-bis(trifluoromethyl)cyclopentenylene) vinylene] ( $\sigma_t = 0.996$ )

As mentioned in chapter two, physical measurements indicate that this highly trans material is syndiotactic (a very high dielectric constant above its glass transition point suggests alignment of the polar  $\text{CF}_3$  groups along the polymer backbone). This would seem to suggest that the more intense of the two resonances observed at 125MHz, (37.32ppm) is due to rr triads, whilst the less intense peak, (37.21ppm) represents tt rm. As for poly[1,4-(2,3-bis(trifluoromethyl)cyclopentenylene) vinylene] with a cis content of 98%, the predicted third signal (mm) is not observed. Quantitative  $^{13}\text{C}$  N.M.R. gives a value for  $(\sigma_r)_t$  of 0.92; therefore the mm resonance would contribute just 0.64% of the total tt signal.

Two other signals are seen in the methylene region of the high trans material, at 37.93 and 36.78ppm. Comparisons with spectra (b) and (c) in figure 3.14 suggest that these peaks are related as a pair, growing in at the same rate from  $\sigma_c=0.02$ , reaching a maximum at  $\sigma_c\approx 0.50$ , before decreasing in intensity as  $\sigma_c$  approaches unity. These two peaks are believed to be ct ( $\equiv$ tc) signals. Since the polymer tends to syndiotacticity at both high cis and high trans, the larger of these two ct peaks is believed to be ct rr, whilst the other is ct rm (which, of course, includes ct mr). The third signal (ct mm) is not observed due to its low abundance.

The overall assignment of the C7 methylene region is tabulated below.

Resonance /ppm		Assignment
100MHz in D <sub>6</sub> -Acetone	125MHz in D <sub>6</sub> -Acetone	
38.33		cc rr
37.93		ct rr
37.54		cc mr
37.02	37.32	tt rr
	37.21	tt rm
36.78		ct rm
36.40		cc mm

Table 3.3 Microstructural assignment for poly[1,4-(2,3-bis(trifluoromethyl)cyclopentenylene)vinylene] via <sup>13</sup>C N.M.R. spectroscopic analysis of the C7 methylene environments

### 3.4.2 Further microstructural information from other resonances in the <sup>13</sup>C N.M.R. spectra

Both olefinic and vinylic carbons (i.e. C2, C3 and C1, C4) also show splitting in their high frequency <sup>13</sup>C N.M.R. spectra, although the effect is far less pronounced than

in the methylene region discussed under 3.4.1. The phenomenon is most noticeable in the olefinic resonances between 131 and 134 ppm, and a tentative assignment of tetrads has been made.

The trans olefinic peak in the very high trans sample ( $\sigma_t = 0.996$ ) is shown in figure 3.16. The major resonance (133.9 ppm) is believed to arise from a ttt rrr tetrad (i.e. all trans syndiotactic).

The two shoulders either side of and immediately adjacent to this major signal are almost certainly related; they grow in and then disappear at roughly equal intensities all the way through the series of samples of the polymer from high trans to high cis. Since the trans polymer is known to be highly syndiotactic ( $\sigma_t = 0.92$ ) it seems reasonable to assume that any meso dyads will be located in runs of racemic dyads. In other words there will be several examples of hexads of the sequence rrrrrr. The two shoulders (of equal intensity) observed at 133.45 and 133.70 ppm are therefore assigned as ttt rrm and ttt mrr (although it is not possible to say which is the low field signal and which is the high field). Another signal, namely ttt rmr, is presumably lost beneath the ttt rrr resonance.

The fourth discernible peak in the trans olefinic region occurs at 133.37 ppm. It is thought that this signal arises from a trans olefinic carbon in the near vicinity of a cis vinylene bond. This argument is based on the series of spectra (figure 3.16); this signal clearly grows in intensity with an increasing cis content, until in the  $\sigma_c = 0.98$  sample it appears as a well-resolved singlet. This is probably ttc and again is likely to be an all syndiotactic tetrad. The other possibilities, tct and ctt are more likely to occur closer to the main cis olefinic resonance at 132.0ppm.

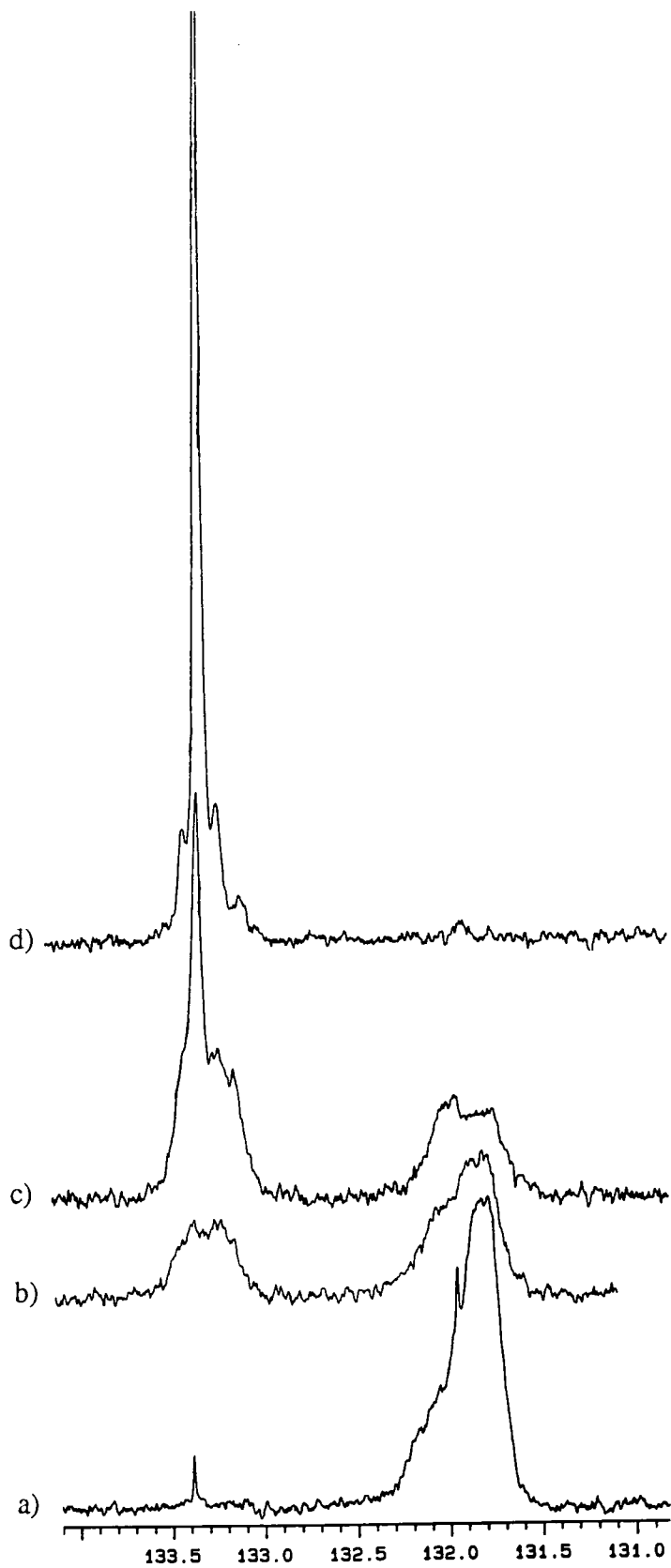


Figure 3.16 The variation of the C2,3 resonances with increasing trans content (100MHz;  $\{CD_3\}_2CO$ ) a)  $\sigma_c = 0.98$ , b)  $\sigma_c = 0.68$ , c)  $\sigma_c = 0.35$ , d)  $\sigma_c = 0.02$

Resonance / ppm	Assignment
133.45	t t t r r m
133.70	t t t m r r
133.9	t t t r r r
133.37	t t c r r r

Table 3.4 Summary of proposed assignments for the trans olefin carbon environments observed in the 100MHz  $^{13}\text{C}$  N.M.R. spectrum of poly[1,4-(2,3-bis(trifluoromethyl)cyclopentenylene)vinylene].

To date, fine structure information has not been obtained from studying the cis olefin signal which is broad and unresolved even at 100MHz (figure 3.17). Nonetheless a 150MHz study is underway on these samples and it is hoped that some further assignments can be made.

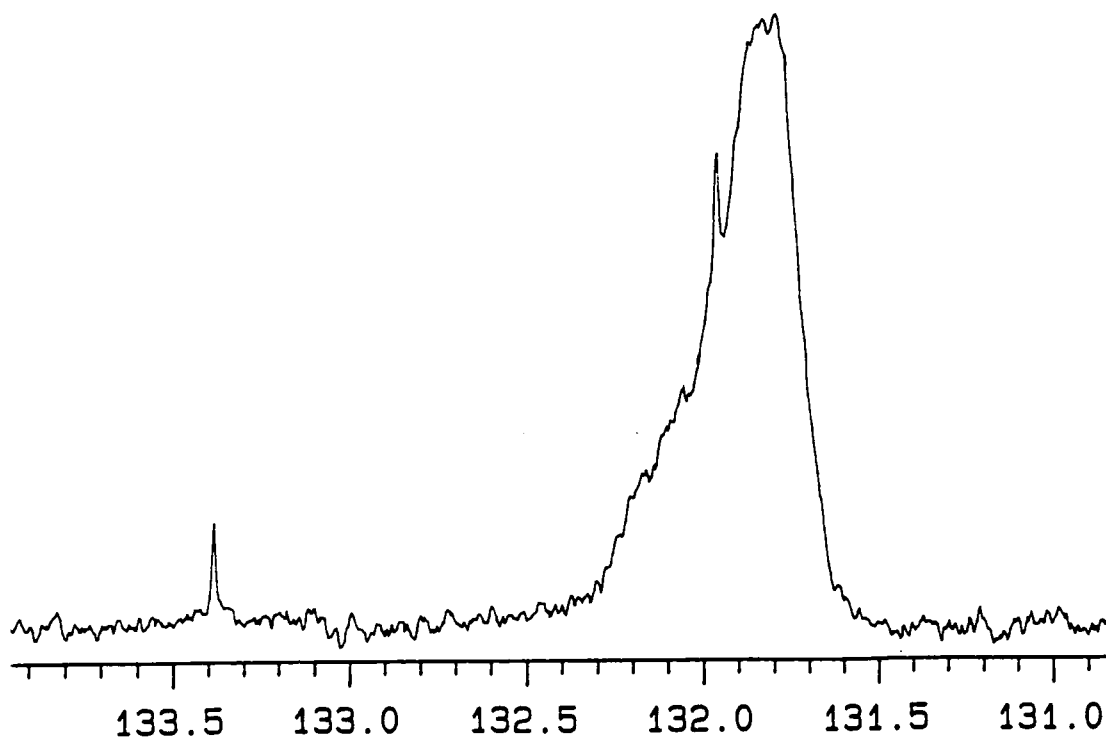


Figure 3.17 The C2,3 olefinic resonance for the very highly cis polymer (100MHz;  $(\text{CD}_3)_2\text{CO}$ )

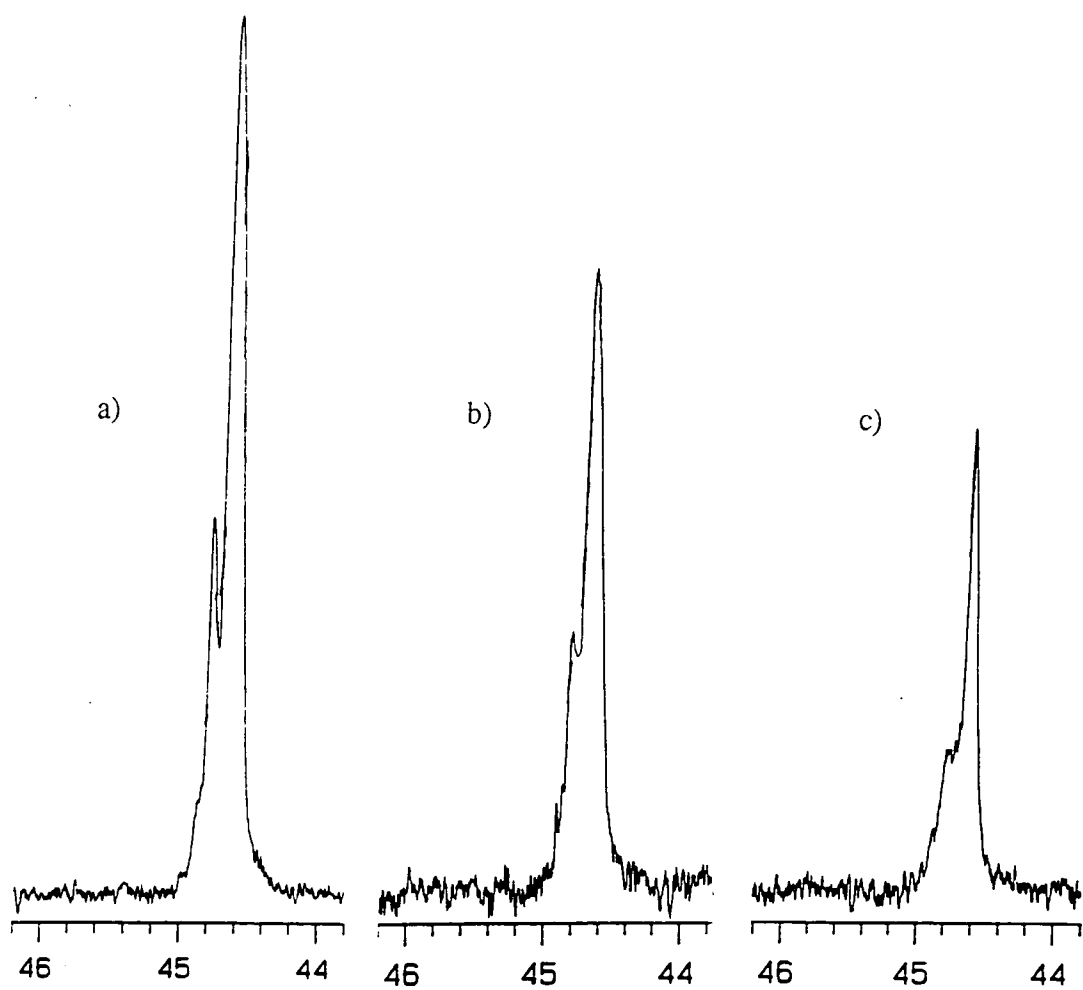


Figure 3.18 The C1,4 cis resonance with increasing trans content  
(100MHz;  $(\text{CD}_3)_2\text{CO}$ ) a)  $\sigma_c = 0.98$ , b)  $\sigma_c = 0.68$ , c)  $\sigma_c = 0.32$

Similarly the vinylene carbons adjacent to a trans double bond in the polymer backbone (i.e. C1 and C4) yield little microstructural data in their  $^{13}\text{C}$  signals. However, their cis analogues (a characteristic 5ppm upfield at 44.6ppm) do display some splitting, and this becomes more noticeable as the trans vinylene content falls (figure 3.18).

Unfortunately an assignment of the two major resonances and at least two shoulders (44.85 and 44.90ppm) has not yet proved possible. In this particular case it has not been possible to specify whether the fine structure observed arises from triads (e.g. cc rr) or tetrads (ccc rrr).

### 3.4.3 Microstructure assignment via $^{19}\text{F}$ N.M.R. spectroscopy

$^{13}\text{C}$  N.M.R. spectroscopy excels in establishing polymer microstructure. However, as shown above, even in cases where chemical shifts are sensitive to r and m dyad environments, complete assignment can be hampered by overlapping signals. Fortunately, the samples of poly[1,4-(2,3-bis(trifluoromethyl)cyclopentenylene) vinylene] prepared via the living mixed initiator system also tender structural information in their  $^{19}\text{F}$  N.M.R. spectra.

As in the methylene C7 region of the carbon spectra, the  $^{19}\text{F}$  N.M.R. of poly[1,4-(2,3-bis(trifluoromethyl)cyclopentenylene) vinylene] changes dramatically as trans content decreases as shown in figure 3.19. At high trans contents there is one major signal at 59.7ppm, possibly with one or two shoulders, alongside several small peaks barely emerging from baseline noise level. As the cis content rises through the series of spectra this resonance diminishes, whilst a range of signals grow in between 59.9 and 60.3ppm, with one peak at 60.1ppm dominating.

This is immediately consistent with the information obtained from the C7 methylene region. At high trans vinylene contents the polymer is highly stereoregular (92% syndiotactic). However, at the other extreme, the high cis samples are not as well-ordered ( $\{\sigma_r\}_c = 0.75$ ) and hence give rise to more complicated splitting patterns.

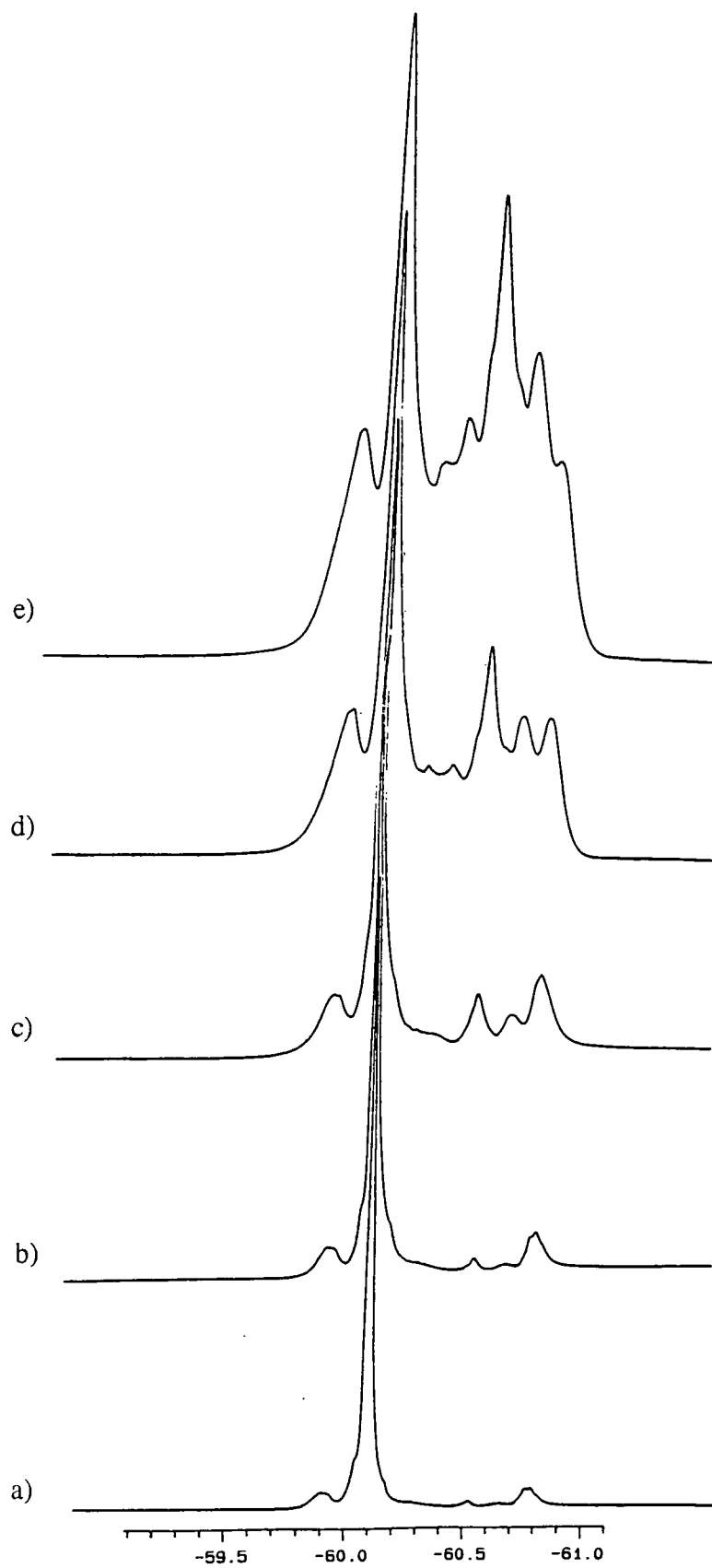


Figure 3.19 The variation in  $^{19}\text{F}$  N.M.R. resonances with increasing cis contents

a)  $\sigma_c = 0.07$ , b)  $\sigma_c = 0.15$ , c)  $\sigma_c = 0.35$ , d)  $\sigma_c = 0.52$ , e)  $\sigma_c = 0.68$

Figure 3.20 shows the 470.599MHz  $^{19}\text{F}$  spectra of the high trans polymer ( $\sigma_t = 0.996$ ); note that it has been vertically expanded several times in order to appreciate the less intense signals. The highest intensity resonance at 60.10ppm can be assigned with confidence to  $\text{CF}_3$  groups on cyclopentenylene rings between two trans bonds, contained within a syndiotactic geometry (i.e. tt rr).

Possible low intensity shoulders on this peak are probably tt rm and maybe even tt mm. It is also possible that the main peak represents fluorines within an all trans-syndiotactic tetrad, in which case the shoulders will correspond to environments such as ttt rrm and ttt rmr. However, at this stage it has not been possible to confirm these minor assignments.

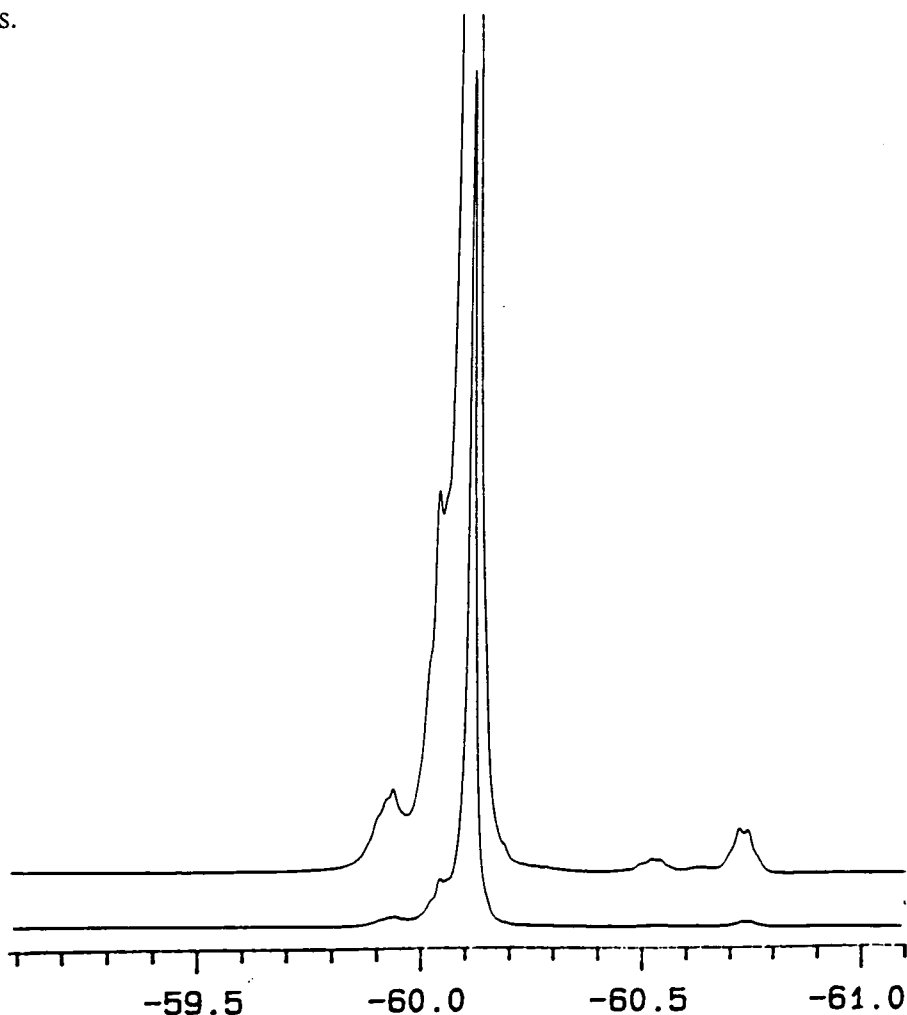


Figure 3.20 The 470MHz  $^{19}\text{F}$  N.M.R. spectrum ( $\{\text{CD}_3\}_2\text{CO}$ ) of 99.6% trans poly[1,4-(2,3-bis(trifluoromethyl)cyclopentenylene) vinylene]

### 3.5 Summary

This chapter has described how living R.O.M.P. can now be exploited to produce polymers of predetermined cis and trans vinylene content, a strategy which should prove applicable to many other R.O.M.P. polymers. The importance of such a system lies in future work, in particular structure-property correlations, which are presently underway.

Furthermore, the system also represents a valuable tool with regard to microstructure assignment; this is particularly so for monomers where the two homobisalkoxides lead to the isolation of high cis and high trans polymers. It seems most likely that this will occur when the monomer olefinic bond is deactivated.

Chapter five describes a preliminary investigation into the R.O.M.P. of several such monomers (again bearing fluorine substituents but in an asymmetric manner). As will be shown, high cis and high trans polymers are afforded, thus laying the tracks for full microstructural studies upon more complicated materials.

### 3.6 References

1. J.H. Wengrovius, R.R. Schrock, M.R. Churchill, J.R. Missert, W.J. Youngs  
J.Am.Chem.Soc. **102** 4515 (1980)
2. M. Jolly, J.P. Mitchell, V.C. Gibson J.Chem.Soc.,Dalton Trans. 1331 (1992)
3. J.P. Mitchell Ph.D. Thesis, University of Durham (1992)
4. D.J. Arney, P.A. Wexler, D.E. Wigley Organometallics **9** 1282 (1990)
5. D.C. Bradley, R.C. Mehrotra, D.P. Gaur 'Metal Alkoxides', Academic Press,  
London (1978)
6. R.R. Schrock, R.T. Depue, J. Feldman, K.B. Yap, D.C. Yang, W.M. Davis,  
L. Park, M. DiMare, M. Schofield, J.T. Anhaus, E. Walborsky, E. Evitt, C. Kruger,  
P.Betz Organometallics **9** 2262 (1990)
7. V.C. Gibson, E.L. Marshall *Unpublished results*
8. K.J. Ivin 'Olefin Metathesis', Academic Press, London (1983)
9. K.J. Ivin, J.J. Rooney, L. Bencze, J.G. Hamilton, L.-M. Lam, G. Lapienis,  
B.S.R. Reddy, H.T. Ho Pure and Appl.Chem **54** 447 (1982)
- 10 J.G. Hamilton, K.J. Ivin, J.J. Rooney J.Mol.Catal. **28** 255 (1985)

## **Chapter Four**

**Studies into Tacticity Control in the Living R.O.M.P. of  
2,3-Bis(trifluoromethyl)bicyclo[2.2.1]hepta-2,5-diene**

## 4.1 Introduction

The previous two chapters of this thesis have shown that it is possible to obtain an unprecedented level of control over the cis and trans contents of ring-opened functionalised norbornene and norbornadienes. This chapter forms a logical extension of this work describing preliminary investigations into tacticity control.

The proposed mechanism for the living metathesis polymerization of 2,3-bis(trifluoromethyl)bicyclo[2.2.1]hepta-2,5-diene with the four-coordinate Schrock-type initiators was outlined in section 2.8. High degrees of tacticity are likely only if, for each propagation step, one face of the N-Mo-C plane is favoured for monomer approach. Consequently any attempt to increase the tacticity in polymers generated from these initiators must be based upon increasing face selectivity.

A possible route to a 'face-selective' initiator would be the synthesis of an analogous complex bearing chiral units either within the imido or alkoxide ligands. However, such a methodology represents a lengthy and laborious task. Potentially, a much simpler way of influencing tacticity might be to polymerize the fluorinated monomer in the presence of an enantiomerically-pure chiral Lewis base. It was envisaged that in such systems the monomer would have to make its approach upon a five-coordinate optically-active adduct of the Schrock initiator, and that this might effect the tacticity of the resultant poly[1,4-(2,3-bis(trifluoromethyl)cyclopentenylene) vinylene].

## 4.2 Five-coordinate chiral base adducts of $\text{Mo}(\text{NAr})(\text{CHR})(\text{OR}')_2$

A considerable amount of work has already been reported on base adducts of the four-coordinate metathesis initiators developed by Schrock and co-workers. The most detailed study yet undertaken investigated the trimethylphosphine adducts of  $\text{Mo}(\text{NAr})(\text{CHCMe}_3)(\text{OCMe}_3)_2$  and  $\text{Mo}(\text{NAr})(\text{CHCMe}_3)(\text{OCMe}(\text{CF}_3)_2)_2$ <sup>1</sup>. Bazan and Schrock have shown that at room temperature base adduct formation with the bis(tert-butoxide) complex is not favoured, although syn and anti adducts are observed under identical conditions with the more electron-withdrawing hexafluorobutoxide species. More recently Grubbs and co-workers have polymerized cyclobutene in a well-behaved living manner using  $\text{W}(\text{NAr})(\text{CHCMe}_3)(\text{OCMe}(\text{CF}_3)_2)_2$  in the presence of  $\text{PMe}_3$ <sup>2</sup>.

For the study described herein, two chirally-resolved nucleophilic molecules were identified as being suitable for base-adduct formation, (*S*)-(-)- $\alpha$ -methylbenzylamine, and (+)-camphor. The two predicted base adducts of  $\text{Mo}(\text{NAr})(\text{CHR})(\text{OCMe}_3)_2$  and  $\text{Mo}(\text{NAr})(\text{CHR})(\text{OCMe}(\text{CF}_3)_2)_2$  are shown in figure 4.1.

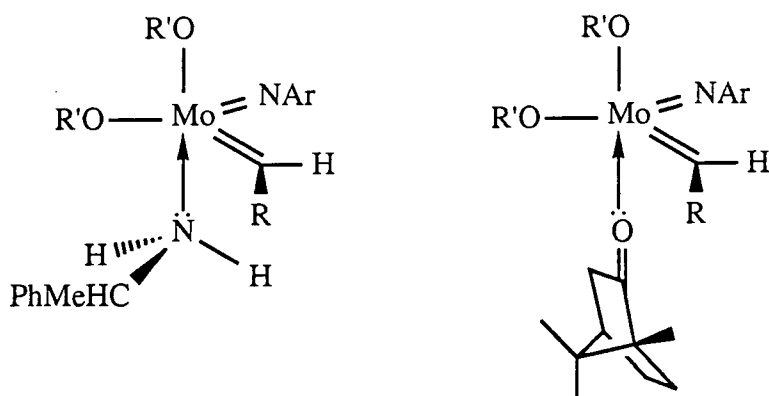


Figure 4.1 The two postulated anti alkylidene rotamers of the five co-ordinate base adducts formed with  $\text{Mo}(\text{NAr})(\text{CHR})(\text{OR}')_2$

The four-coordinate molybdenum initiators have previously been reported to be stable with respect to the amine and ketonic carbonyl functionalities<sup>3</sup>. Previous work has

shown that with *t*-BuNH<sub>2</sub> syn and anti rotamers of the five-coordinate base adduct are observed for Mo(NAr)(CHCMe<sub>2</sub>Ph)(OCMe(CF<sub>3</sub>)<sub>2</sub>)<sub>2</sub>, whilst no reaction is discernible with the bis(*tert*-butoxide) initiator even after several days at elevated temperature. Non-reactivity with respect to ketones has been demonstrated by the addition of several equivalents of benzophenone; no reaction (including metal-oxo or base-adduct formation) is observed for either initiator.

#### 4.2.1 The reaction between Mo(NAr)(CHR)(OR')<sub>2</sub> and

(S)-(-)- $\alpha$ -methylbenzylamine

(R = CMe<sub>2</sub>Ph, R' = CMe<sub>3</sub>, CMe(CF<sub>3</sub>)<sub>2</sub>; R = CMe<sub>3</sub>, R' = CMe<sub>2</sub>CF<sub>3</sub>)

<sup>1</sup>H N.M.R. spectroscopy was employed to study the formation of the five-coordinate chiral base adducts; for each of the three initiators 2 equivalents of the amine were added in a benzene-d<sub>6</sub> solution. As expected adduct formation is strongest for the bis(hexafluorobutoxide) initiator; indeed, for the analogous *tert*-butoxide complex no evidence for any five-coordinate species was detected. Interestingly, Mo(NAr)(CHCMe<sub>3</sub>)(OCMe<sub>2</sub>CF<sub>3</sub>)<sub>2</sub> falls in between these two extremes; at room temperature an equilibrium mixture composed of the syn and anti rotamers of the base adduct and the syn rotamer of the base-free neopentylidene is observed.

Some idea of how strong the adduct formation is with methylbenzylamine can be qualitatively determined by measuring the time required for Mo(NAr)(CHCMe<sub>2</sub>Ph)(OCMe(CF<sub>3</sub>)<sub>2</sub>)<sub>2</sub> to R.O.M.P. 10.0 equivalents of norbornene and comparing this to data recorded for the analogous reaction in the presence of other bases. As a general rule, smaller bases bind more strongly. For example, pyridine forms very strong base adducts; weak adduct formation is even seen at room temperature for Mo(NAr)(CHCMe<sub>2</sub>Ph)(OCMe<sub>3</sub>)<sub>2</sub> (alkylidene resonance at 11.34ppm compared to 11.31 in the absence of the base) and when 2,3-bis(trifluoromethyl)bicyclo[2.2.1]hepta-2,5-diene is added a propagating doublet at 11.40 (compared to 11.35) is observed. However, with the

far bulkier triethylamine no evidence for base adduct formation at room temperature has been observed even for the bis(hexafluorobutoxide) compound.

#### 4.2.2 The polymerization of 2,3-bis(trifluoromethyl)bicyclo[2.2.1]hepta-2,5-diene in the presence of (S)-(-)- $\alpha$ -methylbenzyl amine

The addition of 2,3-bis(trifluoromethyl)bicyclo[2.2.1]hepta-2,5-diene to the base adduct / base-free equilibria described above has also been studied by  $^1\text{H}$  N.M.R. spectroscopy. Although living polymerization does occur, the binding of the amine to the metal centre leads to a marked reduction in the rate of propagation, especially for the fluorinated initiators. The graph in figure 4.2 shows the time required for the bis(trifluorobutoxide) initiator to consume ten equivalents of the fluorinated monomer with and without base present.

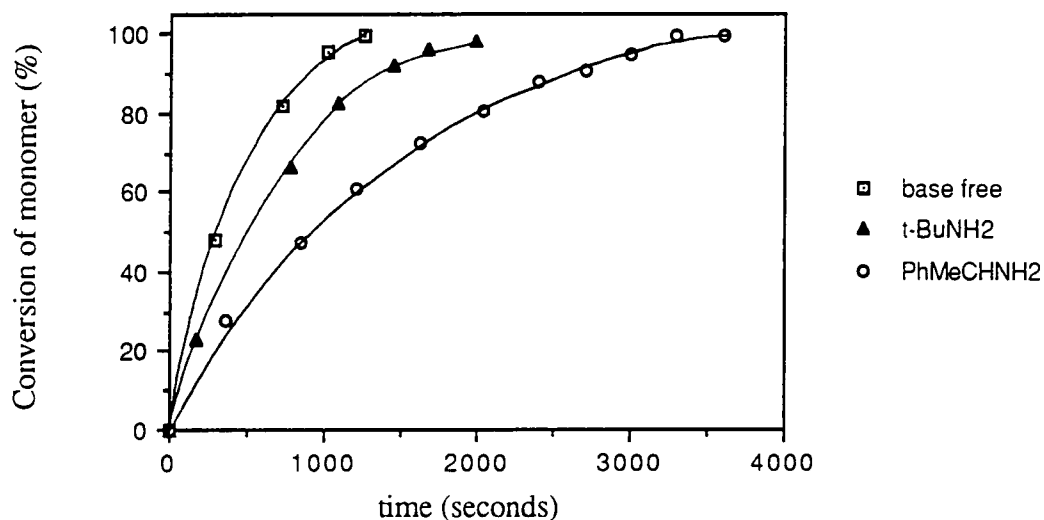


Figure 4.2 The consumption of 2,3-bis(trifluoromethyl)bicyclo[2.2.1]hepta-2,5-diene as a function of time by  $\text{Mo}(\text{NAr})(\text{CHCMe}_3)(\text{OCMe}_2\text{CF}_3)_2$

From the N.M.R. data it also appears that in each case the cis and trans vinylene content of the living polymer chain are unchanged from those observed for the corresponding initiator in the absence of a base. These observations are in agreement with studies on related systems; there is increasing evidence that the base must first dissociate before monomer insertion may occur (similarly base dissociation must also occur prior to syn / anti rotamer isomerization).

The samples of poly[1,4-(2,3-bis(trifluoromethyl)cyclopentenylene) vinylene] were recovered by precipitation from a non-solvent. Analysis of the  $^{13}\text{C}$  N.M.R. spectra confirmed that the cis and trans vinylene contents were indeed the same as those normally observed for the analogous base-free systems. Examination of the C7 methylene region showed that the ring-dyad distributions were also unaffected.

In summary, this short study provides more evidence to support the view that five-coordinate species of the type  $\text{M}(\text{NAr})(\text{CHR})(\text{OR}')_2(\text{B})$  ( $\text{M} = \text{Mo}, \text{W}$ ;  $\text{R} = \text{CMe}_3, \text{CMe}_2\text{Ph}$ ;  $\text{R}' = \text{CMe}_3, \text{CMe}_2\text{CF}_3, \text{CMe}(\text{CF}_3)_2$ ;  $\text{B} = \text{Lewis base}$ ) are inactive with respect to olefin metathesis. In solution, however, these complexes exist in equilibrium with dissociated base and the corresponding four-coordinate base-free initiator. Polymers synthesized from these equilibria possess architectures indicative of propagation through the four-coordinate species only. Therefore even the use of a sterically unhindered, chiral base has no measurable influence over polymer tacticity.

This is an important observation; it implies that the base must dissociate from the metal centre before the monomer can even make its approach towards one of the N-Mo-C faces. A six-coordinate intermediate featuring weak association of the base and the monomer olefinic bond, with metallacycle formation proceeding via an  $\text{S}_{\text{N}}2$  style intermediate (figure 4.3), is therefore unlikely. This may be due to the lack of a suitable empty metal-orbital trans to the base and / or steric hindrance.

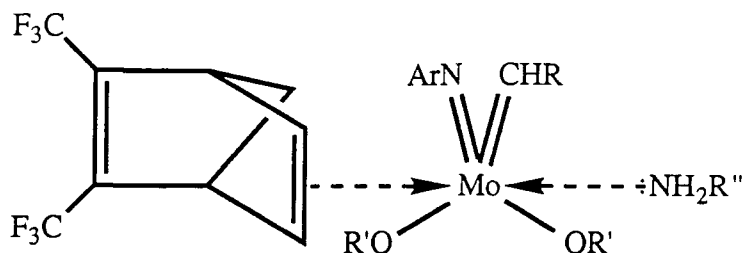


Figure 4.3 Hypothetical  $S_N2$ -related intermediate for base-dissociation / monomer approach

#### 4.2.3 Polymerization of 2,3-bis(trifluoromethyl)bicyclo[2.2.1]hepta-2,5-diene by $\text{Mo}(\text{NAr})(\text{CHCMe}_2\text{Ph})(\text{OR})_2$ in the presence of (+)-camphor

Large scale polymerizations of 2,3-bis(trifluoromethyl)bicyclo[2.2.1]hepta-2,5-diene by the four-coordinate R.O.M.P. initiators in the presence of relatively large amounts of (S)-(-)- $\alpha$ -methylbenzylamine were unsuccessful; this is believed to be due to difficulties in purifying the amine, and also because the rate retardation is likely to become even more significant at the higher concentrations of base employed. Nonetheless, even though the N.M.R. scale polymerizations reported suggest that chiral bases have no influence over polymer tacticity, a second study was undertaken with (+)-camphor.

In order to see what effect, if any, (+)-camphor had upon the level of tacticity in 98% trans poly[1,4-(2,3-bis(trifluoromethyl)cyclopentenylene) vinylene], a THF solution of  $\text{Mo}(\text{NAr})(\text{CHCMe}_2\text{Ph})(\text{OCMe}_3)_2$  was made up and 100 equivalents of the chiral component then added. After exactly ten minutes stirring 1.00g of the monomer was added dropwise to the stirring initiator / camphor solution. An identical experiment was carried out using the bis(hexafluorobutoxide) neophylidene initiator. In both cases the polymer was recovered in the usual way (precipitation from methanol and from hexane respectively).

Unexpectedly the presence of camphor leads not to a change in tacticity, but to a dramatic deviation in the cis and trans vinylene content. The polymer generated from the  $\text{Mo}(\text{NAr})(\text{CHCMe}_2\text{Ph})(\text{OCMe}(\text{CF}_3)_2)_2$  / (+)-camphor mixture contained a trans content of

41.2% (compared to less than 2% in the absence of (+)-camphor), whereas the bis(tert-butoxide)-initiated product had a trans content of 94.5% (reduced from 98%). This observation is reproducible. Further, if the bis(hexafluorobutoxide) reaction is repeated using 200 equivalents of (+)-camphor (again in tetrahydrofuran) the polymer recovered possesses a  $\sigma_c$  value of just 0.14.

These observations have also been found to be solvent dependent. For example, in  $\alpha,\alpha,\alpha$ -trifluorotoluene the effect is lessened.  $\text{Mo}(\text{NAr})(\text{CHCMe}_2\text{Ph})(\text{OCMe}(\text{CF}_3)_2)_2$  and 100 equivalents of the optically active species produce 89.2% cis poly[1,4-(2,3-bis(trifluoromethyl)cyclopentenylene) vinylene].

Furthermore, comparison of the  $^{13}\text{C}$  N.M.R. spectra obtained for these polymers with samples synthesised from the mixed initiator system described in chapter three of similar cis and trans vinylene content suggest that the composition of the dyad tacticities is unchanged. For example figure 4.4 shows the C7 methylene region of two samples of this polymer; spectrum (a) is that of a  $\sigma_t = 0.945$  material prepared from  $\text{Mo}(\text{NAr})(\text{CHCMe}_2\text{Ph})(\text{OCMe}_3)_2$  and 100 equivalents of (+)-camphor, whilst the second trace is that of a 93.5% trans vinylene polymer afforded from a 1:2 mixture of the bis(tert-butoxide) and the bis(hexafluorobutoxide) initiators in THF.

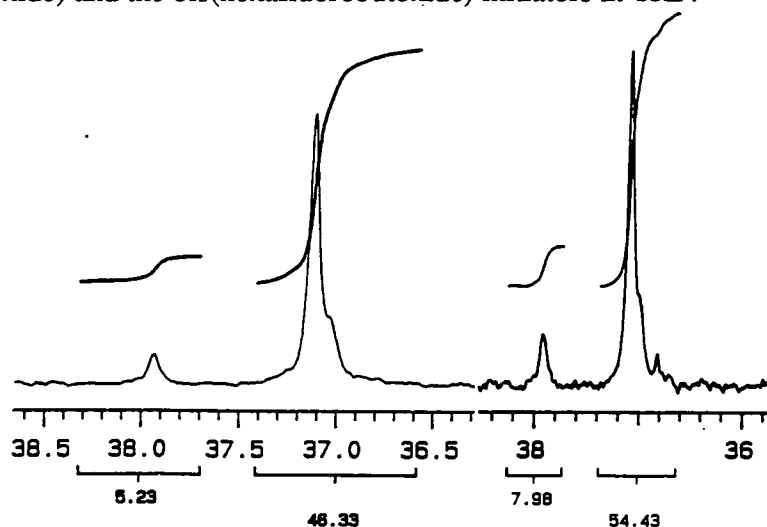


Figure 4.4 The 100MHz  $^{13}\text{C}$  N.M.R.  $\{(\text{CD}_3)_2\text{CO}\}$  methylene C7 regions of the fluoropolymer a) synthesised in the presence of camphor b) synthesised via the mixed initiating system described in chapter three

#### 4.2.4 The reaction between $\text{Mo}(\text{NAr})(\text{CHCMe}_2\text{Ph})(\text{OR})_2$ and (+)-camphor in benzene- $\text{d}_6$

Initially 2 equivalents of (+)-camphor was added to  $\text{C}_6\text{D}_6$  solutions of  $\text{Mo}(\text{NAr})(\text{CHCMe}_2\text{Ph})(\text{OR})_2$  for  $\text{R} = \text{CMe}_3$ ,  $\text{CMe}_2\text{CF}_3$  and  $\text{CMe}(\text{CF}_3)_2$  and the resultant solutions analysed by  $^1\text{H}$  N.M.R. spectroscopy at 250MHz. In the case of the bis(tert-butoxide) and the bis(trifluorobutoxide) initiators no reaction was observed; the alkylidene appears stable with respect to the carbonyl functionality, giving rise to a singlet corresponding in chemical shift to the base free complex. With the bis(hexafluorobutoxide) initiator base-adduct formation is observed, with a single alkylidene at 12.24ppm (no resonance has been located for the other rotamer).

Following the observations reported previously for the effect that camphor has upon the cis and trans content of poly[1,4-(2,3-bis(trifluoromethyl)cyclopentenylene vinylene)] a further sequence of  $^1\text{H}$  N.M.R. experiments were undertaken. The addition of many more equivalents of (+)-camphor and the acquisition of more N.M.R. transients showed that other alkylidene species are indeed present, albeit in relatively small amounts.

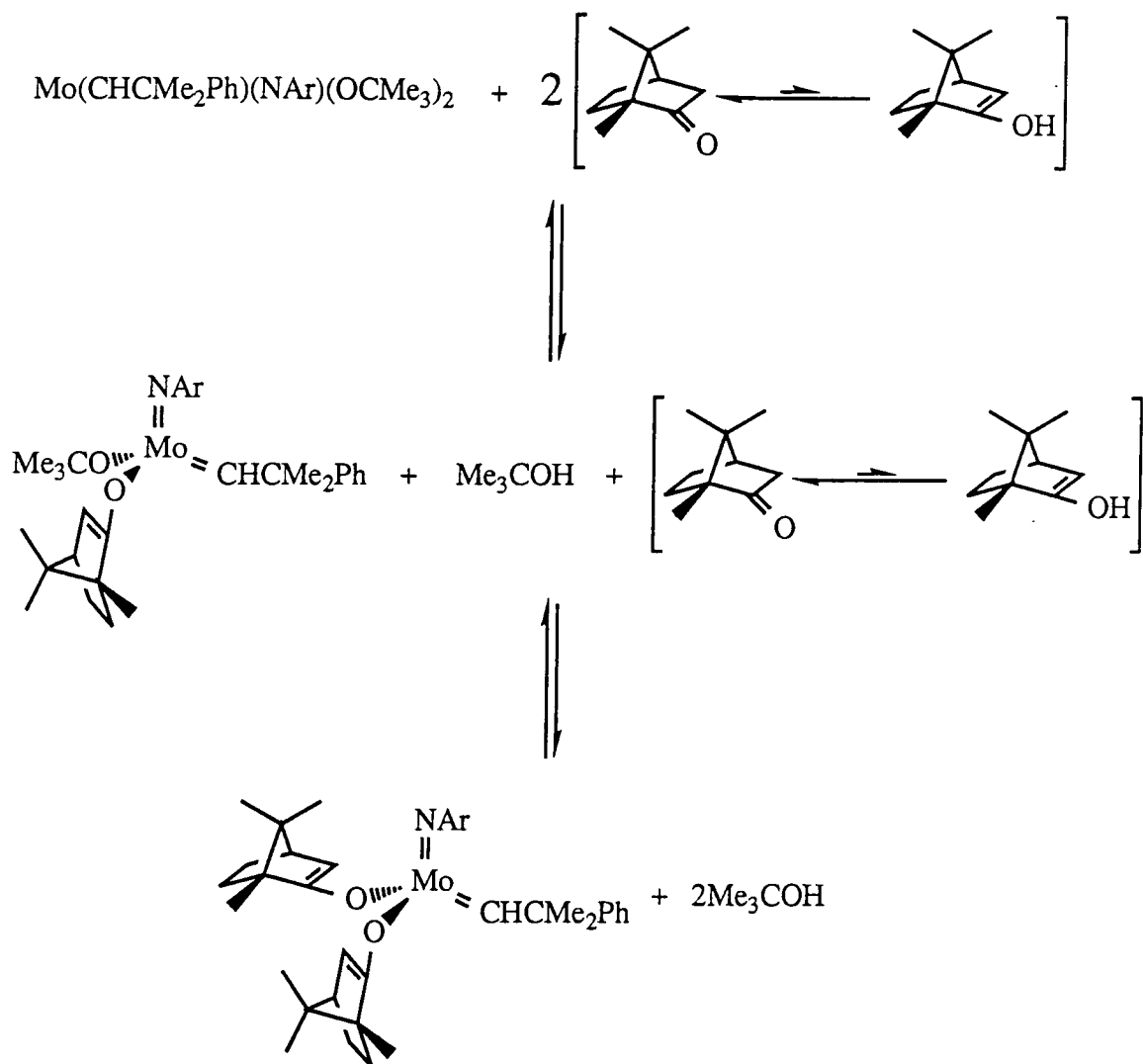
Initiator alkoxides	Equivalents of camphor	Appearance of alkylidene region
$\text{OCMe}_3$	11.4	11.31ppm (96.0%) : 11.23ppm (4.0%)
$\text{OCMe}_3$	21.1	11.31ppm (92.4%) : 11.23ppm (7.60%)
$\text{OCMe}(\text{CF}_3)_2$	12.6	12.23ppm (94.1%) : 11.63ppm (5.9%)
$\text{OCMe}(\text{CF}_3)_2$	22.4	12.29ppm (81.5%) : 11.64ppm (18.5%)

Table 4.1 The observation of minor alkylidene signals following the addition of large excesses of (+)-camphor to the four-coordinate initiators ( $\text{C}_6\text{D}_6$ )

The intensities of the less intense alkylidene resonances remained constant over a period of several days. Given the rapid formation of the equilibrium mixture and the effect over cis and trans content in the experiments to synthesize poly[1,4-(2,3-bis(trifluoromethyl)cyclopentenylene vinylene)] the logical conclusion is that the presence of camphor leads to some form of alkoxide exchange.

Although it has not proved possible to confirm the identities of the new alkylidene resonances it is believed that the initiator undergoes rapid exchange with the enol tautomer of (+)-camphor. As the enol form is removed from the ketone-enol equilibrium so that reaction shifts in favour of more enol production. However, this process exists in a competitive equilibrium with the exchange of the appropriate butanol with the new initiator. Consequently, only a small amount of the camphor-enolate derivative is observed (scheme 4.1).

This theory explains why increasing quantities of the chiral component lead to a larger change in the cis and trans vinylene content. Moreover, the position of a keto / enol tautomerization equilibrium is expected to be solvent dependent (hence the discrepancy between identical experiments in THF and in  $\alpha,\alpha,\alpha$ -trifluorotoluene). It would also appear that the presence of camphor enolate ligands at the active site favours trans metallacycle formation with the fluorinated monomer (presumably syn / anti rotamer interconversion is relatively rapid).



Scheme 4.1

There is no report in the literature concerning the position of the keto-enol equilibrium of camphor in solution at room-temperature. However, consistent with current trends in synthetic methodology, many enolate derivatives have been isolated<sup>4</sup> (figure 4.5).

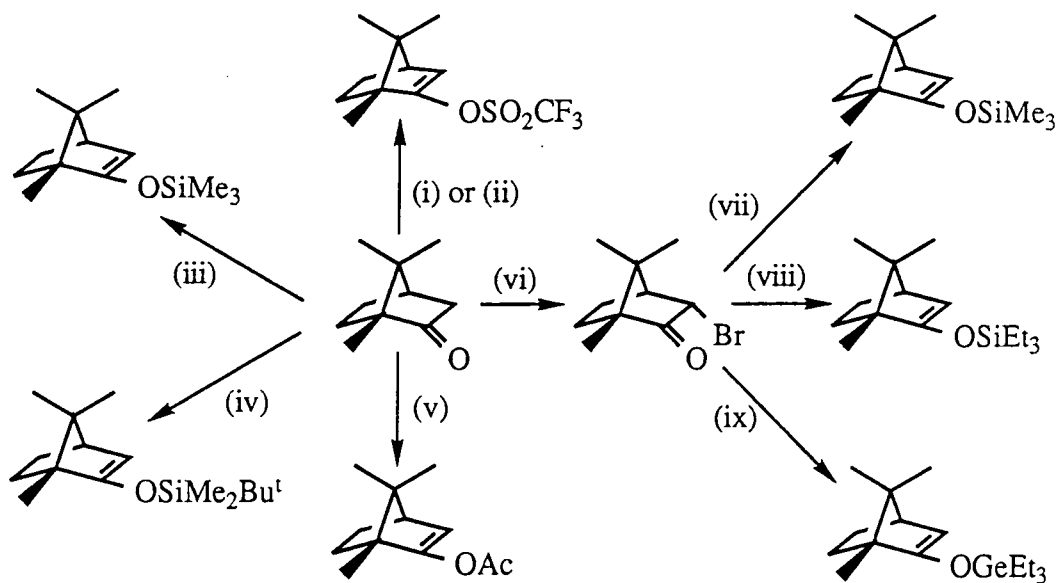


Figure 4.5 (i)  $\text{LiNPr}^i_2$ , DME,  $(\text{CF}_3\text{SO}_3)_2\text{NPh}$ ; (ii) MeLi, THF,  $(\text{CF}_3\text{SO}_3)_2\text{NPh}$ ; (iii)  $\text{LiNPr}^i_2$ , DME,  $\text{Me}_3\text{SiCl}$ ; (iv)  $\text{LiNPr}^i_2$ , THF,  $\text{Bu}^t\text{Me}_2\text{SiCl}$ ; (v)  $\text{Bu}^n\text{Li}$ , THF,  $\text{Ac}_2\text{O}$ ,  $-50^\circ\text{C}$ ; (vi)  $\text{Br}_2$ ,  $\text{AcOH}$ ; (vii) Zn,  $\text{Et}_2\text{O}$ ,  $\text{Me}_3\text{SiCl}$ ; (viii)  $\text{Hg}(\text{SiEt}_3)_2$  (ix)  $\text{Hg}(\text{GeEt}_3)_2$

In order to prove this theory of enolate exchange with the initiator attempts were made to locate the olefinic proton of the mixed butoxide-enolate product, which should possess the same intensity as the alkylidene proton for this species, in the  $^1\text{H}$  N.M.R. spectrum. The corresponding signal for camphor enol acetate<sup>5</sup> is a doublet at 5.54ppm ( $\text{CDCl}_3$ ). Although an unambiguous assignment has not proved feasible, two groups of signals of low intensity are observed between 4 and 6ppm in the proton spectrum arising from a mixture of 19.9 equivalents (+)-camphor and  $\text{Mo}(\text{NAr})(\text{CHCMe}_2\text{Ph})(\text{OCMe}_3)_2$ , (figure 4.6).

Attempts to observe eliminated alcohol have also provided partial evidence for this theory of enolate exchange. Although the signals of many of the camphor protons are found between 0.5 and 1.8ppm, fortuitously the expected resonance of the methyl group of  $(\text{CF}_3)_2\text{MeCOH}$  (1.06ppm) falls in an otherwise unoccupied part of the spectrum. As shown in figure 4.7, when 20.5 equivalents of camphor are mixed with the bis(hexafluorobutoxide) initiator a minor signal is indeed seen at 1.04-1.05ppm. However,

no observation of the hydroxyl proton has been made, and therefore this signal can not yet be confirmed as due to the predicted by-product.

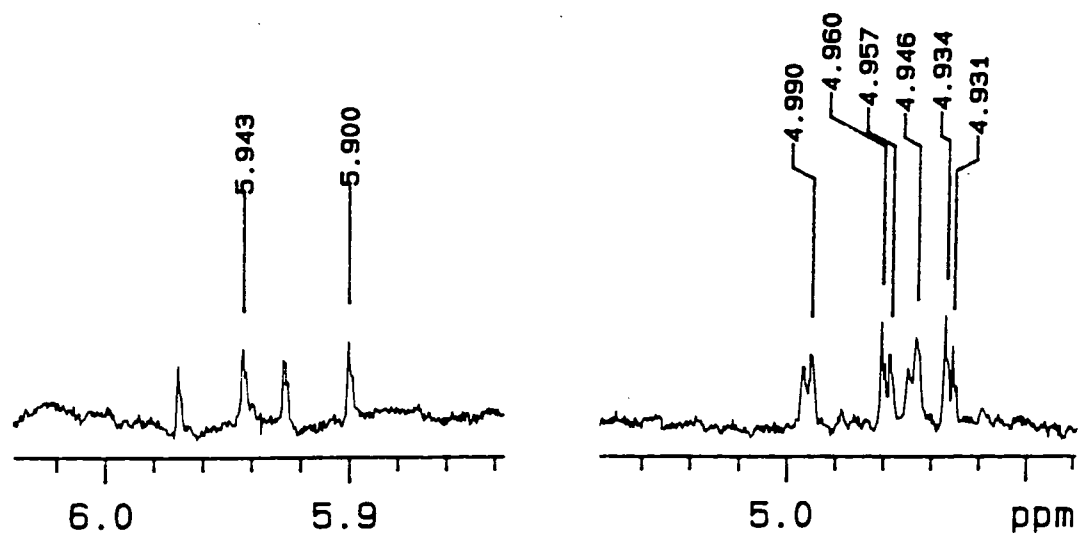


Figure 4.6 400MHz <sup>1</sup>H N.M.R. spectrum of the proposed camphor enolate olefin signals (C<sub>6</sub>D<sub>6</sub>)

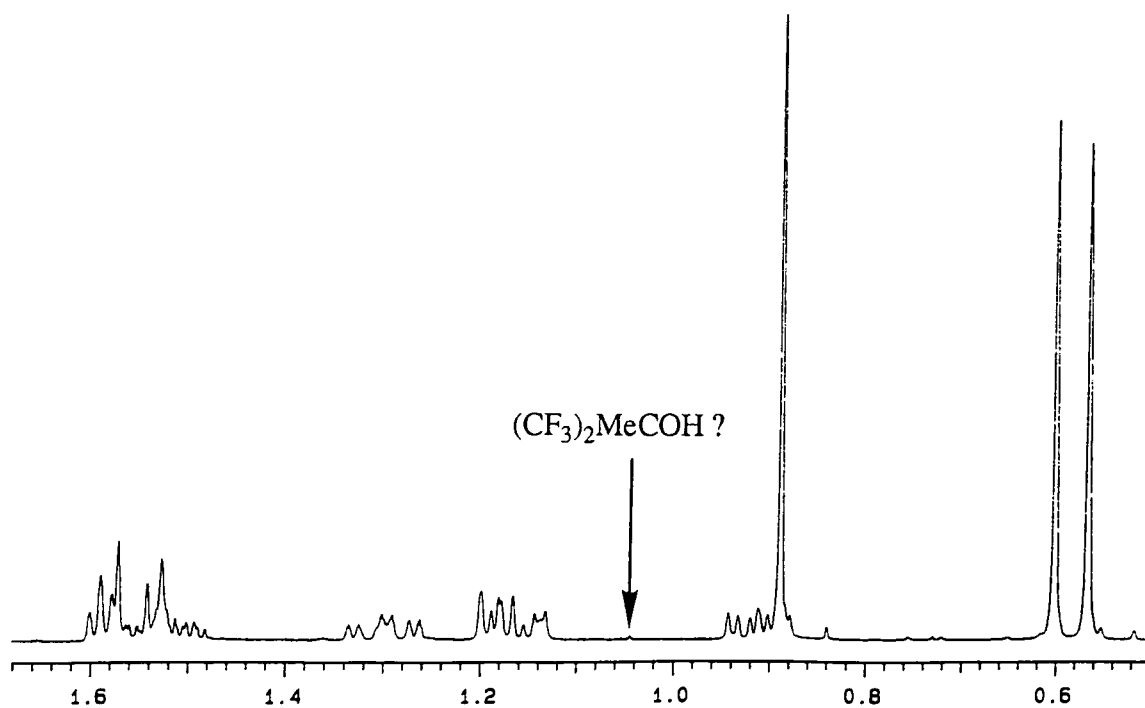


Figure 4.7 A region of the 400MHz <sup>1</sup>H N.M.R. spectrum (C<sub>6</sub>D<sub>6</sub>) of 20.5 equivalents (+)-camphor and Mo(NAr)(CHCMe<sub>2</sub>Ph)(OCMe(CF<sub>3</sub>)<sub>2</sub>)<sub>2</sub> showing the proposed observation of eliminated (CF<sub>3</sub>)<sub>2</sub>MeCOH

### 4.3 Chiral ancillary ligands

The most promising method for controlling tacticity would appear to be the introduction of chiral ancillary ligands at the metal centre. It was hoped that this would result in an initiator which would polymerize norbornenes in a metal-centre controlled fashion.

The observations reported previously with (+)-camphor demonstrate that alkoxide exchange may be the preferred way of introducing chiral ligands at the metal centre. However, the choice of potential chiral ancillary alkoxides is restricted in the light of Schrock's observations concerning the corresponding tungsten-based system<sup>6</sup>. It was found that only a handful of stable bis(alkoxide) complexes of the general formula  $W(NAr)(CHCMe_3)(OR)_2$  were stable, and that these were quite bulky (e.g.  $R = CEt_3$ ) and this resulted in an impaired reactivity as metathesis catalysts.

In order to investigate the feasibility of alkoxide exchange as a synthetic route into chiral-centre containing initiators a series of trial reactions were first carried out using 1-adamantanol. Following initial observations the study was then extended to include two chirally-resolved alcohols, namely (S)-endo-borneol and (-)-menthol.

#### 4.3.1 The $^1H$ N.M.R. reaction of $Mo(NAr)(CHCMe_2Ph)(OCMe_3)_2$ with 1-adamantanol, (S)-endo-borneol, and (-)-menthol in $C_6D_6$

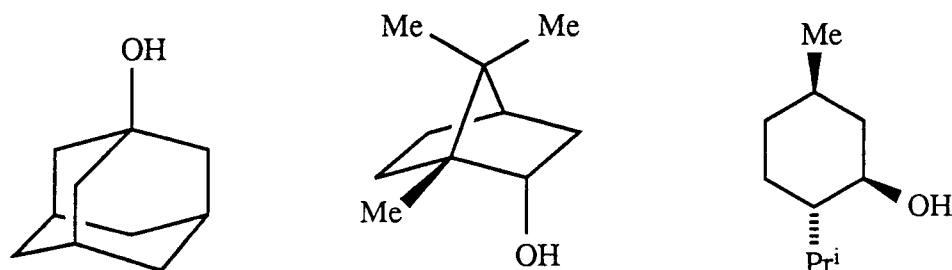


Figure 4.8 (From left to right) Adamantanol, (S)-endo-borneol, (-)-menthol

In all three cases the addition of two equivalents of these alcohols to  $\text{Mo}(\text{NAr})(\text{CHCMe}_2\text{Ph})(\text{OCMe}_3)_2$  leads to rapid alkoxide exchange, as shown by the appearance of three alkylidene signals {in the example of adamantanol arising from the bis(butoxide), the bis(adamantoxide) and the mixed (butoxide - adamantoxide)} and by the presence of methyl resonances corresponding to t-BuOH. The new alkylidene resonances are summarised in table 4.2. The resonances of all the new species possess similar chemical shifts to the bis(butoxide) initiator; consequently a prediction was made at this stage that samples of poly[1,4-(2,3-bis(trifluoromethyl) cyclopentenylene) vinylene] polymerized from the new bis(alkoxide)s would be highly trans.

Alcohol	Alkylidene resonance of the mixed alkoxide-butoxide (ppm)	Alkylidene resonance of the bis(alkoxide) (ppm)
Adamantanol	11.32	11.35
(S)-endo-Borneol	11.22	11.16
(-)-Menthol	11.30	11.28

Table 4.2 The alkylidene signals arising from the addition of 2 equivalents of alcohol to  $\text{Mo}(\text{NAr})(\text{CHCMe}_2\text{Ph})(\text{OCMe}_3)_2$

#### 4.3.2 Synthesis of $\text{Mo}(\text{NAr})(\text{CHCMe}_2\text{Ph})(\text{OR})_2$

{ROH = adamantanol, (S)-endo-borneol, and (-)-menthol}

Rather than synthesize the lithium salts of the three alcohols, followed by reaction with  $\text{Mo}(\text{NAr})(\text{CHCMe}_2\text{Ph})(\text{OSO}_2\text{CF}_3)_2(\text{DME})^7$ , an alternative synthesis of the bis(alkoxide) complexes was devised. The  $^1\text{H}$  N.M.R. spectrum reported in the previous section all show the expected formation of tert-butanol as a product of anionic ligand

metathesis. By removing this volatile compound from the equilibrium production of the desired complex should be promoted.

In order to test whether this would work in practice 0.200g  $\text{Mo}(\text{NAr})(\text{CHCMe}_2\text{Ph})(\text{OCMe}_3)_2$  were dissolved in a small amount of di(ethyl)ether and stirred with an ethereal solution of 2.00 equivalents of (*S*)-endo-borneol. After two minutes all volatiles were removed to yield an orange-brown oil. A further  $5\text{cm}^3$  solvent was added and the solvate-pump cycle was repeated three more times with the product becoming increasingly less oily.  $^1\text{H}$  N.M.R. spectroscopy on the orange solid obtained was indicative of one species only, and included one alkylidene signal, the chemical shift of which coincided with that previously assigned as  $\text{Mo}(\text{NAr})(\text{CHCMe}_2\text{Ph})\{(\text{S})\text{-endo-borneoxide}\}_2$ . This compound is believed to be the first example of a 4-co-ordinate 'Schrock-type' initiator bearing two chiral alkoxide ligands.

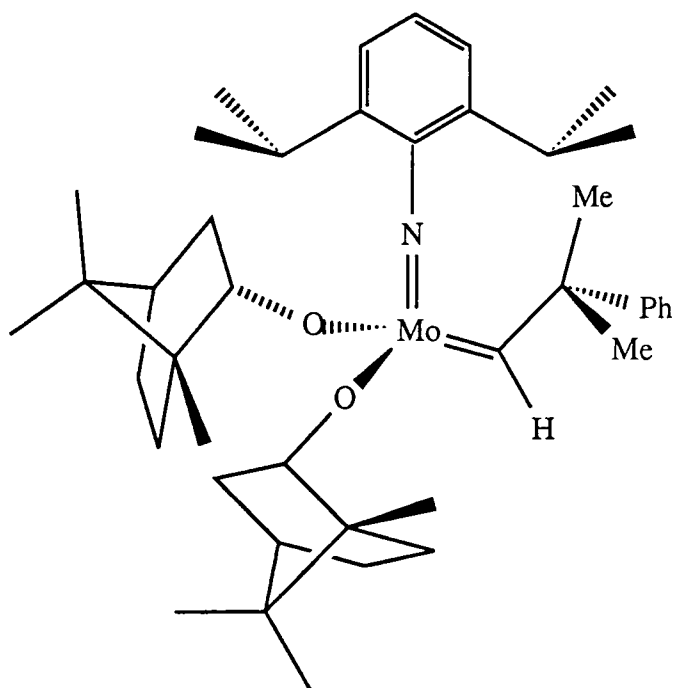


Figure 4.9  $\text{Mo}(\text{NAr})(\text{CHCMe}_2\text{Ph})\{(\text{S})\text{-endo-borneoxide}\}_2$

The bis{(-)-menthoxide} has also be prepared using this technique; removing volatiles from the stirring reaction mixture four times led to the isolation of an orange-brown solid. Recrystallisation from n-pentane at -78°C results in bright orange crystals, which give rise to just one alkylidene signal in their  $^1\text{H}$  and  $^{13}\text{C}$  N.M.R. spectra.

#### 4.3.3 The polymerization of 2,3-bis(trifluoromethyl)bicyclo[2.2.1] hepta-2,5-diene initiated by $\text{Mo}(\text{NAr})(\text{CHCMe}_2\text{Ph})\{(\text{S})\text{-endo-borneoxide}\}_2$

The addition of ten equivalents of the fluorinated monomer to the bis{(S)-endo-borneoxide} complex prepared as described above results in the total consumption of the neophylidene complex within 30 minutes at room temperature. Figure 4.10 shows the  $\text{C}_6\text{D}_6$   $^1\text{H}$  N.M.R. spectrum of the living polymer and an expansion of the propagating alkylidene. The trace is particularly interesting because of the very low intensity of the broad cis olefinic polymer signals at 4.6 - 4.9ppm, confirming previous suspicions that the sample of poly[1,4-(2,3-bis(trifluoromethyl)cyclopentenylene) vinylene] produced is highly trans. Indeed, when the reaction is conducted on a 1.00g scale in  $\alpha,\alpha,\alpha$ -trifluorotoluene the fluoropolymer obtained analyses as 97% trans (measured using  $^{13}\text{C}$  quantitative N.M.R. spectroscopy).

Significantly, the methylene region of this polymer is identical to that seen for 98% trans poly[1,4-(2,3-bis(trifluoromethyl)cyclopentenylene) vinylene] when initiated by  $\text{Mo}(\text{NAr})(\text{CHCMe}_2\text{Ph})(\text{OCMe}_3)_2$ , as shown in figure 4.11. In conclusion, the presence of two monodentate chiral ancillary alkoxide ligands at the active site does not appear to influence the tacticity encountered in the propagating chain.

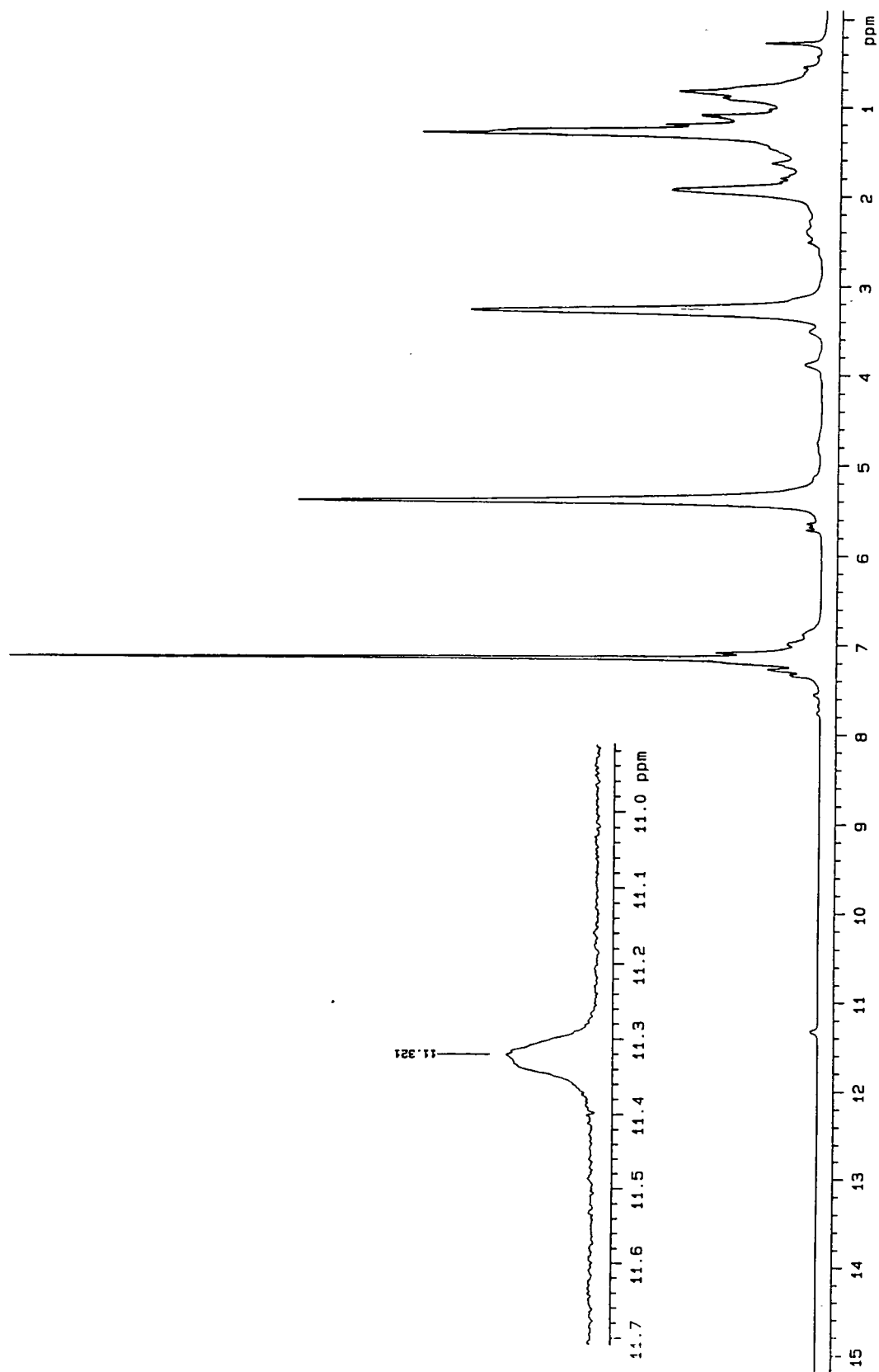


Figure 4.10 The 400MHz <sup>1</sup>H N.M.R. spectrum (C<sub>6</sub>D<sub>6</sub>) of Mo(NAr)(CHCMe<sub>2</sub>Ph)((S)-endo-borneoxide)<sub>2</sub> + 10 equivalents 2,3-bis(trifluoromethyl)bicyclo[2.2.1]hepta-2,5-diene

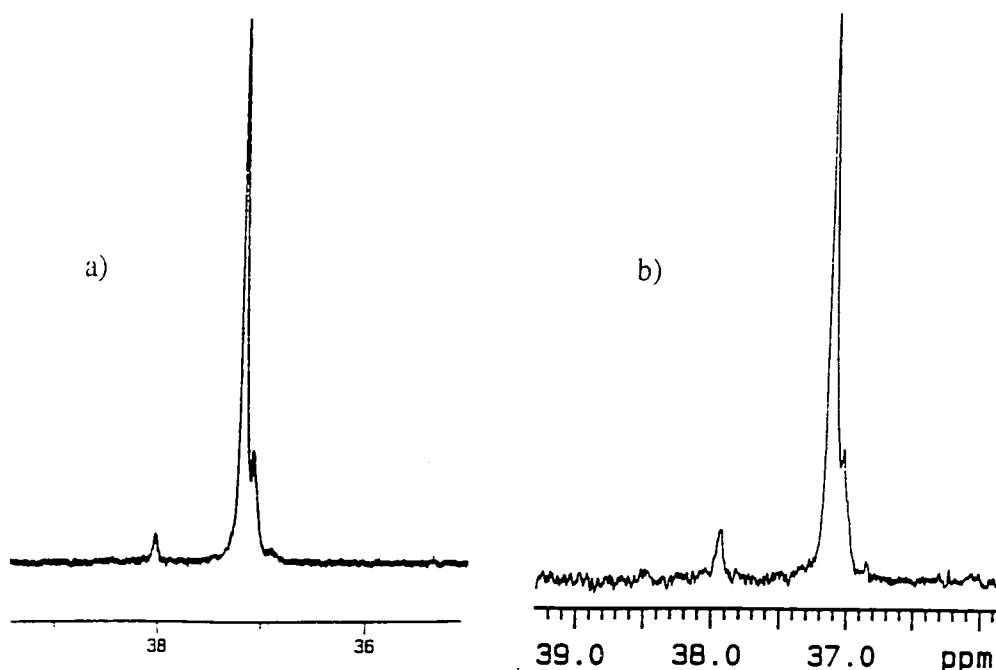


Figure 4.11 C7 Methylene regions ( $\text{CD}_3$ ) $_2$ CO) of the fluoropolymer initiated by  
 a)  $\text{Mo}(\text{NAr})(\text{CHCMe}_2\text{Ph})(\text{OCMe}_3)_2$  (125MHz;  $\sigma_t = 0.98$ )  
 b)  $\text{Mo}(\text{NAr})(\text{CHCMe}_2\text{Ph})\{(\text{S})\text{-endo-borneoxide}\}_2$  (100MHz;  $\sigma_t = 0.97$ )

#### 4.3.4 The polymerization of 2,3-bis(trifluoromethyl)bicyclo[2.2.1]hepta-2,5-diene initiated by $\text{Mo}(\text{NAr})(\text{CHCMe}_2\text{Ph})\{(-)\text{-mentholate}\}_2$

When ten equivalents of 2,3-bis(trifluoromethyl)bicyclo[2.2.1]hepta-2,5-diene are stirred with  $\text{Mo}(\text{NAr})(\text{CHCMe}_2\text{Ph})\{(-)\text{-mentholate}\}$  the  $^1\text{H}$  N.M.R. spectrum of the mixture is similar to that seen for the bis $\{(\text{S})\text{-endo-borneoxide}\}$ ; a trans content of at least 98% has been recorded. The polymerization appears to be living with a propagating alkylidene multiplet shown below (figure 4.12). Once again the methylene C7 region of the  $^{13}\text{C}$  N.M.R. spectrum of the living polymer in benzene- $\text{d}_6$  contains one major peak corresponding to tt rr at 36.10ppm, as well as a broad shoulder towards low frequency (tt rm) and a minor peak at 37.1ppm, believed to be the ct rr signal, confirming the lack of influence over polymer tacticity of monodentate chiral alkoxide ligands in these initiating systems.

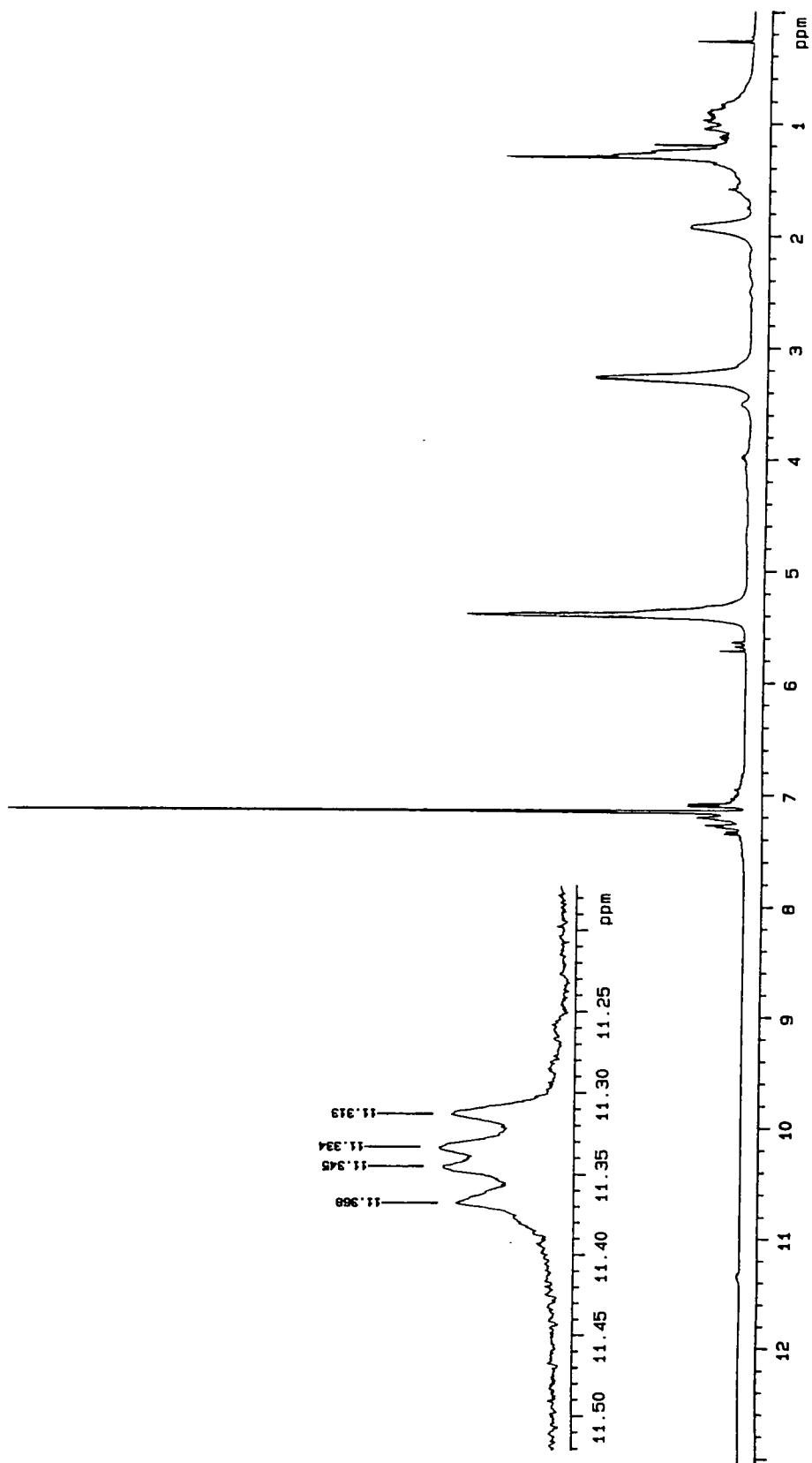


Figure 4.12 The 400MHz <sup>1</sup>H N.M.R. spectrum (C<sub>6</sub>D<sub>6</sub>) of Mo(NAr)(CHCMe<sub>2</sub>Ph){(-)-mentholate}<sub>2</sub> + 10 equivalents 2,3-bis(trifluoromethyl)bicyclo[2.2.1]hepta-2,5-diene

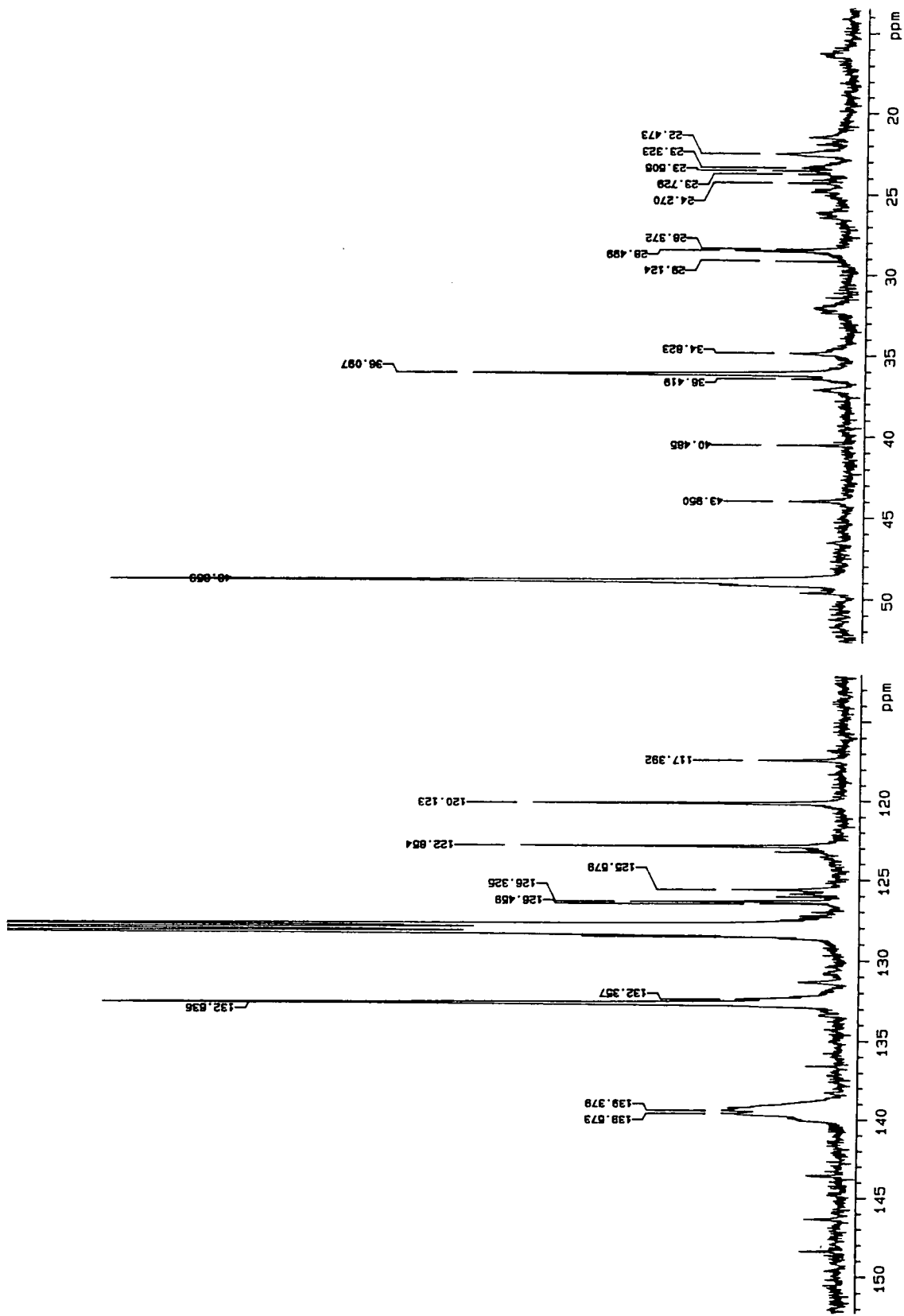


Figure 4.13 The 100MHz  $^{13}\text{C}$  N.M.R. spectrum ( $\text{C}_6\text{D}_6$ ) of living poly[1,4-(2,3-bis(trifluoromethyl)cyclopentenylene) vinylene] initiated by  $\text{Mo}(\text{NAr})(\text{CHCMe}_2\text{Ph})(-)\text{-mentholate}]_2$

#### 4.4 The synthesis of bidentate alkoxide analogues of the molybdenum R.O.M.P. initiators

##### 4.4.1 Studies employing 3,5-di-tert-butylcatechol

Having shown that the two chiral monodentate alkoxide ligands studied above have no effect upon the tacticity of the living fluoropolymer, a logical extension into bidentate ligand chemistry was made.

However, in order to maintain a unstrained tetrahedral environment about the molybdenum centre the two oxygen atoms in any potential bidentate ligand must be well-separated. In order to confirm that sufficient spacer groups are required between the oxygen atoms two equivalents of 3,5-di-tert-butylcatechol (catechol = ortho-dihydroxybenzene) were added to a  $C_6D_6$  solution of  $Mo(N-2,6-i-Pr_2)(CHCMe_2Ph)(OCMe_3)_2$ . The solution turned black instantaneously, and  $^1H$  N.M.R. studies confirmed that the alkylidene had decomposed in an as yet unidentified manner.

When only 1.0 equivalent was added under the same conditions, two alkylidene signals were observed at 12.02 and 12.55ppm in the approximate ratio 4:1. However, the total absence of any discernible resonance due to the alkylidene proton of the bis(butoxide) starting material suggested that these two species were not the expected bis(catecholate) and mixed catecholate-butoxide complexes.

Furthermore, on the addition of one equivalent of the substituted catechol to 0.200g of the bis(butoxide) initiator in di(ethyl) ether, followed by the three pump-solvate cycles, as described earlier in this chapter, a dark brown solid was isolated. As shown in figure 4.14,  $^1H$  N.M.R. spectroscopy upon the product revealed the presence of numerous alkylidene species!

Presumably the mixture of compounds arises due to the inability of one molecule of the catechol to bond to two ligand sites on the molybdenum centre in a tetrahedral

environment. Although no attempt is made to assign all the observed alkylidene signals, it is not difficult to imagine how several different bridged species could be formed.

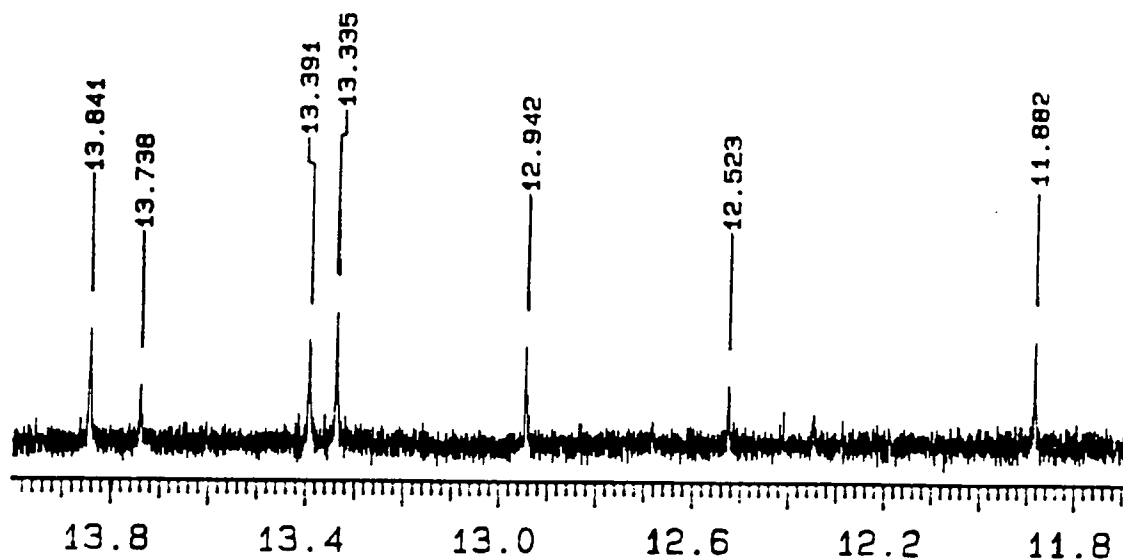


Figure 4.14 The alkylidene region of the 400MHz  $^1\text{H}$  N.M.R. spectrum ( $\text{C}_6\text{D}_6$ ) of the product of the attempted synthesis of  $\text{Mo}(\text{NAr})(\text{CHCMe}_2\text{Ph})(3,5\text{-di-}t\text{-butylcatecholate})$

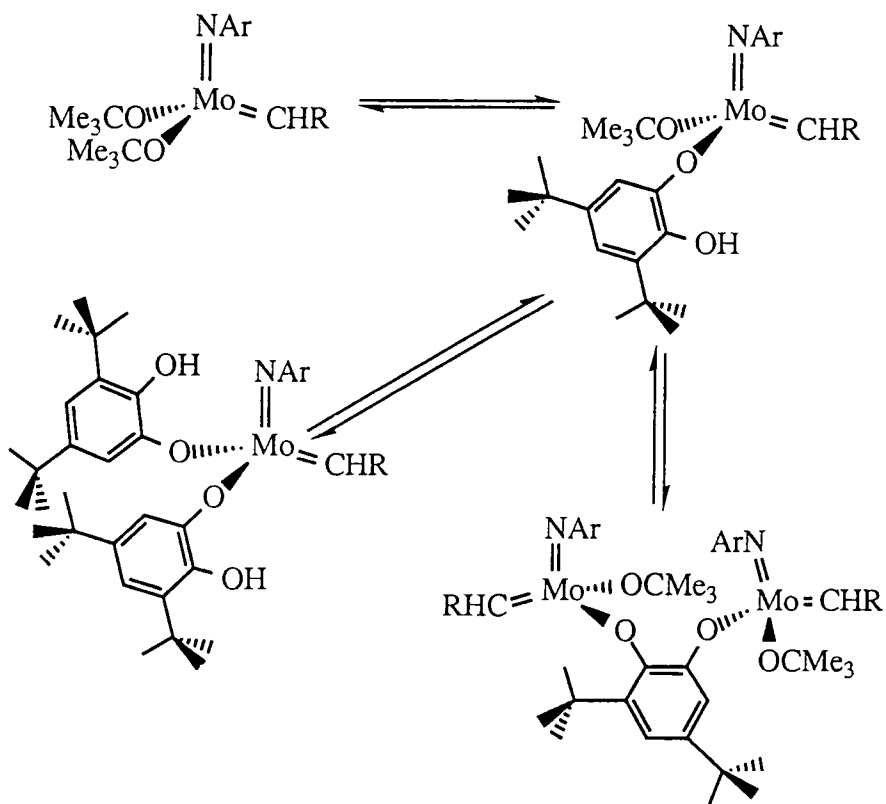


Figure 4.15

#### 4.4.2 Studies on 1,1'-Bi-2-naphthol as a chelating ligand to the Mo(NAr)(CHCMe<sub>2</sub>Ph) fragment

In view of the observations concerning the substituted catechol it was decided to investigate a chelating alkoxide ligand in which the two oxygen atoms are better positioned geometrically for bonding to a single molybdenum-imido-alkylidene fragment. The obvious candidate was 1,1'-bi-2-naphthol<sup>8</sup>, which has a rich history in the field of asymmetric synthesis. More importantly, this ligand possesses a C<sub>2</sub> axis of rotational symmetry and is available in both racemic and enantiomerically-pure forms.

Initially 2 equivalents of (±)-1,1'-bi-2-naphthol, BN(OH)<sub>2</sub> were added to a C<sub>6</sub>D<sub>6</sub> solution of Mo(NAr)(CHCMe<sub>2</sub>Ph)(OCMe<sub>3</sub>)<sub>2</sub>; within seconds the mixture turns a very dark brown colour and oily droplets form on the glass walls of the reaction vessel. <sup>1</sup>H N.M.R. spectroscopy failed to identify any of the products, but did confirm that the molybdenum-alkylidene had decomposed.

The addition of 0.4 equivalents of the racemate to the bis(butoxide) initiator is a far cleaner reaction. Three alkylidenes are observed at 12.00, 11.53, and 11.32ppm in C<sub>6</sub>D<sub>6</sub> in the approximate ratio 7 : 1 : 10. Increasing the number of equivalents upwards to 1.0 results in one major resonance at 12.00, tentatively assigned to Mo(NAr)(CHCMe<sub>2</sub>Ph)(η<sup>2</sup>-BNO<sub>2</sub>), the desired product. A minor signal at 11.53ppm, constituting less than 5% of the total alkylidene intensity, is also seen; presumably this is the mixed species Mo(NAr)(CHCMe<sub>2</sub>Ph)(OCMe<sub>3</sub>){BNO(OH)} in which the binaphtholate ligand binds in a monodentate fashion.

The synthesis of the chelated-binaphtholate complex can be scaled up successfully using the same method as for the bis{(S)-endo-borneoxide} analogue. However, both the binaphtholate complex and the mixed butoxide-binaphtholate are only sparingly soluble in di(ethyl) ether and this can result in incomplete conversion. However, one single solvate-pump cycle in methylene chloride is sufficient to eliminate all the butoxide ligands.

The  $^1\text{H}$  N.M.R. spectrum of  $\text{Mo}(\text{NAr})(\text{CHCMe}_2\text{Ph})(\eta^2\text{-BNO}_2)$  is interesting in many aspects. In  $\text{C}_6\text{D}_6$  many of the signals, including the alkylidene proton, are very broad and show little fine structure. For example, figure 4.16 shows a very broad resonance at 3.97ppm; note also that two well-defined septets of equal intensity are also observed at 4.55 and 4.75ppm.  $^1\text{H}$  COSY experiments<sup>9</sup> have been used to confirm that both the septets are coupled to separate doublets in the methyl region (figure 4.17), and this would appear to suggest that there are at least two iso-propyl environments in the complex. Furthermore, a similar coupling is also seen for the neighbouring broad signal.

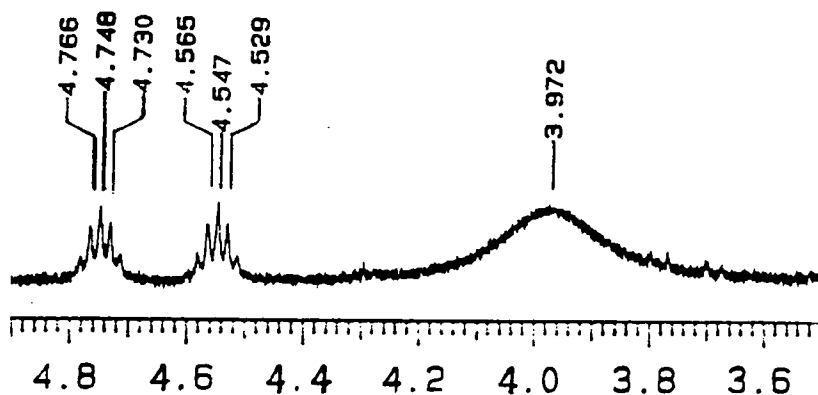


Figure 4.16 A region from the 400MHz  $^1\text{H}$  N.M.R. ( $\text{C}_6\text{D}_6$ ) of  $\text{Mo}(\text{NAr})(\text{CHCMe}_2\text{Ph})(\eta^2\text{-BNO})$

However, upon addition of quinuclidine to the benzene- $\text{d}_6$  solution described above the two septets and the broad peak at 3.97ppm are all replaced by a single septet at 3.85ppm. Furthermore the alkylidene is now a sharp singlet at 11.92ppm (a small singlet at 13.75ppm is believed to be the anti rotamer of the five-coordinate adduct of the nitrogen-base). Indeed, examination of the rest of the spectrum shows that all the previously broad signals have narrowed considerably (the same effect has been observed simply by using THF- $\text{d}_8$  as the N.M.R. solvent).

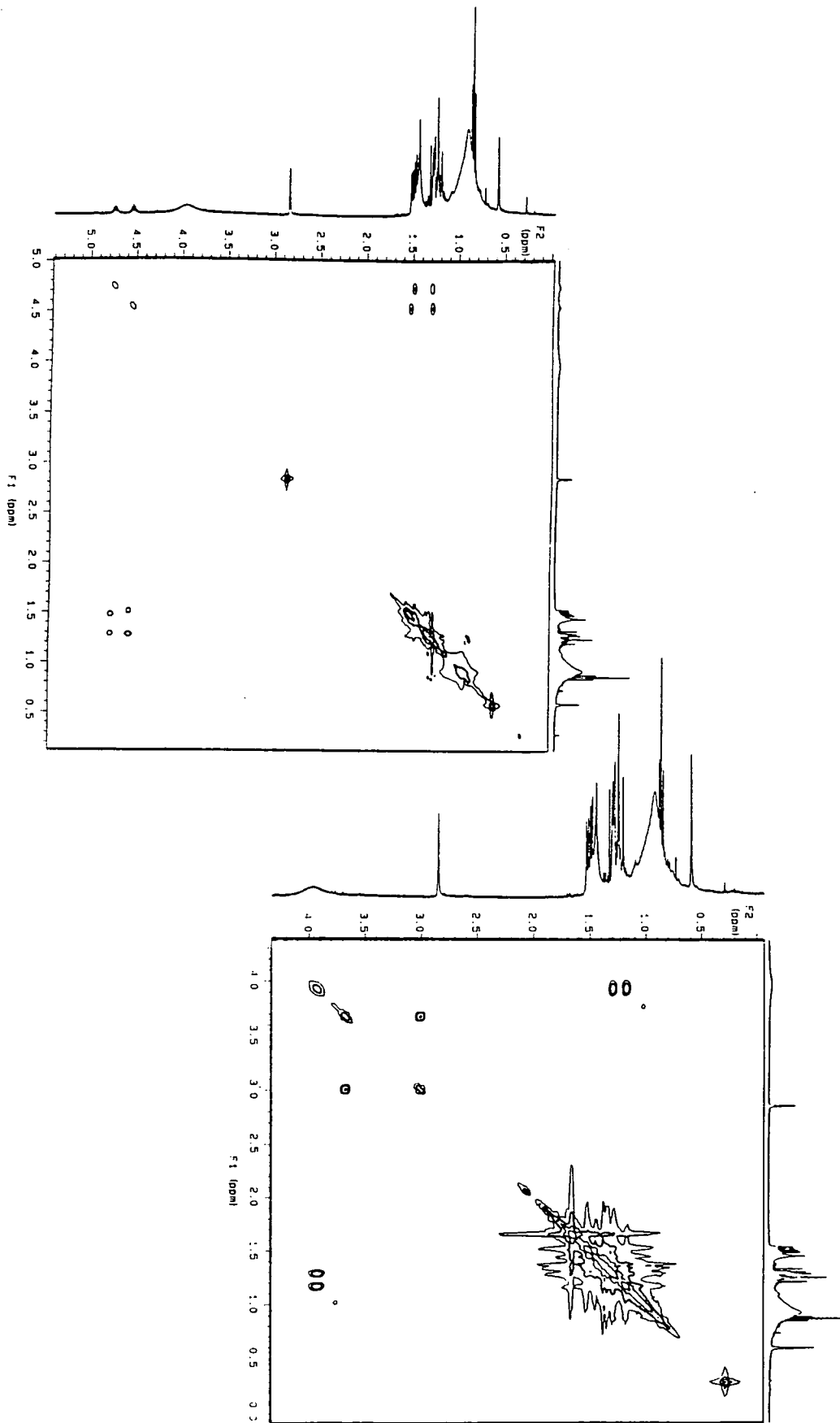


Figure 4.17 <sup>1</sup>H COSY spectra (400MHz; C<sub>6</sub>D<sub>6</sub>) of Mo(NAr)(CHCMe<sub>2</sub>Ph)(η<sup>2</sup>-BNO)

(note the similar coupling of the three signals shown previously in figure 4.16)

It therefore appears that in the base-free form the imido substituent is locked into some geometry which gives rise to two different iso-propyl environments. One of these gives rise to two sharp septets, whilst the other gives a broad multiplet. Although several possible explanations for this have been considered no solution has yet been found. Preliminary low temperature studies have been impeded by low solubility and a tendency for the complex to decompose over extended periods in solution.

However, the spectrum obtained of the base-adduct confirms that just one species is indeed present. Although no parent ion has been observed using solution state mass spectrometry all the other characterising data collected upon this compound supports this belief. Consequently, it was decided to carry out preliminary R.O.M.P. studies upon this initiator, even though substantial structural information is still to be gleaned from the N.M.R. data. Further investigation into this area will almost certainly prove beneficial with regard to providing explanations for the following observations.

2,3-Bis(trifluoromethyl)bicyclo[2.2.1]hepta-2,5-diene can be polymerized by the binaphtholate initiator in  $\alpha,\alpha,\alpha$ -trifluorotoluene in high yield; the recovered polymer analyses as approximately 65% trans. However, the significant region from the  $^{13}\text{C}$  N.M.R. spectrum of this material is once again the C7 methylene signals which are shown in figure 4.18. Comparison with figure 3.14(c) ( $\sigma_t = 0.64$ ) demonstrates that the use of the bidentate binaphtholate ligand results in a change in tacticity. As the figure clearly demonstrates the use of the bidentate ancillary bis(alkoxide) ligand results in a change in tacticity. The resonances toward high frequency are of greater intensity, implying that the binaphtholate initiator promotes an increased level of isotactic dyad formation. This observation therefore shows that it is possible for polymer tacticity to be influenced in these four-coordinate R.O.M.P. initiators, by the use of a bidentate alkoxide.

Further studies on this system have included the synthesis of both the enantiomerically pure (R)-(+)- and the (S)-(-)- binaphtholate analogues shown in figure 4.19 (both these forms are of identical appearance to the ( $\pm$ ) species and give rise to the same spectroscopic characterising data). The metathesis polymerization of 2,3-

bis(trifluoromethyl)bicyclo [2.2.1]hepta-2,5-diene by both these initiators gives an identical polymer microstructure as that observed for the initiator bearing the racemic ligand. This is, of course, exactly what is expected given the  $C_2$ -symmetry of the chiral ligand. The C7 methylene regions of the polymers derived from the two optically-active initiators are shown in figure 4.18.

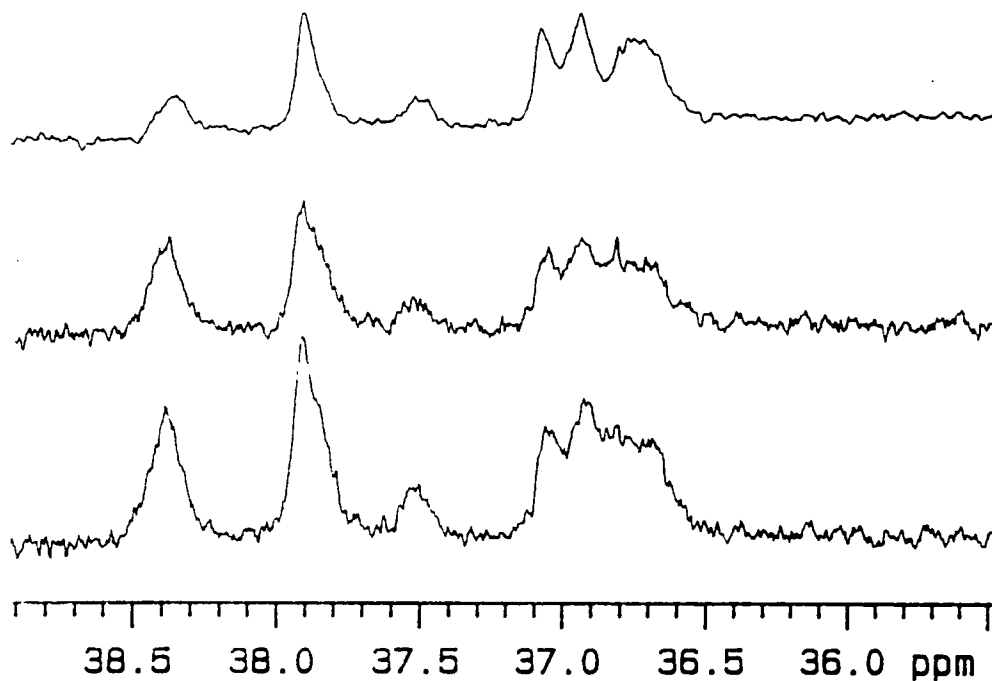


Figure 4.18 The  $^{13}\text{C}$  N.M.R. C7 methylene regions of the fluoropolymer derived from  
 (top to bottom) racemic  $\text{Mo}(\text{NAr})(\text{CHCMe}_2\text{Ph})(\eta^2\text{-BNO})$ ,  
 $(S)\text{-Mo}(\text{NAr})(\text{CHCMe}_2\text{Ph})(\eta^2\text{-BNO})$ ,  $(R)\text{-Mo}(\text{NAr})(\text{CHCMe}_2\text{Ph})(\eta^2\text{-BNO})$

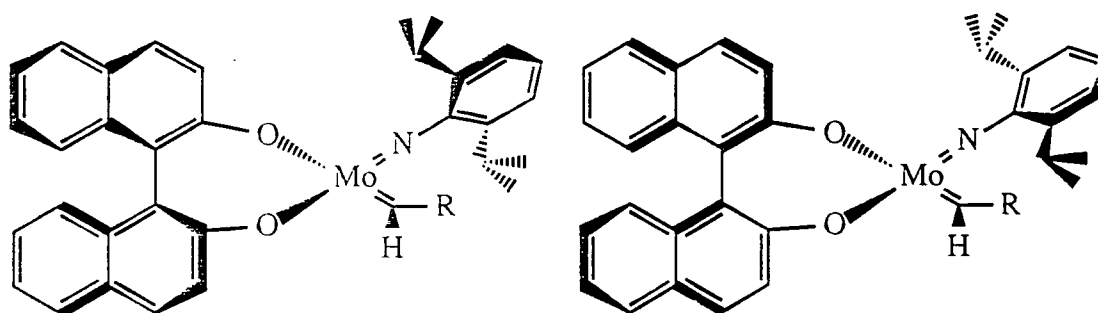


Figure 4.19 (S)- (left) and (R)- forms of  $\text{Mo}(\text{NAr})(\text{CHR})(\eta^2\text{-BNO})$

The binaphtholate ligand must therefore influence the approach of the monomer to the N-Mo-C face; theory predicts that this would lead to a different polymer chain structure than that seen for the bis(butoxide) initiators, and that the presence of racemate or enantiomeric binaphtholates would give rise to the same tacticity.

At the present time, little is known about how the monomer approaches the binaphtholate complex; it is not even clear whether the monomer C7 atom orientates itself towards the imido (which appears to be locked in a sterically favoured geometry) or towards the chelating alkoxide. Furthermore, at the intermediate levels of cis and trans content observed with the binaphtholate complexes, it is difficult to relate increased isotactic dyad intensities to actual mechanistic information.

While this work was in progress, Professor R.R. Schrock independently reported preliminary findings using a 3,3'-bis(dimethylphenylsilane)-1,1'-bi-2-naphthol analogue of the metathesis initiator. He observes a similar trans content to the parent binaphtholate initiator described herein and a similar variation in polymer tacticity.

## 4.5 Conclusions

The work reported in this chapter has moved away from control over cis and trans vinylene content and has focused instead upon controlling tacticity in ring-opened polymers.

The use of chiral base-adducts of the  $\text{Mo}(\text{NAr})(\text{CHR})(\text{OR}')_2$  systems failed to influence the tacticity (a not entirely unexpected observation). However, as part of that study it became apparent that exchange of the metal-alkoxide with the enol form of camphor could be a potential way of introducing chiral units directly at the metal-centre.

Exploiting this methodology led to the synthesis of analogues of the Schrock molybdenum metathesis initiators in which both the alkoxide ligands were chiral and enantiomerically-pure. These systems also fail to alter polymer tacticity

Nonetheless, 1,1'-bi-2-naphtholate derivatives do change the microstructure of poly[1,4-(2,3-bis(trifluoromethyl)cyclopentenylene) vinylene]. As expected for a ligand with a  $C_2$  rotational symmetry the initiator bearing the racemate form of the diol has exactly the same effect as either the all (R) or all (S) analogues.

In conclusion, not only is it possible to completely control the cis and trans vinylene content in the R.O.M.P. of 2,3-bis(trifluoromethyl)bicyclo[2.2.1]hepta-2,5-diene, but we have also shown that the tacticity of the polymer chain can also be influenced by the judicious choice of ancillary ligand at the metal centre.

## 4.6 References

1. G.C. Bazan, PhD Thesis, M.I.T. (1991)
2. Z. Wu, D.R. Wheeler, R.H. Grubbs *J.Am.Chem.Soc.* **114** 146 (1992)
3. J.P. Mitchell, PhD Thesis, University of Durham (1992)
4. T. Money in 'Studies in Natural Product Chemistry: Volume IV Stereoselective Synthesis (Part C)', pp 625 - 697, Ed. A.-U. Rahman, Elsevier Science Publishers, Amsterdam (1989)
5. G.C.Joshi, W.D. Chambers, E.N. Wardhoff *Tetrahedron Lett.* 3613 (1967)
6. R.R. Schrock, R.T. Depue, J. Feldman, K.B. Yap, D.C. Yang, W.M. Davis, L. Park, M. DiMare, M. Schofield, J. Anhaus, E. Walborsky, E. Evitt, C. Kruger, P. Betz *Organometallics* **9** 2262 (1990)
7. R.R. Schrock, J.S. Murdzek, G.C. Bazan, J. Robbins, M. DiMare, M. O'Regan *J.Am.Chem.Soc.* **112** 3875 (1990)
8. 1,1'-Bi-2-naphthol has been used in many application such as:  
*ligand in the enantioselective reduction of ketones;*  
R.Noyori et al. *J.Am.Chem.Soc.* **106** 6709 (1984); *ibid.* **106** 6717 (1984)  
*ligand in a chiral titanium reagent;*  
A.G. Olivero et al. *Helv.Chim.Acta* **64** 2485 (1981);  
K. Mikami et al. *J.Am.Chem.Soc.* **111** 1940 (1989)  
*chiral building block;*  
D.J. Cram et al. *J.Org.Chem.* **42** 4713 (1977); *ibid* **46** 393 (1981);  
J.M. Lehn et al. *Helv.Chim.Acta* **61** 2407 (1978);  
M. Amano et al. *Bull.Chem.Soc.Jpn.* **56** 3672 (1983)  
*chiral auxillary for enantioselective syntheses or resolutions;*  
S. Miyano et al. *Bull.Chem.Soc.Jpn.* **57** 1943 (1984);  
S. Sakane et al. *J.Am.Chem.Soc.* **105** 6154 (1983); *Tetrahedron* **42** 2203 (1986);  
A. Aigner et al. *Chem.Ber.* **118** 3643 (1985);

- S. Sakane et al. *J. Am. Chem. Soc.* **105** 6154 (1983); *Tetrahedron* **42** 2203 (1986);  
A. Aigner et al. *Chem. Ber.* **118** 3643 (1985);  
B.M. Trost, D.J. Murphy *Organometallics* **4** 1143 (1985)
9. A.E. Derome 'Modern N.M.R. Techniques for Chemistry Research', Pergamon Press, Oxford (1987)

## **Chapter Five**

### **The Synthesis of Fluorinated Homopolymers and Block Copolymers via Living ROMP**

## 5.1 Introduction

The previous chapters of this thesis have described a remarkable degree of stereocontrol using the well-defined molybdenum initiator system in the living R.O.M.P. of 2,3-bis(trifluoromethyl)bicyclo[2.2.1]hepta-2,5-diene, **I**. This monomer was initially chosen for study because it is both relatively simple to prepare and purify, and because the lack of head-tail geometries in the stereochemistry of poly[1,4-(2,3-bis(trifluoromethyl)cyclopentylene) vinylene], poly**I**, result in a greatly simplified microstructure analysis. However, in the previous work involving classical initiators many more fluorinated monomers were studied.

In this chapter the investigation is extended to the non-symmetrical, fluorinated monomers **II** - **IV**, and then the living nature of the process is exploited to prepare the first examples of fluorinated di-block copolymers. The monomers studied are 2-trifluoromethylbicyclo[2.2.1]hepta-2,5-diene, **II**, 5-trifluoromethylbicyclo[2.2.1]hept-2-ene, **III**, and 5,5,6-trifluoro-6-trifluoromethylbicyclo[2.2.1]hept-2-ene, **IV**.

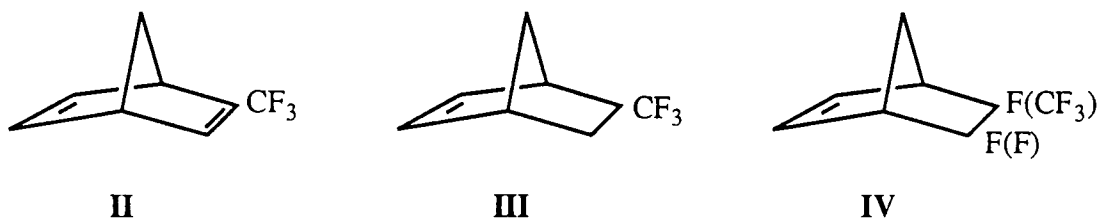


Figure 5.1 presents a general synthesis of a di-block via a living metathesis polymerization mechanism.

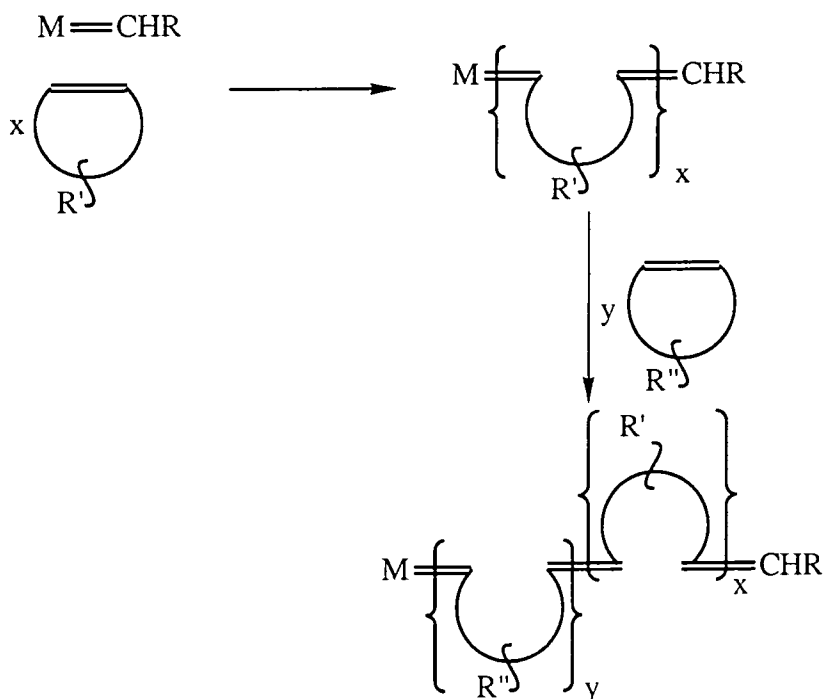


Figure 5.1 General synthesis of a di-block copolymer via living R.O.M.P.

## 5.2 The synthesis of fluorinated homopolymers via living R.O.M.P.

### 5.2.1 The living R.O.M.P. of fluorinated monomers II, III, and IV with $Mo(NAr)(CHCMe_2Ph)(OCMe_3)_2$

These three fluorinated bicyclic olefins undergo R.O.M.P. with the bis(tert-butoxide) initiator to give the ring-opened polymers shown in figure 5.2. The insertion of the first few monomer units into the propagating chain can be conveniently studied by  $^1H$  NMR, as explained in chapter two. The downfield singlet due to the alkylidene proton of the initiator is replaced by a series of signals, the number and multiplicities of which depend upon the nature of the monomer substituents, the arrangement of ligands around the active site, and the living polymer chain structure.

For example, the addition of 10 equivalents of monomer **II** to  $Mo(NAr)(CHCMe_2Ph)(OCMe_3)_2$  in  $C_6D_6$  generates the alkylidene region shown in

figure 5.3. The two multiplets arise from the ability of this unsymmetrical racemic monomer to insert in both head and tail modes.

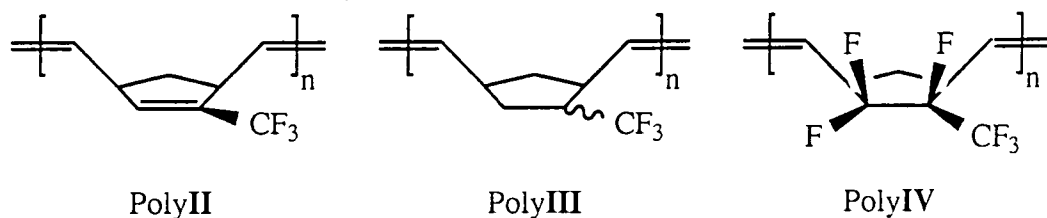


Figure 5.2 The ring-opened polymers of monomers II, III, and IV

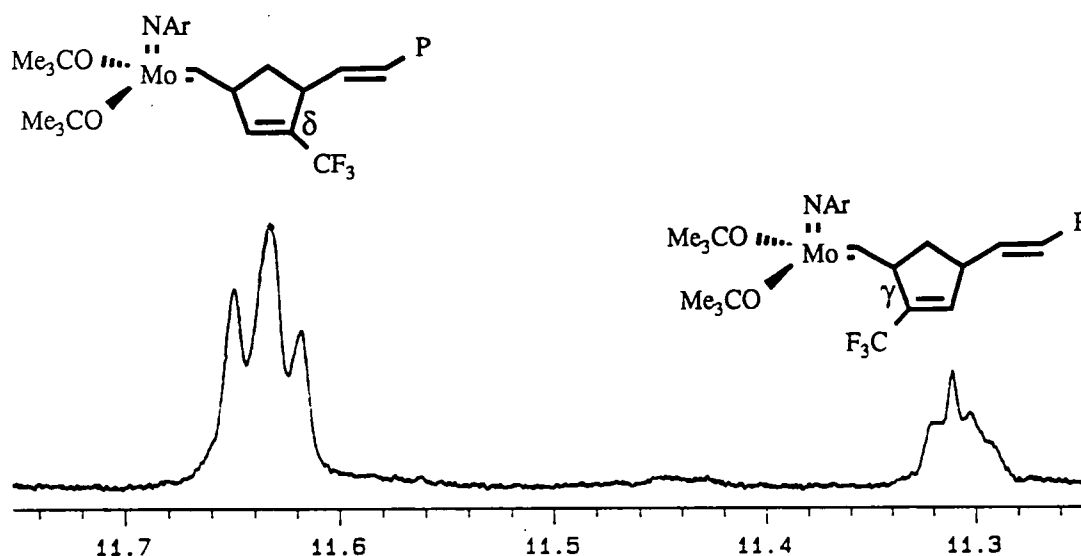


Figure 5.3 The 400MHz  $^1\text{H}$  N.M.R. spectrum ( $\text{C}_6\text{D}_6$ ) of the alkylidene region of living polyII (initiated by  $\text{Mo}(\text{NAr})(\text{CHCMe}_2\text{Ph})(\text{OCMe}_3)_2$ )

The assignment of the two multiplets has been made by considering the analogous  $^1\text{H}$  N.M.R. spectrum observed for living polyI (which features a broadened doublet at 11.34ppm). In living polyII the  $\text{CF}_3$  substituent of the last inserted monomer unit can either be bonded to a  $\gamma$ - or a  $\delta$ - carbon. When the  $\text{CF}_3$  group is nearer the metal centre (i.e.  $\text{C}_\gamma - \text{CF}_3$ ) then the alkylidene proton would experience a similar electronic environment (and consequently possess a similar chemical shift, 11.31ppm) to that found in living polyI. Furthermore, when the  $\text{CF}_3$  substituent in living polyII is bonded to the  $\delta$ -carbon, then the perturbation upon the alkylidene proton from polyI would be far greater,

and hence the alkylidene resonance is likely to differ significantly from polyI. Hence the multiplet from 11.61 - 11.66ppm is assigned to this latter isomer.

In a similar experiment 9.8 equivalents of **III** were polymerized by  $\text{Mo}(\text{NAr})(\text{CHCMe}_2\text{Ph})(\text{OCMe}_3)_2$  (this monomer was supplied by Dr. Ezat Khosravi, and had the composition 65% endo : 35% exo). The  $^1\text{H}$  N.M.R. downfield region recorded in  $\text{C}_6\text{D}_6$  is shown in figure 5.4.

As in the case of living poly**II** two separate multiplets occur separated by about 0.35ppm. Although endo / exo effects can not be dismissed the conclusion again reached is that the two signals arise from the  $\text{CF}_3$  group being bonded to the  $\gamma$ -carbon and to the  $\delta$ -carbon in the last inserted monomer unit.

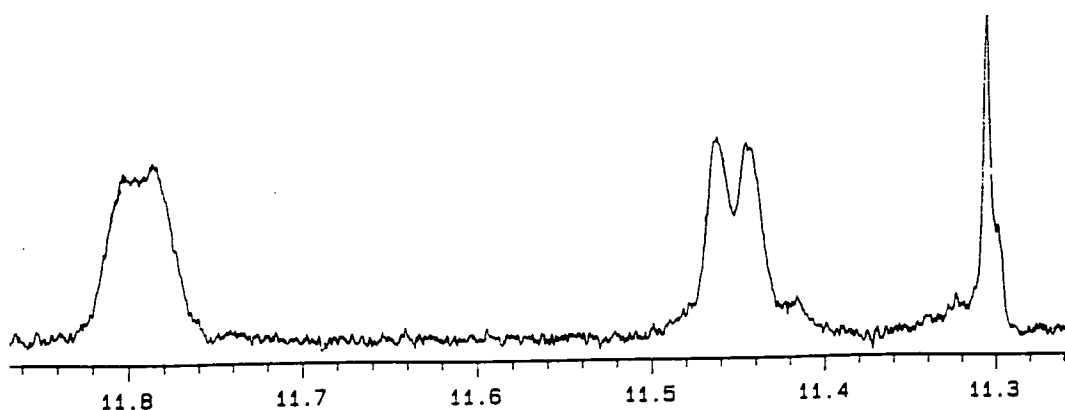


Figure 5.4 The 400MHz  $^1\text{H}$  N.M.R. spectrum of the propagating alkylidene signals of living poly**III** (initiated by  $\text{Mo}(\text{NAr})(\text{CHCMe}_2\text{Ph})(\text{OCMe}_3)_2$ )

Living poly**IV** also gives rise to two propagating multiplets of similar intensities at 11.42-11.45ppm and 11.51-11.55ppm (figure 5.5 shows the 500MHz  $^1\text{H}$  spectrum of the living decamer).

The extremely high frequency used to obtain this trace does highlight the presence of a small residual amount of unconsumed catalyst. However, the precise splitting pattern

of the two multiplets is still not clear. Hence, an unambiguous assignment of the two signals to the four possible isomers (head / tail and endo / exo) has not been achieved.

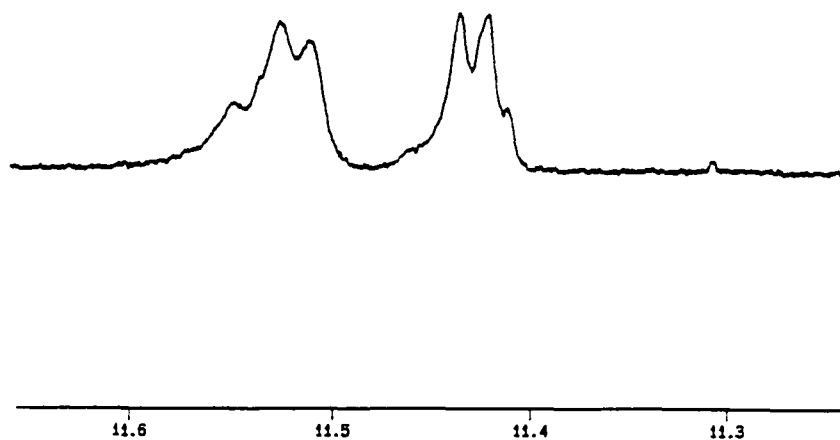


Figure 5.5 The 500MHz <sup>1</sup>H NMR spectrum (C<sub>6</sub>D<sub>6</sub>) of the alkyldiene region of living polyIV (initiated by Mo(NAr)(CHCMe<sub>2</sub>Ph)(OCMe<sub>3</sub>)<sub>2</sub>)

All three monomers have also been studied with Mo(NAr)(CHCMe<sub>2</sub>Ph)(OCMe(CF<sub>3</sub>)<sub>2</sub>)<sub>2</sub> and Mo(NAr)(CHCMe<sub>3</sub>)(OCMe<sub>2</sub>CF<sub>3</sub>)<sub>2</sub>. The propagating alkyldienes observed are recorded in table 5.1. Shifts move to lower field (higher frequency) as methyl groups upon the butoxide ligand are replaced by electron-withdrawing CF<sub>3</sub> groups. All of the signals tend to be broad, unresolved multiplets which consequently are difficult to assign without ambiguity. However, one point to note which is not highlighted by this table is the relative reactivities of the three monomers as revealed by the residual amount of unconsumed initiator.

From the data collated in table 5.2 it would appear that monomers **II** and **III** possess  $k_p$  values which are significantly greater than  $k_i$ . This becomes exaggerated as the ancillary alkoxide ligands become more electron-withdrawing. **IV** behaves similarly to **I**; just a few equivalents consumes nearly all the initiator, indicative of a  $k_p / k_i$  ratio closer to unity (sterically it is unlikely that  $k_i$  will exceed  $k_p$ ).

Monomer	[Mo](OCMe <sub>3</sub> ) <sub>2</sub>	[Mo](OCMe <sub>2</sub> CF <sub>3</sub> ) <sub>2</sub>	[Mo](OCMe(CF <sub>3</sub> ) <sub>2</sub> ) <sub>2</sub>
<b>II</b>	11.28-11.32 (broad, multiplet) 11.61-11.66 (strong multiplet)	12.07-12.10ppm (broad, multiplet)	12.26-12.30 (broad, very weak) 12.59-12.68 (very broad, multiplet)
<b>III</b>	11.45 (broadened doublet) 11.79 (broadened doublet)	11.89, 11.91ppm (broadened doublet) 12.24-12.27ppm (weak multiplet)	11.40-11.45 (weak multiplet)
<b>IV</b>	11.40-11.44 (broad, multiplet) 11.51-11.60 (broad multiplet)	12.04ppm (broadened singlet) 11.91, 11.93ppm (broadened doublet)	12.60-12.64 (broadened doublet) 12.51ppm (broadened singlet)

Table 5.1 Summary of propagating alkylidene proton resonances for monomers **II**, **III**, and **IV** with four-coordinate initiators ([Mo] = Mo(NAr)(CHR); R = CMe<sub>2</sub>Ph, CMe<sub>3</sub>)

Monomer	Number of equivalents	Initiator alkoxide ligands	Propagating alkylidene (%)	Unconsumed initiator (%)
<b>I</b>	10.3	OCMe <sub>3</sub>	>99.0	<1.0
	12.4	OCMe <sub>2</sub> CF <sub>3</sub>	98.4	1.6
	13.6	OCMe(CF <sub>3</sub> ) <sub>2</sub>	96.7	3.3
<b>II</b>	9.9	OCMe <sub>3</sub>	>99.0	<1.0
	10.0	OCMe <sub>2</sub> CF <sub>3</sub>	42.3	57.7
	10.4	OCMe(CF <sub>3</sub> ) <sub>2</sub>	57.2	42.8
<b>III</b>	9.8	OCMe <sub>3</sub>	82.6	17.4
	10.0	OCMe <sub>2</sub> CF <sub>3</sub>	42.6	57.4
	10.1	OCMe(CF <sub>3</sub> ) <sub>2</sub>	18.9	81.1
<b>IV</b>	9.9	OCMe <sub>3</sub>	>99.0	<1.0
	13.0	OCMe <sub>2</sub> CF <sub>3</sub>	94.4	5.6
	16.5	OCMe(CF <sub>3</sub> ) <sub>2</sub>	97.1	2.9

Table 5.2 Percentages of alkylidene resonances attributable to a) propagating species and b) unconsumed initiator for the R.O.M.P. of **I** - **IV** by Mo(NAr)(CHR)(OR')<sub>2</sub> (determined by <sup>1</sup>H N.M.R. in C<sub>6</sub>D<sub>6</sub>)

## 5.2.2 Scaled up homopolymerizations of II, III, and IV

All three monomers have been successfully scaled up in preparations ranging from 0.5 - 1.5g. Typically 1.0g monomer was columned through activated alumina and mixed with 3cm<sup>3</sup> solvent. This was then added to a 2cm<sup>3</sup> stirring solution of 0.010g initiator and left for up to 24hours (the progress of the reaction was monitored via <sup>19</sup>F N.M.R.).

Initially these polymerizations were carried out in mixtures of tetrahydrofuran and toluene (approximately 15-20% tetrahydrofuran). However, samples of polyII and polyIII have also been synthesized in neat tetrahydrofuran, and polyIV initiated by Mo(NAr)(CHCMe<sub>2</sub>Ph)(OCMe(CF<sub>3</sub>)<sub>2</sub>)<sub>2</sub> has also been prepared in  $\alpha,\alpha,\alpha$ -trifluorotoluene.

All the samples prepared in this study were capped with benzaldehyde. Those polymers initiated by Mo(NAr)(CHCMe<sub>2</sub>Ph)(OCMe<sub>3</sub>)<sub>2</sub> were found to precipitate from methanol (suggesting from previous experience a high trans vinylene content); all other samples were recovered from hexane (indicative of an intermediate or high cis vinylene content). <sup>13</sup>C N.M.R. spectroscopy confirmed the general trend of cis and trans content suggested by this behaviour, although several interesting deviations were observed, and these are outlined in the following discussion.

## 5.2.3 <sup>13</sup>C NMR spectroscopic analysis of polyII

Considerable work in the assignment of the <sup>13</sup>C N.M.R. resonances of polyII has been carried out in a previous study using classical initiators<sup>1</sup>. In acetone-d<sub>6</sub> the <sup>13</sup>C NMR spectra of samples of polyII all consist of two major regions just as for polyI; the olefinic carbons (and the CF<sub>3</sub> carbon atom) all give rise to resonances between 115 and 140ppm, whilst the saturated carbon environments are to be found from 30 to 50ppm (figure 5.6).

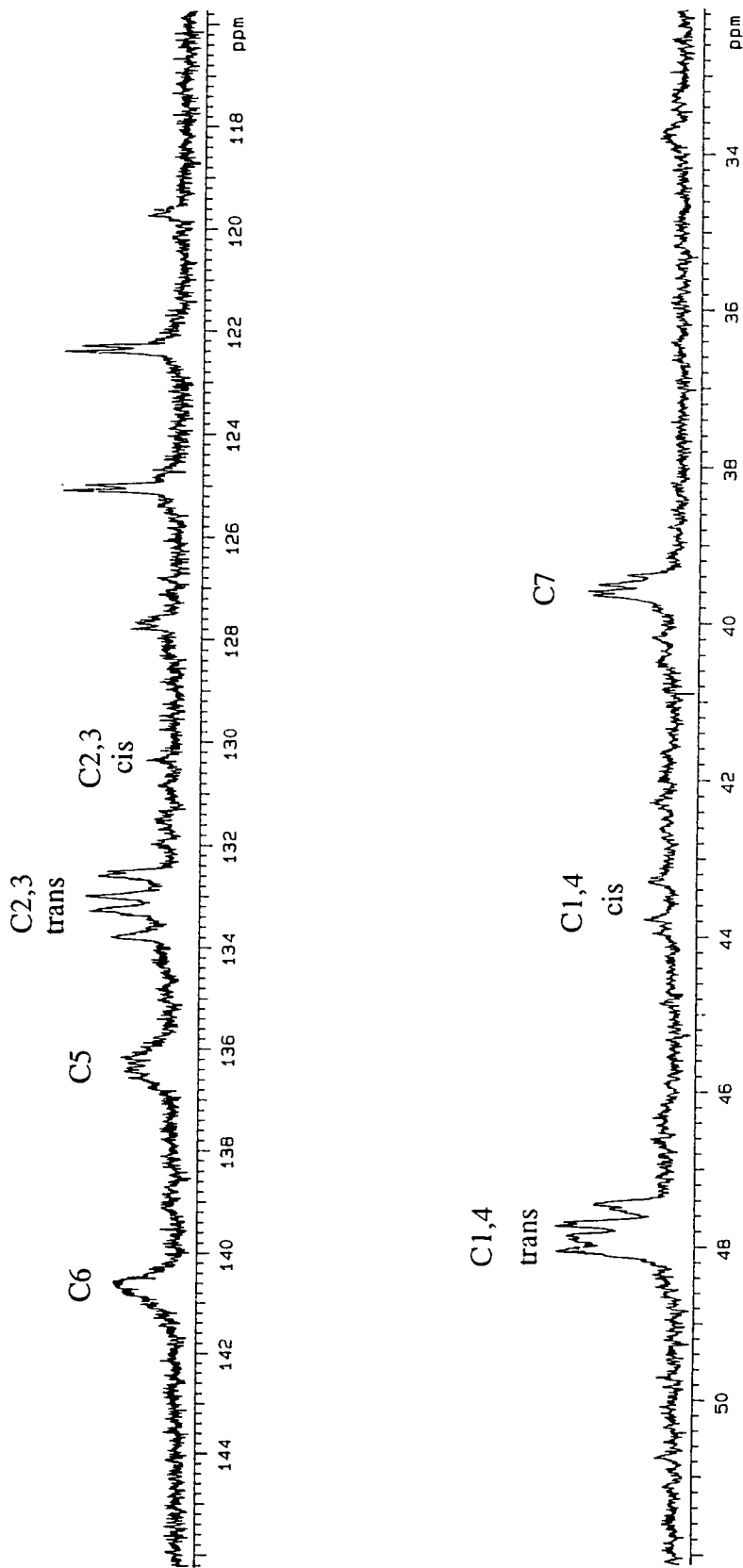


Figure 5.6 The 100MHz  $^{13}\text{C}$  N.M.R. spectrum ( $(\text{CD}_3)_2\text{CO}$ ) of polyII initiated by  $\text{Mo}(\text{NAr})(\text{CHCMe}_2\text{Ph})(\text{OCMe}_3)_2$

As is the case with samples of polyI, cis / trans splitting of about 5ppm is found in C1 and C4 carbon signals (numbering based upon figure 5.7). The trans environments give rise to an asymmetric multiplet centred around 47.9ppm, whilst the cis vinylenes occur as a series of signals between 43.2 and 44.0ppm. The relative intensities of the two sets of resonances suggest that this polymer has a trans content of greater than 90%.

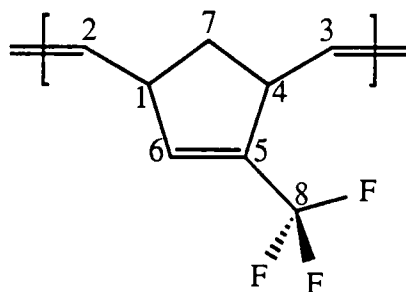


Figure 5.7

This result is not completely unexpected in view of the highly trans nature reported for the ring-opened polymers of **I** with the same initiator. Monomer **II** contains only one CF<sub>3</sub> substituent and therefore the C=C bond to be broken during the propagation stage is less deactivated than in **I**. This results in a small but significant reduction in the stereoselectivity of the polymerization. This proposal supports earlier studies on the R.O.M.P. of this monomer with classical initiators. It was reported that **II** was more susceptible to polymerization than **I** and this results in a greater range of initiators capable of polymerizing **II**.

Comparison of the acetone-d<sub>6</sub> <sup>13</sup>C N.M.R. spectra of poly**II** initiated by ReCl<sub>5</sub> ( $\sigma_c = 0.86$ ) and by OsCl<sub>3</sub> ( $\sigma_c = 0.45$ ) (figure 5.8) shows that although the chemical shifts of the cis and trans signals for C1 and C4 environments are well separated, those for C2

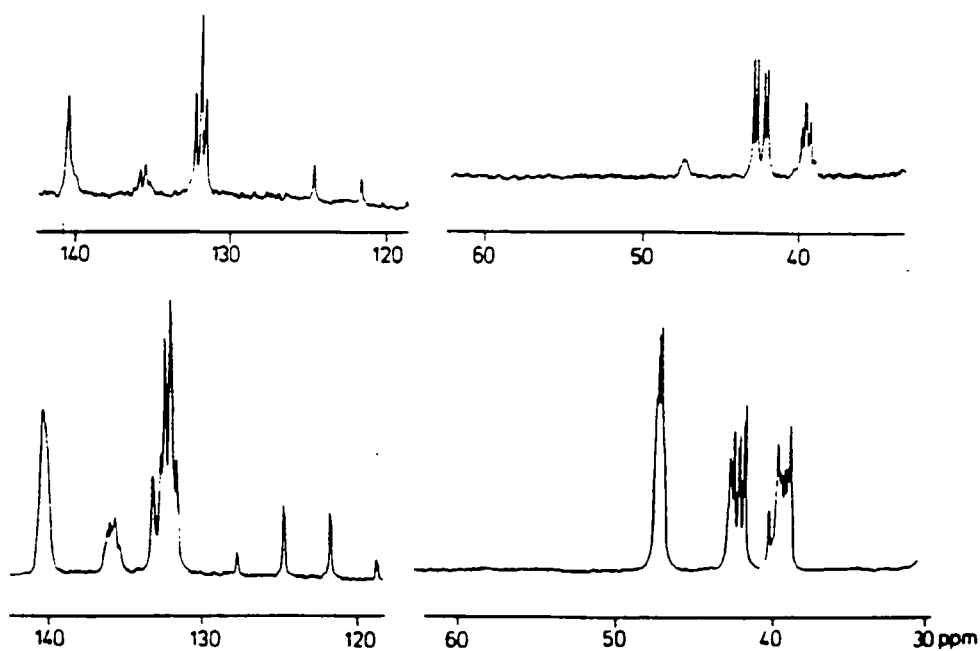


Figure 5.8 The 75MHz  $^{13}\text{C}$  N.M.R. spectra  $\{(\text{CD}_3)_2\text{CO}\}$  of polyII initiated by  $\text{ReCl}_5$  ( $\sigma_c = 0.86$ ; top) and  $\text{OsCl}_3$  ( $\sigma_c = 0.45$ )

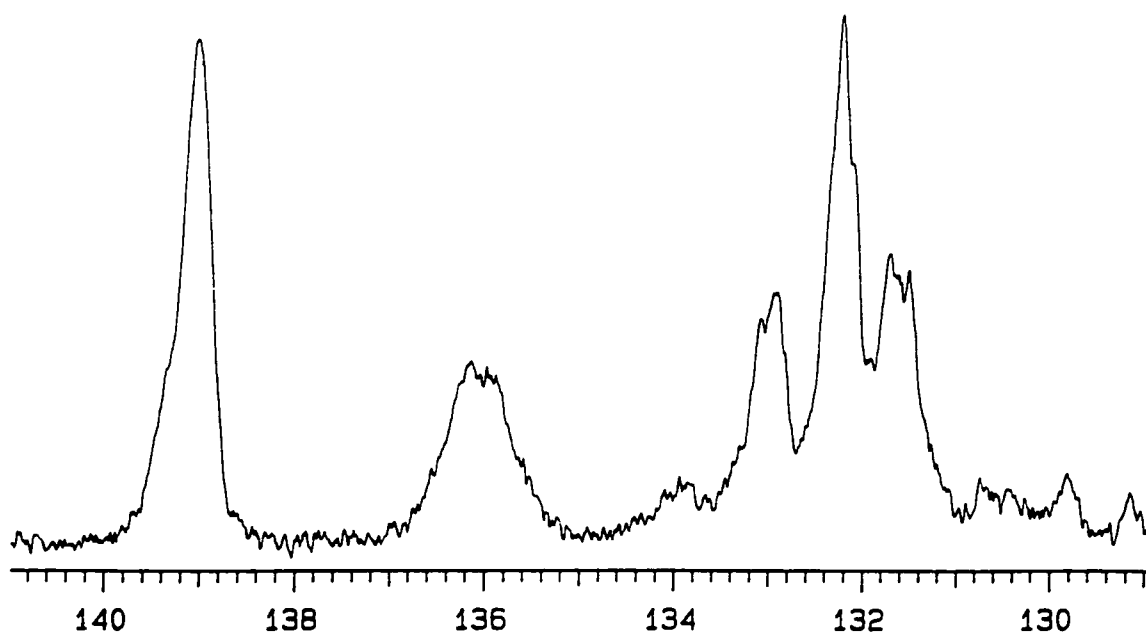


Figure 5.9 The olefinic region of the 100MHz  $^{13}\text{C}$  N.M.R. spectrum of polyII in chloroform- $d_1$  (initiated by  $\text{Mo}(\text{NAr})(\text{CHCMe}_2\text{Ph})(\text{OCMe}_3)_2$ )

and C3 are not. However, it has been found that by changing the solvent to deuterated chloroform (and by increasing the spectrometer frequency to 100.577MHz) the cis and trans C2,C3 resonances become clearly separated (figure 5.9). The region confirms the high trans content of the polymer.

The trans olefinic signal (131.0 - 133.6ppm) has a 'triplet' appearance consisting of unresolved multiplets. This is believed to arise from C2 and C3 trans carbons in HH, HT, TH, and TT environments (H = head, T = tail, where the CF<sub>3</sub> end of the repeat unit is defined as the head). The centre line is caused by coincidental chemical shifts for two of these assembly modes; therefore, the ratio of the three signals (approximately 1 : 2 : 1) implies an equal distribution of all four possible head / tail assemblies.

The fine structure observed is presumably due to different tacticities present in the polymer chain, and this is not unexpected. Although the ring-opened polymers of **I** have only four possible stereoregular assembly modes, the removal of the plane of symmetry in the repeat units for poly**II** leads to a four-fold increase in possible assemblies (figure 5.10 shows the four different environments for an all trans, all syndiotactic poly**II**).

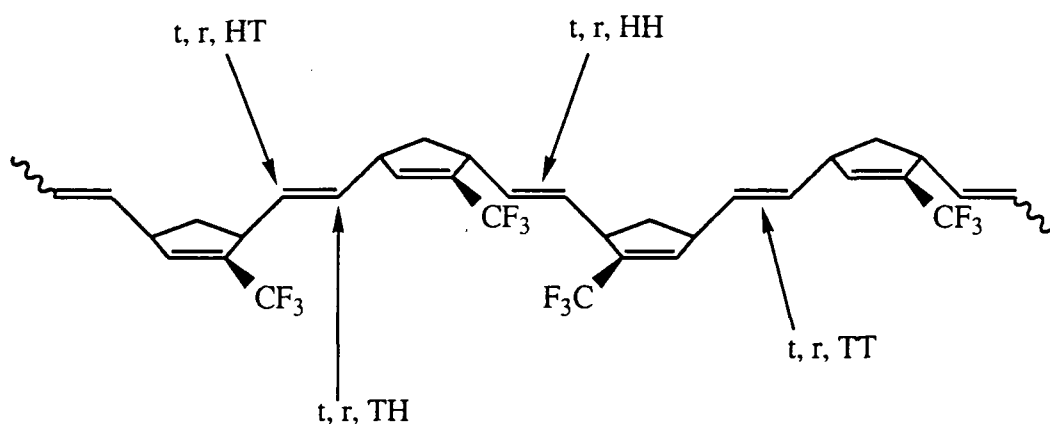


Figure 5.10 Four of the possible sixteen dyad structures for poly**II**

Resonance(s) / ppm	Assignment
38.76, 38.90, 39.52	C7
40.5 - 43.5	C1,4 cis
46.71, 46.95, 47.44	C1,4 trans
118.56, 121.23, 123.92, 126.60	C8
128.0 - 130.7	C2,3 cis
131.52, 131.62, 132.25, 132.93, 133.10	C2,3 trans
136.15	C5
139.05	C6

Table 5.3 The resonances for high trans polyII in CDCl<sub>3</sub>

In view of the increased complexity in the microstructure of this polymer compared with polyI, an attempt has not been made to further define the microstructure of polyII from the C2,C3 signals.

Three lines are also seen for the C1 and C4 trans carbon signals in CDCl<sub>3</sub> (figure 5.11); however, this triplet is not symmetrical and therefore is not a simple case of head / tail splitting effects. Indeed, the <sup>13</sup>C spectrum of the living decamer in benzene-D<sub>6</sub> shows at least four lines for this region as shown in figure 5.12. Even more microstructural information is apparent in the spectrum recorded in acetone-d<sub>6</sub>, in which the C1 and C4 carbons give rise to four unresolved multiplets (figure 5.13). This is similar to the four lines observed for the cis C1 and C4 environments in a highly cis form of polyII initiated by ReCl<sub>5</sub>. The splitting was assigned as two sets of two signals of equal total intensity. However, in the spectrum of the high trans polyII separation of the multiplets is not sufficient to allow for an accurate determination of peak intensities, thus precluding further analysis.

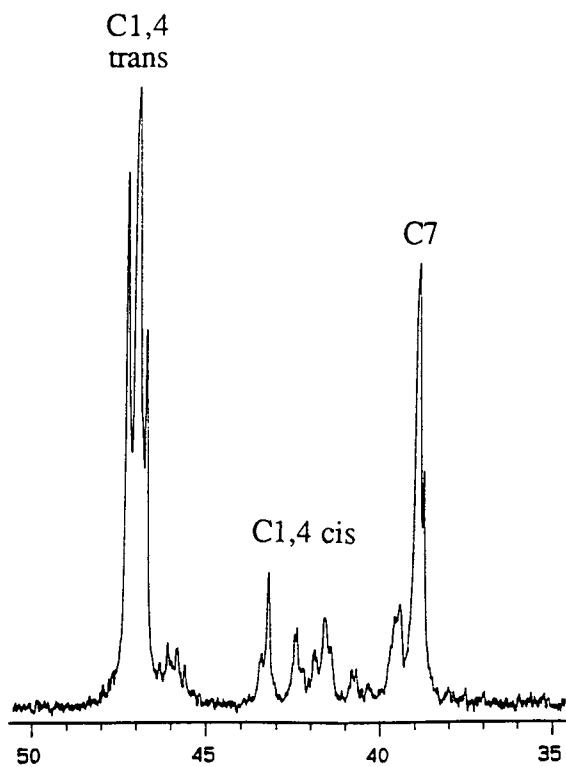


Figure 5.11 The low field region of the 100MHz  $^{13}\text{C}$  N.M.R. spectrum of polyII initiated by  $\text{Mo}(\text{NAr})(\text{CHCMe}_2\text{Ph})(\text{OCMe}_3)_2$  in chloroform- $\text{d}_1$

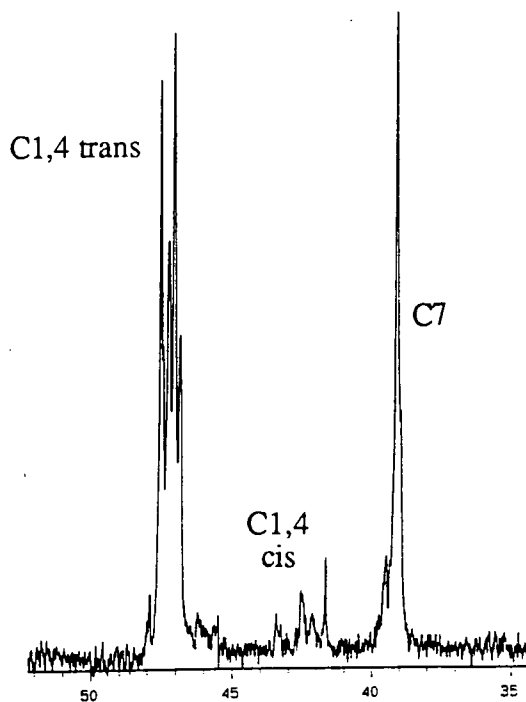


Figure 5.12 The low field region of the 100MHz  $^{13}\text{C}$  N.M.R. spectrum of polyII initiated by  $\text{Mo}(\text{NAr})(\text{CHCMe}_2\text{Ph})(\text{OCMe}_3)_2$  in benzene- $\text{d}_6$

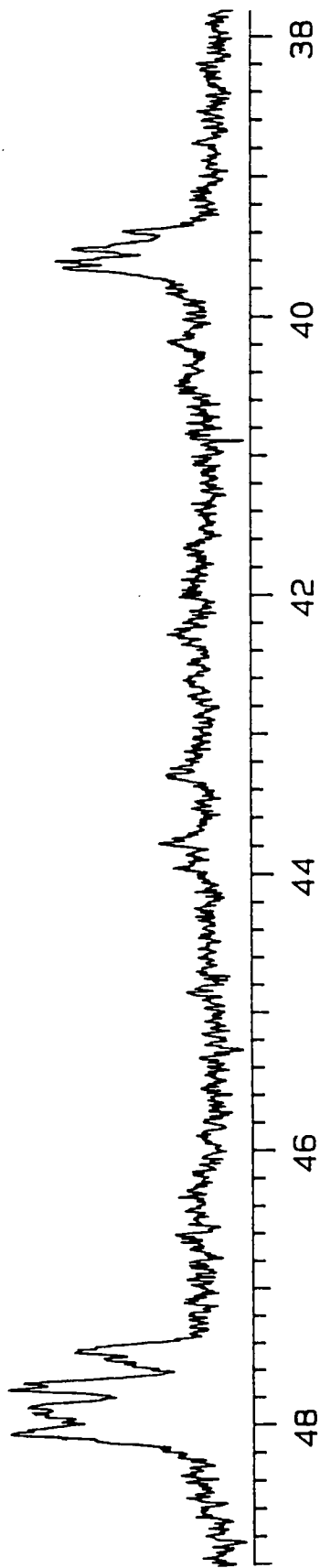


Figure 5.13 The C1,C4 and C7 resonances in the 100MHz  $^{13}\text{C}$  N.M.R. spectrum of highly trans polyII in acetone- $d_6$

The C7 resonance was reported previously as a triplet in  $(\text{CD}_3)_2\text{CO}$  (and again this was explained in terms of head / tail possibilities with two of the four assembly modes possessing coincident chemical shift values). At 100MHz the polymer prepared here displays at least four distinct resonances (figure 5.13), suggesting that at this increased frequency the chemical shifts of the four possible head-tail dyad permutations are no longer coincident. Indeed, rather than simple HT effects, it is believed that the C7 methylene region, as for polyI, is sensitive to tacticity splitting.

In  $\text{CDCl}_3$  the high trans sample of polyII gives rise to the methylene region shown previously in figure 5.11. However, in the absence of any further data (particularly dielectric measurements) no further assignment has yet proved possible.

The final region of this spectrum worthy of consideration is that associated with the carbon (C8) of the trifluoromethyl substituent; this has the appearance of two overlapping quartets. Therefore, the polar substituents may be in two non-equivalent environments within the chain. This may be due to head-tail effects (in which case four overlapping quartets might be observed at higher frequency). However, the precise origin of this splitting is still not known; the belief that it may not be a microstructural phenomenon, but a conformational one instead, can not be discounted.

The reverse from high trans to high cis polyI when the initiator is changed to  $\text{Mo}(\text{NAr})(\text{CHCMe}_2\text{Ph})(\text{OCMe}(\text{CF}_3)_2)_2$  is also seen for monomer II. Figure 5.14 presents the acetone- $d_6$   $^{13}\text{C}$  NMR spectrum from 38 to 50ppm of a sample of polyII generated from the bis(hexafluorobutoxide) initiator. The C1 and C4 signals are marked and clearly reveal a cis vinylene content in excess of 95%.

The cis resonances are particularly interesting, especially compared to the two doublets seen in the same region for the  $\text{ReCl}_5$  initiated analogue (figure 5.8). The simplicity of the classically-initiated sample implies a high degree of stereoregularity.

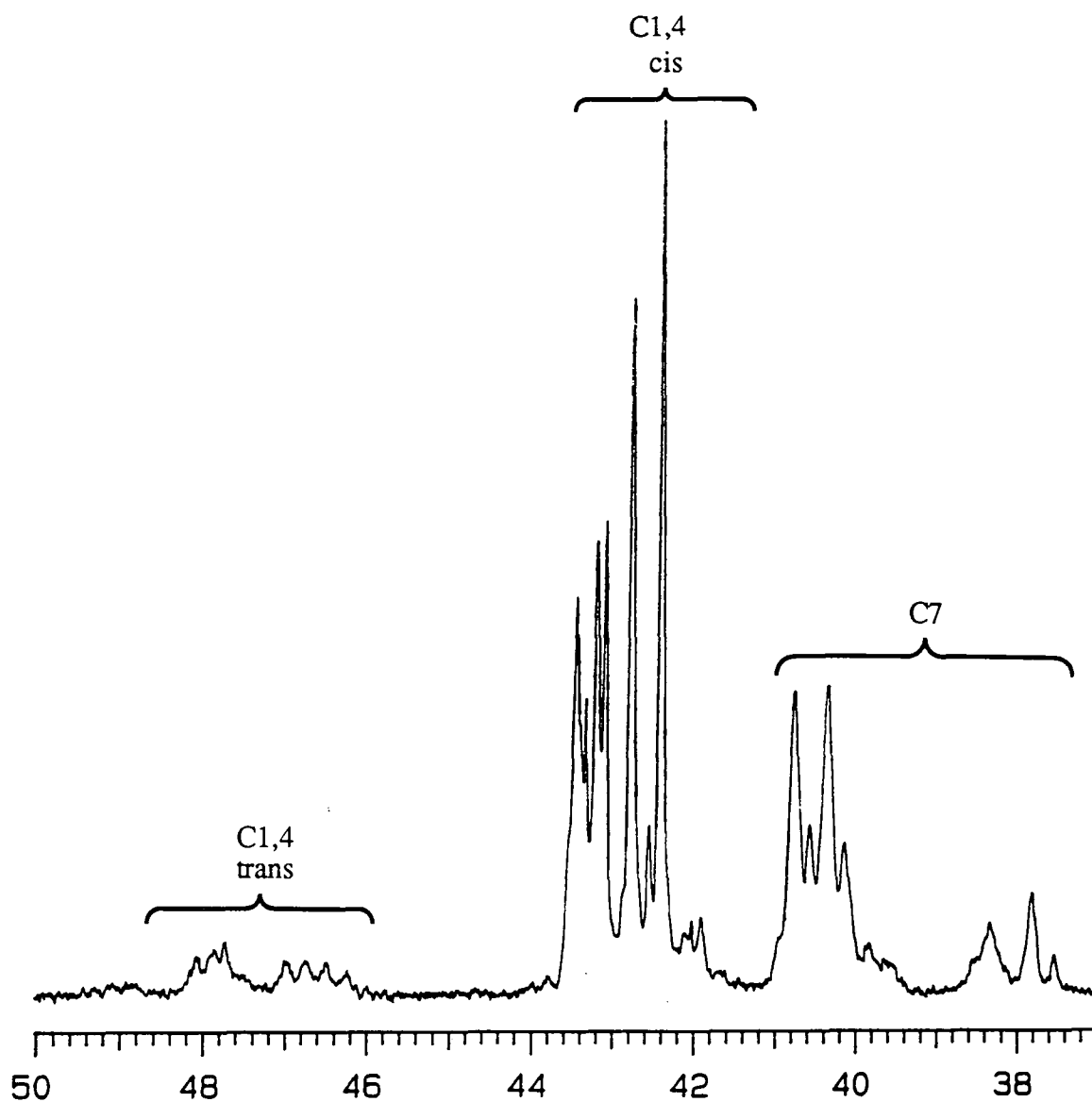


Figure 5.14 The C1,C4 and C7 signals in the 100MHz  $^{13}\text{C}$  N.M.R. spectrum  $\{(\text{CD}_3)_2\text{CO}\}$  of polyII initiated by  $\text{Mo}(\text{NAr})(\text{CHCMe}_2\text{Ph})(\text{OCMe}(\text{CF}_3)_2)_2$

Indeed, in the original report on the R.O.M.P. of **II** it was suggested that a cis-syndiotactic architecture might be favoured. Similarly the C7 methylene region is more complex in the  $\sigma_c = 0.95$  sample of poly**II** than in the  $\text{ReCl}_5$ -initiated version ( $\sigma_c = 0.86$ ).

The high cis content of this sample of poly**II** is also confirmed by analysis of the olefinic C2 and C3 signals which are shown in figure 5.15. Although in acetone- $d_6$  cis and trans environments lead to overlapping signals in this part of the spectrum, the appearance of a relatively well-resolved triplet implies that one olefinic geometry predominates. Note also from figure 5.15 that the trifluoromethyl substituent carbon (C8) again appears as a quartet of doublets (In deuterio-acetone  $J_q = 270.08\text{Hz}$ ,  $J_d = 7.72\text{Hz}$ ).

The most informative region of this spectrum may prove to be the C6 resonances. Figure 5.8 shows that when  $\text{ReCl}_5$  is used to polymerize **II** this signal appears as a singlet with a small shoulder towards high field. Like poly**I** ( $\sigma_c = 0.98$ ) the ring-opened polymer of **II** initiated by  $\text{Mo}(\text{NAr})(\text{CHCMe}_2\text{Ph})(\text{OCMe}(\text{CF}_3)_2)_2$  is not believed to be completely tactic; hence the multiplicity of the C6 signal in its  $^{13}\text{C}$  NMR spectrum. Combining the evidence of both spectra together it would seem to provide further weight to the claim that the  $\text{ReCl}_5$ -initiated polymer is predominantly syndiotactic (the main signal is assigned as rr with the small shoulder arising from mr dyads).

In summary, both a high trans and a high cis form of poly**II** can be synthesized via initiators of the type  $\text{Mo}(\text{NAr})(\text{CHR})(\text{OR}')_2$ . It should therefore prove possible to carry out a full microstructure assignment via  $^{13}\text{C}$  NMR spectroscopy over a range of samples initiated by a mixed initiator equilibrium as described in chapter three with poly**I**. However, due to the small quantity of monomer **II** available, this has not yet been carried out. Nonetheless, in order to obtain at least one intermediate sample of poly**II**, the monomer was polymerized using  $\text{Mo}(\text{NAr})(\text{CHCMe}_3)(\text{OCMe}_2\text{CF}_3)_2$ . The acetone- $d_6$   $^{13}\text{C}$  NMR of the isolated product is shown overleaf (figure 5.16), as well as expansions of the two regions from 118 to 142ppm and from 33 to 49ppm. Astonishingly, comparison with

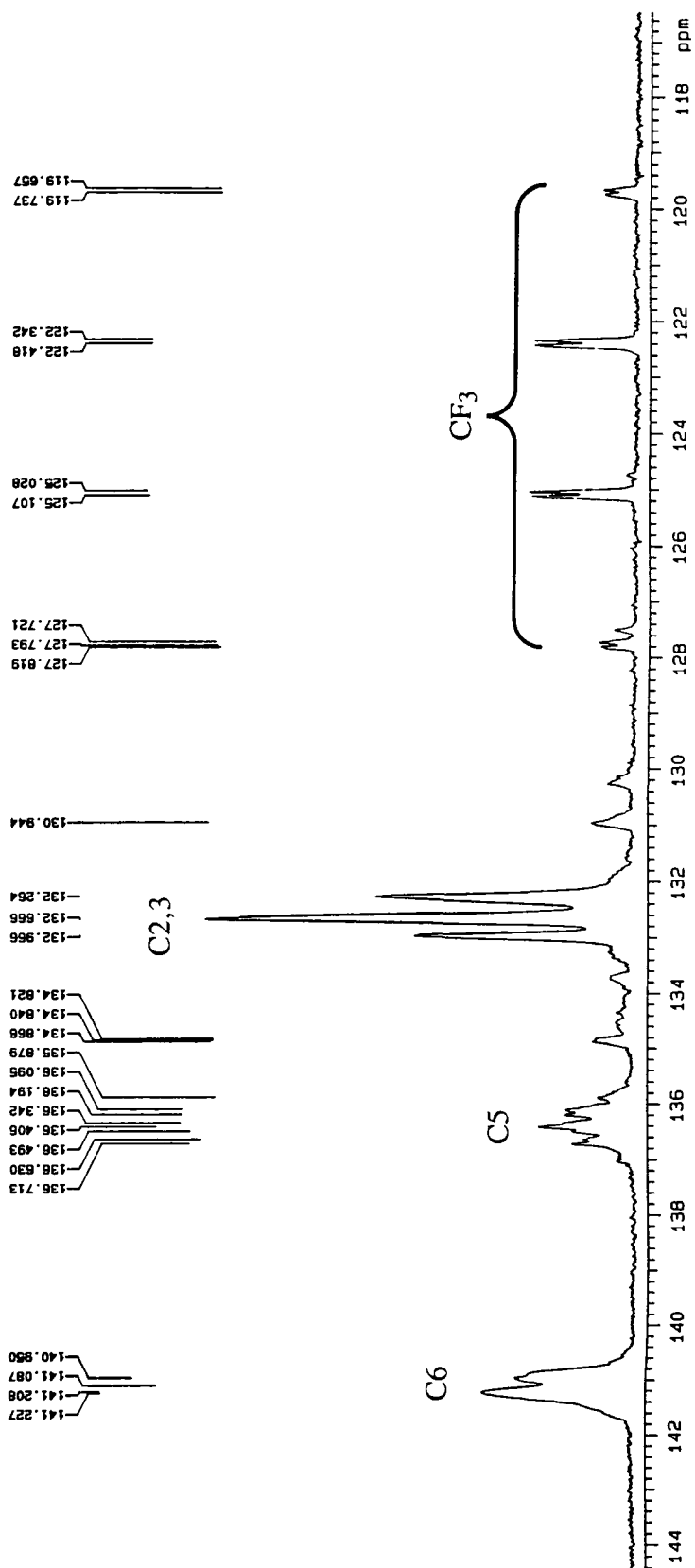


Figure 5.15 The olefinic region of the 100MHz  $^{13}\text{C}$  N.M.R. spectrum  $\{(\text{CD}_3)_2\text{CO}\}$  of poly II initiated by  $\text{Mo}(\text{NAr})(\text{CHCMe}_2\text{Ph})(\text{OCMe}(\text{CF}_3)_2)_2$

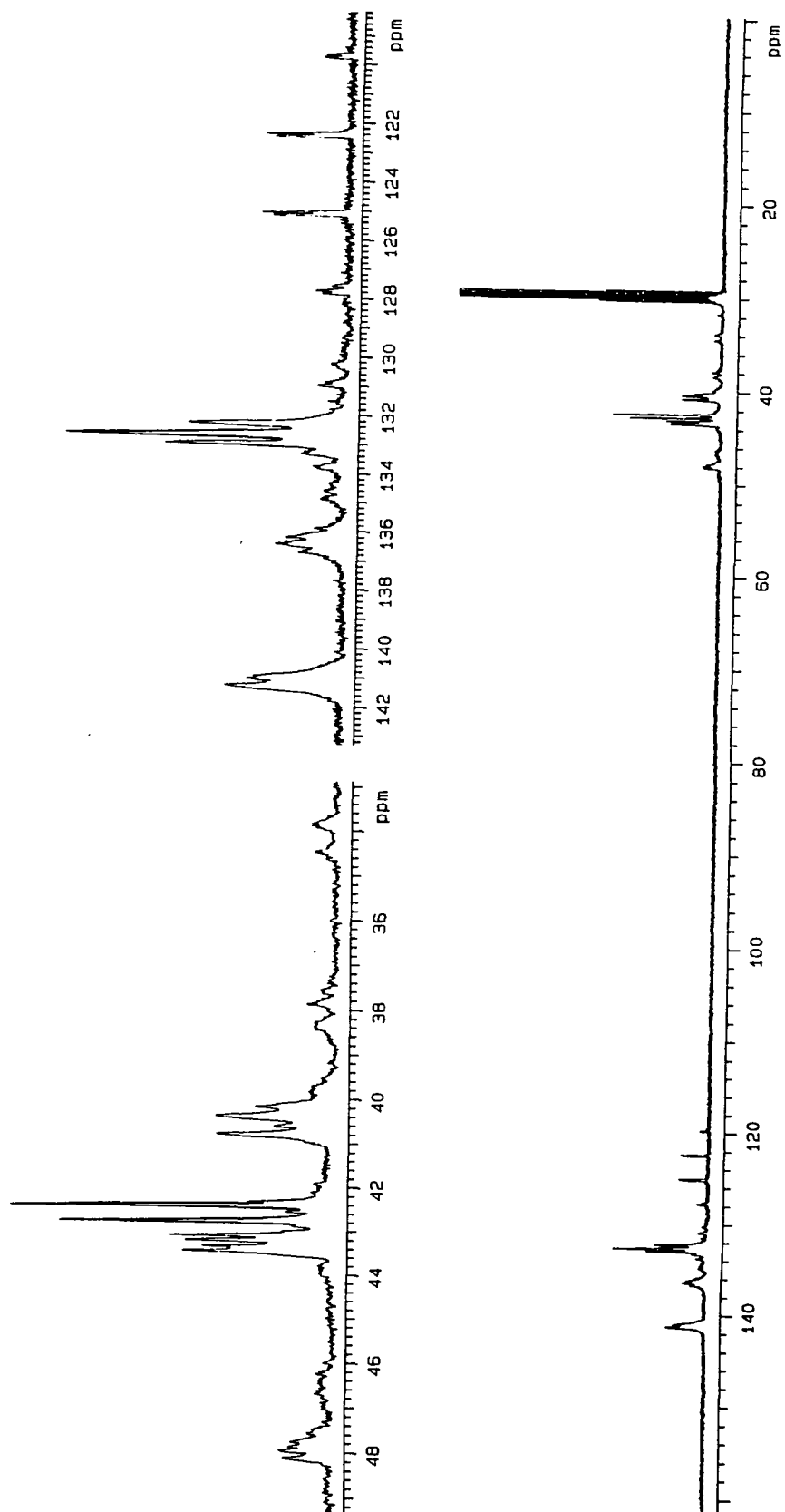


Figure 5.16 The 100MHz  $^{13}\text{C}$  N.M.R. spectrum  $\{(\text{CD}_3)_2\text{CO}\}$  of poly**II** initiated by  $\text{Mo}(\text{NAr})(\text{CHCMe}_3)(\text{OCMe}_2\text{CF}_3)_2$

figures 5.14 and 5.15 shows that this sample also possesses a very high cis vinylene content, estimated at approximately 90%.

Indeed, apart from the slight increase in the intensity of the C1,C4 trans signals between 47.5 and 48.1ppm, and the minor change in the appearance of the C2,C3 cis triplet, this spectrum is practically super-imposable upon that obtained for the polymer initiated by  $\text{Mo}(\text{NAr})(\text{CHCMe}_2\text{Ph})(\text{OCMe}(\text{CF}_3)_2)_2$ .

This unexpected finding is particularly surprising in view of the data reported for polyI which has a  $\sigma_c$  value of 0.65 when initiated via the bis(trifluorobutoxide) initiator. However, the effect can still be rationalised in terms of Schrock's observation that cis and trans stereochemistries are governed by syn / anti rotamer interconversion rates. Monomer I propagates at a slow enough rate to allow for appreciable syn / anti interconversion. As a result 65% of I can polymerize via the anti form of  $\text{Mo}(\text{NAr})(\text{CHP})(\text{OCMe}_2\text{CF}_3)_2$  {P = propagating chain}. However, the double bond to be opened during the R.O.M.P. of II is less deactivated than in I. As a consequence propagation is more rapid and considerably more of the propagation occurs via the syn rotamer (90%). Therefore the polymer produced is predominantly cis. By the same rationale the sample of polyII generated from the bis(butoxide) initiator is not quite as highly trans as the corresponding samples of polyI.

#### 5.2.4 $^{13}\text{C}$ NMR spectroscopic analysis of polyIII

Ring-opened polymers of **III** have the potential for an even more complicated microstructure than the series of polymers of monomer **II** discussed above. The presence of exo and endo substituent orientations results in 32 possible stereoregular assembly modes (the racemic sample of **III** used in this study consisted of 65% endo : 35% exo). Consequently, analysis of polymer microstructure via  $^{13}\text{C}$  NMR is unlikely to lead to an unambiguous assignment.

When **III** is R.O.M.P.ed using  $\text{Mo}(\text{NAr})(\text{CHCMe}_2\text{Ph})(\text{OCMe}_3)_2$  as the initiator, the polymer which results gives the  $^{13}\text{C}$  N.M.R. spectrum shown in figure 5.17.

The assignment of this polymer's spectrum is again facilitated by a previous study using classical initiators<sup>2</sup>. The first point of interest is that this polymer is mostly trans (not surprising in view of the previous work with monomers **I** and **II**). A  $\sigma_1$  value of approximately 0.80 is estimated.

The C2 and C3 signals are well separated and the cis and trans signals for both these carbons are also quite distinct. The C3 trans head-head (t HH) is particularly interesting since it appears as a doublet whilst the C2 t TT, C2 t TH, and C3 t HT signals are all single lines. Note that the C2 carbons can only occur in TT and TH environments, and the C3 atoms can only be found in HH and HT sites. Also the intensities of all four signals should be equal.

In the previous report the splitting of the C3 t HH resonance was assigned as due to r and m dyads. Certainly, the equal intensity of the lines would appear to rule out an endo / exo effect. However, assuming that the high trans nature of this polymer is accompanied by a tendency to form syndiotactic dyads, as is the case with **I**, then an equal splitting of the C3 signal is difficult to justify using a tacticity argument. Possible explanations as to the origin of such splitting include repulsive interactions between the fluorines leading to two different conformational structures, or hydrogen-bonding between the substituents and solvent molecules.

\* = cis signals (further assignment not made)

† = unassigned

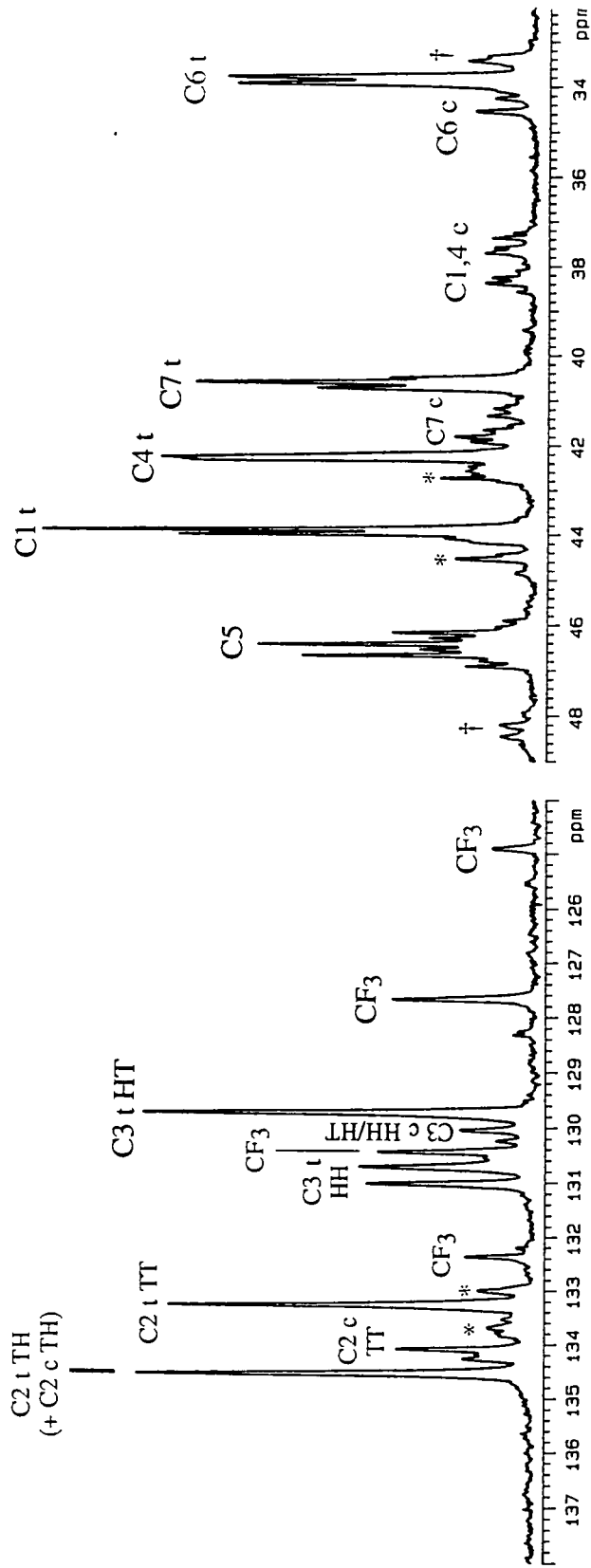


Figure 5.17 The 100MHz  $^{13}\text{C}$  N.M.R. spectrum  $\{(\text{CD}_3)_2\text{CO}\}$  of poly(III) initiated by  $\text{Mo}(\text{NAr})(\text{CHCMe}_2\text{Ph})(\text{OCMe}_3)_2$

In view of the differences obtained between spectra of polyII in deuterated acetone and chloroform, a spectrum of high trans polyIII was also obtained in CDCl<sub>3</sub>. However, no extra information was gleaned from this spectrum which was essentially the same as that obtained in acetone-d<sub>6</sub>. Table 5.4 records the <sup>13</sup>C trans resonances for this sample of polyIII in both solvents, as well as assignments.

Resonances in (CD <sub>3</sub> ) <sub>2</sub> CO / ppm	Resonances in CDCl <sub>3</sub> / ppm	Assignment
33.92, 33.77	33.20, 33.05	C6 t
40.72, 40.59, 40.50	39.77, 39.73	C7 t
42.32, 42.29, 42.24	41.66	C4 t
43.97, 43.87	43.44, 43.34	C1 t
45.90 - 46.95 (major signals: 46.66, 46.41, 46.16)	45.40 - 46.50 (46.18, 45.98, 45.87, 45.75)	C5
129.72	128.74	C3 t HT
132.36, 130.44, 127.66, 125.90	132.0, 129.22, 126.45, 123.7	C8
131.02, 130.71	130.18, 129.82	C3 t HH
133.26	132.37	C2 t TH
134.54	133.70	C2 t TT

Table 5.4 The trans carbon resonances for polyIII in acetone-d<sub>6</sub> and chloroform-D<sub>3</sub> at 100.577MHz

With Mo(NAr)(CHCMe<sub>2</sub>Ph)(OCMe<sub>2</sub>CF<sub>3</sub>)<sub>2</sub> monomer II can be polymerized in THF to give a white fibrous material the <sup>13</sup>C N.M.R. spectrum of which is shown in figure 5.18. The intensities of all the cis signals are appreciably higher than for the bis(tert-butoxide) initiated sample. However, an accurate determination of cis and trans vinylene content is hampered by overlapping resonances and in some cases ambiguities concerning their assignments. Nonetheless, from comparison of the C3 HH cis and trans

signals (at 130.04 and 129.72ppm respectively) it would appear that this polymer is approximately 50% trans.

As for polyI and II, a highly cis stereoisomer of polyIII is formed when the initiator is  $\text{Mo}(\text{NAr})(\text{CHCMe}_2\text{Ph})(\text{OCMe}(\text{CF}_3)_2)_2$ . Assignment of the  $^{13}\text{C}$  N.M.R. resonances is made on figure 5.19 and a  $\sigma_c$  value of 0.90 is determined from the relative intensities of the C1 trans signal (44.0ppm) and the C1 and C4 cis multiplet (36.4 - 38.0ppm). As before, the presence of endo and exo possibilities complicates further assignment and therefore a discussion of tacticity in this potentially interesting sample is hampered. Dielectric measurements are presently underway<sup>3</sup>, and may help to clarify microstructural details.

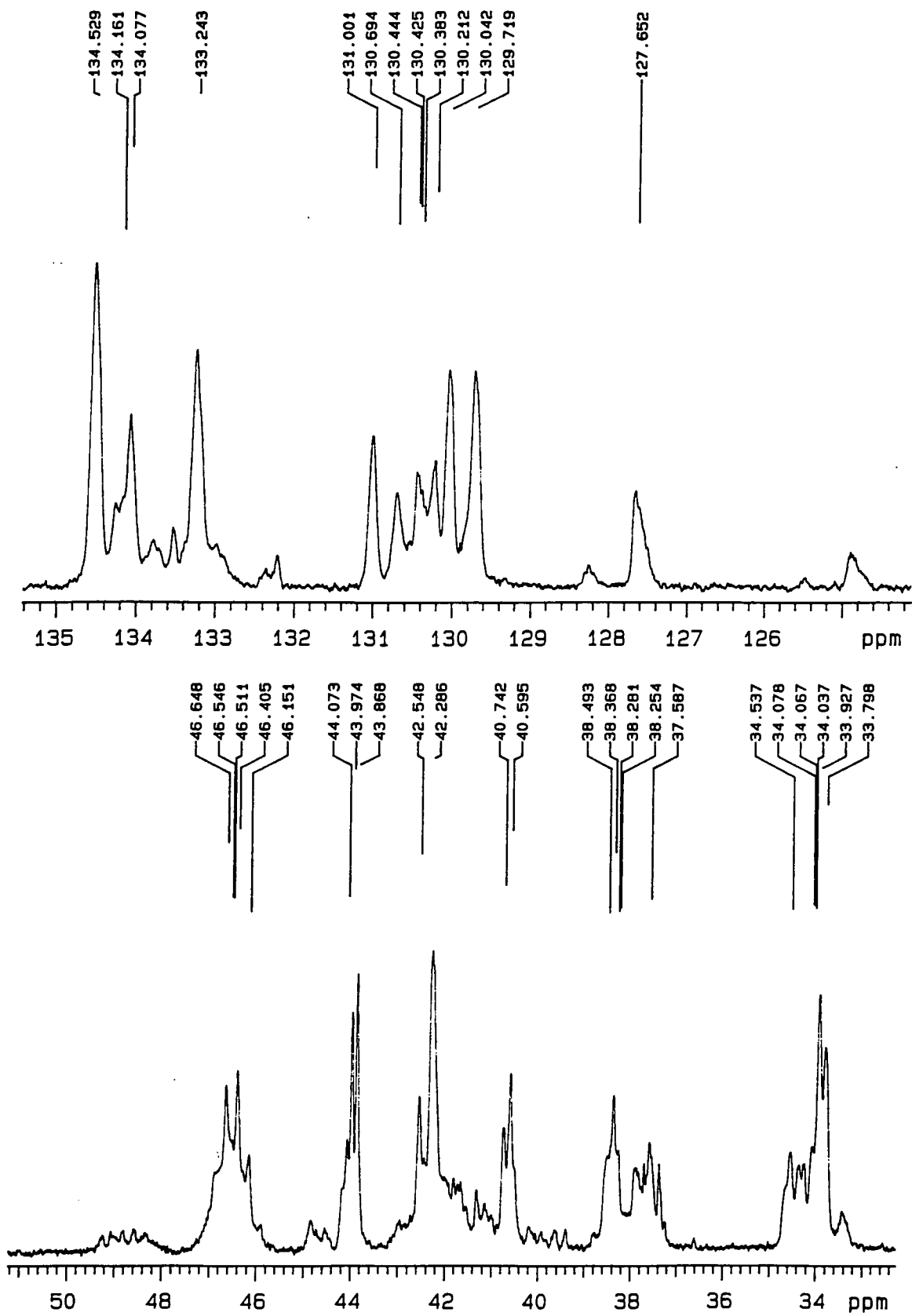


Figure 5.18 The 100MHz  $^{13}\text{C}$  N.M.R. spectrum  $\{(\text{CD}_3)_2\text{CO}\}$  of polyIII initiated by  $\text{Mo}(\text{NAr})(\text{CHCMe}_2\text{Ph})(\text{OCMe}_2\text{CF}_3)_2$

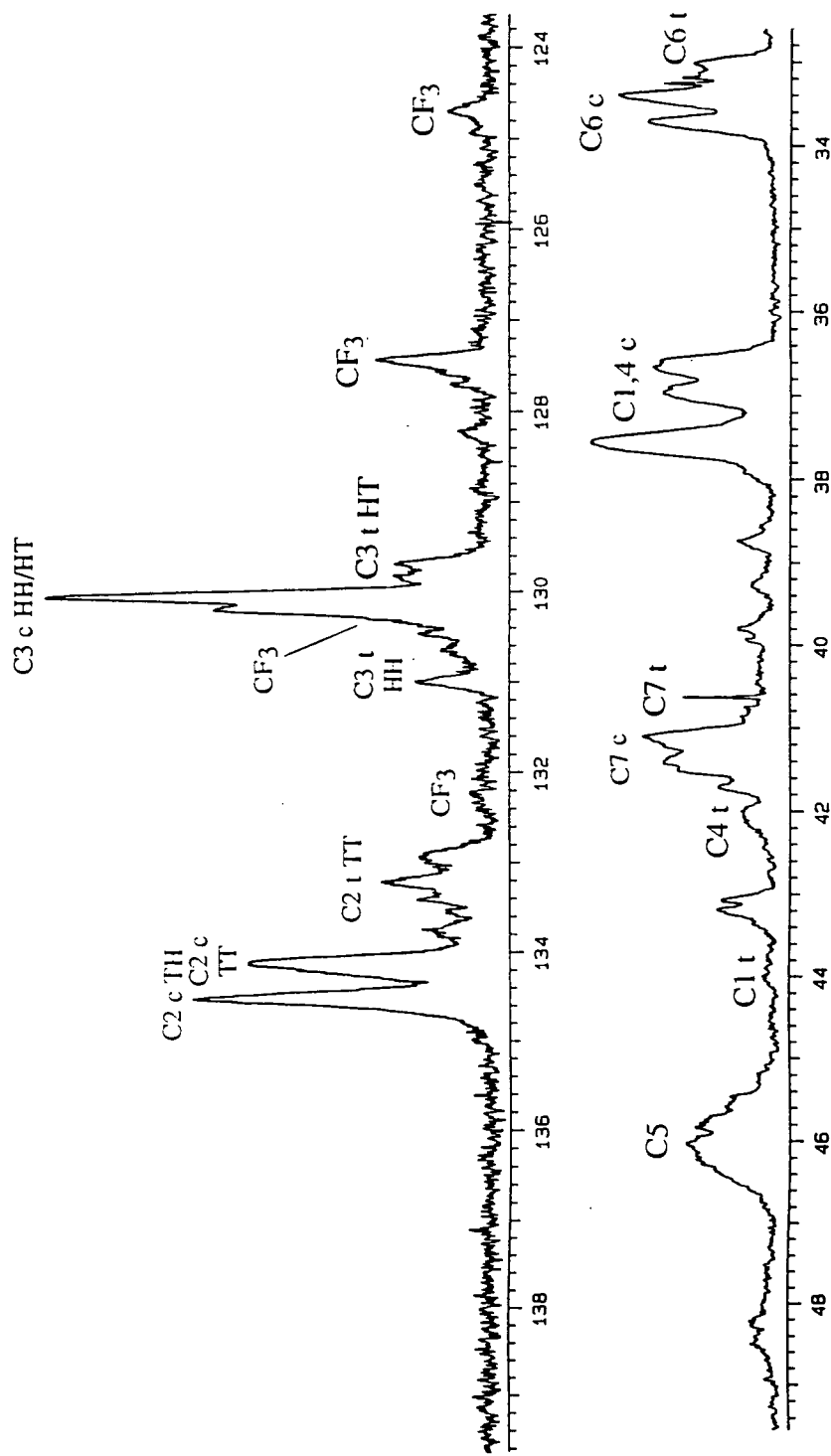


Figure 5.19 The 100MHz  $^{13}\text{C}$  N.M.R. spectrum  $\{(\text{CD}_3)_2\text{CO}\}$  of poly(III) initiated by  $\text{Mo}(\text{NAr})(\text{CHCMe}_2\text{Ph})(\text{OCMe}(\text{CF}_3)_2)_2$

### 5.2.5 $^1\text{H}$ and $^{13}\text{C}$ N.M.R. spectroscopic analysis of polyIV

Attention has already been drawn to the fact that in terms of substituent effects monomer IV is more closely related to I than either II or III. It might therefore be expected that it should undergo R.O.M.P. to give a highly trans polymer with  $\text{Mo}(\text{NAr})(\text{CHCMe}_2\text{Ph})(\text{OCMe}_3)_2$  and a high cis stereoisomer with the bis(hexafluorobutoxide) initiator.

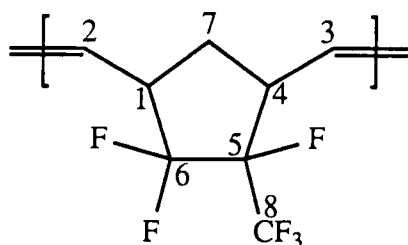


Figure 5.20

Less work has been carried out on this monomer than with either of the other three with classical initiating systems. As a result rather more detailed analysis has been required in order to assign  $^{13}\text{C}$  N.M.R. resonances.

The  $^1\text{H}$  N.M.R. spectrum of the living oligomer bearing tert-butoxide ancillary ligands is shown in figure 5.21a. Its relative simplicity and similarity to trans living polyI does support the prediction of a high trans content. For comparison, the corresponding spectrum for  $\text{Mo}(\text{NAr})(\text{CHCMe}_2\text{Ph})(\text{OCMe}(\text{CF}_3)_2)_2$  - initiated polyIV is shown in figure 5.21b; noticeably it contains several extra signals (especially between 2.8 and 3.6ppm) and the intense resonance at 5.5ppm is much broader. However all of the signals seen in the first trace are also present in the latter case; this does not lend support to an all cis polymer, but rather an intermediate stereochemistry.

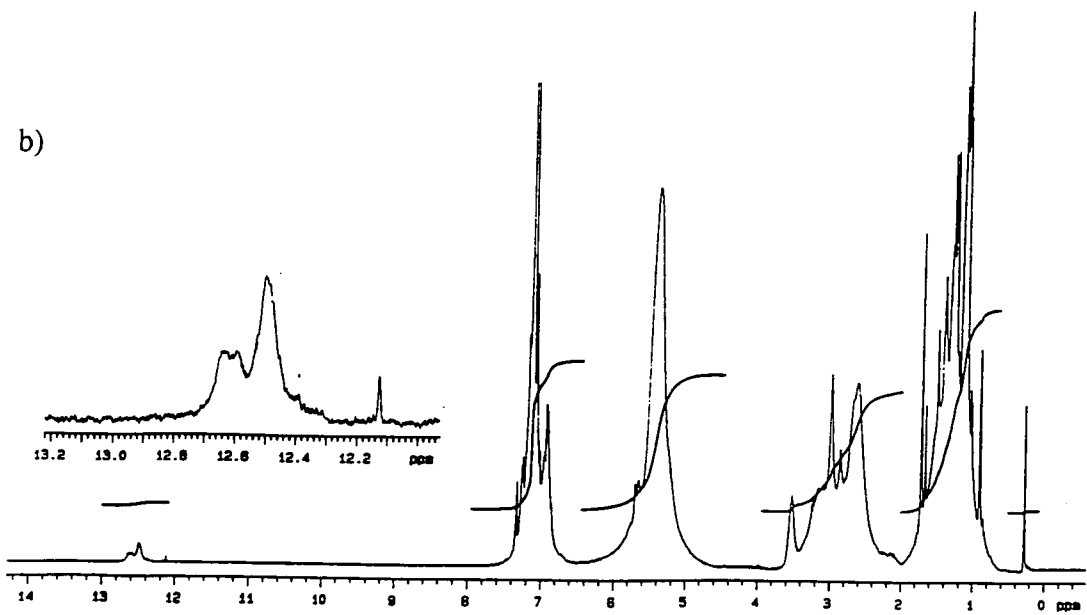
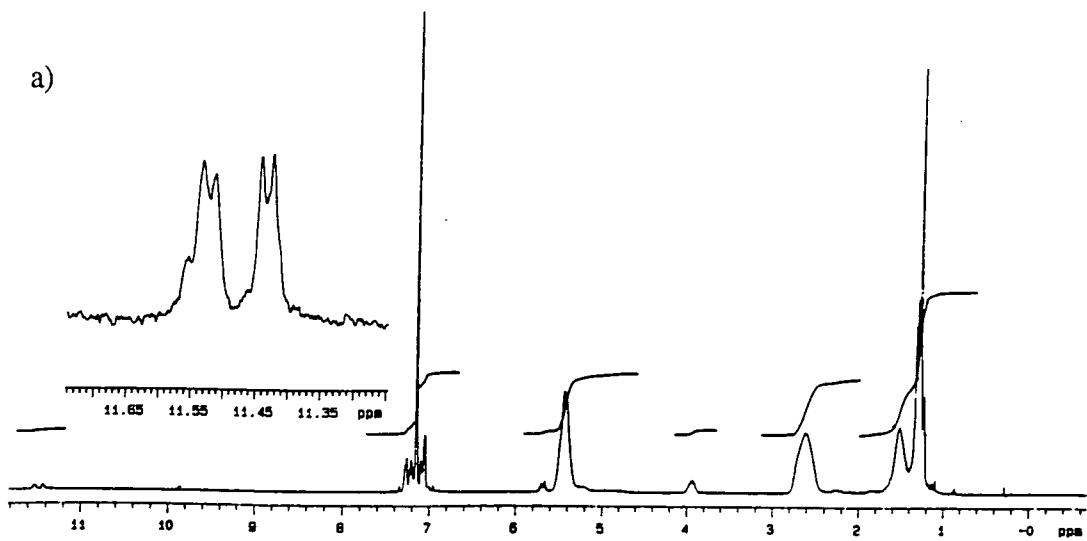


Figure 5.21 The 400MHz N.M.R. spectra ( $C_6D_6$ ) of living polyIV initiated by

a)  $Mo(NAr)(CHCMe_2Ph)(OCMe_3)_2$

b)  $Mo(NAr)(CHCMe_2Ph)(OCMe(CF_3)_2)_2$

The  $^{13}\text{C}$  N.M.R. of a sample of polyIV (initiated by the bis(butoxide) neophylidene complex) is noticeably more complex than any of the spectra shown previously in this chapter, a consequence of the increased potential for fluorine coupling (as well as possessing 32 possible assembly modes). The complexity is particularly exaggerated in the downfield region of the spectrum (figure 5.22).

Nevertheless, the remainder of the spectrum is relatively well-resolved. In order to aid the assignment of these signals a series of  $^{13}\text{C}$  DEPT N.M.R. experiments<sup>4</sup> were carried out, which led to the assignments in figure 5.23.

A large scale polymerization of IV was also conducted using  $\text{Mo}(\text{NAr})(\text{CHCMe}_2\text{Ph})(\text{OCMe}(\text{CF}_3)_2)_2$ , and the same  $^{13}\text{C}$  N.M.R. experiments were carried out as before. Figure 5.24 displays the  $^{13}\text{C}[^1\text{H}]$  decoupled N.M.R. spectrum of the homopolymer. An obvious difference between these spectra is the occurrence of new, quite intense signals at 43.8-44.2, 38.9, 34.6 and 33.9ppm, as well as a weak broad multiplet between 41.2 and 42.8ppm. Further, the intense signals at 43.77 and 44.00ppm probably comprise at least two signals, just one of which is seen in figure 5.23. As in the proton spectrum all of the resonances recorded for the bis(butoxide) - initiated sample of polyIV are also present but are of much weaker intensity. The new signals are believed to arise from carbon environments in cis geometry dyads. The complete lack of such resonances in the first spectrum therefore implies that very high trans polymer is indeed accessible from  $\text{Mo}(\text{NAr})(\text{CHCMe}_2\text{Ph})(\text{OCMe}_3)_2$ .

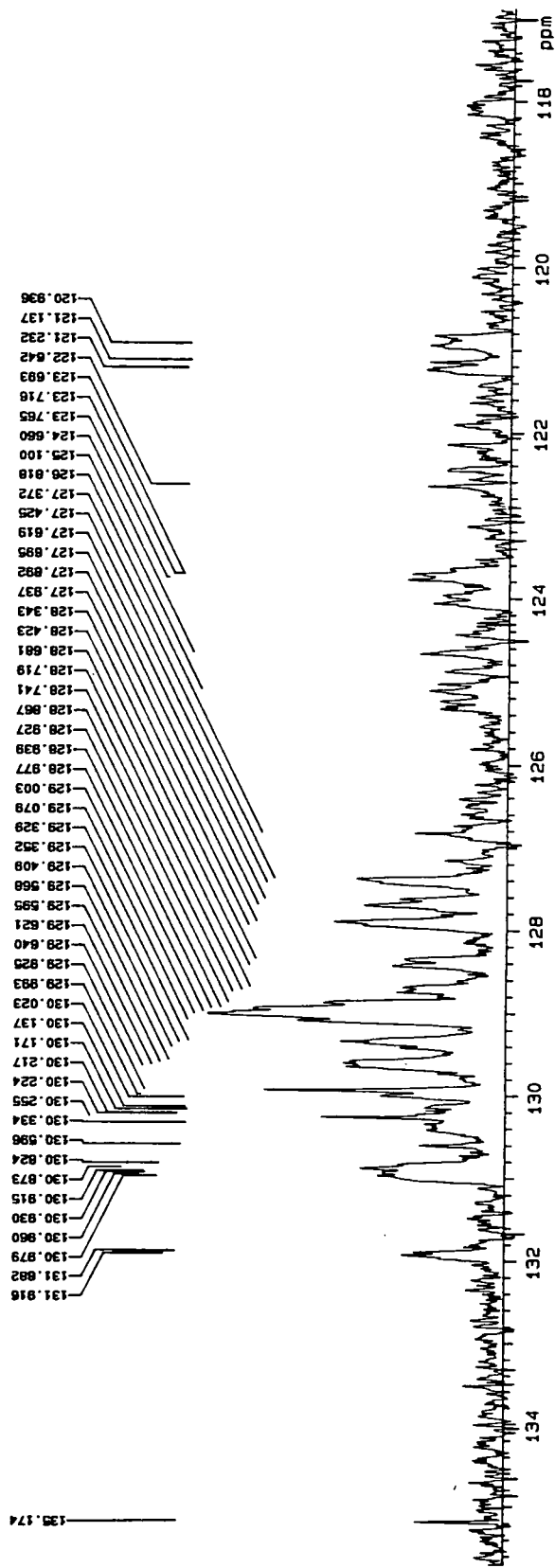


Figure 5.22 The olefinic region of the 100MHz  $^{13}\text{C}$  N.M.R. spectrum  $\{(\text{CD}_3)_2\text{CO}\}$  of poly**IV** initiated by  $\text{Mo}(\text{NAr})(\text{CHCMe}_2\text{Ph})(\text{OCMe}_3)_2$

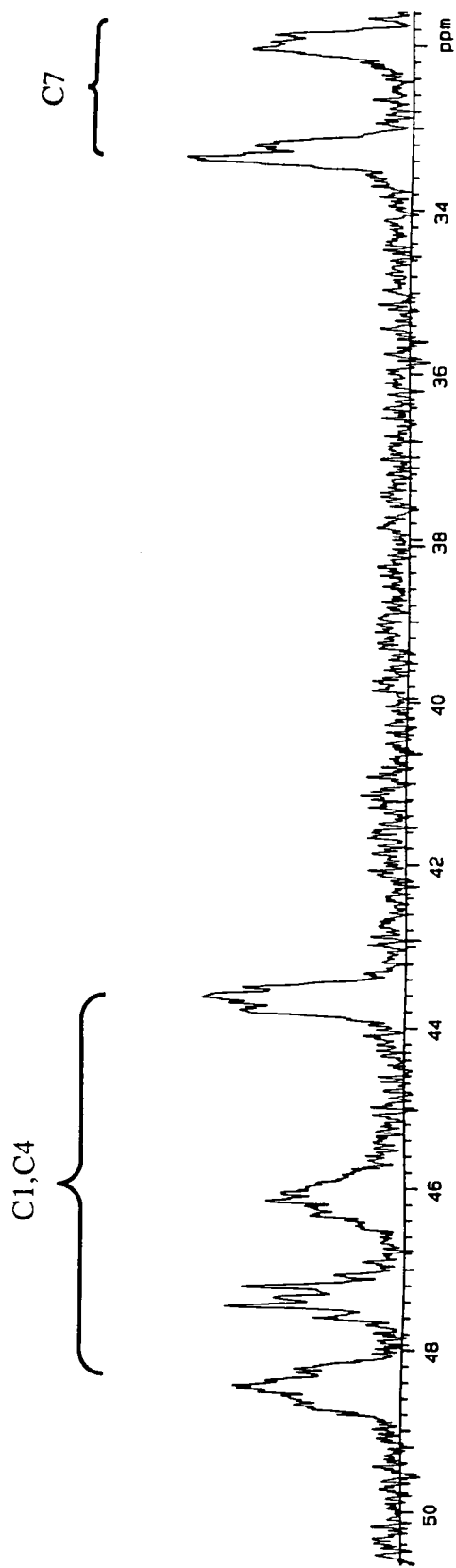


Figure 5.23 The C1,C4 and C7 signals of the 100MHz  $^{13}\text{C}$  N.M.R. spectrum  $\{(\text{CD}_3)_2\text{CO}\}$  of polyIV initiated by  $\text{Mo}(\text{NAr})(\text{CHCMe}_2\text{Ph})(\text{OCMe}_3)_2$  (including preliminary assignments)

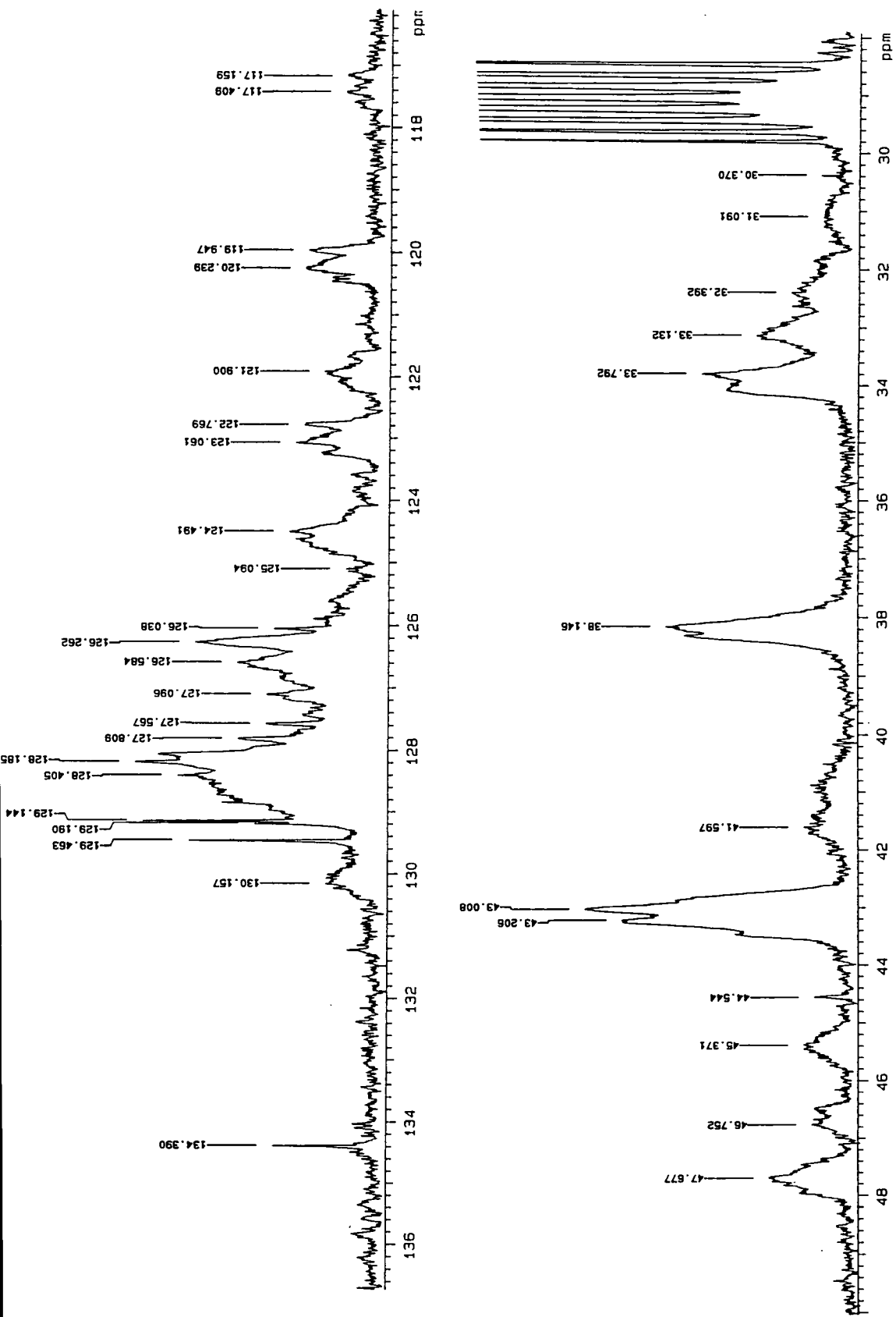


Figure 5.24 The 100MHz  $^{13}\text{C}$  N.M.R. spectrum  $\{(\text{CD}_3)_2\text{CO}\}$  of poly $\text{IV}$  initiated by  $\text{Mo}(\text{NAr})(\text{CHCMe}_2\text{Ph})(\text{OCMe}(\text{CF}_3)_2)_2$

Using the fluorinated tert-butoxide initiator a cis vinylene content of 75% is estimated, somewhat less than anticipated by comparison with **I**. This may be a reflection of the extra deactivation of the double bond in monomer **IV** than that found in **I**. High trans poly**IV** is preparable when the ancillary alkoxides at the active site permit relatively fast syn / anti rotamer interconversion. However, even when the initiator carries (OCMe(CF<sub>3</sub>)<sub>2</sub>) substituents the inherently less reactive nature of monomer **IV** (compared to **D**) may result in significant polymerization via the anti rotamer state (thus reducing the cis stereoselectivity of this polymerization). The reason for the increased deactivation of the unsaturated bond in **IV** is the closer proximity of the fluorine atom substituents. In a molecule of **IV** half of the six fluorine atoms are bonded to a carbon β to the double bond, whereas in **I** all of the fluorine atoms are attached to a carbon atom one more bond removed.

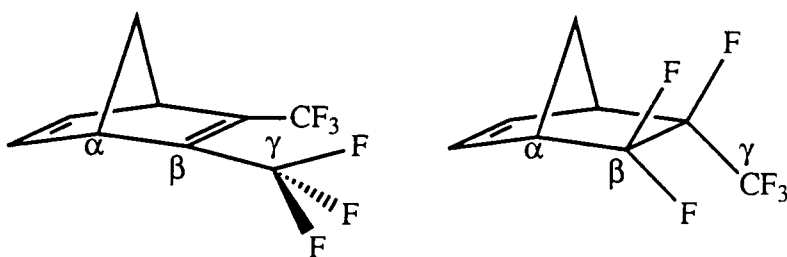


Figure 5.25

### 5.2.6 Gel permeation chromatographic analysis of the fluoropolymers

In general, the fluorinated homopolymers reported in this chapter have molecular weight distributions that approach unity, a feature characteristic of living R.O.M.P.. Table 5.5 reveals that typical values of  $M_w/M_n$  are less than 1.30.

However, the traces obtained in every case are bimodal. For example, when initiated via Mo(NAr)(CHCMe<sub>2</sub>Ph)(OCMe<sub>3</sub>)<sub>2</sub> poly**II** and poly**III** contain a small fraction

(<5%) with a molecular mass twice that of the major component (the same effect is also seen for IV but is even less pronounced).

Monomer	[Mo](OCMe <sub>3</sub> ) <sub>2</sub>		[Mo](OCMe <sub>2</sub> CF <sub>3</sub> ) <sub>2</sub>		[Mo](OCMe(CF <sub>3</sub> ) <sub>2</sub> ) <sub>2</sub>	
	M <sub>w</sub>	PDI	M <sub>w</sub>	PDI	M <sub>w</sub>	PDI
II	2.47 x 10 <sup>4</sup>	1.19	6.39 x 10 <sup>4</sup>	1.26	1.66 x 10 <sup>5</sup>	1.52
III	1.31 x 10 <sup>5</sup>	1.09	8.48 x 10 <sup>4</sup>	1.20	1.48 x 10 <sup>5</sup>	1.16
IV	4.22 x 10 <sup>4</sup>	1.03	-	-	-	-

Table 5.5 GPC data for the ring-opened polymers of II, III, and IV.

$$\left\{ \text{PDI} = \text{polydispersity index} = \frac{M_w}{M_n} \right\}$$

This phenomenon is believed to arise from trace quantities of dioxygen in the reaction mixture which can cap the active carbene site prior to the addition of an aldehydic termination reagent<sup>5</sup>. The resultant polymer possesses a carbonyl end-group which can also cap a further metal centre to yield a dimer (figure 5.26).

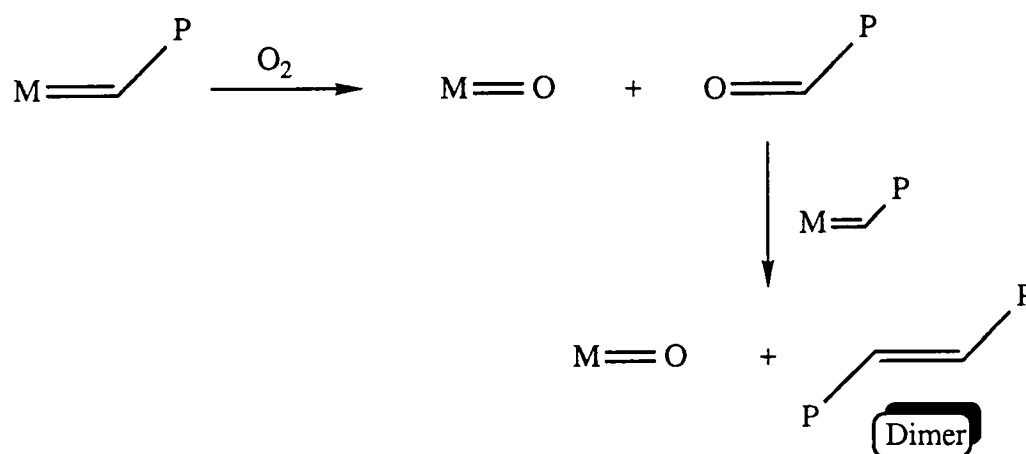


Figure 5.26 The origin of 'polymeric dimer' in living R.O.M.P. systems

With both of the two fluorinated initiators the dimeric fraction represents significantly more than 5% of the total mixture for both polyII and polyIII (figure 5.27). This effect is probably just a reflection of a higher oxygen content, either in the solvents used or in the glove box atmosphere (all four samples were synthesised at the same time). As a result the polydispersity indices (calculated across both peaks) are probably significantly greater than they could be.

Interestingly the samples of polyII prepared seem to be more air-sensitive than any of the other polymers. Consequently, although low polydispersities may be observed if the sample is analysed soon after synthesis, after standing for a few days the molecular weight distributions rise considerably (in one case  $M_w / M_n = 4.27$ ). Whether this is due to cross-linking on contact with air or light has yet to be established.

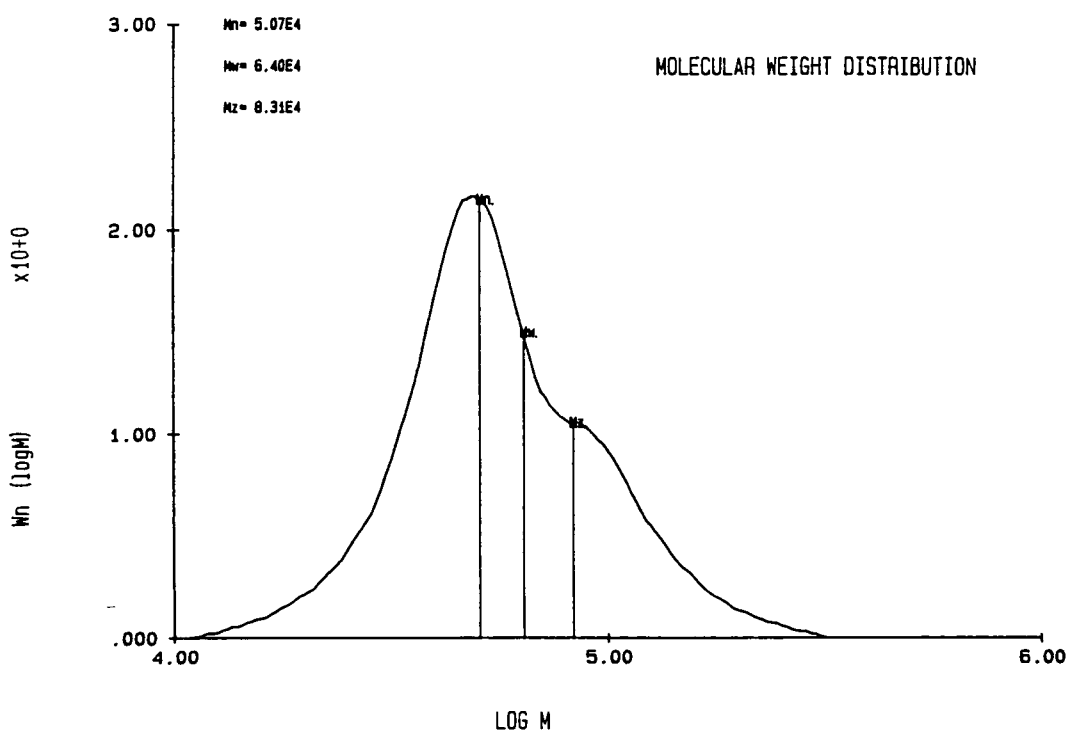


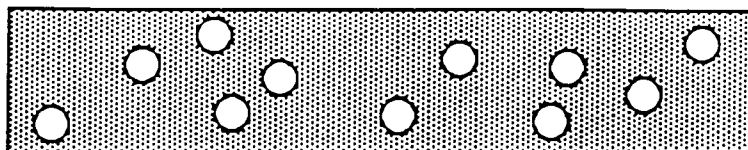
Figure 5.27 Molecular weight distribution plot (determined by gel permeation chromatography) for a sample of polyII initiated by  $\text{Mo}(\text{NAr})(\text{CHCMe}_3)(\text{OCMe}_2\text{CF}_3)_2$  {PDI = 1.26}

### 5.3 The synthesis of fluorinated block copolymers:- a model for PVDF

As well as synthesizing potentially piezoelectric materials, one of the aims of the research carried out towards this thesis was the synthesis of a model for understanding better the mechanisms which lead to the high piezoelectric effect observed in poly(vinylidene fluoride), PVDF. Although much research has been conducted on this subject some areas of confusion still exist.

For example, in the glass transition region of PVDF there is a considerable contribution to the overall piezoelectricity of a poled sample from the amorphous phase. Davies<sup>6</sup> has shown that this piezoelectric response requires an electric field to be produced in the amorphous phase from the polar crystalline region. Further, for such a mechanism to operate the amorphous regions adjacent to the embedded crystalline phases must first be extended. In other words, it appears that the polar crystalline regions can somehow reversibly induce a form of crystallization in the neighbouring amorphous surroundings. The conclusion drawn from such a hypothesis is that in a semi-crystalline sample it may be necessary to consider the physical properties observed in terms of a crystalline phase, an amorphous phase, and also an interfacial region.

One possibility for testing this theory is via the synthesis of fluorinated block copolymers of well-defined structures. By raising the temperature of the sample through the T<sub>g</sub> of the block of lowest T<sub>g</sub> a soft amorphous region would be created containing dispersed phases of the second hard polar block (which would still be below its T<sub>g</sub>). This is represented schematically in figure 5.28.



○ = Hard, polar phase

▒ = Soft, polar phase

Figure 5.28 Schematic representation of a model for the amorphous and crystalline regions of PVDF

PolyI would appear to be a good candidate for the hard, dispersed, polar phase. In order to carry out the dielectric measurements envisaged it became apparent that the amorphous phase would have to be constructed from a polymer of much lower  $T_g$  (approximately  $40^\circ\text{C}$ ). This material would also have to be appreciably polar.

The following section describes the synthesis of several such block copolymers and preliminary dielectric measurements are reported.

### 5.3.1 $^1\text{H}$ NMR study of living fluorinated block copolymers

Table 5.6 lists the materials targeted in this study. Before attempting to synthesize these materials a preliminary investigation was undertaken on an N.M.R. scale.

For example, when 12.9 equivalents of **I** were added to  $\text{Mo}(\text{NAr})(\text{CHCMe}_2\text{Ph})(\text{OCMe}_3)_2$  in benzene- $\text{D}_6$  a doublet at 11.34ppm was observed in the  $^1\text{H}$  NMR spectrum of the mixture, characteristic of the propagating alkylidene of living poly**I**. Upon addition of 21.2 equivalents of **III** the doublet completely disappeared and was replaced by two multiplets at 11.45 and 11.79ppm. These signals correspond to the alkylidene  $\text{H}_\alpha$  of living poly**III**. The broad signals of the poly**I** block are still discernible in the second spectrum as shown in figure 5.29. The extra signals in the lower trace all correlate with proton environments recorded previously in living poly**III**.

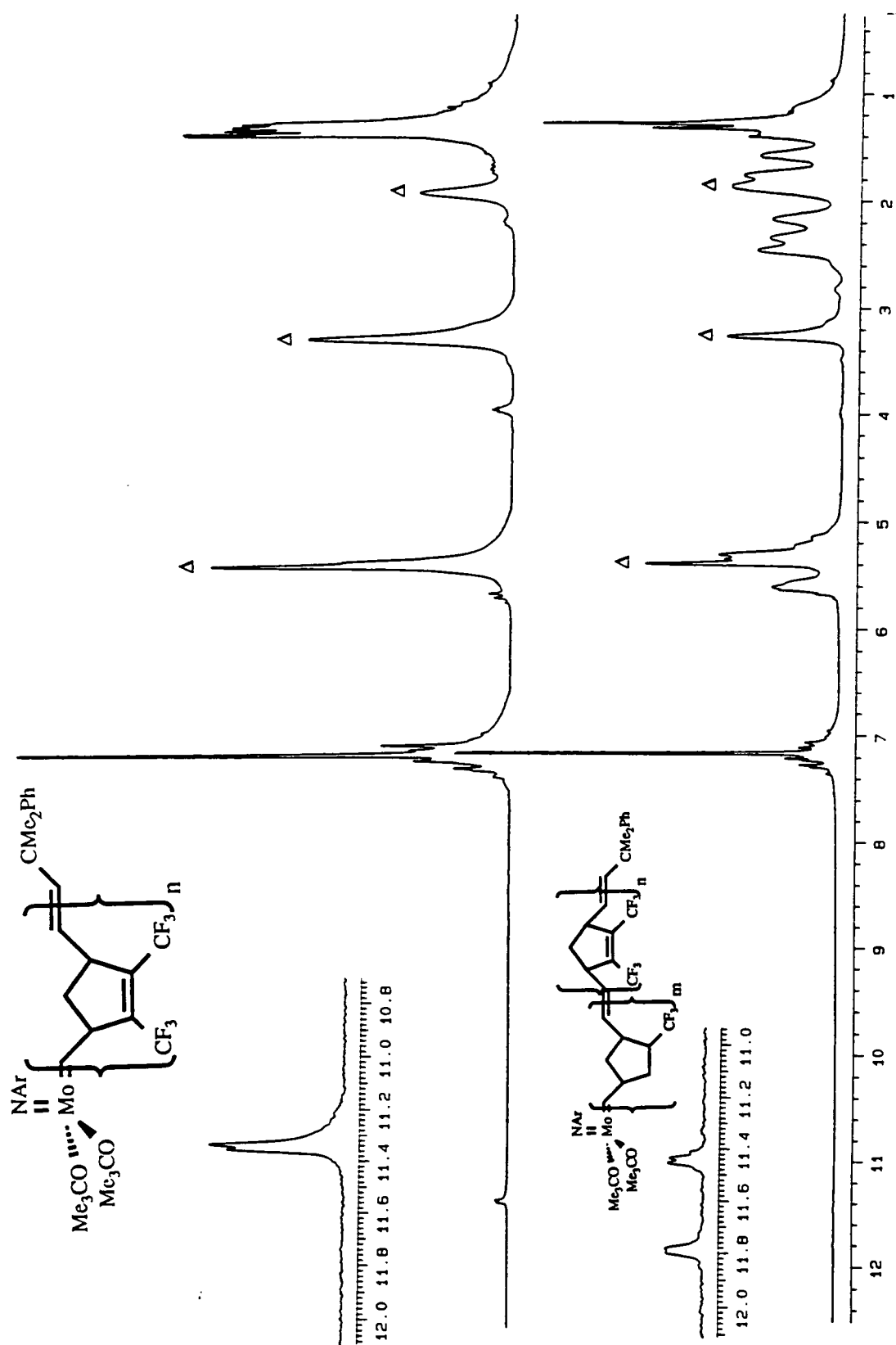


Figure 5.29 The living block copolymerization of monomers **I** and **III** by  $\text{Mo}(\text{NAr})(\text{CHCMe}_2\text{Ph})(\text{OCMe}_3)_2$  in  $\text{C}_6\text{D}_6$

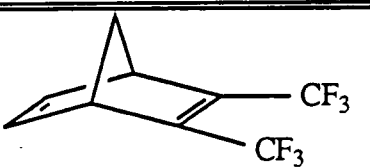
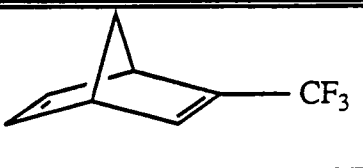
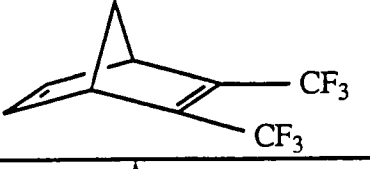
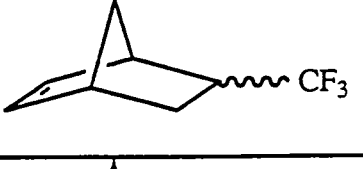
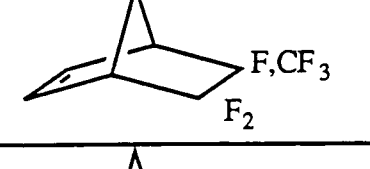
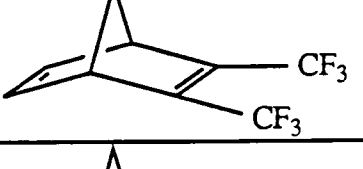
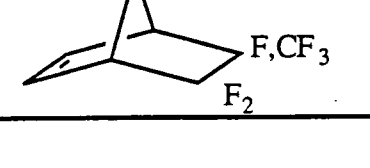
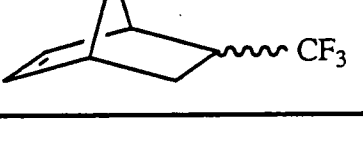
First monomer	Second monomer	Terminology
		Copoly I - II
		Copoly I - III
		Copoly IV - I
		Copoly IV - III

Table 5.6 The fluorinated block-copolymers synthesized as part of this investigation

In each of the four cases highlighted in table 5.7 the addition of 10 - 20 equivalents of the second monomer results in complete consumption of the modified initiator formed from the neophylidene complex and the first monomer.

Copolymer	Alkylidene region after addition of first monomer (ppm)	Alkylidene region after addition of second monomer (ppm)
<b>I - II</b>	11.34 (d)	11.31 (m) 11.64 (m)
<b>I - III</b>	11.34 (d)	11.45 (d) 11.79 (m)
<b>IV - I</b>	11.42 (m) 11.53 (m)	11.34 (d)
<b>IV - III</b>	11.42 (m) 11.53 (m)	11.45 (d) 11.79 (m)

Table 5.7 Alkylidene signals observed via  $^1\text{H}$  NMR during the synthesis of the fluorinated block co-polymers

### 5.3.2 Scaled-up syntheses of the fluorinated block copolymers

In general, the scaled-up (1.0 - 2.0g) block copolymerizations are more temperamental than the homopolymerizations discussed earlier in this chapter. This is believed to be a consequence of the longer reaction times (typically each monomer addition was followed by 24 hours stirring in order to ensure high conversion) leading to slow decomposition of the active site.

Block copolymers **I - III**, **IV - I**, and **IV - III** were all prepared in a solvent mixture of 85% toluene : 15 % tetrahydrofuran. Curiously, several attempts to synthesize block copolymer **I - III** in neat tetrahydrofuran all resulted in the isolation of the homopolymer of **I**.

Block copolymer **I - II** has only been prepared successfully from  $\alpha,\alpha,\alpha$ -trifluorotoluene allowing for just 4 hours stirring after each monomer pulse.

## 5.4 Structural characterisation of the fluorinated block copolymers

Characterization of block copolymers, although an area of increasingly active research, is still not as highly developed as that of homopolymers. Only a select few, notably the styrene-diene systems, have been subjected to an exhaustive structural study.

For the samples prepared in this study characterization has been achieved using  $^{13}\text{C}$ ,  $^{19}\text{F}$ , and  $^1\text{H}$  nuclear magnetic resonance spectroscopy, differential scanning calorimetry, and gel permeation chromatography. Preliminary dielectric measurements are also reported.

### 5.4.1 $^{13}\text{C}$ N.M.R. spectroscopic analysis of the block copolymers

One method of determining whether or not a copolymer system possesses a block structure, a random arrangement of repeat units, or is a completely alternating sequence of monomer groups is N.M.R. spectroscopy. In a block co-polymer, if the length of the blocks are long enough so as to discount signals from the interchange units, then the spectrum of the block material should be the simple sum of the two component homopolymer spectra.

### 5.4.2 $^{13}\text{C}$ N.M.R. analysis of the copolymer of I and III

The  $^{13}\text{C}$  N.M.R. spectrum of the ring-opened homopolymer of **III** initiated by  $\text{Mo}(\text{NAr})(\text{CHCMe}_2\text{Ph})(\text{OCMe}_3)_2$  has already been discussed. It is quite complex and many of the minor signals have still to be assigned unambiguously. However, as explained above the spectrum of a block co-polymer should have an additive basis. Therefore the characteristic 'N.M.R. fingerprint' of the block of poly**III** can be used to confirm its presence in the copolymer.

Figure 5.30 shows the acetone- $d_6$   $^{13}\text{C}$  NMR spectrum for a sample of copolyI-III prepared using the bis(butoxide) neophylidene initiator. Although the spectrum suffers from a low signal-to-noise ratio the resonances due to the block of polyI are readily discernible ( $\text{I}_{\text{C}5,6}$  at 139.71;  $\text{I}_{\text{C}2,3}$  trans at 133.43;  $\text{I}_{\text{C}2,3}$  cis at c.132.0;  $\text{I}_{\text{C}8}$  at c.126.1, 123.34, 120.61, and c.118.0ppm).

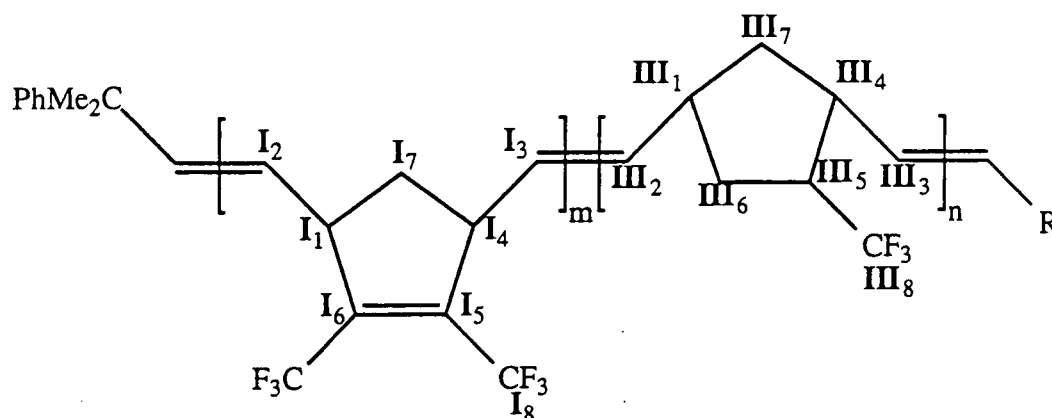


Figure 5.28 The labelling used in the discussion of the  $^{13}\text{C}$  NMR spectrum of polyI - III

The remaining signals correspond to those due to poly III. A similar picture is found upfield in the  $\text{sp}^3$  carbon region; full assignments of both sections are detailed in table 5.8.

Not all of the predicted resonances have been located due to their low intensity and the overlapping of certain signals. For example, the signal due to  $\text{I}_{\text{C}1,4}$  cis which would be expected to occur at 44.6ppm is difficult to find. Nonetheless the general appearance of the spectrum indicates that the block of polyI is ca.98% trans, whilst the second component is estimated to be at least 90% trans (cis signals for this block are certainly more evident than for the block of polyI).

This is of course exactly what would be expected, given that the cis / trans geometry of the living polymer blocks is metal-centre controlled; i.e. it is the nature of the alkoxides that determine the syn / anti rotamer interconversion rate. However, if tacticity

\* = resonance arising from a block of polyI

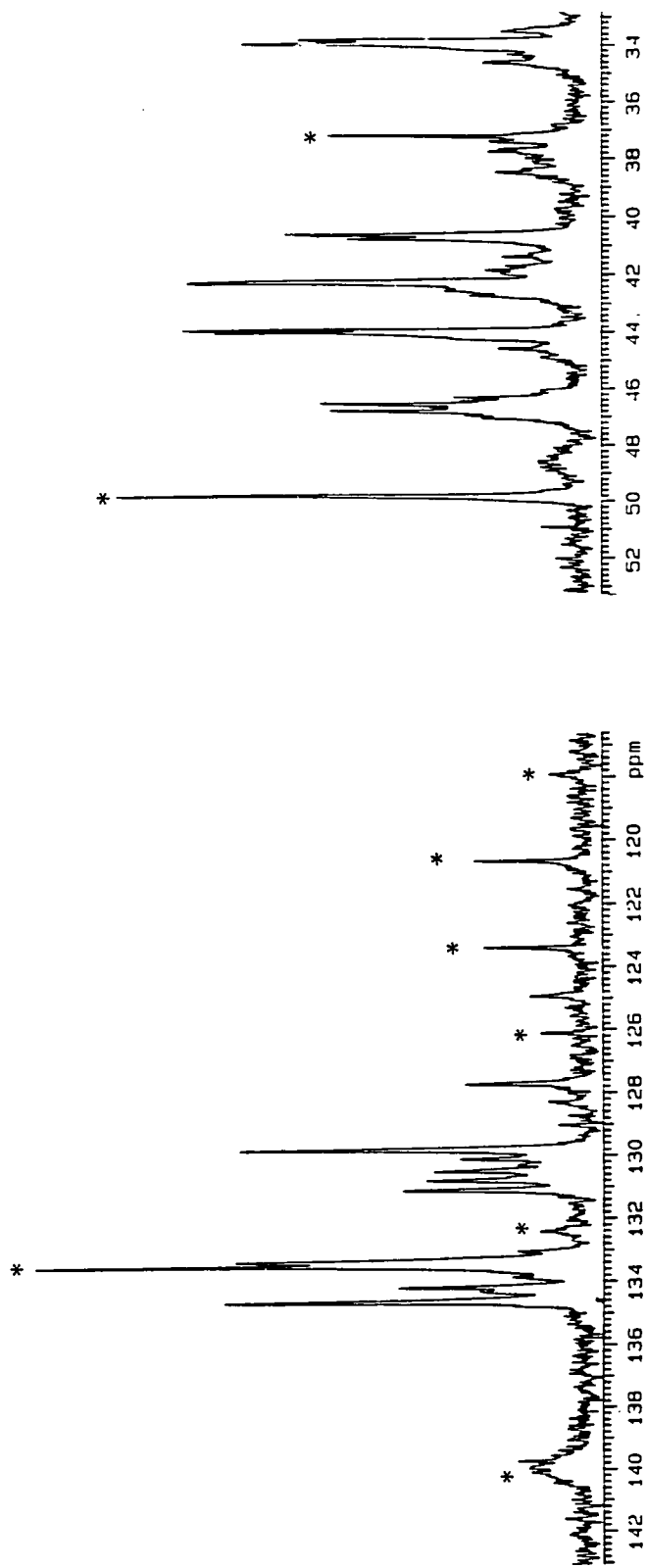


Figure 5.30 The 100MHz  $^{13}\text{C}$  N.M.R. spectrum  $\{(\text{CD}_3)_2\text{CO}\}$  of block copoly I - III

is influenced by interactions between incoming monomer units and the last inserted unit.

then the interchange junction may well comprise a short run of tapered tacticity.

Block CopolyI-III resonance observed in acetone-d <sub>6</sub> at 100.577MHz (ppm)	Assignment	Corresponding resonance for the isolated homopolymer of I or III
33.95, 33.81	III C6	33.92, 33.77
37.17	I C7 tt rr	37.12
40.75, 40.60	III C7	40.72, 40.59
42.26	III C4 trans	42.24
44.01, 43.90	III C1 trans	43.97, 43.87
46.76, 46.52, 46.26	III C5 trans	46.66, 46.41, 46.16
49.74	I C1,4 trans	49.76
126.1, 123.34, 120.62, 118.0	I C8	126.05, 123.33, 120.61, 117.89
133.10, 130.46, 127.69, 124.91	III C8	132.36, 130.44, 127.66, 124.95
129.74	III C3 trans HT	129.72
130.06	III unassigned	130.04
131.05, 130.74	III C3 trans HH	130.71, 131.02
132.0	I C2,3 cis	132.02
132.39	III C2 cis TH	132.36
133.29	III C2 trans TH	133.26
133.43	I C2,3 trans	133.40
134.14	III C2 cis TT	134.09
134.58	III C2 trans TT	134.54
139.90	I C5,6	139.88

Table 5.8 <sup>13</sup>C N.M.R. assignments for block copolymer I - III

### 5.4.3 $^{13}\text{C}$ and $^{19}\text{F}$ N.M.R. analysis of block copolymers I-II, IV-I and IV-III

As for the block copolymer of monomer **I** and **III**, the other three block copolymers also give  $^{13}\text{C}$  and  $^{19}\text{F}$  N.M.R. spectra corresponding to the sum of the spectra of their two component homopolymers. The spectra obtained therefore offer little in the way of extra information from that already gleaned from studying the homopolymers traces, but nonetheless confirm that the materials are di-block copolymers.

The broadening of certain  $^{13}\text{C}$  resonances does tend to mask the true proportions of the compounds. For example, figure 5.31 shows a section of the spectrum of a sample of copoly**I-II**. At first glance the narrow resonances of the high trans block of poly**I** are clearly recognisable; however, the signals associated with the block of poly**II** are much broader because of the asymmetric nature of the repeat unit substituents. Nonetheless, quantitative  $^{13}\text{C}$  N.M.R. confirms that the proportion of **I** to **II** in the sample analysed is 2.62 : 1.00.

$^{19}\text{F}$  N.M.R. studies on the same polymer provide a simpler picture; the chemical shifts of the fluorine substituents in the two blocks are well separated and the signals are quite clear (figure 5.32). Furthermore, they can be integrated to reveal a ratio of 2.55 : 1.00 **I** : **II**, in good agreement with the figure obtained above.

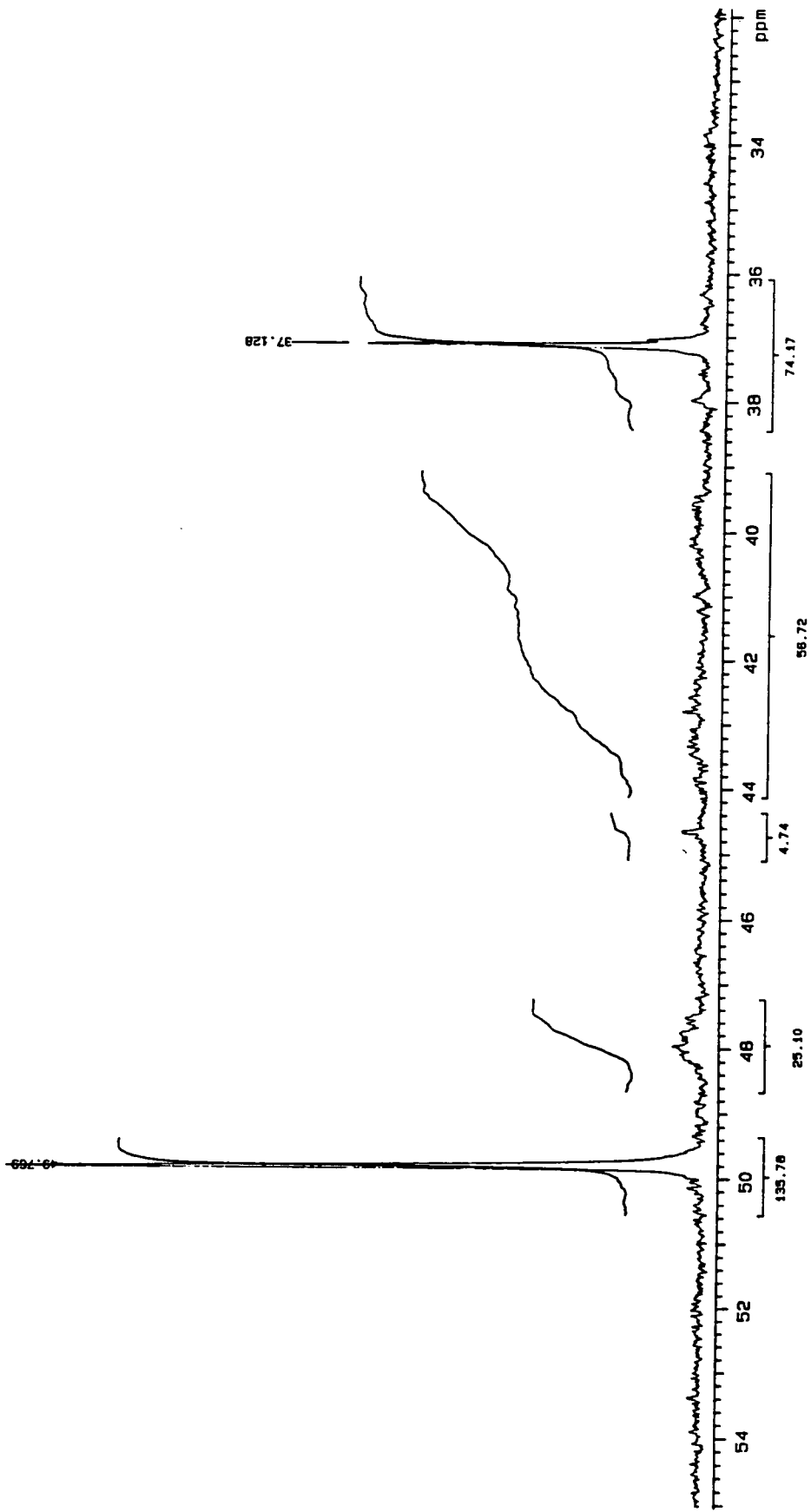


Figure 5.31 The C1, C4 and C7 region from the 100MHz  $^{13}\text{C}$  N.M.R. spectrum of block copoly I - II

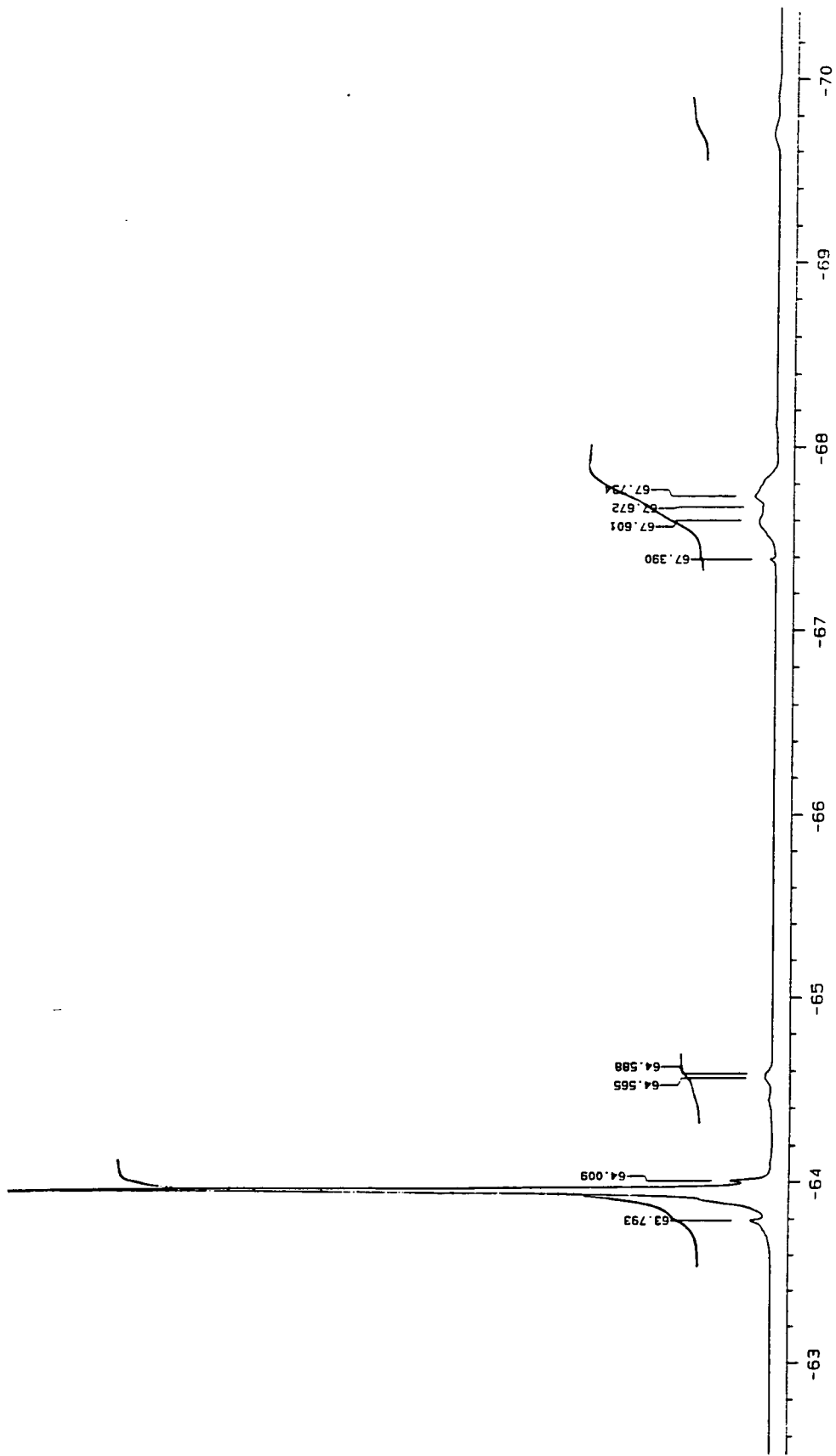


Figure 5.32 The  $^{19}\text{F}$  N.M.R. spectrum  $(\text{CD}_3)_2\text{CO}$  of block copoly I - II

#### 5.4.4 Differential Scanning Calorimetric analysis

One of the reasons for the interest in block copolymer systems is their ability to exhibit unique properties as a result of the general thermodynamic incompatibility of the blocks ('microphase separation'). Consequently several sophisticated techniques have been employed to investigate morphological structures, such as small-angle X-ray scattering (SAXS), small-angle light scattering (SALS) and wide-angle X-ray diffraction (WAXD).

However, D.S.C. also provides useful data for inferring the degree of the phase separations, as well as revealing the compositional dependence of thermal transitions. D.S.C. is also used to distinguish between genuine block systems and other polymer hybrids (blends and random copolymers).

Two-phase systems generally display two separate and distinct T<sub>g</sub>s, characteristic of the components. In contrast, homogenous random copolymers display a single T<sub>g</sub> which is a compositionally-weighted average of the T<sub>g</sub> values of the corresponding homopolymers. An exception to this rule is a block copolymer in which the segments are mutually compatible (e.g. styrene -  $\alpha$ -methyl styrene). Furthermore, while crystallinity is possible in block or graft copolymers (due to long sequences), the disruption encountered in chain regularity in a random copolymer reduces the probability of crystalline domains dramatically.

Therefore in order to confirm that the materials synthesized in this study possess genuine block structures it is first necessary to record the transitions observed for the homopolymers when initiated by Mo(NAr)(CHCMe<sub>2</sub>Ph)(OCMe<sub>3</sub>)<sub>2</sub>.

Monomer	T <sub>g</sub> / °C	T <sub>m</sub> / °C
I	96	191
II	70	-
III	73	-
IV	105	217

Table 5.9 T<sub>g</sub> and T<sub>m</sub> values recorded for the ring-opened fluoropolymers



Glass transition temperatures and melting points for the homopolymers are shown in table 5.9. Endotherms corresponding to the melting process are only seen for polyI and polyIV. However, all the transitions have been found to be relatively weak and hence difficult to detect using D.S.C. (thus leading to some ambiguity in the figures reported in both table 5.9 and table 5.10).

Nonetheless, D.S.C. does reveal two glass transitions for the block copolymer of I and III, as shown in figure 5.34. A T.S.C. measurement at the University of Leeds upon the same sample of polyI - III confirms the presence of two T<sub>g</sub> temperatures which are well-defined and provide clear evidence that the two components are not compatible (figure 5.33). Interestingly, even though only one component is known to crystallise as a homopolymer, two melting point endotherms are also observed in the D.S.C. An explanation for this is that block of polyIII can crystallize, but requires some other crystalline regions to be present (polyI) in order for crystallization to be induced.

The transitions (and assignments) observed for all four block co-polymers are tabulated below. In general the D.S.C. traces recorded do show two glass transition temperatures, which correspond to the T<sub>g</sub>s of the two homopolymer components.

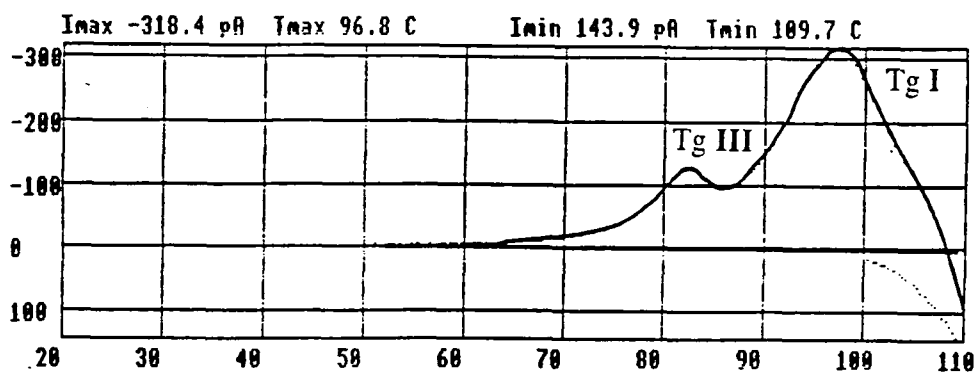


Figure 5.33 A T.S.C. trace of a sample of copolyI - III

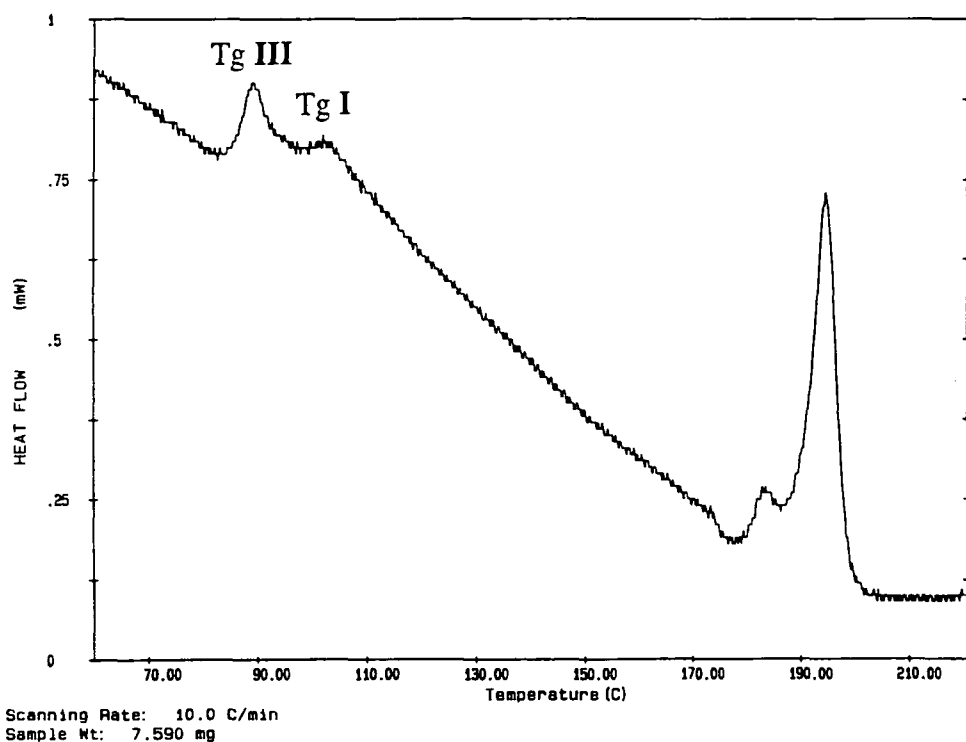


Figure 5.34 A D.S.C. trace of a sample of copolyI - III

Copolymer	Transitions observed / °C	Assignment
I - II	Needs rerunning	
I - III	80	Tg phase III
	96	Tg phase I
	183	Tm phase III
	194	Tm phase I
IV - I	84	-
	87	Tg phase I
	100	Tm phase I
	190	-
IV - III	79	-
	83	-

Table 5.10 D.S.C. transitions observed for the block-copolymers

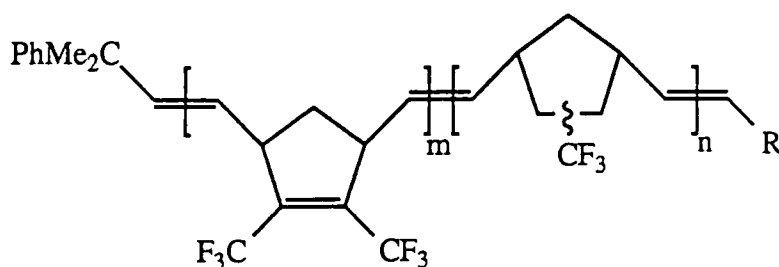
#### 5.4.5 Dielectric measurements

As mentioned in the immediately preceding section T.S.C. measurements have been carried out upon one of the block copolymers synthesised as part of this study, copoly I - III. Dielectric measurements have also been recorded for a sample of poly III initiated by  $\text{Mo}(\text{NAr})(\text{CHCMe}_2\text{Ph})(\text{OCMe}_3)_2$ , which has been shown to be approximately 80% trans earlier in this chapter.

The T.S.C. trace for the ring-opened homopolymer of III shows a Tg at 79°C (compared to 73°C when measured by D.S.C.). Dielectric measurements reveal a very low  $\epsilon_R$  value of 5.9. A slightly higher figure (6.1) is reached when measured via pyroelectric studies.

The block copolymer sample analysed in this study had the constitution outlined in figure 5.35. The two glass transition temperatures mentioned previously (at 82.0 and

96.8°C) confirm the block-like nature of its architecture, and  $^{13}\text{C}$  has already been used to show that the two blocks are both highly trans, and that the block of polyI was 92% syndiotactic.



Mass block polyI  $\approx$  80,000  
 Mass block polyIII  $\approx$  40,000

Polydispersity = 1.08

Figure 5.35

The dielectric constant for the block of **III** is again very low (dielectric measurements imply a value for  $\epsilon_R$  of 5.5, whilst pyroelectric studies give 4.5). However, the trans syndiotactic block of polyI has a  $\epsilon_R$  value of just 11.5 (by dielectric measurements; 11.9 via T.S.C. / pyroelectric measurements).

For some reason the incompatible nature of this block copolymer appears to have resulted in a dramatic decrease in the alignment of dipoles in the phase containing polyI. Further work is currently underway to try to explain this observation, which could have interesting implications for the PVDF model study.

#### 5.4.6 Gel Permeation Chromatographic analysis

The interpretation of molecular weight determination experiments on block copolymers are notoriously difficult. Usual light-scattering techniques are inaccurate

since, in general, the two units will differ in refractive index increment. Similarly in a block system intrinsic viscosities are not necessarily proportional to molecular weight.

G.P.C. is no exception; frequently the column medium will solubilize one component preferentially and the copolymer may then aggregate irreversibly to form micelles (swollen cores of insoluble blocks surrounded by a flexible fringe of soluble component). However, G.P.C. can be used to reveal the presence of more than one macromolecular population (if they differ sufficiently in molecular size). In other words, G.P.C. can not be used to provide accurate molecular weight measurements, but is still useful for the detection of impurities. A block-copolymer should display just one peak, and no material corresponding to either homopolymer should be detectable.

Despite this argument the GPC traces obtained for tetrahydrofuran solutions of block copolymers I - III, IV - I, and IV - III are all bimodal (e.g. figure 5.36). Nonetheless, this observation has still been rationalised as arising from genuine block structures. In each case, the major peak appears quite narrow (polydispersity calculations across both peaks are reported below), with a small shoulder towards high molecular weight. Although no curve-fitting analysis has been applied the peak of the shoulder and of the major peak have been converted into molecular weight values and are tabulated below.

The obvious trend is that the smaller peak corresponds to material with twice the molecular weight of the main fraction. Reference has already been made to a proposed binuclear termination step as a result of trace amounts of dioxygen in the monomer feed(s). In the examples described above the product of such a decomposition mechanism possesses an A-B-A triblock architecture, the origin of which is shown schematically in figure 5.37.

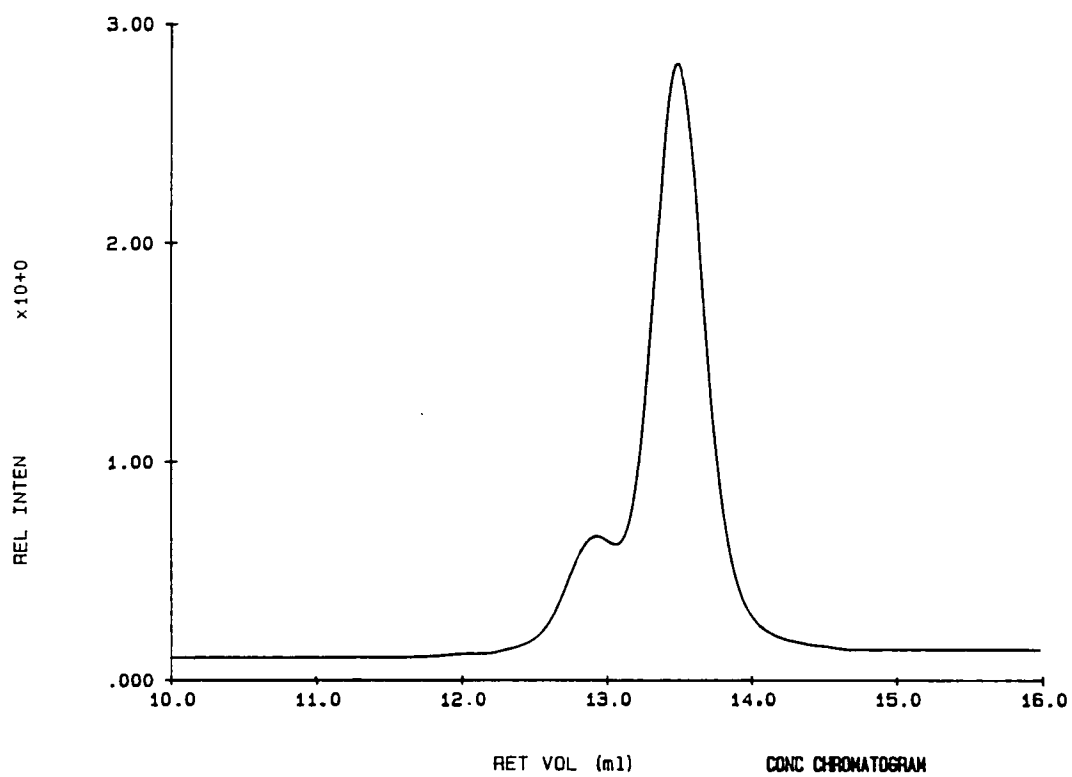


Figure 5.36 Gel permeation chromatogram of a sample of block copolyIV - III

Copolymer	Polydispersity	Molecular weight of the major peak	Molecular weight of the shoulder
I - III	1.08	120,200	229,000
IV - I	1.07	125,900	240,000
IV - III	1.08	69,200	125,900

Table 5.11 The bimodal nature of the G.P.C. traces obtained on the fluorinated block copolymers (polydispersity =  $M_n / M_w$  ; measured across both the major peak and the shoulder)

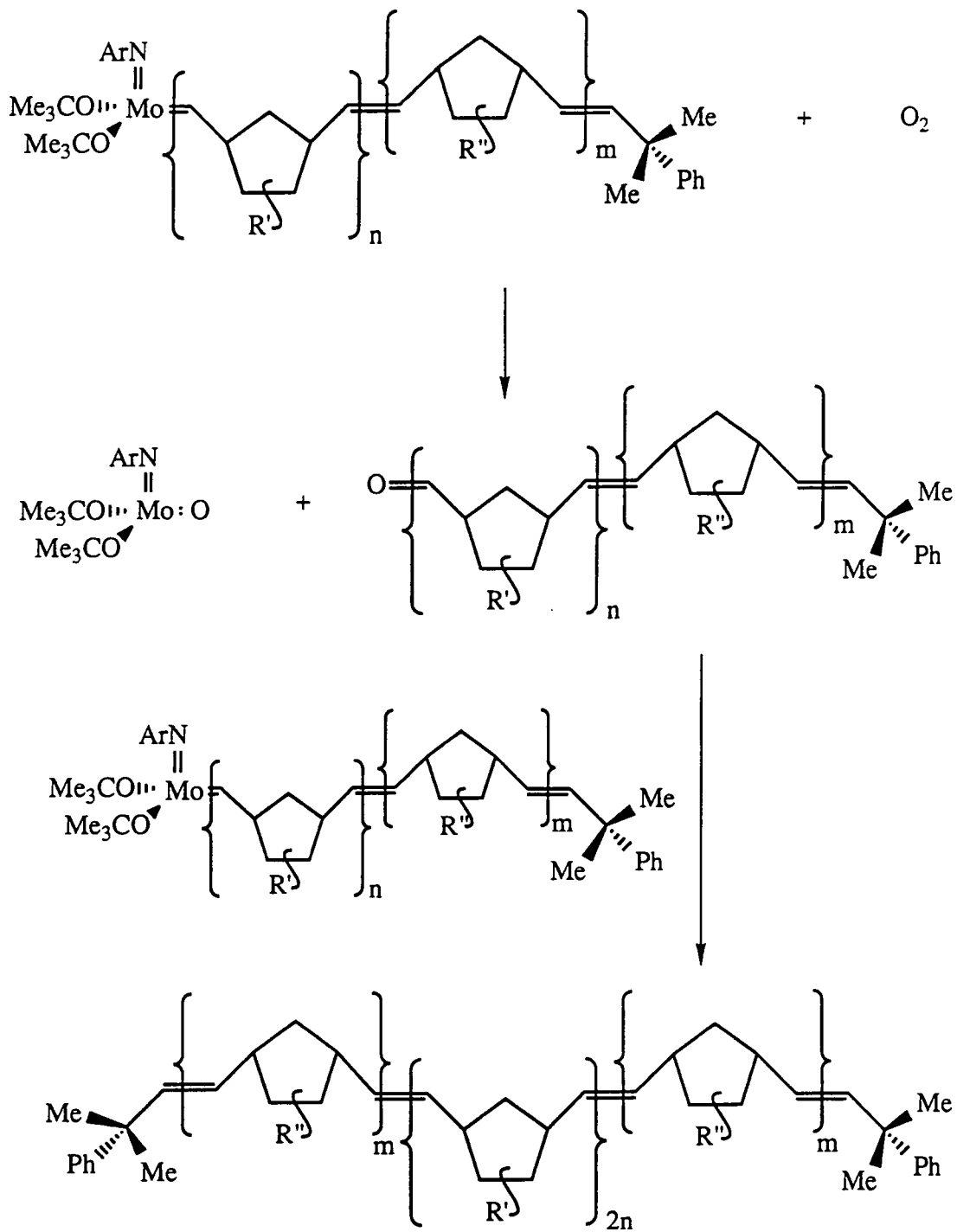


Figure 5.37 Bimolecular termination in living R.O.M.P.

## 5.5 Summary

This chapter has described the synthesis of several fluorinated homopolymers via living R.O.M.P., and several have been shown to be highly stereoregular. Di-block copolymers of these materials contain the same highly stereoregular architectures and this should have a major influence over their physical properties.

Attempts to characterize the block copolymers have been largely successful. However, a more detailed study may be required in order to understand certain observations, such as the dielectric measurements reported on co-polyI - III.

The use of these systems for investigating the origin of induced crystallization of the amorphous phases immediately neighbouring crystalline domains in poly(vinylidene fluoride) samples has not yet been made. Indeed, one of the requirements of such a model is that the  $T_g$  of the two blocks should be well separated, and this has not yet proved possible. Recent studies by Dr. B. Wilson and Miss L.M. Hamilton have shown that replacing the fluorine and trifluoromethyl substituents with long-chain fluorinated alkyl groups leads to a dramatic drop in glass transition temperature. However, even this material may not prove ideal as the desired soft phase; the presence of the long-chain substituent might hinder polymer chain alignment in areas neighbouring the hard phase domains.

## 5.6 References

1. P. M. Blackmore, W.J. Feast, P.C. Taylor *Brit.Pol.J.* **19** 205 (1987)
2. P.M. Blackmore, W.J. Feast *Polymer* **27** 1296 (1986)
3. G.R. Davies, H.V.St.A. Hubbard, I.M. Ward *Work in progress*
4. A.E. Derome, 'Modern N.M.R. Techniques for Chemistry Research', Pergamon Press, Oxford (1987)
5. W.J. Feast, V.C. Gibson, E. Khosravi, E.L. Marshall, J.P. Mitchell *Polymer* **30** 872 (1992)
6. G.R. Davies in 'Physics of Dielectric Solids', Conference Series Number 58 (The Institute of Physics, Bristol) (1987) pp50 - 63

## **Chapter Six**

### **Experimental Details**

## 6.1 General

### 6.1.1 Experimental Techniques

All manipulations of air and / or moisture sensitive materials were performed on a conventional vacuum / inert atmosphere (nitrogen or argon) line using standard Schlenk and cannular techniques, or in an inert atmosphere filled glove box.

Elemental analyses were performed by the micro-analytical services of this department.

Infrared spectra were recorded on Perkin-Elmer 577 and 457 grating spectrophotometers using either KBr or CsI windows. Absorptions are abbreviated in the text as follows: vs (very strong), s (strong), m (medium), w (weak), br (broad), sp (sharp), sh (shoulder).

Mass spectra were recorded on a VG 7070E Mass Spectrometer.

NMR spectra were recorded on the following instruments at the frequencies listed: Bruker AMX 500,  $^1\text{H}$  (500.140MHz),  $^{13}\text{C}$  (125.760MHz),  $^{19}\text{F}$  (470.599MHz); Varian VXR400,  $^1\text{H}$  (399.95 MHz),  $^{13}\text{C}$  (100.58 MHz),  $^{19}\text{F}$  (376.29 MHz); Bruker AC250,  $^1\text{H}$  (250.13 MHz),  $^{19}\text{F}$  (235.36 MHz); Varian Gemini 200,  $^1\text{H}$  (199.98 MHz),  $^{13}\text{C}$  (50.29 MHz). The following abbreviations have been used for band multiplicities and shapes: s (singlet), d(doublet), t (triplet), q (quartet), sept (septet), m (multiplet), br (broad). Chemical shifts are quoted as  $\delta$  in ppm downfield from the following references:  $^1\text{H}$  ( $\text{C}_6\text{D}_6$ , 7.15ppm;  $(\text{CD}_3)_2\text{CO}$ , 2.20ppm;  $\text{C}_4\text{D}_8\text{O}$ , 1.7 and 3.8ppm;  $\text{CD}_2\text{Cl}_2$ , 5.35ppm);  $^{13}\text{C}$  ( $\text{C}_6\text{D}_6$ , 128.0ppm;  $(\text{CD}_3)_2\text{CO}$ , 29.8ppm;  $\text{CDCl}_3$ , 77.7ppm);  $^{19}\text{F}$  (all shifts referenced to either internal or external  $\text{CFCl}_3$ ).

GPC traces were recorded on a Viscotek differential refractometer fitted with a Knauer HPLC pump 64 and two PLgel  $10\mu$  mixed columns (tetrahydrofuran solvent, flow rate  $1\text{ cm}^3\text{ min}^{-1}$ ). Samples (0.1 - 0.3% w/v) were filtered through a Millex SR  $0.5\mu\text{m}$  filter before injection to remove particulates. The columns were calibrated using commercially available polystyrene standards (Polymer Laboratories Ltd.) ranging from 1206 to  $1.03 \times 10^6$  MW.

Differential Scanning Calorimetry analyses were carried out on a Perkin Elmer Series 7, calibrated against metallic zinc and indium (melting points = 156.2°C and 419.5°C respectively).

### 6.1.2 Solvents and Reagents

The following NMR solvents were dried by storing over a suitable drying agent (in parenthesis) and vacuum distilled immediately prior to use: benzene-d<sub>6</sub> (phosphorus (V) oxide), methylene chloride-d<sub>2</sub> (calcium hydride), tetrahydrofuran-d<sub>8</sub> (potassium benzophenone ketyl), chloroform-d<sub>1</sub> (phosphorus (V) oxide), and toluene-d<sub>8</sub> (phosphorus (V) pentoxide). Acetone-d<sub>6</sub> was used as received.

The following solvents were dried by prolonged reflux over a suitable drying agent, and distilled and deoxygenated immediately prior to use (drying agent in parenthesis); toluene (sodium metal), pentane (lithium aluminium hydride), tetrahydrofuran (sodium benzophenone ketyl), dichloromethane (calcium hydride), diethyl ether (lithium aluminium hydride),  $\alpha,\alpha,\alpha$ -trifluorotoluene (calcium hydride), dimethoxy ethylene glycol (potassium metal) and heptane (lithium aluminium hydride). All polymerization solvents, with the exception of tetrahydrofuran, were also passed through a column of activated alumina prior to use.

The following chemicals were prepared by previously published procedures:

Mo(N-2,6-*i*-Pr<sub>2</sub>-C<sub>6</sub>H<sub>3</sub>)(CHCMe<sub>2</sub>Ph)(OCMe<sub>3</sub>)<sub>2</sub><sup>1</sup>, Mo(N-2,6-*i*-Pr<sub>2</sub>-C<sub>6</sub>H<sub>3</sub>)(CHCMe<sub>2</sub>Ph)(OCMe(CF<sub>3</sub>)<sub>2</sub>)<sub>2</sub><sup>1</sup>, LiOCMe<sub>3</sub><sup>2</sup>, LiOCMe(CF<sub>3</sub>)<sub>2</sub><sup>3</sup>, 2,3-bistrifluoromethylbicyclo[2.2.1]hepta-2,5-diene<sup>4</sup> and 2-trifluoromethylbicyclo[2.2.1]hepta-2,5-diene<sup>5</sup>. 5-Trifluoromethylbicyclo[2.2.1]hept-2-ene<sup>6</sup> and 5,5,6-trifluoro-6-trifluoromethylbicyclo[2.2.1]hept-2-ene<sup>7</sup> were synthesised by Dr. Ezat Khosravi in Durham.

The following chemicals were obtained commercially and used as received unless stated otherwise:

Molybdenum (IV) oxide (Fluorchem); chlorine (BOC) bubbled through concentrated sulphuric acid; anhydrous sodium molybdate (Aldrich); 2,6-di-isopropylaniline (Aldrich) distilled repeatedly until colourless; triethylamine (Aldrich),

distilled; chlorotrimethylsilane (Aldrich) distilled; 2,6-lutidine (Aldrich), distilled; 1-chloro-2-methyl-2-phenylpropane ('neophyl chloride', Aldrich), washed with concentrated sulphuric acid, dried over anhydrous magnesium sulphate and distilled onto 4A molecular sieves; trifluoromethylsulphonic acid (Aldrich); n-butyl lithium (Aldrich); 2-methylpropan-2-ol (Aldrich), distilled; hexafluoro-2-methylpropan-2-ol (Fluorochem), distilled; dicyclopentadiene (Aldrich); tungsten (VI) chloride (Aldrich); hexafluoro-2-butyne (Fluorochem); trifluoropropyne (Fluorochem); 1,1,2-trichloro-3,3,3-trifluoro-propene (Fluorochem) distilled; zinc dust (Aldrich); N,N-dimethylacetamide (Aldrich) distilled; alumina (Aldrich), activated *in vacuo* in a furnace; maleic anhydride (Aldrich); hydroquinone (Aldrich); benzaldehyde (Aldrich) distilled; (+)-camphor (Fluka), recrystallised from toluene; (-)-menthol (Fluka), recrystallised from toluene; 1-adamantanol (Aldrich); 3,5-di-tert-butylcatechol (Aldrich); racemic-1,1'-bi-2-naphthol (Aldrich), sublimed (room temperature  $10^{-3}$ mmHg); (R)- and (S)- 1,1'-bi-2-naphthol (Aldrich); (S)-endo-borneol (Aldrich), recrystallised from toluene; (S)-(-)- $\alpha$ -methylbenzylamine (Aldrich), distilled onto 4A molecular sieves and passed through a column of activated alumina immediately prior to use; tert-butylamine (Aldrich) distilled; pyridine (Aldrich) distilled; trimethylaluminium (Aldrich) distilled.

## 6.2 Experimental details to chapter two

### 6.2.1 Investigations into the effect of reaction conditions upon the trans content of poly[1,4-(2,3-bis(trifluoromethyl)cyclopentenylene) vinylene]

The reaction conditions employed in this series of experiments varied according to the reaction parameters under investigation. The following account outlines a general procedure for the ring-opening metathesis polymerization of 2,3-bis(trifluoromethyl)bicyclo[2.2.1]hepta-2,5-diene by  $\text{Mo}(\text{NAr})(\text{CHCMe}_2\text{Ph})(\text{OCMe}_3)_2$ .

Typically 1.00g 2,3-bis(trifluoromethyl)bicyclo[2.2.1]hepta-2,5-diene (4.38mmol) was dissolved in  $5.0\text{cm}^3$  solvent and then added dropwise over 5 minutes to a  $5.0\text{cm}^3$  rapidly stirring solution of  $\text{Mo}(\text{NAr})(\text{CHCMe}_2\text{Ph})(\text{OCMe}_3)_2$  (0.0100g,  $1.82 \times 10^{-2}$ mmol). Almost instantaneously upon the addition of the monomer the reaction mixture deepened to a cherry-red colour which returned to the original orange colour of the initiator within 10-15 minutes.

The reaction was allowed to stir for 16-24 hours (monomer conversion was monitored via  $^{19}\text{F}$  N.M.R. spectroscopy) before the polymerization was terminated by the addition of a large excess of benzaldehyde ( $50\mu\text{l}$ ,  $4.91 \times 10^{-1}$ mmol). After a further 30 minutes stirring the reaction vial was removed from the glove box and its contents added dropwise to  $250\text{cm}^3$  vigorously stirring methanol. The precipitated polymer was then recovered by decantation and subsequent washing ( $2 \times 50\text{cm}^3$  methanol) before residual volatiles were removed *in vacuo*. Yields varied depending upon conditions but in most cases were in excess of 80%. A typical set of characterizing data is given below.

Elemental analysis for  $(\text{C}_9\text{H}_6\text{F}_6)_n$  Found (required): %C 47.46 (47.38), %H 2.71 (2.65), %F 49.71 (49.97).

Infra-red data (polymer film cast from acetone,  $\text{cm}^{-1}$ ) 3020 (m), 2979 (s), 2948 (s), 2878 (m), 2630 (w,br), 2440 (w,br), 2270 (w,br), 2080 (w,br), 1808 (w,br), 1717 (m), 1682

(s), 1665 (m,sh), 1660 (m,sh), 1455 (s), 1370-1030 (v.s,v.br), 990-960 (v.s,br), 920 (s), 910 (s,sh), 847 (m), 824 (w,br), 750 (m,sh), 728 (s), 715 (s), 633 (w,br), 568 (m), 514 (m), 466 (m,br), 422 (w,br), 370 (w,br), 323 (m), 310 (w,sh), 271 (w), 260 (w,sh).

$^1\text{H N.M.R. data}$  (500MHz,  $(\text{CD}_3)_2\text{CO}$ , 298K): (major resonances only; see text for assignment)

5.76 - 5.66 (m), 5.62 (dm), 4.23 (m), 3.81 (s,br), 2.89 (s,br), 2.78 - 2.69 (qt), 1.65 (dm)

$^{19}\text{F NMR data}$  (235MHz,  $(\text{CD}_3)_2\text{CO}$ , 298K): (major resonance only; see text for assignment)

59.92.

$^{13}\text{C N.M.R. data}$  (125.77MHz,  $(\text{CD}_3)_2\text{CO}$ , 298K): (major resonances only; see text for assignment)

139.88 (m), 132.02 , 133.43 , 126.05, 123.33, 120.61, 117.89, 49.76, 44.61, 37.12.

#### Gel permeation chromatography

$M_n$  calc =  $5.5 \times 10^4$   $M_n$  obs =  $4.6 \times 10^4$

$M_w / M_n = 1.06$

### **6.2.2 The reaction between 2,3-bis(trifluoromethyl)bicyclo[2.2.1]hepta-2,5-diene and $\text{Mo}(\text{NAr})(\text{CHCMe}_2\text{Ph})(\text{OCMe}(\text{CF}_3)_2)_2$ in $\text{C}_6\text{D}_6$**

To a rapidly stirring solution of 0.0100g  $\text{Mo}(\text{NAr})(\text{CHCMe}_2\text{Ph})(\text{OCMe}(\text{CF}_3)_2)_2$  ( $1.31 \times 10^{-2}$ mmol in 400 $\mu\text{l}$   $\text{C}_6\text{D}_6$ ) was added a 400 $\mu\text{l}$   $\text{C}_6\text{D}_6$  solution of 0.0298g of 2,3-bis(trifluoromethyl)bicyclo [2.2.1]hepta-2,5-diene ( $1.31 \times 10^{-1}$ mmol). After 30 minutes the reaction mixture was transferred to a 5mm N.M.R. tube and sealed under  $\text{N}_2$ .

$^1\text{H N.M.R. data}$  (400MHz,  $\text{C}_6\text{D}_6$ , 298K)

Alkylidene region: 12.47 -12.39 (m, 10H) and 12.38 - 12.26 (m,24H) Mo=CHP

12.13 (s, 1H) Mo=CHCMe<sub>2</sub>Ph.

**6.2.3 The scaled-up reaction between 2,3-bis(trifluoromethyl)bicyclo  
[2.2.1]hepta-2,5-diene and Mo(NAr)(CHCMe<sub>2</sub>Ph)(OCMe(CF<sub>3</sub>)<sub>2</sub>)<sub>2</sub>  
in  $\alpha,\alpha,\alpha$ -trifluorotoluene**

1.11g Bis(trifluoromethyl)bicyclo[2.2.1]hepta-2,5-diene (4.87 mmol) in 1.30cm<sup>3</sup> trifluorotoluene was added dropwise to a rapidly stirring solution of Mo(N-2,6-C<sub>6</sub>H<sub>3</sub>-i-Pr<sub>2</sub>)(CHCMe<sub>2</sub>Ph)(OCMe(CF<sub>3</sub>)<sub>2</sub>)<sub>2</sub> (0.008g, 1.05 x 10<sup>-2</sup> mmol, in 1.3cm<sup>3</sup> trifluorotoluene; 464 equivalents of monomer). No apparent colour change was observed, but within 3 minutes the reaction mixture became extremely viscous and turned noticeably cloudy. In order to maintain the homogenous nature of the polymerization a further 4.00cm<sup>3</sup> trifluorotoluene was added and stirring continued for 24 hours.

After terminating the polymerization (reaction stirred for 60 minutes following the addition of 50 $\mu$ l benzaldehyde) the product was isolated by precipitation from hexane. The non-solvent was then filtered off and the product dried *in vacuo* to afford 0.880g white fibrous material (79.3%).

Elemental analysis for (C<sub>9</sub>H<sub>6</sub>F<sub>6</sub>)<sub>n</sub> Found (required): %C 48.00 (47.38), %H 2.69 (2.65), %F 50.13 (49.97).

Infra-red data (polymer film cast from acetone, cm<sup>-1</sup>):

3013 (w), 2963 (m), 2939 (m), 2880 (w), 1717 (m), 1684 (m), 1462 (w,sh), 1453 (w), 1402 (w), 1344 (s), 1307 (s) 1294 (s), 1281 (s,sh), 1260 (m,sh), 1185-1130 (v.s, v.br), 1091 (m), 1050 (m,sh), 1024 (m), 988 (m), 950 (w), 924 (m), 905 (w,sh), 900 (w,sh), 895 (w,sh), 885 (w,sh), 862 (w), 801 (w,br,sh) 768 (w), 724 (m,sh), 719 (m), 708 (m,sh) 678 (w), 654 (w,br).

<sup>1</sup>H N.M.R. data (400MHz, (CD<sub>3</sub>)<sub>2</sub>CO, 298K): (major resonances only; see text for assignment) 5.61 (br), 5.55 (br), 4.23 (s,br), 2.85 (s), 2.82 (br), 1.53 (br).

$^{19}\text{F}$  NMR data (235MHz,  $(\text{CD}_3)_2\text{CO}$ , 298K): (see text for assignment)

59.9 - 60.3 (m).

$^{13}\text{C}$  N.M.R. data (100.577MHz,  $(\text{CD}_3)_2\text{CO}$ , 298K): (major resonances only; see text for assignment) 140.2 (m), 133.38, 131.86, 126.02, 123.29, 120.56, 117.84, 49.73, 44.18, 38.39, 37.57.

#### Gel permeation chromatography

$M_n$  calc =  $1.06 \times 10^6$   $M_n$  obs =  $7.28 \times 10^5$

$M_n/M_w = 1.11$

#### 6.2.4 Determination of $k_p / k_i$ for the R.O.M.P. of 2,3-bis(trifluoromethyl) bicyclo[2.2.1]hepta-2,5-diene initiated by $\text{Mo}(\text{NAr})(\text{CHR})(\text{OCMe}(\text{CF}_3)_2)_2$ {R = $\text{CMe}_3$ and $\text{CMe}_2\text{Ph}$ }

For a system in which  $[\text{M}]$  is the concentration of monomer,  $[\text{M}]_0$  is the concentration of monomer at time  $t = 0$ ,  $[\text{I}]$  the concentration of the initiator, and  $[\text{I}]_0$  the initial concentration of the initiator, then (as shown in Appendix II) if a given quantity of monomer is added to the initiator, then as  $[\text{M}]$  tends to zero the ratio of  $k_p$  (the rate constant of propagation) to  $k_i$  (the rate constant of initiation) can be found from the expression...

$$\frac{[\text{M}]_0}{[\text{I}]_0} + \frac{k_p}{k_i} \ln \left\{ \frac{[\text{I}]}{[\text{I}]_0} \right\} + \left\{ 1 - \frac{k_p}{k_i} \right\} \left\{ \frac{[\text{I}]}{[\text{I}]_0} - 1 \right\} = 0$$

0.0201g  $\text{Mo}(\text{NAr})(\text{CHCMe}_2\text{Ph})(\text{OCMe}(\text{CF}_3)_2)_2$  ( $2.63 \times 10^{-2}$ mmol) was dissolved in 400 $\mu\text{l}$   $\text{C}_6\text{D}_6$  and stirred rapidly. To this solution was added approximately 0.006g of 2,3-bis(trifluoromethyl)bicyclo[2.2.1]hepta-2,5-diene in a further 400 $\mu\text{l}$   $\text{C}_6\text{D}_6$  (1 equivalent of monomer = 5.99mg). After 30 minutes the number of equivalents actually added was determined by  $^{19}\text{F}$  N.M.R. spectroscopy (polymer signals occur at 57 - 61ppm, ancillary fluorinated alkoxides at 77 - 80ppm). The ratio of  $[\text{I}] / [\text{I}]_0$  was obtained by

integrating the  $^1\text{H}$  N.M.R. signal for unconsumed neopentylidene initiator at 12.06ppm (the neophylidene analogue has a chemical shift of 12.13ppm) against the total alkylidene proton resonances.

Three determinations were carried out for the neopentylidene complex and gave ratios of 2.73, 2.64, 2.57; therefore  $k_p / k_i = 2.65 (\pm) 0.08$ .

#### **6.2.5 Determination of $k_p$ for the R.O.M.P. of 2,3-bis(trifluoromethyl)bicyclo[2.2.1]hepta-2,5-diene initiated by $\text{Mo}(\text{NAr})(\text{CHR})(\text{OCMe}(\text{CF}_3)_2)_2$ {R = $\text{CMe}_3$ and $\text{CMe}_2\text{Ph}$ }**

To a stirring solution of 0.0101g  $\text{Mo}(\text{NAr})(\text{CHCMe}_2\text{Ph})(\text{OCMe}(\text{CF}_3)_2)_2$  ( $1.32 \times 10^{-2}\text{mmol}$ ) in 2.9864g benzene was added 0.1505g 2,3-bis(trifluoromethyl)bicyclo[2.2.1]hepta-2,5-diene ( $6.60 \times 10^{-1}\text{mmol}$ ) in 2.0027g benzene and 0.1928g ( $1.32\text{mmol}$ )  $\alpha,\alpha,\alpha$ -trifluorotoluene (to act as an internal  $^{19}\text{F}$  N.M.R. standard and to help maintain the homogeneous nature of the polymerization).

At set intervals  $50\mu\text{l}$  aliquots were removed and capped with  $20\mu\text{l}$  benzaldehyde. The samples were analyzed by  $^{19}\text{F}$  N.M.R. spectroscopy which displayed a broad multiplet from 59.1-59.9ppm for the polymer, a singlet at 62.5ppm for the monomer, and a singlet at 63.03ppm for the internal reference. The reaction was followed by monitoring the loss of monomer with time. The data were evaluated by assuming pseudo-first-order kinetics. Three determinations of  $k_p$  were made (0.62, 0.63, 0.60) to give a mean value of  $0.62 (\pm) 0.02$ .

#### **6.2.6 The reaction between 2,3-bis(trifluoromethyl)bicyclo[2.2.1]hepta-2,5-diene and $\text{Mo}(\text{NAr})(\text{CHCMe}_3)(\text{OCMe}_2\text{CF}_3)_2$ in $\text{C}_6\text{D}_6$**

0.0520g 2,3-Bis(trifluoromethyl)bicyclo[2.2.1]hepta-2,5-diene ( $2.28 \times 10^{-1}\text{mmol}$ ) were dissolved in  $400\mu\text{l}$   $\text{C}_6\text{D}_6$  and the resultant mixture added to a rapidly stirring  $\text{C}_6\text{D}_6$  solution of  $\text{Mo}(\text{NAr})(\text{CHCMe}_3)(\text{OCMe}_2\text{CF}_3)_2$  (0.0134g,  $2.25 \times 10^{-2}\text{mmol}$  in  $400\mu\text{l}$ ). After 30 minutes the reaction was analyzed by  $^1\text{H}$  N.M.R. spectroscopy.

**6.2.7 The scaled-up reaction between 2,3-bis(trifluoromethyl)bicyclo  
[2.2.1]hepta-2,5-diene and Mo(NAr)(CHCMe<sub>3</sub>)(OCMe<sub>2</sub>CF<sub>3</sub>)<sub>2</sub>  
in  $\alpha,\alpha,\alpha$ -trifluorotoluene**

0.0118g Mo(N-2,6-C<sub>6</sub>H<sub>3</sub>-i-Pr<sub>2</sub>)(CHCMe<sub>3</sub>)(OCMe<sub>2</sub>CF<sub>3</sub>)<sub>2</sub> ( $1.98 \times 10^{-2}$  mmol) was dissolved in 2.00cm<sup>3</sup> trifluorotoluene. To this stirring solution was then added dropwise over 60 seconds a solution of bis(trifluoromethyl) bicyclo[2.2.1]hepta-2,5-diene (0.973g 4.26 mmol in 1.80cm<sup>3</sup> trifluorotoluene).

After 60 minutes the reaction mixture was still orange, but had become noticeably cloudy, and very viscous.

50 $\mu$ l Benzaldehyde was added after 16 hours and after a further hour stirring the mixture was added dropwise to methanol (100 cm<sup>3</sup>). This suspension was then reduced to 20 cm<sup>3</sup> before the polymer was recovered by decanting the liquid. Residual volatiles were removed under reduced pressure (10<sup>-3</sup>mmHg for 18 hours) to yield 0.86g cream powder (89%).

Elemental analysis for (C<sub>9</sub>H<sub>6</sub>F<sub>6</sub>)<sub>n</sub> Found (required): %C 47.42 (47.38), %H 2.69 (2.65), % F 49.61 (49.97).

Infra-red data (polymer film cast from acetone, cm<sup>-1</sup>) 3020 (w), 2975, (m), 2951 (m), 2903 (w,sh), 2877(w), 1750 (w,sh), 1722 (m,sh), 1716 (m), 1703 (w,sh), 1688 (m,sh), 1682 (m), 1674 (m,sh), 1649 (w,sh), 1451 (m), 1400 (w), 1366 (m,sh), 1358 (m,sh), 1352 (s), 1342 (s), 1295 (s,br), 1260 (m), 1220 (m,sh), 1180-1130 (s,v,br), 1108 (m,sh), 1093 (m,sh), 1044 (m), 989 (m), 970 (m,sh), 923 (m), 776 (w), 746 (w), 725 (m,sh), 716 (m), 709 (m,sh), 704 (w,sh), 650 (w,br), 560 (w,br), 535 (w,sh), 521 (w).

<sup>1</sup>H N.M.R. data (400MHz, (CD<sub>3</sub>)<sub>2</sub>CO, 298K): 5.70 (m,br), 5.57 (m,br), 4.20 (m,br), 3.82 (s,br), 3.30 (s,br), 3.08 (s), 2.77 (m), 1.57 (m,br).

$^{19}\text{F}$  NMR data (385MHz,  $(\text{CD}_3)_2\text{CO}$ , 298K) 63.67, 63.90, 64.07, 64.30, 64.42, 64.42  
(all are broad singlets).

$^{13}\text{C}$  N.M.R. data (100MHz,  $(\text{CD}_3)_2\text{CO}$ , 298K) 140.42-139.64 (m), 133.45, 133.31, 133.22, 131.98, 131.84, 131.75, 121.96 (q,  $J_{\text{CF}} = 272.76\text{Hz}$ ), 49.73, 49.60, 49.45, 44.90, 44.81, 44.60, ca. 38.4, 37.84, 37.57, 37.0-36.4 (m).

Gel permeation chromatography

$M_n$  calc =  $1.06 \times 10^6$   $M_n$  obs =  $7.28 \times 10^5$

$M_w/M_n = 1.11$

## 6.3 Experimental details to chapter three

### 6.3.1 Reaction of $\text{Mo}(\text{NAr})(\text{CHCMe}_2\text{Ph})(\text{OCMe}(\text{CF}_3)_2)_2$ with one equivalent of $\text{Mo}(\text{NAr})(\text{CHCMe}_2\text{Ph})(\text{OCMe}_3)_2$

0.0118g  $\text{Mo}(\text{NAr})(\text{CHCMe}_2\text{Ph})(\text{OCMe}_3)_2$  ( $2.15 \times 10^{-2}$  mmol) and 0.0165g  $\text{Mo}(\text{NAr})(\text{CHCMe}_2\text{Ph})(\text{OCMe}(\text{CF}_3)_2)_2$  ( $2.15 \times 10^{-2}$  mmol) were mixed together in a sealable 5mm glass NMR tube. The tube was then placed on a vacuum line and 750 $\mu\text{l}$   $\text{C}_6\text{D}_6$  vacuum distilled directly onto the solid mixture. The tube was then sealed and a  $^1\text{H}$  N.M.R. spectrum was obtained.

### 6.3.2 Reaction of $\text{Mo}(\text{NAr})(\text{CHCMe}_2\text{Ph})(\text{OCMe}_3)_2$ with 2 equivalents of $\text{LiOCMe}(\text{CF}_3)_2$

0.0145g  $\text{Mo}(\text{NAr})(\text{CHCMe}_2\text{Ph})(\text{OCMe}_3)_2$  ( $2.64 \times 10^{-2}$  mmol) were dissolved in 400 $\mu\text{l}$   $\text{C}_6\text{D}_6$  and to this stirring solution was then added a 400 $\mu\text{l}$   $\text{C}_6\text{D}_6$  solution of  $(\text{CF}_3)_2\text{MeCOLi}$  (0.0098g,  $5.30 \times 10^{-2}$  mmol).

### 6.3.3 Reaction of $\text{Mo}(\text{NAr})(\text{CHCMe}_2\text{Ph})(\text{OCMe}(\text{CF}_3)_2)_2$ with 2 equivalents of $\text{Me}_3\text{COLi}$

To a solution of 0.0131g  $\text{Mo}(\text{NAr})(\text{CHCMe}_2\text{Ph})(\text{OCMe}(\text{CF}_3)_2)_2$  ( $1.71 \times 10^{-2}$  mmol in 400 $\mu\text{l}$   $\text{C}_6\text{D}_6$ ) was added 0.0027g  $\text{Me}_3\text{COLi}$  ( $3.37 \times 10^{-2}$  mmol in 400 $\mu\text{l}$   $\text{C}_6\text{D}_6$ ). After stirring at room temperature for 10 minutes the reaction was transferred into a 5mm NMR tube and sealed under nitrogen.

#### **6.3.4 Reaction of Mo(NAr)(CHCMe<sub>2</sub>Ph)(OCMe<sub>3</sub>)<sub>2</sub> with 2 equivalents of (CF<sub>3</sub>)<sub>2</sub>MeCOH**

To a stirring solution of Mo(NAr)(CHCMe<sub>2</sub>Ph)(OCMe<sub>3</sub>)<sub>2</sub> (0.0153g, 2.78 x 10<sup>-2</sup> mmol in 400μl C<sub>6</sub>D<sub>6</sub>) was added 0.0100g (CF<sub>3</sub>)<sub>2</sub>MeCOH (5.59 x 10<sup>-2</sup> mmol in 400μl C<sub>6</sub>D<sub>6</sub>). After 10 minutes stirring the reaction vial contents were placed in a 5mm NMR tube, and the contents froze until just prior to obtaining the <sup>1</sup>H NMR spectrum.

#### **6.3.5 Reaction of Mo(NAr)(CHCMe<sub>2</sub>Ph)(OCMe(CF<sub>3</sub>)<sub>2</sub>)<sub>2</sub> with 2 equivalents of Me<sub>3</sub>COH**

0.0020g Me<sub>3</sub>COH (2.70 x 10<sup>-2</sup> mmol, previously columned through activated alumina) were dissolved in 400μl C<sub>6</sub>D<sub>6</sub>. The resultant solution was then added to a stirring solution of Mo(NAr)(CHCMe<sub>2</sub>Ph)(OCMe(CF<sub>3</sub>)<sub>2</sub>)<sub>2</sub> (0.0102g 1.33 x 10<sup>-2</sup> mmol in 400μl C<sub>6</sub>D<sub>6</sub>), before transferral into a sealable NMR tube.

#### **6.3.6 The addition of 2,3-bis(trifluoromethyl)bicyclo[2.2.1]hepta-2,5-diene to a 1:1 mixture of Mo(NAr)(CHCMe<sub>2</sub>Ph)(OCMe(CF<sub>3</sub>)<sub>2</sub>)<sub>2</sub> and Mo(NAr)(CHCMe<sub>2</sub>Ph)(OCMe<sub>3</sub>)<sub>2</sub> in C<sub>6</sub>D<sub>6</sub>**

The contents of the NMR tube described in 6.3.1 were recovered and placed in a small glass vial fitted with a magnetic stirrer flea. To this C<sub>6</sub>D<sub>6</sub> solution was added 0.0966g 2,3-bis(trifluoromethyl)bicyclo[2.2.1]hepta-2,5-diene (4.23 x 10<sup>-1</sup> mmol, 19.7 equivalents); the polymerization was allowed to stir for 60 minutes before being transferred to another sealable NMR tube.

**6.3.7 The large scale polymerization of 2,3-bis(trifluoromethyl)bicyclo [2.2.1]hepta-2,5-diene with a 1:1 mixture of Mo(NAr)(CHCMe<sub>2</sub>Ph)(OCMe(CF<sub>3</sub>)<sub>2</sub>)<sub>2</sub> and Mo(NAr)(CHCMe<sub>2</sub>Ph)(OCMe<sub>3</sub>)<sub>2</sub>**

Both initiators were dissolved into 3.00cm<sup>3</sup> tetrahydrofuran and left to stir for ten minutes in order to reach a steady equilibrium (0.0132g Mo(NAr)(CHCMe<sub>2</sub>Ph)(OCMe<sub>3</sub>)<sub>2</sub> 2.40 x 10<sup>-2</sup> mmol : 0.0184g Mo(NAr)(CHCMe<sub>2</sub>Ph)(OCMe(CF<sub>3</sub>)<sub>2</sub>)<sub>2</sub> 2.40 x 10<sup>-2</sup> mmol). 2.00g Bis(trifluoromethyl)bicyclo[2.2.1]hepta-2,5-diene (8.77 mmol in 3.00cm<sup>3</sup> THF) was then added, imparting an immediate red-orange colouration to the stirring mixture, which returns to its original orange colour shortly afterwards.

After 24 hours 50µl benzaldehyde (4.91 x 10<sup>-1</sup>mmol) was added to terminate the living metal centre. Precipitation from hexane, followed by filtration and removal of residual volatiles *in vacuo* lead to the isolation of 0.63g pale pink flakes (31.5% yield). Much higher yields are obtainable if the mother liquor from the precipitation stage is kept and left to stand overnight.

## 6.4 Experimental details to chapter four

### 6.4.1 The reaction of $\text{Mo}(\text{NAr})(\text{CHR})(\text{OR}')_2$ with (S)-(-)- $\alpha$ -methylbenzylamine in $\text{C}_6\text{D}_6$

A known mass of each of the three initiators was dissolved in 400  $\mu\text{l}$   $\text{C}_6\text{D}_6$  and transferred to a small vial fitted with a stirrer flea. Approximately two equivalents of the amine (precise quantities are detailed in table 6.1) were then added in a further 400  $\mu\text{l}$   $\text{C}_6\text{D}_6$ . Each of the mixtures was allowed to stir for 60 minutes before being added to a 5mm N.M.R. tube which was sealed under an  $\text{N}_2$  atmosphere and frozen (kept at  $-40^\circ\text{C}$ ) until a  $^1\text{H}$  N.M.R. spectrum was obtained.

Initiator alkoxides	Mass of initiator / g	mmol of initiator	Mass of amine / g	mmol of amine	Equivalents of amine
$\text{OCMe}_3$	0.0133	0.0242	0.0050	0.0413	1.71
$\text{OCMe}_2\text{CF}_3$	0.0200	0.0336	0.0081	0.0688	2.05
$\text{OCMe}(\text{CF}_3)_2$	0.0096	0.0125	0.0038	0.0314	2.51

Table 6.1

### 6.4.2 The R.O.M.P. of 2,3-bis(trifluoromethyl)bicyclo[2.2.1]hepta-2,5-diene by $\text{Mo}(\text{NAr})(\text{CHR})(\text{OR}')_2$ in the presence of (S)-(-)- $\alpha$ -methylbenzylamine

To the stirring solutions made up in section 6.4.1 was added approximately 10 equivalents of 2,3-bis(trifluoromethyl)bicyclo[2.2.1]hepta-2,5-diene in 200  $\mu\text{l}$   $\text{C}_6\text{D}_6$  (table 6.2). After 60 minutes at room temperature the increasingly viscous orange solutions were transferred into fresh N.M.R. tubes and again were frozen until just prior to  $^1\text{H}$  N.M.R. spectroscopic analysis.

Initiator alkoxides	Mass of monomer / g	mmol of monomer	Equivalents of monomer
OCMe <sub>3</sub>	0.0630	0.276	11.4
OCMe <sub>2</sub> CF <sub>3</sub>	0.0559	0.245	7.3
OCMe(CF <sub>3</sub> ) <sub>2</sub>	0.0388	0.170	13.6

Table 6.2

#### 6.4.3 The R.O.M.P. of 2,3-bis(trifluoromethyl)bicyclo[2.2.1]hepta-2,5-diene by Mo(NAr)(CHR)(OR')<sub>2</sub> in the presence of (+)-camphor

Several such experiments were carried out, all following the general procedure described below.

0.0080g Mo(NAr)(CHCMe<sub>2</sub>Ph)(OCMe(CF<sub>3</sub>)<sub>2</sub>)<sub>2</sub> ( $1.04 \times 10^{-2}$ mmol) in 1.5cm<sup>3</sup>  $\alpha,\alpha,\alpha$ -trifluorotoluene and 0.1590g (+)-camphor (1.04mmol in 2.5cm<sup>3</sup>  $\alpha,\alpha,\alpha$ -trifluorotoluene) were mixed together and left to stir for ten minutes. After this time period, during which no apparent colour change had been detected, 0.500g 2,3-bis(trifluoromethyl)bicyclo[2.2.1]hepta-2,5-diene (2.19mmol) in 1.5cm<sup>3</sup>  $\alpha,\alpha,\alpha$ -trifluorotoluene was added. The polymerization was then allowed to stir overnight (16 hours).

Excess benzaldehyde (50 $\mu$ l) was then added and after a further 30 minutes stirring the red solution (not noticeably viscous) was added dropwise to 150cm<sup>3</sup> heptane, forming an immediate cloudy precipitate, which settles out as a pale pink powder. The yellow solution was filtered off and the polymer dried *in vacuo* for 24 hours to afford a yield of 0.440g (88%).

#### 6.4.4 The reaction of $\text{Mo}(\text{NAr})(\text{CHR})(\text{OR}')_2$ with (+)-camphor in $\text{C}_6\text{D}_6$

Benzene- $d_6$  solutions (200 $\mu\text{l}$ ) of  $\text{Mo}(\text{NAr})(\text{CHCMe}_2\text{Ph})(\text{OCMe}_3)_2$  and  $\text{Mo}(\text{NAr})(\text{CHCMe}_2\text{Ph})(\text{OCMe}(\text{CF}_3)_2)_2$  were made up and to these were added 600 $\mu\text{l}$   $\text{C}_6\text{D}_6$  solutions of (+)-camphor (masses used and equivalents are recorded in table 6.3). After stirring for 10 minutes the mixtures were pipetted into 5mm N.M.R. tubes and sealed under  $\text{N}_2$ .

Initiator alkoxides	Mass of initiator / g	mmol of initiator	Mass of (+)-camphor / g	mmol of (+)-camphor	Equivalents of camphor
$\text{OCMe}_3$	0.0104	0.0189	0.0327	0.215	11.4
$\text{OCMe}_3$	0.0104	0.0189	0.0609	0.400	21.1
$\text{OCMe}(\text{CF}_3)_2$	0.0141	0.0184	0.0351	0.231	12.6
$\text{OCMe}(\text{CF}_3)_2$	0.0141	0.0184	0.0627	0.412	22.4

Table 6.3

#### 6.4.5 The reaction between $\text{Mo}(\text{NAr})(\text{CHCMe}_2\text{Ph})(\text{OCMe}_3)_2$ and 2 equivalents ROH in $\text{C}_6\text{D}_6$

2.00 Equivalents of 1-adamantanol, (-)-menthol, and (S)-endo-borneol in 400 $\mu\text{l}$   $\text{C}_6\text{D}_6$  were added to three 400 $\mu\text{l}$  solutions of  $\text{Mo}(\text{NAr})(\text{CHCMe}_2\text{Ph})(\text{OCMe}_3)_2$  (quantities used are shown in table 6.4). After ten minutes stirring at room temperature the mixtures were analysed by  $^1\text{H}$  N.M.R. spectroscopy (further monitoring showed that the equilibrium position had already been reached).

Mass of initiator / g	mmol of initiator	Alcohol	Mass of alcohol / g	mmol of alcohol	Equivalents of alcohol
0.0163	0.0297	adamantanol	0.0090	0.0591	1.99
0.0178	0.0324	borneol	0.0103	0.0668	2.06
0.0182	0.0331	menthol	0.0103	0.0676	2.04

Table 6.4

#### 6.4.6 The synthesis of $\text{Mo}(\text{NAr})(\text{CHCMe}_2\text{Ph})\{(\text{S})\text{-endo-borneoxide}\}_2$

0.1492g  $\text{Mo}(\text{NAr})(\text{CHCMe}_2\text{Ph})(\text{OCMe}_3)_2$  (0.271mmol) and 0.0837g (S)-endo-borneol (0.543mmol) were both loaded into the same schlenk and  $10\text{cm}^3$  di(ethyl) ether was added to give an orange-brown solution. After stirring for 5 minutes volatiles were removed *in vacuo*; the schlenk was then transferred into a dinitrogen-atmosphere glove box and some of the orange oil was extracted into  $800\mu\text{l}$   $\text{C}_6\text{D}_6$ . N.M.R. spectroscopy showed three alkylidene signals in the ratio 60% {bis(borneoxide)} : 30% (mixed borneoxide-butoxide) : 10% {bis(butoxide)}, confirming that a substantial amount of eliminated t-BuOH had indeed been removed from the system.

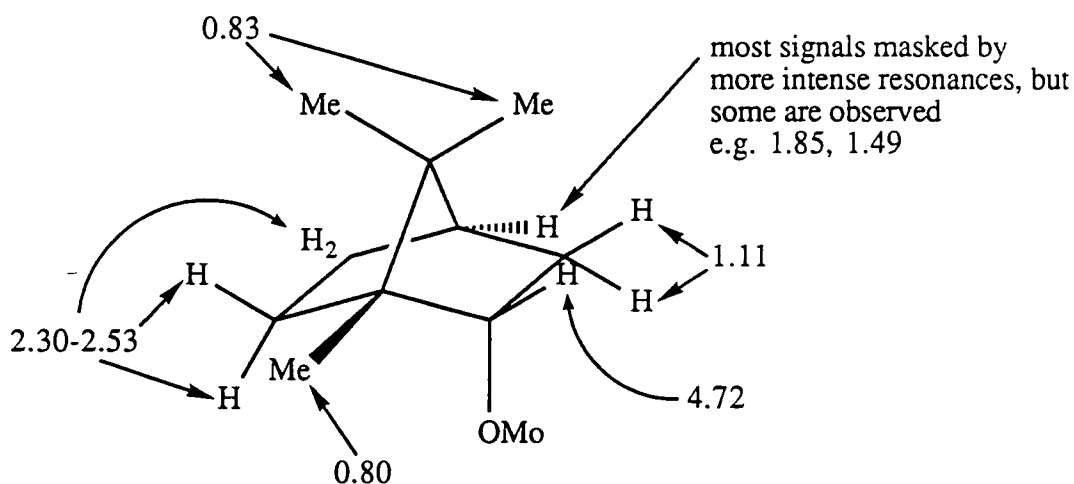
The contents of the N.M.R. tube were recovered and poured back into the original schlenk. The residual deuterated benzene was removed *in vacuo* to give another orange-brown oil.  $10\text{cm}^3$   $\text{Et}_2\text{O}$  was again added and the mixture stirred for a further five minutes, before stripping off the solvent. This cycle was repeated twice more; each time the volatiles were removed the involatiles became increasingly less oily, forming yellow flakes of solid after the fourth cycle. The material was analysed again by N.M.R. and shown to be the bis(borneoxide).

Recrystallisation from the minimum amount of n-pentane at  $-78^\circ\text{C}$  yielded 0.124g orange crystals (64%).

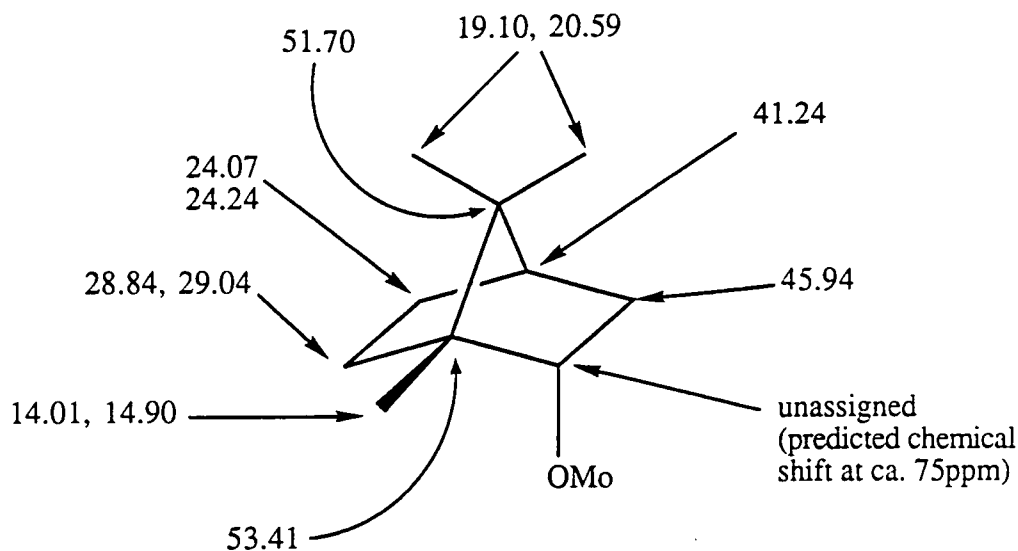
Elemental analysis for  $\text{MoC}_4\text{H}_6\text{NO}_2$  Found (required) C (71.06%) H (8.94%) N (1.97%).

Infra-red data (nujol mull,  $\text{cm}^{-1}$ ) 2450 (w,br), 1600 (w,br), 1337 (w), 1308 (w), 1277 (w,sh), 1264 (m), 1233 (w), 1207 (w,sh), 1200 (w), 1164 (w), 1146 (w,sh), 1137 (m), 1110 (s), 1080 (m), 1053 (s,br), 1031 (s), 1020 (s), 1007 (m,sh), 992 (m), 979 (w,sh), 950 (w,sh), 945 (w,sh), 935 (w), 920 (w), 888 (w), 844 (m), 800 (m,br), 783 (w,sh), 762 (m), 757 (m), 750 (w,sh), 699 (s), 695 (m,sh), 669 (m,sh), 636 (m,br), 589 (w), 516 (w,br), 450 (w,br).

$^1\text{H N.M.R. data}$  (400MHz,  $\text{C}_6\text{D}_6$ , 298K) 11.16 (s, 1H,  $\text{Mo}=\text{CHCMe}_2\text{Ph}$ ), 7.36 (d, aromatics), 7.07 (s, aromatics), 4.72 (br,m, 1H), 4.00 (sept, 2H,  $\text{NAr-CHMe}_2$ ), 3.91 (br,m), 3.25 (m), 2.52 (br), 2.41 (br), 2.30 (br), 1.83 (d), 1.64 (d, 6H,  $\text{CHCMe}_2\text{Ph}$ ), 1.49 (br), 1.32 (d, 12H,  $\text{NAr-CHMe}_2$ ), 1.11 (d), 0.83 (d, 12H), 0.80 (s, 6H).



$^{13}\text{C N.M.R. data}$  (100MHz,  $\text{C}_6\text{D}_6$ , 298K) 267.39 ( $\text{Mo}=\text{CHCMe}_2\text{Ph}$ ), 153.71 ( $\text{NAr-C}_{\text{ipso}}$ ), 150.58, 146.34 ( $\text{NAr-C}_{\text{ortho}}$ ), 126.70, 126.34, 123.37 ( $\text{Mo}=\text{CHCMe}_2\text{Ph}$  and  $\text{NAr-C}_{\text{meta + para}}$ ), 53.41, 51.70, 48.31 ( $\text{Mo}=\text{CHCMe}_2\text{Ph}$ ), 45.94, 41.24, 31.81 ( $\text{Mo}=\text{CHCMe}_2\text{Ph}$ ), 31.55 ( $\text{NAr-CHMe}_2$ ), 29.37, 29.04, 28.84, 27.85, 26.77 ( $\text{NAr-CHMe}_2$ ), 24.24, 24.07, 20.59, 19.10, 14.90, 14.10.



#### 6.4.7 The synthesis of $\text{Mo}(\text{NAr})(\text{CHCMe}_2\text{Ph})\{(-)\text{-mentholate}\}_2$

A similar procedure to that followed for the synthesis of the bis(borneoxide) complex was also used for the bis(mentholate). Di(ethyl) ether ( $5\text{cm}^3$ ) was added to a solid mixture of  $\text{Mo}(\text{NAr})(\text{CHCMe}_2\text{Ph})(\text{OCMe}_3)_2$  (0.0812g,  $1.48 \times 10^{-1}\text{mmol}$ ) and (-)-menthol (0.0462g,  $2.95 \times 10^{-1}\text{mmol}$ ), and the resultant orange solution was left to stir for five minutes before the removal of volatiles *in vacuo*. After four cycles a sticky orange-brown oil results; although solid flakes appear upon the sides of the reaction vessel almost immediately, prolonged exposure to vacuum did not induce crystallisation. Two more solvate-pump cycles also failed to yield a solid product. Nonetheless  $^1\text{H}$  N.M.R. of the oil revealed the presence of just one alkydene with a chemical shift previously assigned to the bis(mentholate) complex.

The oil was dissolved into twice its volume of n-pentane and left overnight at  $-40^\circ\text{C}$  to afford 0.056g orange crystals (53%).

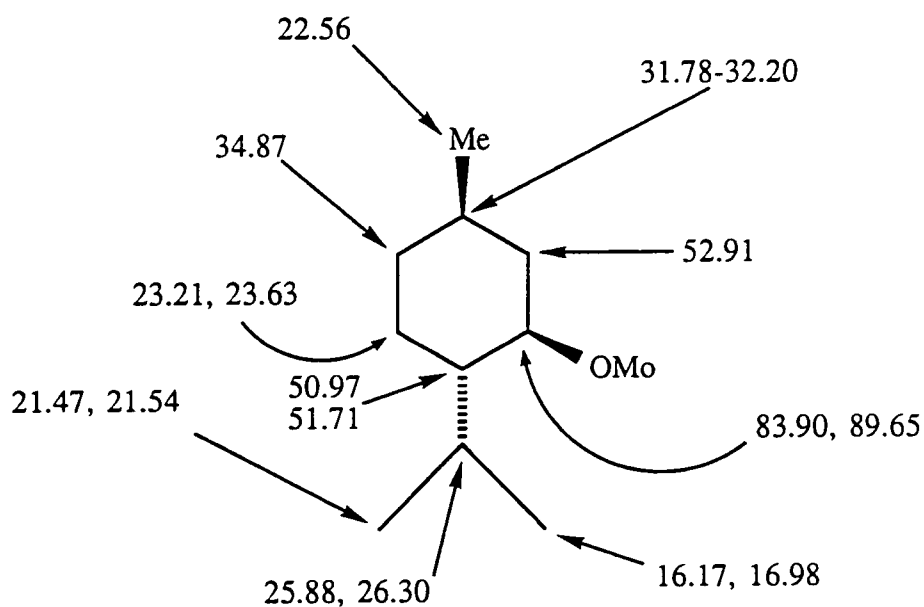
Elemental analysis for  $\text{MoC}_{42}\text{H}_{67}\text{NO}_2$  Found (required) C (70.86%), H (9.20%), N (1.97%).

Infra-red data (nujol mull,  $\text{cm}^{-1}$ ) 1603 (w,br), 1588 (w,br), 1345 (m), 1320 (w,br), 1293 (w), 1265 (m), 1233 (w), 1210 (w), 1179 (w), 1155 (w), 1100 (m,br), 1078 (m), 1060

(m,sh), 1042 (m), 1018 (s,br), 991 (s), 978 (m,sh), 968 (m,sh), 934 (w,sh), 925 (w), 878 (w), 852 (w), 810 (m,sh), 801 (m), 760 (s), 752 (m,sh), 732 (m), 718 (m), 700 (s), 596 (w), 500 (w,br), 451 (w,br).

$^1\text{H N.M.R. data}$  (400MHz,  $\text{C}_6\text{D}_6$ , 298K) 11.27 (s, 1H,  $\text{Mo}=\text{CHCMe}_2\text{Ph}$ ), 7.43 (br), 7.41 (br), 7.20 (m), 7.18 (s), 7.10-7.01 (m) all aromatic protons, 4.05 (m, 2H,  $\text{NAr-CHMe}_2$ ), 2.62-2.48 (m, 2H, menthol- $\text{CHMe}_2$ ), 2.07 (d m, unassigned menthol protons), 1.70 (d, 6H,  $\text{Mo}=\text{CHCMe}_2\text{Ph}$ ), 1.56 (br,m, unassigned), 1.32 1.30 (two overlapping doublets, 24H,  $\text{NAr-CHMe}_2$  and menthol- $\text{CHMe}_2\text{Ph}$ ), 1.03 (d), 1.02 (s), 1.01 (s, unassigned), 0.91 (m, 6H, menthol-Me), 0.81 (br,m, unassigned).

$^{13}\text{C N.M.R. data}$  (100MHz,  $\text{C}_6\text{D}_6$ , 298K) 258.03 ( $\text{Mo}=\text{CHCMe}_2\text{Ph}$ ), 153.36 ( $\text{NAr-C}_{\text{ipso}}$ ), 150.33, 146.18 ( $\text{NAr-C}_{\text{ortho}}$ ), 136.56, 126.10, 126.03, 123.23 (neophyl aromatics +  $\text{NAr-C}_{\text{m+p}}$ ), 89.65, 83.90, 52.91, 51.71, 50.97, 47.31 ( $\text{Mo}=\text{CHCMe}_2\text{Ph}$ ), 34.87, 32.20, 32.07, 31.87, 31.78, 28.43 ( $\text{NAr-CHMe}_2$ ), 26.30, 25.88, 24.22 ( $\text{NAr-CHMe}_2$ ), 23.92, 23.63, 23.21, 22.56, 21.54, 21.47, 16.98, 16.17.



no observation of the hydroxyl proton has been made, and therefore this signal can not yet be confirmed as due to the predicted by-product.

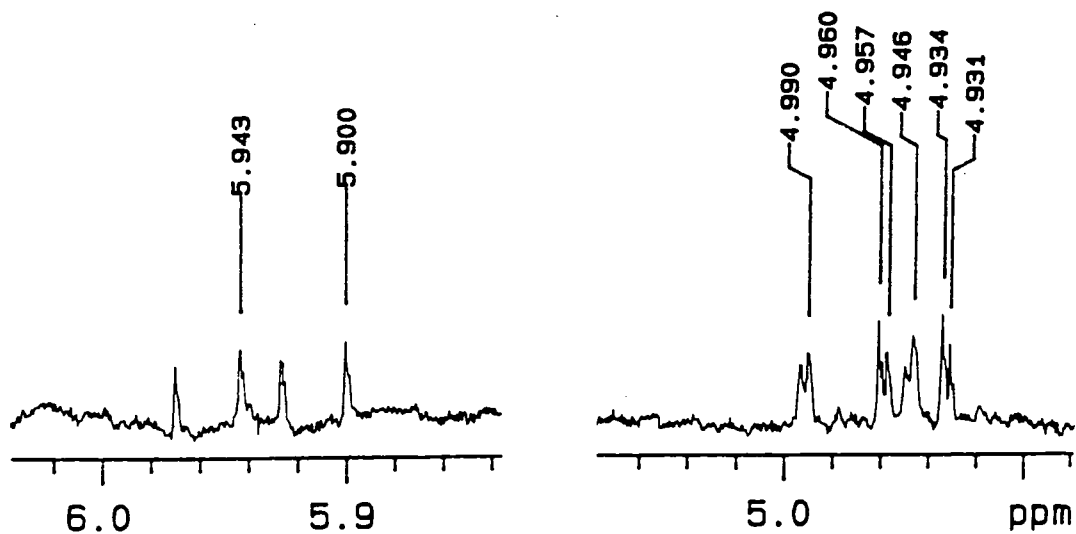


Figure 4.6 400MHz  $^1\text{H}$  N.M.R. spectrum of the proposed camphor enolate olefin signals ( $\text{C}_6\text{D}_6$ )

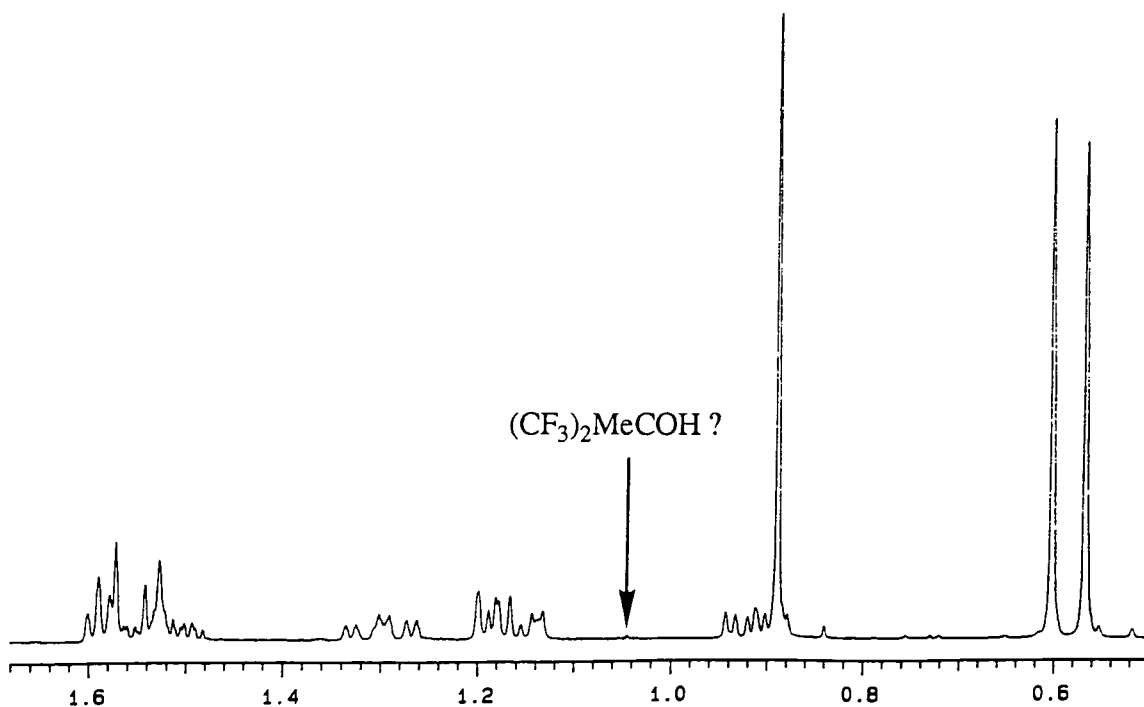


Figure 4.7 A region of the 400MHz  $^1\text{H}$  N.M.R. spectrum ( $\text{C}_6\text{D}_6$ ) of 20.5 equivalents (+)-camphor and  $\text{Mo}(\text{NAr})(\text{CHCMe}_2\text{Ph})(\text{OCMe}(\text{CF}_3)_2)_2$  showing the proposed observation of eliminated  $(\text{CF}_3)_2\text{MeCOH}$

The solid was recrystallised from hot (80°C) heptane to give 0.059g orange-brown microcrystalline powder (a yield of 42%).

Elemental analysis for  $\text{MoC}_{42}\text{H}_{41}\text{NO}_2$  Found (required) C 71.60% (73.35%), H 6.07% (6.00%), N 1.86% (2.04%).

Infra-red data (nujol mull,  $\text{cm}^{-1}$ ) 1620 (w), 1589 (m), 1580 (w,sh), 1511 (w,sh), 1502 (m,br), 1495 (m,sh), 1330 (m,br), 1272 (m, sh), 1262 (m), 1241 (s), 1220 (m), 1210 (m,sh), 1146 (w,br), 1129 (w), 1092 (w,br), 1073 (m), 1060 (w), 1042 (w), 1032 (m), 1020 (m), 993 (w), 947 (m), 936 (m), 861 (w), 818 (s), 810 (s,sh), 800 (s), 795 (m,sh), 760 (m,sh), 748 (s), 722 (w,sh), 700 (m), 692 (m,sh), 668 (m), 632 (w), 604 (w), 579 (w), 561 (w,br), 520 (w,br), 494 (w,br), 450 (w,br), 418 (w,br).

$^1\text{H N.M.R. data}$  (400MHz,  $\text{C}_6\text{D}_6$ , 298K) 12.00 (Mo=CHCMe<sub>2</sub>Ph), 7.86 (d), 7.57 (m), 7.39-6.50 (m, aromatics), 4.75 (sept, NAr-CHMe<sub>2</sub>), 4.55 (sept, NAr-CHMe<sub>2</sub>), 3.98 (br), 2.85 (s), 1.52 (d, Mo=CHCMe<sub>2</sub>Ph), 1.49 (d, Mo=CHCMe<sub>2</sub>Ph), 1.45 (s), 1.32 (d, NAr-CHMe<sub>2</sub>), 1.30 (d, NAr-CHMe<sub>2</sub>), 1.25 (s), 1.20 (d), 0.92 (br), 0.87 (m), 0.59 (s).

$^{13}\text{C N.M.R. data}$  (100MHz,  $\text{C}_6\text{D}_6$ , 298K) 267.5, 163.79, 162.99, 154.23, 153.48, 153.00, 152.04, 148.91, 136.45, 134.38, 134.22, 133.82, 131.52, 131.13, 130.89, 130.21, 129.88, 129.61, 129.30, 128.76, 128.70, 127.19, 126.98, 126.58, 126.42, 126.13, 125.97, 125.14, 124.96, 124.34, 123.94, 123.73, 123.58, 123.47, 122.67, 122.49, 121.99, 119.20, 93.74, 56.10, 44.43, 34.39, 30.40, 30.17, 29.13, 29.02, 28.61, 28.36, 25.94, 24.85, 24.44, 22.82, 22.68, 14.24.

## 6.5 Experimental details to chapter five

### 6.5.1 The reaction between $\text{Mo}(\text{NAr})(\text{CHR})(\text{OR}')_2$ and 10 equivalents of the fluorinated monomers II, III, and IV

To a stirring solution of 0.010 - 0.020g of the initiator (400 $\mu\text{l}$   $\text{C}_6\text{D}_6$ ) was added approximately 10 equivalents of the monomer under study (again dissolved in 400 $\mu\text{l}$   $\text{C}_6\text{D}_6$ ). Stirring was allowed to continue for 30 minutes before the contents of the reaction vial were pipetted into a 5mm N.M.R. tube which was sealed under nitrogen and kept frozen until immediately before obtaining a  $^1\text{H}$  N.M.R. spectrum.

Initiator alkoxides	Monomer	Mass of initiator / g	mmol initiator	Mass of monomer / g	mmol monomer	Monomer equivalents
OCMe <sub>3</sub>	II	0.0111	0.0202	0.0320	0.200	9.9
	III	0.0103	0.0184	0.0288	0.177	9.8
	IV	0.0122	0.0222	0.0478	0.221	9.9
OCMe <sub>2</sub> CF <sub>3</sub>	II	0.0085	0.0143	0.0229	0.143	10.0
	III	0.0094	0.0158	0.0256	0.158	10.0
	IV	0.0096	0.0161	0.0452	0.209	13.0
OCMe(CF <sub>3</sub> ) <sub>2</sub>	II	0.0109	0.0144	0.0228	0.150	10.4
	III	0.0094	0.0123	0.0201	0.0124	10.1
	IV	0.0093	0.0121	0.0431	0.200	16.5

Table 6.5

### 6.5.2 Scaled-up homopolymerizations of monomers II, III, and IV

initiated by  $\text{Mo}(\text{NAr})(\text{CHR})(\text{OR}')_2$

The homopolymerizations were carried out using an identical procedure as for that followed for the polymerization of 2,3-bis(trifluoromethyl)bicyclo[2.2.1]hepta-2,5-diene. Solvents, reaction times and yields are all summarised in table 6.6, and this is followed by characterising data for the three polymers initiated by  $\text{Mo}(\text{NAr})(\text{CHCMe}_2\text{Ph})(\text{OCMe}_3)_2$ .

Initiator alkoxides + monomer	Mass of monomer / g	Monomer equivalents	Solvent	Reaction time / hrs	Yield / %
$\text{OCMe}_3$ + II	0.996	228	Toluene:THF (90:10)	24	74.9
$\text{OCMe}_3$ + III	1.490	722	Toluene:THF (80:20)	18	78.7
$\text{OCMe}_3$ + IV	0.700	155	Toluene:THF (85:15)	24	31.1
$\text{OCMe}_2\text{CF}_3$ + II	0.516	231	THF	18	67.8
$\text{OCMe}_2\text{CF}_3$ + III	0.886	254	THF	18	87.6
$\text{OCMe}(\text{CF}_3)_2$ + II	0.958	346	THF	18	85.4
$\text{OCMe}(\text{CF}_3)_2$ + III	1.013	342	THF	18	82.9
$\text{OCMe}(\text{CF}_3)_2$ + IV	0.426	175	$\text{C}_6\text{H}_5\text{CF}_3$	12	35.7

Table 6.6

### 6.5.3 Characterising data on the high trans ring-opened polymer of 2-trifluoromethylbicyclo[2.2.1]hepta-2,5-diene

Elemental analysis for  $(C_8H_7F_3)_n$  Found (required) %C 60.12 (60.00), %H 4.47 (4.41), %F 35.89 (35.59).

Infra-red data (film cast from acetone,  $cm^{-1}$ ) 3001 (m), 2965 (m), 2920 (m,sh), 2864 (w), 1742 (m,sh), 1717 (s,br), 1707 (s,sh), 1657 (m,sh), 1442 (m,sh), 1424 (m), 1368 (s), 1360 (s,sh), 1348 (s,sh), 1313 (m), 1281 (m), 1224 (s), 1200 (m,sh), 1155 (s), 1122 (s), 1090 (m), 1049 (m), 971 (m), 930 (w), 893 (w), 870 (w), 719 (w).

$^1H$  N.M.R. data (400MHz,  $(CD_3)_2CO$ , 298K) 6.18 (br,s trans vinylene), 6.11 (s, cis vinylene), 5.43 (br), 5.35 (s), 5.31 (m), 3.84 (s), 3.68 (s), 3.46 (br), 3.34 (br), 2.47 (m), 1.51, 1.49, 1.48, 1.43 (all singlets), 1.26 (m), 1.17 (d), 0.99 (s), 0.88 (d).

$^{13}C$  N.M.R. data (100MHz,  $(CD_3)_2CO$ , 298K) (major resonances only; see text for assignments) 140.59, 136.30 (m), 133.79, 133.29, 132.98, 132.60, 127.79, 125.10, 124.99, 122.41, 122.30, 119.73, 48.04 (m), 47.85 (d), 47.47 (d), 47.44 (m), 43.76 (m), 39.58 (m).

$^{19}F$  N.M.R. data (370MHz,  $(CD_3)_2CO$ , 298K) 64.42 (m), 64.57 (m), 67.39 (s), 67.60 (m), 67.73 (m), 69.75 (m), 69.95 (m).

### 6.5.4 Characterisation data on the high trans ring-opened polymer of endo/exo-5-trifluoromethylbicyclo[2,2,1]hept-2-ene

Elemental analysis for  $(C_8H_9F_3)_n$  Found (required) %C 59.20 (59.26), %H 5.40 (5.59), %F 35.55 (35.15).

Infra-red data (film cast from acetone,  $\text{cm}^{-1}$ ) 3040 (w,sh), 2952 (m,br), 2877 (m), 1725 (m,sh), 1718 (m), 1707 (m,sh), 1464 (m), 1452 (m), 1392 (s), 1370 (m,sh), 1308 (m), 1275 (s,br), 1253 (s,sh), 1223 (m), 1170-1140 (s,br), 1114 (s), 1082 (s), 1058 (m,sh), 1008 (m), 970 (s,br), 929 (m,br), 894 (w,br), 760 (w,br), 697 (w), 660 (w,br).

$^1\text{H N.M.R. data}$  (400MHz,  $\text{CD}_3\text{Cl}$ , 298K) 6.18 (m), 5.96 (s), 3.08 (s), 2.99 (s), 2.91 (s), 2.72 (m), 1.94 (m), 1.67 (m), 1.45 (m), 1.28 (d), 1.14 (m), 1.09 (m).

$^{13}\text{C N.M.R. data}$  (100MHz,  $\text{CD}_3\text{Cl}$ , 298K) (major resonances only; see text for assignments) 133.70, 132.37, 129.82, 129.22, 128.74, 126.45, 45.98 (m), 43.60 (m), 41.84 (m), 39.77 (m), 33.13 (br).

$^{19}\text{F N.M.R. data}$  (370MHz,  $\text{CD}_3\text{Cl}$ , 298K) 60.71 (s), 60.84 (s), 60.99 (m), 65.96 (m), 66.16 (m).

#### **6.5.5 Characterisation data on the high trans ring-opened polymer of 5,5,6-trifluoro-6-trifluoromethylbicyclo[2.2.1]hept-2-ene**

Elemental analysis for  $(\text{C}_8\text{H}_6\text{F}_6)_n$  Found (required) %C 44.00 (44.46), %H 2.85 (2.80), %F 52.89 (52.74).

Infra-red data (film cast from acetone,  $\text{cm}^{-1}$ ) 1462 (w), 1387 (m,sh), 1350 (s), 1310 (m), 1240 (s), 1209 (s,br), 1155 (m,sh), 1120 (m,sh), 1095 (m,br), 1076 (m), 1012 (w), 976 (m), 965 (w,sh), 930 (w), 910 (w,sh), 902 (w), 829 (w), 807 (w), 744 (w), 729 (w), 717 (w).

$^{13}\text{C N.M.R. data}$  (100MHz,  $(\text{CD}_3)_2\text{CO}$ , 298K) (major resonances only; see text for partial assignment) 131.92 (m), 130.93 (m), 130.60 (s), 130.33, 129.93, 128.68, 128.34, 127.87 (m), 127.62 (m), 127.37 (m), 126.82 (m), 125.10 (m), 124.66 (s), 123.76 (br),

122.64 (s), 123.76 (br), 122.64 (s), 121.1-120.8 (m), 48.46 (m), 47.20 (m), 46.15 (m), 43.62 (m), 33.30 (m), 31.90 (m).

*<sup>19</sup>F N.M.R. data* (370MHz, C<sub>6</sub>D<sub>6</sub>, 298K) 72.83, 72.99, 76.18, 76.48, 104.08, 105.14, 117.39, 118.45, 125.20, 126.24, 159.76, 192.16.

#### 6.5.6 N.M.R. scale block copolymer synthesis

Once again a similar procedure was followed for all the block copolymer synthesis. For the sake of brevity, therefore, the preparation of just one of them, namely co-poly I - III is described in detail. The reader is referred to table 6.7 for more information on the synthesis of the other systems. Characterisation of all of the block copolymers is deferred until after the synthetic details.

An 80% toluene : 20% THF solution of 2,3-bis(trifluoromethyl)bicyclo[2.2.1]hept-2,5-diene (0.613g, 2.69mmol in 5cm<sup>3</sup> solvent) was added to a 5cm<sup>3</sup> stirring solution of 0.0090g Mo(NAr)(CHCMe<sub>2</sub>Ph)(OCMe<sub>3</sub>)<sub>2</sub> (1.64 x 10<sup>-2</sup>mmol). The solution immediately reddens, returning to its original orange colour after five minutes. After 24 hours <sup>19</sup>F N.M.R. on an aliquot of the reaction mixture confirmed the complete consumption of the monomer.

1.297g 5-trifluoromethylbicyclo[2.2.1]hept-2-ene (8.00mmol in a further 5cm<sup>3</sup> solvent) was then added and the mixture was allowed to stir overnight (18 hours). After this time period the solution was extremely viscous and so a further 5cm<sup>3</sup> neat THF was added before the addition of an excess of a capping reagent (50µl benzaldehyde).

After a further 2 hours stirring the block copolymer was precipitated from 200cm<sup>3</sup> methanol via the dropwise addition of the reaction mixture over 30 minutes. Filtration and removal of residual volatiles *in vacuo* lead to the isolation of 1.52g of a pale cream-coloured, fibrous material (79.6%).

Block copolymer	Mass of initiator / g	Equivalents of block A	Equivalents of block B	Solvent	Yield / %
I - II	0.0090	164	488	Toluene :THF (80 : 20)	79.6
I - III	0.0110	64	44	C <sub>6</sub> H <sub>5</sub> CF <sub>3</sub>	64.6
IV - I	0.0160	64	124	Toluene :THF (80 : 20)	70.3
IV - III	0.0070	91	247	Toluene :THF (85: 15)	96.2

Table 6.7

### 6.5.7 Characterisation data on block copolymer I - III

*Infra-red data* (film cast from acetone, cm<sup>-1</sup>) 1800 (w), 1622 (m,sh), 1615 (m), 1605 (m,sh), 1600 (m,sh), 1588 (m,sh), 1582 (m), 1565 (m,sh), 1555 (m,sh), 1464 (m,sh), 1454 (m), 1349 (s,br), 1302 (s,br), 1262 (s,sh), 1240 (s), 1190-1140 (s, v.br), 1073 (s,sh), 1040 (s,sh), 1011 (m), 977 (s,br), 922 (s), 912 (s,sh), 905 (s,sh), 848 (w), 835 (w), 804 (w), 743 (m,sh), 729 (s), 718 (s), 713 (m,sh), 705 (m,sh).

*<sup>13</sup>C N.M.R. data* (100MHz, (CD<sub>3</sub>)<sub>2</sub>CO, 298K) (major resonances only; see text for assignments) 139.90, 134.58, 134.14, 133.43, 133.29, 132.39, 132.0, 131.05, 130.74, 130.06, 129.74, 129.01 (q, J<sub>CF</sub> = 274.58Hz), 122.05 (q, J<sub>CF</sub> = 270.89), 49.74, 46.76, 46.52, 46.26, 44.01, 43.90, 42.26, 40.75, 40.60, 37.17, 33.95, 33.81.

*<sup>19</sup>F N.M.R. data* (370MHz, (CD<sub>3</sub>)<sub>2</sub>CO, 298K) 59.34 (s,I), 65.06 (III), 65.20 (III), 65.33 (III), 70.33 (III), 70.34 (III), 70.38 (III), 70.51 (III).

### 6.5.8 Characterisation data on block copolymer I - II

*Infra-red data* (film cast from acetone,  $\text{cm}^{-1}$ ) 1800 (w,br), 1740 (w,sh), 1722 (m,sh), 1714 (m), 1705 (m,sh), 1700 (m,sh), 1688 (m,sh), 1682 (m), 1660 (m,sh), 1638 (w,sh), 1462 (w,sh), 1453 (m), 1420 (m,sh), 1385 (m,sh), 1346 (s,br), 1298 (s,br), 1263 (s,sh), 1225 (s,sh), 1185-1130 (s,br), 1095 (s,sh), 1060 (s,br), 1025 (m,sh), 989 (s,sh), 970 (s), 921 (s), 913 (s,sh), 870 (m), 848 (w), 758 (w,br), 727 (m), 718 (s), 712 (m,sh), 698 (w,sh).

*$^{13}\text{C}$  N.M.R. data* (100MHz,  $(\text{CD}_3)_2\text{CO}$ , 298K) (major resonances only; see text for discussion) 139.90 (m, I C5,6), 133.44 (m, I C2,3 t), 132.65 (m, II), 123.36 (q,  $J_{\text{CF}} = 273.74\text{Hz}$ , I C8), 49.77 (s, I C1,4 t), 47.95 (m,br, II), 44.6 (s, I C1,4 c), 37.13 (s, I C7 tt rr), 37.05 (s, I C7 tt rm).

*$^{19}\text{F}$  N.M.R. data* (235MHz,  $(\text{CD}_3)_2\text{CO}$ , 298K) 59.34 (s, I), 64.41 (m, II), 64.56 (m, II), 67.36 (s, II), 67.60 (m, II), 67.73 (m, II), 69.74 (m, II), 69.95 (m).

### 6.5.9 Characterisation data on block copolymer IV - I

*Infra-red data* (film cast from acetone,  $\text{cm}^{-1}$ ) 1805 (w), 1750 (w,sh), 1723 (m,sh), 1715 (m), 1706 (m,sh), 1699 (m,sh), 1689 (m,sh), 1682 (m), 1665 (m,sh), 1656 (m,sh) 1649 (m,sh), 1464 (m,sh), 1455 (m), 1349 (s,br), 1301 (s,br), 1260 (s,sh), 1240 (s,br), 1190-1140 (s,v.br), 1072 (s), 1042 (s,sh), 1012 (m), 977 (s,br), 922 (s), 914 (m,sh), 904 (m,sh), 848 (w), 824 (w), 804 (w,br), 744 (w), 728 (m), 717 (s), 712 (m,sh), 705 (m,sh), 696 (w,sh).

*$^{13}\text{C}$  N.M.R. data* (100MHz,  $(\text{CD}_3)_2\text{CO}$ , 298K) (major resonances only) 139.92 (m, I C5,6), 133.44 (m, I C2,3 t), 132.0 (m, I C2,3 c), 131.0 (br, IV), 129.0 (m, IV), 123.36 (q,  $J_{\text{CF}} = 273.74\text{Hz}$ , I C8), 49.92 (s, I C1,4 t), 48.5 (br, IV), 47.4 (m, IV), 46.1 (br, IV), 44.6 (s, I C1,4 c), 43.6 (br, IV), 37.14 (s, I C7 tt rr), 37.05 (s, I C7 tt rm), 33.38 (m, IV), 32.0 (br, IV).

*<sup>19</sup>F N.M.R. data* 59.34 (s, I), 72.74 (s, IV), 72.97 (m, IV), 76.29 (s, IV), 76.45 (m, IV), 76.57 (s, IV), 103.93 (m, IV), 104.58 (m, IV), 104.62 (s, IV), 115.62 (d, IV), 116.26 (d, IV), 117.3 (m, IV), 118.05 (m, IV), 125.1 (m, IV), 125.75 (m, IV), 160.19 (m, IV), 192.31 (s, IV).

#### 6.5.10 Characterisation data on block copolymer IV - III

*Infra-red data* 1712 (w,br), 1467 (w,sh), 1462 (m), 1454 (m,sh), 1400 (m,sh), 1391 (s), 1350 (m,br), 1308 (s,br), 1270 (s,br), 1250 (s), 1238 (s,sh), 1210 (s,br,sh), 1190-1145 (s,br), 1118 (s,br), 1088 (s), 1060 (m,sh), 1011 (m), 981 (m,sh), 973 (s), 928 (m,br), 901 (m), 800 (w,br).

*<sup>13</sup>C N.M.R. data* (major resonances only) 134.53 (III), 134.15 (III), 133.25 (III), 131.01 (IV), 130.70 (III), 130.43 (IV), 129.71 (III), 127.66 (IV), 46.66 (m, III), 46.42 (m, III), 43.86 (IV), 40.58 (m, III), 33.92 (III), 33.77 (III).

*<sup>19</sup>F N.M.R. data* 65.06 (s, III), 65.20 (s, III), 65.35 (s, III), 70.32 (s, III), 70.33 (s, III), 70.37 (s, III), 70.50 (s, III), 72.73 (s, IV), 72.97 (s, IV), 76.28 (s, IV), 76.42 (s, IV), 103.95 (w, IV), 104.58 (s, IV), 104.61 (s, IV), 115.61 (d, IV), 116.34 (d, IV), 117.38 (m, IV), 118.05 (m, IV), 125.02 (m, IV), 125.75 (m, IV), 160.18 (m, IV), 192.31 (s, IV).

## 6.6 References

1. R.R. Schrock, J.S. Murzdek, G.C. Bazan, J. Robbins, M. DiMare, M. O'Regan  
J.Am.Chem.Soc. **112** 3875 (1990)
2. T.V. Lubben, P.T. Wolczanski, G.D. Van Duyne Organometallics **3** 982 (1984)
3. Prepared using an analogous technique to that described for LiOCMe<sub>3</sub> in reference 2.
4. A.b. Alimuniar, P.M. Blackmore, J.H. Edwards, W.J. Feast, B. Wilson Polymer  
**27** 1281 (1986)
5. P.M. Blackmore, W.J. Feast, P.C. Taylor Brit.Pol.J. **19** 205 (1987)
6. P.M. Blackmore, W.J. Feast Polymer **27** 1296 (1986)
7. B. Wilson, Ph.D. Thesis, University of Durham, (1979).

## **Appendices**

**Appendix I The relationship between dielectric constants and polymer microstructure**

In a gaseous sample polarization is predicted using the Debye theory for uncorrelated and isolated permanent dipoles. In such cases the average angle,  $\theta$ , of a dipole in an electric field,  $E$ , is given by the Langevin function which states...

$$\langle \cos\theta \rangle = \coth\left(\frac{\mu E}{kT}\right) - \frac{kT}{\mu E}$$

Furthermore the polarization,  $\Delta P$ , of the sample is given by

$$\Delta P = P_{\max} \left\{ \coth\left(\frac{\mu E}{kT}\right) - \frac{kT}{\mu E} \right\}$$

where	$\Delta P$	=	polarisation (charge per unit area)
	$E$	=	poling field (voltage per unit area)
	$\mu$	=	dipole moment
	$k$	=	Boltzmann constant
	$T$	=	temperature (degree Kelvin)

At the limit of small electric fields...

$$\begin{aligned} \frac{\Delta P}{\epsilon_0 E} &= \frac{n\mu^2}{3kT} \\ &= \epsilon_R - \epsilon_U \\ &= \chi_p \end{aligned}$$

where $n$	=	dipole density (dipoles per unit volume)
$\epsilon_R$	=	relaxed dielectric constant (measured above $T_g$ )
$\epsilon_U$	=	unrelaxed dielectric constant (measured below $T_g$ )
$\chi_p$	=	relaxed electric susceptibility

However, the Debye theory only applies to uncorrelated dipoles in a rarefied medium. For a solid large approximations to the previous equations become necessary. This is most easily done by the introduction of the Kirkwood g-factor which attempts to make some allowance for the non-independent nature of dipoles in a solid.

$$\epsilon_R - \epsilon_U = \frac{n g \mu^2}{3kT}$$

$$g = \text{Kirkwood 'g'-factor}$$

$$= 1 + z \langle \cos \psi \rangle$$

where  $z$  = the number of nearest neighbours of a molecule in a system  
 $\psi$  = the angle of the molecule with respect to the nearest neighbour

In other words if  $g = 1$  (i.e.  $z = 0$  or  $\psi = 90^\circ$ ) then adjacent dipoles behave independently of one another.

From the stance of dielectric measurements, the most important parameter in all these equations is 'n', which represents the number of dipoles per unit volume. As a consequence the relaxed dielectric constant is dependent upon the density of dipoles in a sample; hence poly(vinylidene fluoride) with a large number of highly polar aligned C-F bonds in a relatively small volume possesses such a high dielectric constant.

The importance of dipole alignment is emphasised in the following two extreme cases of orientation of two adjacent dipoles.

i) two parallel dipoles ( $\uparrow \uparrow$ )

$$\begin{aligned} \text{number of dipoles per unit volume} &= \frac{n}{2} \\ \text{dipole moment} &= 2\mu \\ \therefore \epsilon_R - \epsilon_U &= \frac{\frac{n}{2}(2\mu^2)g}{3kT} \end{aligned}$$

ii) two antiparallel dipoles ( $\uparrow\downarrow$ )

$$\text{dipole moment} = 0$$

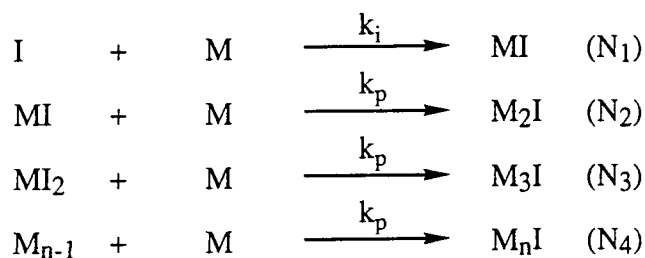
$$\therefore \epsilon_R - \epsilon_U = 0$$

Therefore the more aligned the dipoles are, the greater will be the dielectric constant.

## Appendix II Kinetic derivation for the calculation of $\frac{k_p}{k_i}$

The ratio of rate constants of propagation to initiation has proven useful in cases where the individual rates are too fast to measure. The kinetic formulation presented here follows that of Bazan, and is based closely upon that of Gold.

Consider the polymerization process as the following set of equations...



where

- I = initiating species
- M = monomer
- $k_i$  = rate constant of initiation
- and  $k_p$  = rate constant of propagation.

For the following derivation the following are also defined:

- $[\text{I}]_0$  = initial concentration of the initiating species
- $[\text{M}]_0$  = initial concentration of monomer
- $[\text{I}]$  = instantaneous concentration of the initiating species
- $[\text{M}]$  = instantaneous concentration of the monomer
- $\text{N}_i$  = concentration of the propagating species with  $i^{\text{th}}$  degree of polymerization

For a living polymerization the following conditions exist:

$$\sum_{x=1}^n N_x = [I]_0 - [I]$$

(i.e. no termination or transfer of the propagating species)

$$\text{and } \sum_{x=1}^n x N_x = [M]_0 - [M]$$

(i.e. the concentration of monomer consumed equals the concentration multiplied by the degree of polymerization {DP(n)} of the propagating species)

From the equations representing the polymerization process:

$$\frac{-d[I]}{dt} = k_i[M][I]$$

$$\text{and } \frac{-d[M]}{dt} = k_i[M][I] + k_p[M] \sum_{x=1}^n N_x$$

$$\text{Therefore, } \frac{d[M]}{d[I]} = \frac{k_i[I] + k_p \sum_{x=1}^n N_x}{k_i[I]}$$

$$\text{and since } \sum_{x=1}^n N_x = [I]_0 - [I], \quad \frac{d[M]}{d[I]} = \frac{k_i[I] + k_p\{[I]_0 - [I]\}}{k_i[I]}$$

$$= 1 - \frac{k_p}{k_i} + \frac{k_p [I]_0}{k_i [I]}$$

Hence,

$$\int_{[M]_0}^{[M]} = \int_{[I]_0}^{[I]} \left( 1 - \frac{k_p}{k_i} + \frac{k_p}{k_i} \frac{[I]_0}{[I]} \right) d[I]$$

$$\therefore [M] = [M]_0 + \left( 1 - \frac{k_p}{k_i} \right) ([I] - [I]_0) + \frac{k_p}{k_i} [I]_0 \ln \left( \frac{[I]}{[I]_0} \right)$$

When the polymerization has finished, (i.e. as  $[M]$  tends towards zero)...

$$0 = [M]_0 + \left( 1 - \frac{k_p}{k_i} \right) ([I] - [I]_0) + \frac{k_p}{k_i} [I]_0 \ln \left( \frac{[I]}{[I]_0} \right)$$

$$\therefore \boxed{0 = \frac{[M]_0}{[I]_0} + \frac{k_p}{k_i} \ln \left( \frac{[I]}{[I]_0} \right) + \left( 1 - \frac{k_p}{k_i} \right) \left( \frac{[I]}{[I]_0} - 1 \right)}$$

This is the equation used to determine  $\frac{k_p}{k_i}$  since

$\frac{[M]_0}{[I]_0}$  = number of equivalents of monomer added to the initiating species

and  $\frac{[I]}{[I]_0}$  = ratio of unreacted initiator to total reactive species.

As described in chapter two, both of these quantities can be found from simple N.M.R. spectroscopic experiments.

#### References:

1. G.C. Bazan Ph.D. Thesis, M.I.T. (1990)
2. L.J. Gold J.Chem.Phys 28 91 (1958)

**Appendix III**  
**First Year Induction Courses: October 1989**

The course consists of a series of one hour lectures on the services listed below

1. Departmental Organisation
2. Safety Matters
3. Electrical appliances and infrared spectroscopy
4. Chromatography and Microanalysis
5. Atomic absorption and inorganic analysis
6. Library facilities
7. Mass spectroscopy
8. Nuclear Magnetic Resonance
9. Glass blowing techniques

## Appendix IV

### Colloquia, Lectures and Seminars given by invited speakers during the period 1st August 1989 to 31st July 1990

(\* indicates attendance by the author)

- BADYAL, Dr J.P.S. (Durham University) 1st November 1989  
Breakthroughs in Heterogeneous Catalysis
- \*BECHER, Dr.J. (Odense University) 13th November 1989  
Synthesis of New Macrocyclic Systems using  
Heterocyclic Building Blocks.
- \*BERCAW, Prof. J.E. (California Institute of Technology) 10th November 1989  
Synthetic and Mechanistic Approaches to  
Zieger-Natta Polymerisation of Olefins
- BLEASDALE, Dr. C. (Newcastle University) 21st February 1990  
The Mode of Action of some anti-tumour Agents
- BOWMAN, Prof. J.M. (Emory University) 23rd March 1990  
Fitting Experiment with Theory in Ar-OH
- BUTLER, Dr. A. (St. Andrews University) 7th December 1989  
The Discovery of Penicillin: Facts and Fancies
- CHEETHAM, Dr.A.K. (Oxford University) 8th March 1990  
Chemistry of Zeolite Cages
- CLARK, Prof. D.T. (ICI Wilton) 22nd February 1990  
Spatially Resolved Chemistry (using Nature's  
Paradigm in the Advanced Materials Arena).
- \*COLE-HAMILTON, Prof. D.J. (St. Andrews University) 29th November 1989  
New Polymers from Homogeneous Catalysis
- CROMBIE, Prof. L. (Nottingham University) 15th February 1990  
The Chemistry of Cannabis and Khat

- DYER, Dr. U. (Glaxo) 31st January 1990  
Synthesis and Conformation of C-Glycosides
- \*FLORIANI, Prof. C. (Lausanne Univ., Switzerland) 25th October 1989  
Molecular Aggregates- A Bridge Between  
Homogeneous and Heterogeneous Systems
- GERMAN, Prof. L.S. (USSR Academy of Sciences) 9th July 1990  
New Syntheses in Fluoroaliphatic Chemistry:  
Recent Advances in the Chemistry of Fluorinated Oxiranes.
- GRAHAM, Dr.D. (B.P. Research Centre) 4th December 1989  
How Proteins Absorb to Interfaces
- \*GREENWOOD, Prof. N.N. (University of Leeds) 9th November 1989  
Novel Cluster Geometries in Metalloborane  
Chemistry
- HOLLOWAY, Prof. J.H. (University of Leicester) 1st February 1990  
Noble Gas Chemistry
- \*HUGHES, Dr.M.N. (King's College, London) 30th November 1989  
A Bug's Eye View of the Periodic Table
- HUISGEN, Prof. R. (Universität München) 15th December 1989  
Recent Mechanistic Studies of [2+2] Additions
- KLINOWSKI, Dr.J. (Cambridge University) 13th December 1989  
Solid State NMR Studies of Zeolite Catalysts
- LANCASTER, Rev. R. (Kimbolton Fireworks) 8th February 1990  
Fireworks - Principles and Practice.
- LUNAZZI, Prof. L. (University of Bologna) 12th February 1990  
Application of Dynamic NMR to the Study of  
Conformational Enantiomerism
- \*PALMER, Dr. F. (Nottingham University) 17th October 1989  
Thunder and Lightning

- PARKER, Dr. D. (Durham University) 16th November 1989  
Macrocycles, Drugs and Rock'N'Roll
- \*PERUTZ, Dr. R.N. (York University) 24th January 1990  
Plotting the Course of C-H Activations with  
Organometallics.
- PLATONOV, Prof. V.E. (USSR Academy of Sciences) 9th July 1990  
Polyfluoroindanes: Synthesis and Transformation
- \*POWELL, Dr.R.L. (ICI) 6th December 1989  
The Development of CFC Replacements
- POWIS, Dr. I. (Nottingham University) 21st March 1990  
Spinning off in a Huff: Photodissociation  
of Methyl Iodide
- ROZHKOVA, Prof. I.N. (USSR Academy of Sciences) 9th July 1990  
Reactivity of Perfluoroalkyl Bromides
- \*STODDART, Dr.J.F. (Sheffield University) 1st March 1990  
Molecular Lego
- \*SUTTON, Prof. D. (Simon Fraser Univ., Vancouver B.C.) 14th February 1990  
Synthesis and Applications of Dinitrogen and Diazo  
Compounds of Rhenium and Iridium.
- THOMAS, Dr.R.K. ( Oxford University) 28th February 1990  
Neutron Reflectometry from Surfaces
- THOMPSON, Dr. D.P. (Newcastle University) 7th February 1990  
The Role of Nitrogen in Extending Silicate  
Crystal Chemistry.

**During the period 1st August 1990 to 31st July 1991**

- ALDER, Dr. B.J. (Lawrence Livermore Labs., California) 15th January 1991  
Hydrogen in all its glory

- \*BELL, Prof. T. (SUNY, Stony Brook, U.S.A.) 14th November 1990  
Functional Molecular Architecture and Molecular Recognition
- \*BOCHMANN, Dr. M. (University of East Anglia) 24th October 1990  
Synthesis, Reactions and Catalytic Activity of Cationic Titanium Alkyls
- BRIMBLE, Dr. M.A. (Massey University, New Zealand) 29th July 1991  
Synthetic Studies Towards the Antibiotic Griseusin-A
- \*BROOKHART, Prof. M.S. (University of N. Carolina) 20th June 1991  
Olefin Polymerizations, Oligomerizations and Dimerizations Using Electrophilic Late Transition Metal Catalysts
- BROWN, Dr. J. (Oxford University) 28th February 1991  
Can Chemistry Provide Catalysts Superior to Enzymes?
- BUSHBY, Dr. R. (Leeds University) 6th February 1991  
Biradicals and Organic Magnets
- COWLEY, Prof. A.H. (University of Texas) 13th December 1990  
New Organometallic Routes to Electronic Materials
- CROUT, Prof. D. (Warwick University) 29th November 1990  
Enzymes in Organic Synthesis
- DOBSON, Dr. C.M. (Oxford University) 6th March 1991  
NMR Studies of Dynamics in Molecular Crystals
- GERRARD, Dr. D. (British Petroleum) 7th November 1990  
Raman Spectroscopy for Industrial Analysis
- HUDLICKY, Prof. T. (Virginia Polytechnic Institute) 25th April 1991  
Biocatalysis and Symmetry Based Approaches to the Efficient Synthesis of Complex Natural Products

- JACKSON, Dr. R. (Newcastle University) 31st October 1990  
New Synthetic Methods:  $\alpha$ -Amino Acids and Small Rings
- \*KOCOVSKY, Dr. P. (Uppsala University) 6th November 1990  
Stereo-Controlled Reactions Mediated by Transition and Non-Transition Metals
- LACEY, Dr. D. (Hull University) 31st January 1991  
Liquid Crystals
- LOGAN, Dr. N. (Nottingham University) 1st November 1990  
Rocket Propellants
- MACDONALD, Dr. W.A. (ICI Wilton) 11th October 1990  
Materials for the Space Age
- \*MARKAM, Dr.J. (ICI Pharmaceuticals) 7th March 1991  
DNA Fingerprinting
- \*PETTY, Dr. M. (Durham University) 14th February 1991  
Molecular Electronics
- \*PRINGLE, Dr. P.G. (Bristol University) 5th December 1990  
Metal Complexes with Functionalised Phosphines
- PRITCHARD, Prof. J. (Queen Mary and Westfield College, London University) 21st November 1990  
Copper Surfaces and Catalysts
- SADLER, Dr. P.J. (Birbeck College, London) 24th January 1991  
Design of Inorganic Drugs: Precious Metals, Hypertension + HIV
- \*SARRE, Dr. P. (Nottingham University) 17th January 1991  
Comet Chemistry
- \*SCHROCK, R.R. (Massachusetts Institute of Technology) 24th April 1991  
Metal-ligand Multiple Bonds and Metathesis Initiators

- \*SCOTT, Dr. S.K. (Leeds University) 8th November 1990  
Clocks, Oscillations and Chaos
- \*SHAW, Prof. B.L. (Leeds University) 20th February 1991  
Syntheses with Coordinated, Unsaturated Phosphine  
Ligands
- \*SINN, Prof. E. (Hull University) 30th January 1991  
Coupling of Little Electrons in Big Molecules.  
Implications for the Active Sites of (Metalloproteins  
and other) Macromolecules
- \*SOULEN, Prof. R. (South Western University, Texas) 26th October 1990  
Preparation and Reactions of Bicycloalkenes
- WHITAKER, Dr. B.J. (Leeds University) 28th November 1990  
Two-Dimensional Velocity Imaging of State-Selected  
Reaction Products

**During the period 1st August 1991 to 31st July 1992**

- ANDERSON, Dr. M. (Shell Research) 30th January 1992  
Recent Advances in the Safe and Selective Chemical  
Control of Insect Pests
- \*BILLINGHAM, Dr. N.C. (University of Sussex) 5th March 1992  
Degradable Plastics - Myth or Magic?
- BUTLER, Dr. A.R. (St. Andrews University) 7th November 1991  
Traditional Chinese herbal drugs: a different  
way of treating disease
- COOPER, Dr. W.D. (Shell Research) 11th December 1991  
Colloid science: theory and practice
- FENTON, Prof. D.E. (Sheffield University) 12th February 1992  
Polynuclear complexes of molecular clefts as models  
for copper biosites

- GANI, Prof. R. (St. Andrews University) 13th November 1991  
The chemistry of PLP-dependent enzymes
- GEHRET, Dr. J-C (Ciba-Geigy, Basel) 13th May 1992  
Some aspects of industrial agrochemical research
- GRIGG, Prof. R. (Leeds University) 4th December 1991  
Palladium-catalysed cyclisation and ion-capture processes
- HANN, Dr. R.A. (ICI Imagedata) 12th March 1992  
Electronic Photography - An Image of the Future
- HARRIS, Dr. K.D.M. (St. Andrews University) 22nd January 1992  
Understanding the properties of solid-inclusion compounds
- HITCHMAN, Prof. M.L. (Strathclyde University) 26th February 1992  
Chemical vapour deposition
- HOLMES, Dr. A. (Cambridge University) 29th January 1992  
Cycloaddition reactions in the service of the synthesis of piperidine and indolizidine natural products
- JOHNSON, Prof. B.F.G. (Edinburgh University) 6th November 1991  
Cluster-surface analogies
- KEELEY, Dr. R. 31st October 1991  
Modern forensic science
- KNIGHT, Prof. D.M. (University of Durham) 7th April 1992  
Interpreting experiments: the beginning of electrochemistry
- MASKILL, Dr. H. (Newcastle University) 18th March 1992  
Concerted or stepwise fragmentation in a deamination-type reaction
- MORE O'FERRALL, Dr. R. (University College, Dublin) 20th November 1991  
Some acid-catalysed rearrangements in organic chemistry

- \*NIXON, Prof J.F. (University of Sussex) 25th February 1992  
*The Tilden Lecture* Phosphaalkynes: new building blocks  
in inorganic and organometallic chemistry
- SALTHOUSE, Dr. J.A. (University of Manchester) 17th October 1991  
Son et Lumiere - a demonstration lecture
- SAUNDERS, Dr. J. (Glaxo Group Research Limited) 13th February 1992  
Molecular Modelling in Drug Discovery
- SMITH, Prof. A.L. (ex Unilever) 5th December 1991  
Soap, detergents and black puddings
- THOMAS, Prof. E.J. (Manchester University) 19th February 1992  
Applications of organostannanes to organic synthesis
- THOMAS, Dr. S.E. (Imperial College) 11th March 1992  
Recent advances in organoiron chemistry
- \*VOGEL, Prof. E. (University of Cologne) 20th February 1992  
*The Musgrave Lecture* Porphyrins: Molecules of  
Interdisciplinary Interest
- \*WARD, Prof. I.M. (IRC in Polymer Science and  
Technology, University of Leeds) 28th November 1991  
*The SCI Lecture* The science and technology of  
orientated polymers

## Appendix V

### Conferences and Lectures Attended

(\* denotes poster presentation, † denotes lecture given)

1. “North East Graduate Symposium”,  
University of Newcastle-Upon-Tyne, 2<sup>nd</sup> April 1990
2. “Symposium in Honour of Professor Peter L. Pauson - Organometallic Chemistry  
in the Transition Metals”  
University of Strathclyde, 19<sup>th</sup> October 1990
3. “Aspects of Contemporary Polymer Chemistry”  
University of Lancaster, April 1991
4. “Transition Metal Mediated Polymerizations”  
Macro Group UK, SCI, Belgrave Square, London, 25<sup>th</sup> June 1991
- 5.\* “Physical Aspects of Polymer Science”,  
University of Leeds, 9<sup>th</sup> - 11<sup>th</sup> September 1991
6. “IRC Industrial Club Seminar”  
University of Durham, 17<sup>th</sup> - 18<sup>th</sup> September 1991
7. “Autumn Meeting of the Royal Society of Chemistry”,  
University of York, 29<sup>th</sup> September 1991
8. “Fluoropolymers ‘92: Synthesis, Properties and Commercial Applications”  
UMIST, Manchester, 6<sup>th</sup> - 8<sup>th</sup> January 1992
- 9.† “North East Graduate Symposium”  
University of Durham, 3<sup>rd</sup> April 1993
- 10.\* “Aspects of Contemporary Polymer Chemistry”,  
University of Durham, 6<sup>th</sup> - 8<sup>th</sup> April 1992

## Appendix VI

### Publications

1. "A remarkable ancillary ligand effect in living ring-opening metathesis polymerization"  
W.J. Feast, V.C. Gibson, E.L. Marshall  
J.Chem.Soc.,Chem.Comm. 1157 (1992)
2. "Bimolecular termination in living ring-opening metathesis polymerization"  
W.J. Feast, V.C. Gibson, E. Khosravi, E.L. Marshall, J.P. Mitchell  
Polymer **33** 872 (1992)
3. "Fluorinated block copolymers via living ring-opening metathesis polymerization"  
E. Khosravi, W.J. Feast, V.C. Gibson, E.L. Marshall  
Proceedings of the International Symposium on Metathesis 1991, July 22<sup>nd</sup> - 25<sup>th</sup>  
1991, Philadelphia.
4. "Ring-opening metathesis polymerization of syn- and anti-7-methylbicyclo[2.2.1]hept-2-ene initiated by  $Mo(CHCMe_3)(NC_6H_3-2,6-i-Pr_2)(OCMe_3)_2$ "  
W.J. Feast, V.C. Gibson, K.J. Ivin, E. Khosravi, A.M. Kenwright,  
E.L. Marshall, J.P. Mitchell  
Makromol.Chem. **193** 2103 (1992)
5. "Synthesis and properties of novel, highly polar polymers"  
W.J. Feast, E. Khosravi, V.C. Gibson, E.L. Marshall, B. Wilson  
Polymer Preprints, Japan **41** 45 (1992)
6. "Synthesis and Properties of Stereoregular Fluoropolymers via ring-opening metathesis polymerization of fluorinated norbornenes and norbornadienes. An overview and progress report"  
G. R. Davies, W.J. Feast, V.C. Gibson, H.V.St.A. Hubbard, K.J. Ivin,  
A.M. Kenwright, E. Khosravi, E.L. Marshall, J.P. Mitchell, I.M. Ward,  
B.Wilson  
Makromolekulare Symposium, Lyon 1992
7. "Proceedings of the Symposium Functionele Polymeren - de Polymeren van Morgen" (pp1 - 14), TU Delft, the Netherlands (1992)  
G.R. Davies, W.J. Feast, V.C. Gibson, H.V.St.A. Hubbard, E. Khosravi,  
E.L. Marshall, M. Petty, M.C. Petty, J. Tsbouklis, I.M. Ward, S.C. Wellings

